OAK RIDGE NATIONAL LABORATORY LIBRARY
3 4456 0024744 5

ORNL-4553

CENTRAL RESEARCH LIBRARY

THEORETICAL AND EXPERIMENTAL STRESS ANALYSIS OF ORNL THIN-SHELL CYLINDER-TO-CYLINDER MODEL NO. 1

J. M. Corum
S. E. Bolt
W. L. Greenstreet
R. C. Gwaltney

OAK RIDGE NATIONAL LABORATORY
CENTRAL RESEARCH LIBRARY
DOCUMENT COLLECTION
LIBRARY LOAN COPY
DO NOT TRANSFER TO ANOTHER PERSON
If you wish someone else to see this document, send in name with document and the library will arrange a loan.

OAK RIDGE NATIONAL LABORATORY
OPERATED BY UNION CARBIDE CORPORATION • FOR THE U.S. ATOMIC ENERGY COMMISSION

Printed in the United States of America. Available from
National Technical Information Service
U.S. Department of Commerce
5285 Port Royal Road, Springfield, Virginia 22151
Price: Printed Copy $3.00; Microfiche $0.95

This report was prepared as an account of work sponsored by the United States Government. Neither the United States nor the United States Atomic Energy Commission, nor any of their employees, nor any of their contractors, subcontractors, or their employees, makes any warranty, express or implied, or assumes any legal liability or responsibility for the accuracy, completeness or usefulness of any information, apparatus, product or process disclosed, or represents that its use would not infringe privately owned rights.

ORNL-4553
UC-80 — Reactor Technology

Contract No. W-7405-eng-26

Reactor Division

THEORETICAL AND EXPERIMENTAL STRESS ANALYSIS OF ORNL THIN-SHELL CYLINDER-TO-CYLINDER MODEL NO. 1

J. M. Corum
S. E. Bolt
W. L. Greenstreet
R. C. Gwaltney

OCTOBER 1972

OAK RIDGE NATIONAL LABORATORY
Oak Ridge, Tennessee 37830
operated by
UNION CARBIDE CORPORATION
for the
U.S. ATOMIC ENERGY COMMISSION

OAK RIDGE NATIONAL LABORATORY LIBRARY
3 4456 0024744 5

CONTENTS

Page

LIST OF FIGURES v

ABSTRACT 1

1. INTRODUCTION 2

2. EXPERIMENTAL ANALYSIS 5

2.1 Model Construction 5
2.2 Strain-Gage Layout 6
2.3 Test Description 7
2.4 Data Acquisition and Reduction 8
2.5 Variations of Maximum Measured Stresses around Nozzle-Cylinder Junction 10

3. FINITE-ELEMENT ANALYSIS 24

3.1 Background 24
3.2 Finite-Element Method 25
3.3 Finite-Element Idealization of Model 30

4. COMPARISON OF THEORY AND EXPERIMENT 34

4.1 Internal Pressure 34
4.2 Out-of-Plane Moment Loading, M_{XN}, on Nozzle 36
4.3 Torsional Moment Loading, M_{YN}, on Nozzle 37
4.4 In-Plane Moment Loading, M_{ZN}, on Nozzle 38
4.5 In-Plane Force, F_{XN}, on Nozzle 39
4.6 Axial Force, F_{YN}, on Nozzle 39
4.7 Out-of-Plane Force, F_{ZN}, on Nozzle 39
4.8 Torsional Moment Loading, M_{XC}, on Cylinder 40
4.9 Out-of-Plane Moment Loading, M_{YC}, on Cylinder 40
4.10 In-Plane Moment Loading, M_{ZC}, on Cylinder 41
4.11 Axial Force, F_{XC}, on Cylinder 41
4.12 In-Plane Force, F_{YC}, on Cylinder 42
4.13 Out-of-Plane Force, F_{ZC}, on Cylinder 42

5. CONCLUSIONS 95

ACKNOWLEDGMENTS 99

REFERENCES 100

APPENDIX. TABULATION OF EXPERIMENTAL DATA 103

A.1 Internal Pressure 105
A.2 Out-of-Plane Moment Loading, M_{XN}, on Nozzle 113
A.3 Torsional Moment Loading, M_{YN}, on Nozzle 121
A.4 In-Plane Moment Loading, M_{ZN}, on Nozzle 129
A.5 In-Plane Force, F_{XN}, on Nozzle 137
A.6 Axial Force, F_{YN}, on Nozzle 145
A.7 Out-of-Plane Force, F_{ZN}, on Nozzle 153
A.8 Torsional Moment Loading, M_{XC}, on Cylinder 161

A.9 Out-of-Plane Moment Loading, M_{YC}, on Cylinder 169
A.10 In-Plane Moment Loading, M_{ZC}, on Cylinder 177
A.11 Axial Force, F_{XC}, on Cylinder 185
A.12 In-Plane Force, F_{YC}, on Cylinder 193
A.13 Out-of-Plane Force, F_{ZC}, on Cylinder 201

LIST OF FIGURES

Page

1. Thin-Shell Cylinder-to-Cylinder Model 1 and Table Showing Dimensions of All Four Models in Test Series 4

2. Schematic of First Model Showing Applied External Loadings 4

3. Strain-Gage Layout 13

4. Closeup of Assembly of Five Strain-Gage Rosettes on a Common Foil Backing 14

5. Model During Instrumentation 15

6. Closeup of Gages in Junction Region 16

7. Instrumented Model in Test Frame Being Subjected to an In-Plane Moment Loading on the Nozzle 17

8. Variation of Maximum Principal Stress Ratios around Nozzle-Cylinder Junction for Internal Pressure 18

9. Variation of Maximum Principal Stress Ratios around Nozzle-Cylinder Junctions for Out-of-Plane Moment, M_{XN}, on Nozzle ... 18

10. Variation of Maximum Principal Stress Ratios around Nozzle-Cylinder Junction for Torsional Moment, M_{YN}, on Nozzle 18

11. Variation of Maximum Principal Stress Ratios around Nozzle-Cylinder Junction for In-Plane Moment, M_{ZN}, on Nozzle 19

12. Variation of Maximum Principal Stress Ratios around Nozzle-Cylinder Junction for In-Plane Force, F_{XN}, on Nozzle 19

13. Variation of Maximum Principal Stress Ratios around Nozzle-Cylinder Junction for Axial Force, F_{YN}, on Nozzle 20

14. Variation of Maximum Principal Stress Ratios around Nozzle-Cylinder Junction for Out-of-Plane Force, F_{ZN}, on Nozzle 20

15. Variation of Maximum Principal Stress Ratios around Nozzle-Cylinder Junction for Torsional Moment, M_{XC}, on Cylinder 21

16. Variation of Maximum Principal Stress Ratios around Nozzle-Cylinder Junction for Out-of-Plane Moment, M_{YC}, on Cylinder .. 21

17. Variation of Maximum Principal Stress Ratios around Nozzle-Cylinder Junction for In-Plane Moment, M_{ZC}, on Cylinder 22

18. Variation of Maximum Principal Stress Ratios around Nozzle-Cylinder Junction for Axial Force, F_{XC}, on Cylinder 22

19. Variation of Maximum Principal Stress Ratios around Nozzle-Cylinder Junction for In-Plane Force, F_{YC}, on Cylinder 23

20. Variation of Maximum Principal Stress Ratios around Nozzle-Cylinder Junction for Out-of-Plane Force, F_{ZC}, on Cylinder ... 23

21. Flat-Plate and Curved-Shell Finite-Element Idealizations 32

22. Quadrilateral Element and Component Triangles 32

23. Constraint at Junction Nodes 33

24. Finite-Element Idealization of Model 33

25. Measured and Predicted Stress Distributions at 0° for Internal Pressure of 50 psi 43

26. Measured and Predicted Stress Distributions at 180° for Internal Pressure of 50 psi 43

27. Measured and Predicted Stress Distributions at 330° for Internal Pressure of 50 psi 44

28. Measured and Predicted Stress Distributions at 150° for Internal Pressure of 50 psi 44

29. Measured and Predicted Stress Distributions at 300° for Internal Pressure of 50 psi 45

30. Measured and Predicted Stress Distributions at 120° for Internal Pressure of 50 psi 45

31. Measured and Predicted Stress Distributions at 270° for Internal Pressure of 50 psi 46

32. Measured and Predicted Stress Distributions at 90° for Internal Pressure of 50 psi 46

33. Measured and Predicted Stress Distributions at 0° for Out-of-Plane Moment, M_{XN}, on Nozzle 47

34. Measured and Predicted Stress Distributions at 180° for Out-of-Plane Moment, M_{XN}, on Nozzle 47

35. Measured and Predicted Stress Distributions at 330° for Out-of-Plane Moment, M_{XN}, on Nozzle 48

36. Measured and Predicted Stress Distributions at 150° for Out-of-Plane Moment, M_{XN}, on Nozzle 48

37. Measured and Predicted Stress Distributions at 300° for Out-of-Plane Moment, M_{XN}, on Nozzle 49

38. Measured and Predicted Stress Distributions at 120° for Out-of-Plane Moment, M_{XN}, on Nozzle 49

39. Measured and Predicted Stress Distributions at 270° for Out-of-Plane Moment, M_{XN}, on Nozzle 50

40. Measured and Predicted Stress Distributions at 90° for Out-of-Plane Moment, M_{XN}, on Nozzle 50

41. Measured and Predicted Stress Distributions at 0° for Torsional Moment, M_{YN}, on Nozzle 51

42. Measured and Predicted Stress Distributions at 180° for Torsional Moment, M_{YN}, on Nozzle 51

43. Measured and Predicted Stress Distributions at 330° for Torsional Moment, M_{YN}, on Nozzle 52

44. Measured and Predicted Stress Distributions at 150° for Torsional Moment, M_{YN}, on Nozzle 52

45. Measured and Predicted Stress Distributions at 300° for Torsional Moment, M_{YN}, on Nozzle 53

46. Measured and Predicted Stress Distributions at 120° for Torsional Moment, M_{YN}, on Nozzle 53

47. Measured and Predicted Stress Distributions at 270° for Torsional Moment, M_{YN}, on Nozzle 54

48. Measured and Predicted Stress Distributions at 90° for Torsional Moment, M_{YN}, on Nozzle 54

49. Measured and Predicted Stress Distributions at 0° for In-Plane Moment, M_{ZN}, on Nozzle 55

50. Measured and Predicted Stress Distributions at 180° for In-Plane Moment, M_{ZN}, on Nozzle 55

51. Measured and Predicted Stress Distributions at 330° for In-Plane Moment, M_{ZN}, on Nozzle 56

52. Measured and Predicted Stress Distributions at 150° for In-Plane Moment, M_{ZN}, on Nozzle 56

53. Measured and Predicted Stress Distributions at 300° for In-Plane Moment, M_{ZN}, on Nozzle 57

54. Measured and Predicted Stress Distributions at 120° for In-Plane Moment, M_{ZN}, on Nozzle 57

55. Measured and Predicted Stress Distributions at 270° for In-Plane Moment, M_{ZN}, on Nozzle 58

56. Measured and Predicted Stress Distributions at 90° for In-Plane Moment, M_{ZN}, on Nozzle 58

57. Measured and Predicted Stress Distributions at 0° for In-Plane Force, F_{XN}, on Nozzle 59

58. Measured and Predicted Stress Distributions at 180° for In-Plane Force, F_{XN}, on Nozzle 59

59. Measured and Predicted Stress Distributions at 330° for In-Plane Force, F_{XN}, on Nozzle 60

60. Measured and Predicted Stress Distributions at 150° for In-Plane Force, F_{XN}, on Nozzle 60

61. Measured and Predicted Stress Distributions at 300° for In-Plane Force, F_{XN}, on Nozzle 61

62. Measured and Predicted Stress Distributions at 120° for In-Plane Force, F_{XN}, on Nozzle 61

63. Measured and Predicted Stress Distributions at 270° for In-Plane Force, F_{XN}, on Nozzle 62

64. Measured and Predicted Stress Distributions at 90° for In-Plane Force, F_{XN}, on Nozzle 62

65. Measured and Predicted Stress Distributions at 0° for Axial Force, F_{YN}, on Nozzle 63

66. Measured and Predicted Stress Distributions at 180° for Axial Force, F_{YN}, on Nozzle 63

67. Measured and Predicted Stress Distributions at 330° for Axial Force, F_{YN}, on Nozzle 64

68. Measured and Predicted Stress Distributions at 150° for Axial Force, F_{YN}, on Nozzle 64

69. Measured and Predicted Stress Distributions at 300° for Axial Force, F_{YN}, on Nozzle 65

70. Measured and Predicted Stress Distributions at 120° for Axial Force, F_{YN}, on Nozzle 65

71. Measured and Predicted Stress Distributions at 270° for Axial Force, F_{YN}, on Nozzle 66

72. Measured and Predicted Stress Distributions at 90° for Axial Force, F_{YN}, on Nozzle 66

73. Measured and Predicted Stress Distributions at 0° for Out-of-Plane Force, F_{ZN}, on Nozzle 67

74. Measured and Predicted Stress Distributions at 180° for Out-of-Plane Force, F_{ZN}, on Nozzle 67

75. Measured and Predicted Stress Distributions at 330° for Out-of-Plane Force, F_{ZN}, on Nozzle 68

76. Measured and Predicted Stress Distributions at 150° for Out-of-Plane Force, F_{ZN}, on Nozzle 68

77. Measured and Predicted Stress Distributions at 300° for Out-of-Plane Force, F_{ZN}, on Nozzle 69

78. Measured and Predicted Stress Distributions at 120° for Out-of-Plane Force, F_{ZN}, on Nozzle 69

79. Measured and Predicted Stress Distributions at 270° for Out-of-Plane Force, F_{ZN}, on Nozzle 70

80. Measured and Predicted Stress Distributions at 90° for Out-of-Plane Force, F_{ZN}, on Nozzle 70

81. Measured and Predicted Stress Distributions at 0° for Torsional Moment, M_{XC}, on Cylinder 71

82. Measured and Predicted Stress Distributions at 180° for Torsional Moment, M_{XC}, on Cylinder 71

83. Measured and Predicted Stress Distributions at 330° for Torsional Moment, M_{XC}, on Cylinder 72

84. Measured and Predicted Stress Distributions at 150° for Torsional Moment, M_{XC}, on Cylinder 72

85. Measured and Predicted Stress Distributions at 300° for Torsional Moment, M_{XC}, on Cylinder 73

86. Measured and Predicted Stress Distributions at 120° for Torsional Moment, M_{XC}, on Cylinder 73

87. Measured and Predicted Stress Distributions at 270° for Torsional Moment, M_{XC}, on Cylinder 74

88. Measured and Predicted Stress Distributions at 90° for Torsional Moment, M_{XC}, on Cylinder 74

89. Measured and Predicted Stress Distributions at 0° for Out-of-Plane Moment, M_{YC}, on Cylinder 75

90. Measured and Predicted Stress Distributions at 180° for Out-of-Plane Moment, M_{YC}, on Cylinder 75

91. Measured and Predicted Stress Distributions at 330° for Out-of-Plane Moment, M_{YC}, on Cylinder 76

92. Measured and Predicted Stress Distributions at 150° for Out-of-Plane Moment, M_{YC}, on Cylinder 76

93. Measured and Predicted Stress Distributions at 300° for Out-of-Plane Moment, M_{YC}, on Cylinder 77

94. Measured and Predicted Stress Distributions at 120° for Out-of-Plane Moment, M_{YC}, on Cylinder 77

95. Measured and Predicted Stress Distributions at 270° for Out-of-Plane Moment, M_{YC}, on Cylinder 78

96. Measured and Predicted Stress Distributions at 90° for Out-of-Plane Moment, M_{YC}, on Cylinder 78

97. Measured and Predicted Stress Distributions at 0° for In-Plane Moment, M_{ZC}, on Cylinder 79

98. Measured and Predicted Stress Distributions at 180° for In-Plane Moment, M_{ZC}, on Cylinder 79

99. Measured and Predicted Stress Distributions at 330° for In-Plane Moment, M_{ZC}, on Cylinder 80

100. Measured and Predicted Stress Distributions at 150° for In-Plane Moment, M_{ZC}, on Cylinder 80

101. Measured and Predicted Stress Distributions at 300° for In-Plane Moment, M_{ZC}, on Cylinder 81

102. Measured and Predicted Stress Distributions at 120° for In-Plane Moment, M_{ZC}, on Cylinder 81

103. Measured and Predicted Stress Distributions at 270° for In-Plane Moment, M_{ZC}, on Cylinder 82

104. Measured and Predicted Stress Distributions at 90° for In-Plane Moment, M_{ZC}, on Cylinder 82

105. Measured and Predicted Stress Distributions at 0° for Axial Force, F_{XC}, on Cylinder 83

106. Measured and Predicted Stress Distributions at 180° for Axial Force, F_{XC}, on Cylinder 83

107. Measured and Predicted Stress Distributions at 330° for Axial Force, F_{XC}, on Cylinder 84

108. Measured and Predicted Stress Distributions at 150° for Axial Force, F_{XC}, on Cylinder 84

109. Measured and Predicted Stress Distributions at 300° for Axial Force, F_{XC}, on Cylinder 85

110. Measured and Predicted Stress Distributions at 120° for Axial Force, F_{XC}, on Cylinder 85

111. Measured and Predicted Stress Distributions at 270° for Axial Force, F_{XC}, on Cylinder 86

112. Measured and Predicted Stress Distributions at 90° for Axial Force, F_{XC}, on Cylinder 86

113. Measured and Predicted Stress Distributions at 0° for In-Plane Force, F_{YC}, on Cylinder 87

114. Measured and Predicted Stress Distributions at 180° for In-Plane Force, F_{YC}, on Cylinder 87

115. Measured and Predicted Stress Distributions at 330° for In-Plane Force, F_{YC}, on Cylinder 88

116. Measured and Predicted Stress Distributions at 150° for In-Plane Force, F_{YC}, on Cylinder 88

117. Measured and Predicted Stress Distributions at 300° for In-Plane Force, F_{YC}, on Cylinder 89

118. Measured and Predicted Stress Distributions at 120° for In-Plane Force, F_{YC}, on Cylinder 89

119. Measured and Predicted Stress Distributions at 270° for In-Plane Force, F_{YC}, on Cylinder 90

120. Measured and Predicted Stress Distributions at 90° for In-Plane Force, F_{YC}, on Cylinder 90

121. Measured and Predicted Stress Distributions at 0° for Out-of-Plane Force, F_{ZC}, on Cylinder 91

122. Measured and Predicted Stress Distributions at 180° for Out-of-Plane Force, F_{ZC}, on Cylinder 91

123. Measured and Predicted Stress Distributions at 330° for Out-of-Plane Force, F_{ZC}, on Cylinder 92

124. Measured and Predicted Stress Distributions at 150° for Out-of-Plane Force, F_{ZC}, on Cylinder 92

125. Measured and Predicted Stress Distributions at 300° for Out-of-Plane Force, F_{ZC}, on Cylinder 93

126. Measured and Predicted Stress Distributions at 120° for Out-of-Plane Force, F_{ZC}, on Cylinder 93

127. Measured and Predicted Stress Distributions at 270° for Out-of-Plane Force, F_{ZC}, on Cylinder 94

128. Measured and Predicted Stress Distributions at 90° for Out-of-Plane Force, F_{ZC}, on Cylinder 94

THEORETICAL AND EXPERIMENTAL STRESS ANALYSIS OF ORNL THIN-SHELL CYLINDER-TO-CYLINDER MODEL NO. 1

J. M. Corum W. L. Greenstreet
S. E. Bolt R. C. Gwaltney

ABSTRACT

The first in a series of four thin-shell cylinder-to-cylinder models was tested, and the experimentally determined elastic stress distributions were compared with theoretical predictions obtained from a thin-shell finite-element analysis. The models in the series are idealized thin-shell structures consisting of two circular cylindrical shells intersecting at right angles. There are no transitions, reinforcements, or fillets in the junction region. The series of model tests serves two basic purposes: (1) the experimental data will provide design information directly applicable to nozzles in cylindrical vessels, and (2) the idealized models serve a basic need for test results for use in developing and evaluating theoretical analyses applicable to nozzles in cylindrical vessels and to thin piping tees.

The cylinder of the model tested had an outside diameter of 10 in., and the nozzle had an outside diameter of 5 in., giving a d_o/D_o ratio of 1/2. The OD/thickness ratio for both cylinder and nozzle was 100. Thirteen separate loading cases were analyzed. In each, one end of the cylinder was rigidly held. In addition to an internal pressure, three mutually perpendicular force components and three mutually perpendicular moment components were individually applied at the free end of the cylinder and at the end of the nozzle. The experimental stress distributions for each of the 13 loadings were obtained using 322 three-gage strain rosettes located on the inner and outer surfaces.

Each of the 13 loading cases was also analyzed theoretically using a finite-element shell analysis developed at the University of California, Berkeley. The analysis used flat-plate elements and considered five degrees of freedom per node in the final assembled equations. The comparisons between theory and experiment show reasonably good general agreement, and it is felt that the analysis would be satisfactory for most engineering purposes.

1. INTRODUCTION

Intersecting cylindrical shells are common configurations in structural components for nuclear reactor systems. Piping tees and nozzles in cylindrical vessels are specific examples. Despite their common occurrence, however, proven elastic stress analysis methods for such configurations have not been generally available, and only recently have potential analyses, both analytical and numerical, been developed. This is true even for the case of an idealized configuration consisting of two thin-shell cylinders intersecting normally with no transitions, reinforcements, or fillets in the junction region.

To meet the need for experimental data obtained from carefully machined models, Oak Ridge National Laboratory is testing a series of four thin-shell cylinder-to-cylinder models. In addition to serving a basic need for test results for use in developing and evaluating potential analytical techniques, the models in the series will provide design information directly applicable to nozzles in cylindrical vessels and to a class of thin piping tees as well. The test results will be particularly applicable to liquid-metal fast breeder reactor components in which relatively low internal pressures and high thermal transients dictate thin-walled structures.

The first model in the series has been tested, and the results have been compared with theoretical predictions obtained from a finite-element thin-shell analysis. The purpose of this report is to discuss the testing and analysis of this first model and to present the comparisons of theory and experiment.

The first model, which has been tested, is shown in Fig. 1, together with a table listing the significant dimensions of all four models in the series. As the figure indicates, these models are truly idealized shell structures. There are no transitions, fillets, or reinforcing in the junction region. The outside diameter D_o of the cylinder of the first model was 10.0 in. and the outside diameter d_o of the nozzle was 5.0 in., giving a d_o/D_o ratio of 1/2. The cylinder thickness T was 0.1 in., and the nozzle thickness t was 0.05 in. Thus the OD/thickness ratio of both shells was 100.

The remaining three models have outside diameters of 10.0 in. for the cylinder. However, in the second model the outside diameter of the nozzle is also 10.0 in., giving a d_o/D_o ratio of 1.0. In the third and fourth models the outside diameter of the nozzle is 1.29 in. The fourth model will actually be obtained from the third by boring out the nozzle to provide a thinner wall thickness.

The first model is shown schematically in Fig. 2, together with the applied forces and moments to which it was subjected. The major dimensions are also shown. One end of the model was rigidly fixed, or "built-in," as shown, while external loads were applied to the free end of the cylinder and to the end of the nozzle. Three mutually perpendicular force components and three mutually perpendicular moment components were applied individually at each location. Thus, including internal pressure, there was a total of 13 loading cases. These loading cases were examined both experimentally and analytically, and the results were compared for each loading case.

Chapter 2 of this report describes the testing aspects of the experimental analysis and also the strain-gage data-acquisition and reduction techniques used. Representative experimental results, in the form of maximum measured stress distributions around the nozzle-cylinder junction, are presented for each loading. The finite-element analysis is discussed in Chapter 3. A brief description of the formulation used is given, and the specific element layout for the model is presented. Complete comparisons of theory and experiment are presented and discussed in Chapter 4 for all 13 loading cases. Chapter 5 contains a concise summary of the conclusions drawn from the study of this first thin-shell cylinder-to-cylinder configuration. For the benefit of the reader who might want to use the experimental data for comparisons with his own analyses, an appendix is included in which a complete set of experimental data is tabulated for each of the 13 loading cases.

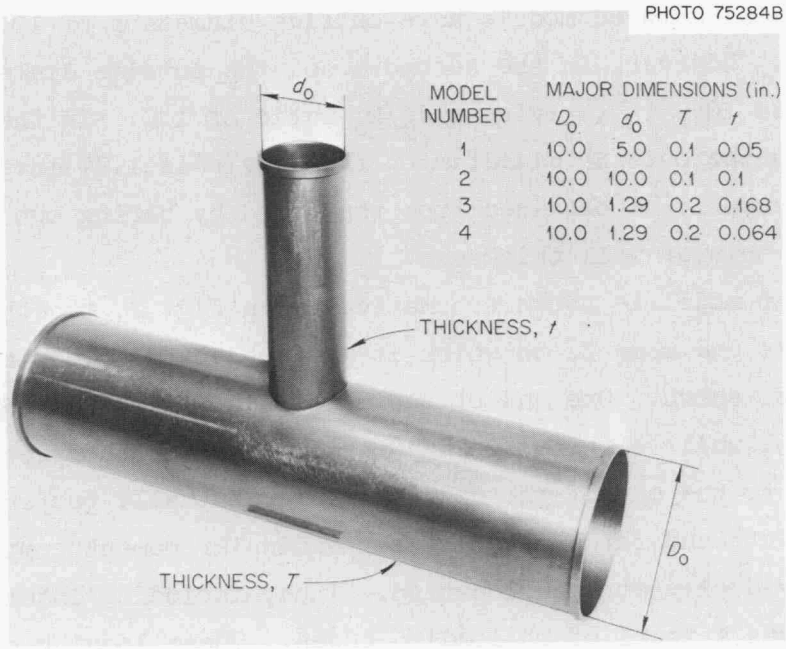

MODEL NUMBER	MAJOR DIMENSIONS (in.) D_o	d_o	T	t
1	10.0	5.0	0.1	0.05
2	10.0	10.0	0.1	0.1
3	10.0	1.29	0.2	0.168
4	10.0	1.29	0.2	0.064

Fig. 1. Thin-shell cylinder-to-cylinder model 1 and table showing dimensions of all four models in test series.

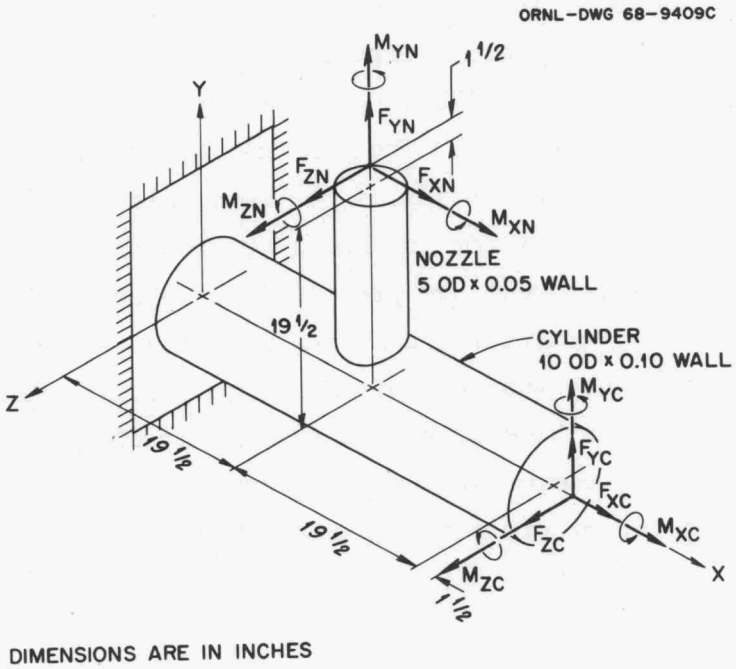

Fig. 2. Schematic of first model showing applied external loadings.

2. EXPERIMENTAL ANALYSIS

Experimental investigations of thin-shell cylinder-to-cylinder pressure vessel configurations have used both strain-gage metal models and photoelastic models. Strain-gage studies for internal pressure and for external nozzle loadings have been carried out by Hardenbergh, Zamrik, and Edmondson,[1] by Hardenbergh and Zamrik,[2] and by Riley.[3] In the first two studies, contoured and reinforced outlets were used, while in the third, the model was fabricated from hot rolled sheet steel by welding. Photoelastic studies have been carried out by Taylor and Lind[4] and by Leven.[5] In both cases, reinforced openings were examined. Thus, of the previous studies, only that of Riley[3] used a thin-shell idealized cylinder-to-cylinder metal model, and it was of welded construction rather than being carefully machined.

2.1 Model Construction

One of the primary objectives of the experimental analysis described in this report was to obtain experimental data on a carefully machined cylinder-to-cylinder model so that the effects of geometrical imperfections would be minimized. As will be discussed later, geometrical imperfections can play a very significant role in the behavior of thin shells; consequently, extreme care was used in making the first model.

The basic configuration was obtained by welding together two thick-walled carbon steel cylinders. The resulting weldment was then annealed, and the inside surfaces were machined to their final dimensions by boring. The structure was annealed a second time at this point. To maintain the correct dimensions during annealing, tight-fitting graphite mandrels were machined and inserted in both the nozzle and cylinder. These mandrels were used throughout the subsequent machining of the outer surfaces, which was done by turning on a lathe, milling, and finally by hand finishing in the immediate vicinity of the junction.

Despite the care used in machining the model, slight geometrical imperfections were inevitably present, and they did have a noticeable but relatively small effect on the experimentally determined stresses. In an

effort to reduce the magnitude of the geometrical imperfections even further, the remaining models in the series have been machined from solid, one-piece carbon steel forgings. After conventional machining to rough dimensions, the final surfaces were machined on a tracing-type milling machine using a carefully constructed mahogany wood pattern.

2.2 Strain-Gage Layout

The model was extensively instrumented with electrical resistance strain gages on both the outside and inside surfaces. A sufficient number of gages was used on this first model to provide a good description of the stress distributions for comparison with predictions and for identifying the high-stress regions. Subsequent models in the series of four will have fewer gages.

The strain-gage layout for the first model is shown in Fig. 3 on developed views of the nozzle and cylinder. A total of 322 three-gage strain-gage rosettes was used, making 966 individual strain gages. Half of these were on the outer surface, and half were on the inner surface. They were, in all cases, located "back to back" at the locations shown in the figure.

The gages were arranged in two opposite quadrants as shown, with each quadrant having four lines, or strings, of gages. On the nozzle these lines were spaced at 30° intervals and ran axially along the nozzle. On the cylinder, the gage lines were actually helical curves that were perpendicular to the junction line at the points where the nozzle gage lines intersected the junction line.

There were two principal reasons for gaging two opposite quadrants. First, for the majority of the 13 loadings the behavior in the two quadrants was expected to be different, and second, for loadings such as internal pressure, where the behavior should be identical, experimental data from two supposedly identical quadrants allow a check of the data and provide some indication of the effects of geometrical imperfections in the model.

The three-gage rosettes used were Micro-Measurements type EA-06-030YB-120, option SE, which is a very compact three-gage foil rosette.

The three individual gages are arranged in a "Y" pattern and have an individual gage length of 0.030 in. As can be seen in the inset in the upper right-hand corner of Fig. 3, five complete rosettes were located along each gage line within the first 5/8 in. from the junction. These first five rosettes were supplied mounted on a common backing by the gage manufacturer. These assemblies have the same designation as the single rosettes except that the option becomes B27. One of the five-rosette assemblies is shown in Fig. 4.

The rosettes were applied with an epoxy adhesive, BR-610, which is available from W. T. Bean, Inc. Curing times and temperatures ranged from 10 hr at 250°F to 24 hr at 200°F. Uninsulated 4-mil-diam wire was used to connect the gages to terminal tabs to which larger lead wires were connected. Bridge completion and dummy compensation were provided by similar gages mounted on unstressed pieces. One dummy gage was used for approximately 23 to 24 active gages. The strain-gage data were recorded by a Beckman-Dextir data-acquisition system (Sect. 2.4).

The model is shown in Fig. 5 with the strain gages applied but not completely wired. The four lines of gages in the fourth quadrant can be clearly seen. They are in the longitudinal plane at 0°, at 30° around from the longitudinal plane, at 60° around, and finally in the transverse plane at 90° around from the longitudinal plane. A close-up view of the rosettes in the junction region is shown in Fig. 6.

2.3 Test Description

Figure 7 shows the instrumented model in a loading frame being subjected to an in-plane moment loading on the nozzle. The right end of the cylinder was rigidly clamped to the heavy flat plate as shown. A split ring arrangement acting over the flange on the end of the cylinder (see Fig. 5) was used for this purpose. The loading fixtures on the other end of the cylinder and on the end of the nozzle were attached in a similar manner. These heavy fixtures in effect constrained the end circles of the shell to remain plane circles. The end fixtures were counterbalanced by weights attached to the cables (Fig. 7).

The external loads were applied by hydraulic rams acting through load cells, and the loads were controlled by the load cell indications. The pressure loading was applied using a hydraulic fluid. To avoid undue straining of the model, weights were used to counterbalance the weight of the pressurizing fluid in the model.

For all 13 loading cases, data were taken at 0, 20, 40, 60, 80, 100, 80, 60, 40, 20, and 0% of full load. The procedure was then repeated, so that two complete sets of data were taken for each gage for every loading.

Since the available data-acquisition equipment was limited to 250 channels, it was necessary to repeat the above procedure four times for each loading with approximately one-fourth of the 966 gages being monitored each time.

2.4 Data Acquisition and Reduction

The strain-gage data were recorded by a Beckman-Dextir automatic data-acquisition system. The system consists of a data-acquisition unit composed of a number of remotely located data-gathering boxes assigned to different experiments, a central data-processing unit, and a central data-recording unit. Each remotely located data-gathering box is capable of accepting 25 analog inputs and 25 user-related digital inputs from decimal switches or other contact-closure devices. The individual boxes are connected to the central processing and recording units by a party-line arrangement. This party line carries the control sequence signals to the data-gathering boxes and also carries the analog voltages and digital constants back to the data-processing unit.

Ten data-gathering boxes, or 250 analog channels, were available for the test of the first cylinder-to-cylinder model. These boxes were modified to provide bridge excitation and completion for the strain-gage circuits by the use of internal switching and external power supplies.

The low-level analog signals from the data-gathering boxes of the Beckman-Dextir system are transmitted to the central data processor, where they are amplified to ±5 V full scale. These amplified voltages are then digitized and passed on to the data-recording unit, where they are recorded on IBM-compatible magnetic tape and if desired printed on paper

tape. The user-related digital information from each data-gathering box is also recorded in the same format as the digitized analog information. Immediately after a complete data scan is taken, the user may recall, by means of a teletypewriter at the experiment, the data recorded from any single box in the group scanned.

The central data processor records the time of day to the nearest minute in four digits from a time-of-day clock and the day of the year from a day-of-year calendar. These data are recorded along with box number and channel number data.

Each data-gathering box may be scanned automatically at 5-, 15-, 30-, or 60-min intervals or on a continuous basis. Also a push-button switch on each box allows for one scan of the data entered through that box. The scanning rate within each box is eight channels per second. The system accuracy is stated to be ±0.07% of full scale, and the system repeatability, 0.04% of full scale.

All data from all experiments for a 24-hr period are recorded on a single magnetic tape. At the end of the 24-hr period the tape is sent to an IBM 360/75 computer, where the millivolt readings for each experiment are converted to engineering units (strains in this case). All data for that 24-hr period are then printed out for each experiment and returned to the experimenter. In addition, the data are recorded on a master tape for storage.

The experimental results presented later in this report, and tabulated in the Appendix, are generally based on the strain-gage readings at maximum load and on the first of the two sets of data taken from each gage and loading. If the first set of data was questionable for some reason, the second set was used. The strain-gage readings at fractional values of the maximum load were used to check linearity and drift of the gages. In those cases where nonlinearity or drift was excessive, or where an individual gage or circuit was otherwise obviously malfunctioning, the rosette of which the gage was a part was not used in the final results for the specific loading case under consideration. In some instances, a gage that behaved erratically during one loading behaved normally during others. Thus, in the final plots showing the experimental stresses,

results from a given rosette may be included for some loadings but not for others.

Stresses were calculated from the experimental strains by using a modulus of elasticity value of 30×10^6 psi and a Poisson's ratio of 0.3.

2.5 Variations of Maximum Measured Stresses Around Nozzle-Cylinder Junction

In all cases, the maximum measured stresses occurred at the junction between nozzle and cylinder. Consequently, in this section representative experimental results, in the form of maximum measured stress distributions around the nozzle-cylinder junction, are presented and discussed for each loading. Plots of all the experimental points along each gage line are presented in Chapter 4 for each loading and compared with theoretical predictions.

To examine the maximum stresses, stress ratios were considered. These ratios were determined by dividing the maximum absolute principal stress value at a point by a nominal membrane stress value. The membrane hoop stress in the cylinder, and nozzle, was used as the nominal stress level for the pressure loading. For the moment loadings on the nozzle, or cylinder, the maximum membrane bending stresses (computed by Mc/I) or the membrane shear stress (computed by Tc/J and equal to the maximum normal stress) in the nozzle, or cylinder, were used as the nominal stresses. For the axial forces on nozzle and cylinder, the axial membrane stress (calculated by P/A) was used. For the in-plane and out-of-plane forces on the nozzle, the nominal stress was somewhat arbitrarily chosen as the maximum bending stress in the nozzle (calculated by Mc/I) at the level of the top of the cylinder. Finally, for the in-plane and out-of-plane forces on the cylinder, the nominal stress was arbitrarily chosen as the maximum bending stress in the cylinder at its midlength (at the center line of the nozzle).

The applied loads used in the experimental analyses are given in Table 1, together with the nominal membrane stress levels calculated by the above procedures.

Table 1. Applied loads and nominal stress levels

Loading case	Load level	Nominal membrane stress (psi)
Internal pressure, p	50 psi	2475
Out-of-plane moment, M_{XN}	600 in.-lb	624
Torsional moment, M_{YN}	2000 in.-lb	1040
In-plane moment, M_{ZN}	2400 in.-lb	2495
In-plane force, F_{XN}	200 lb	3339
Axial force, F_{YN}	300 lb	386
Out-of-plane force, F_{ZN}	100 lb	1669
Torsional moment, M_{XC}	20,000 in.-lb	1300
Out-of-plane moment, M_{YC}	20,000 in.-lb	2600
In-plane moment, M_{ZC}	20,000 in.-lb	2600
Axial force, F_{XC}	5000 lb	1608
In-plane force, F_{YC}	2000 lb	5464
Out-of-plane force, F_{ZC}	1200 lb	3279

The variations in the experimentally determined maximum stresses around the junction between nozzle and cylinder are shown in Figs. 8 through 20 for each of the 13 individual loading cases. In each case, the stresses shown were determined from the strain-gage rosettes immediately adjacent to the junction, and of the four possible maximum stress distributions — cylinder inside and outside and nozzle inside and outside — those shown produced the largest stresses in each case.

The points labeled "extrapolated maximum" in the figures are estimated maximum stress ratios at the junction obtained by extrapolating the experimentally determined principal stress distributions along each gage line to the peak stresses at the junction. It should be emphasized that the maximum stress estimates are based on a consideration of the stresses along gage lines only; this does not preclude the existence of slightly higher ratios at locations between gage lines. The maximum stress ratios and the locations of the maximum stresses based on both the experimental

analysis and the finite-element analysis are tabulated and compared in Chapter 5.

Figures 8 through 20 indicate that, in general, the maximum measured stresses varied in a reasonably smooth and consistent manner around the nozzle-cylinder junction. It is particularly significant to note that only for the internal pressure case did the maximum stress occur in the longitudinal plane of symmetry. For all other loadings the maximum occurred in the transverse plane of symmetry or at an intermediate position between the two planes of symmetry.

The consistency of the experimental data and perhaps some assessment of the geometrical consistency of the model can be obtained by examining the results for those loading cases where symmetry existed. For internal pressure (Fig. 8), the torsional moment on the cylinder (Fig. 15), the in-plane moment on the cylinder (Fig. 17), and the axial force on the cylinder (Fig. 18), the results in the two quadrants would be expected to be equal. A comparison for these cases indicates good agreement except for internal pressure. The variations there will be discussed further in Chapter 4. Some other loadings, such as the in-plane moment on the nozzle (Fig. 11), the in-plane force on the nozzle (Fig. 12), the axial force on the nozzle (Fig. 13), and the in-plane force on the cylinder (Fig. 19), should exhibit longitudinal symmetry (the same maximum stress ratios at 90 and 270°). For these cases the agreement in the transverse plane is generally good. Thus, in general, the plots of maximum stress ratios around the nozzle-cylinder junction illustrate that reliable and consistent data were obtained from this carefully prepared model.

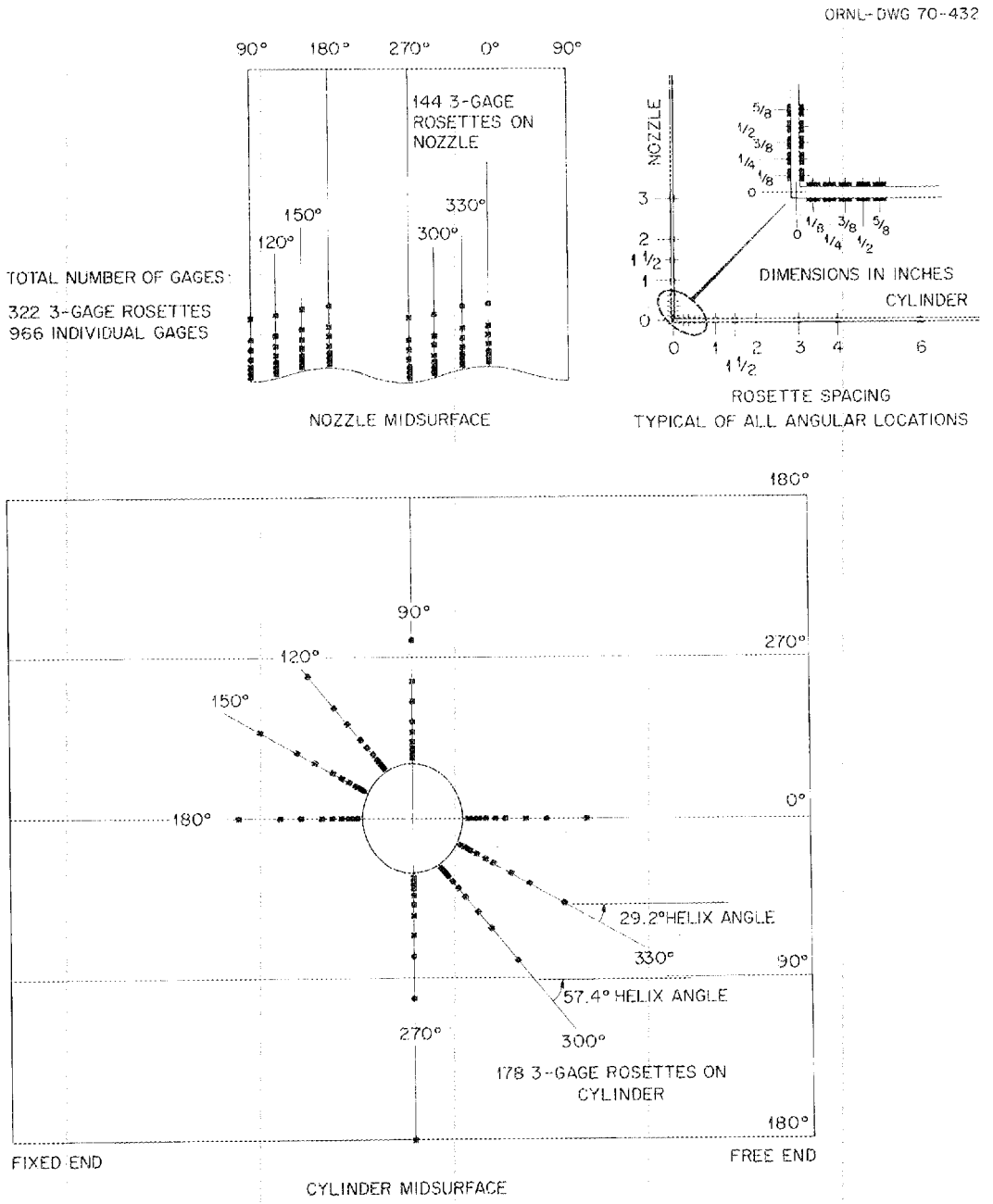

Fig. 3. Strain-gage layout.

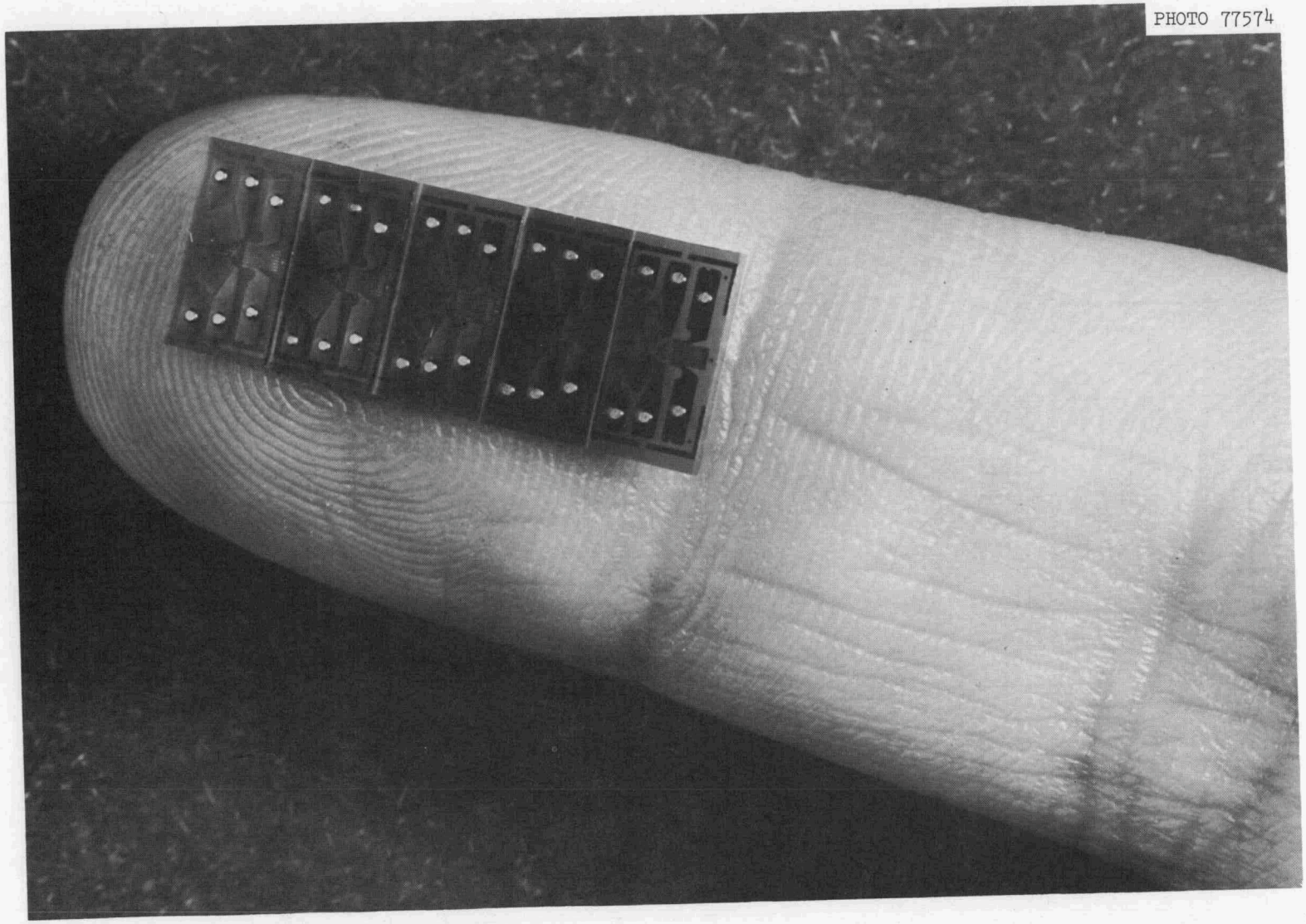

Fig. 4. Closeup of assembly of five strain-gage rosettes on a common foil backing.

PHOTO 76683

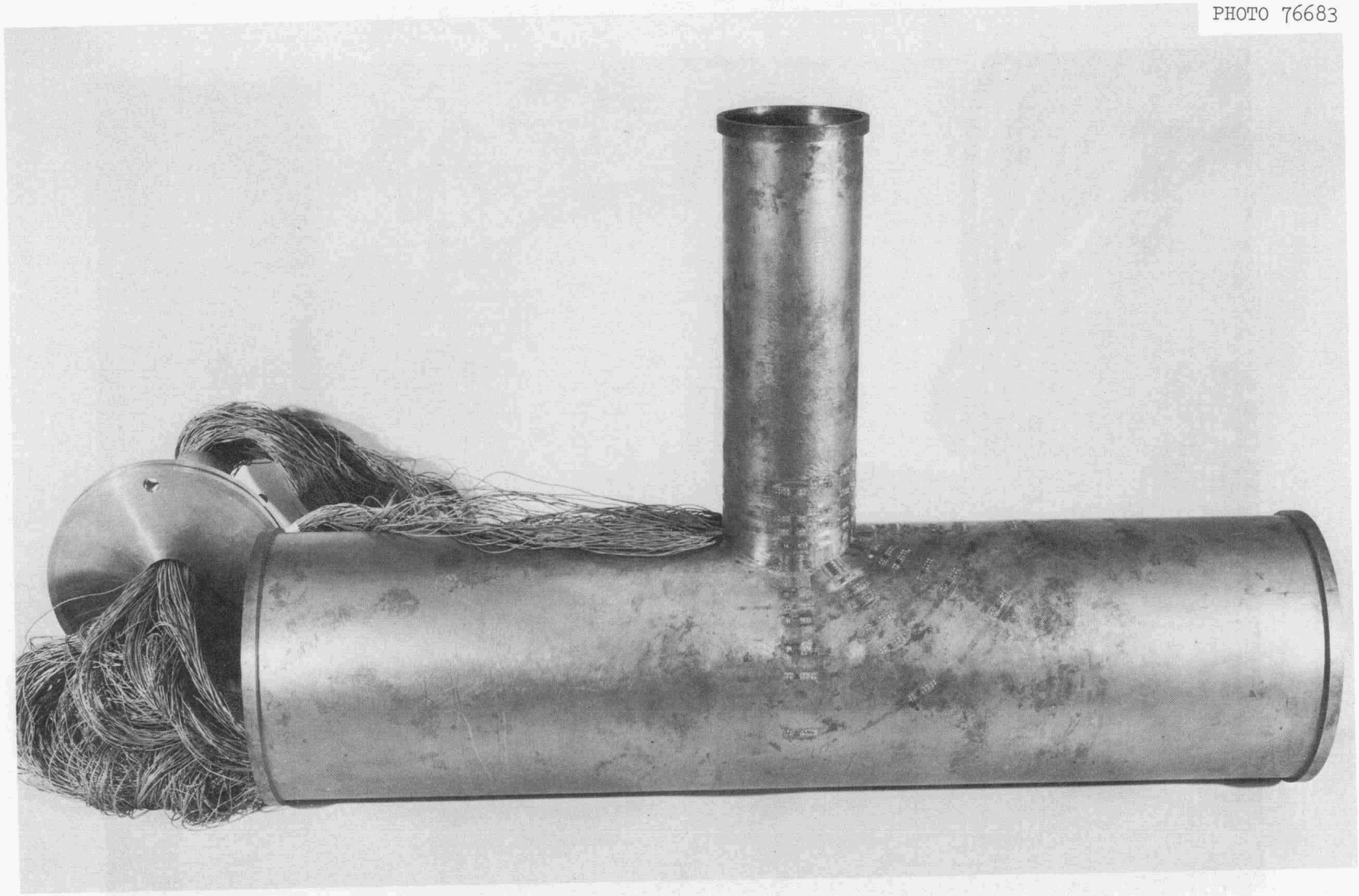

Fig. 5. Model during instrumentation.

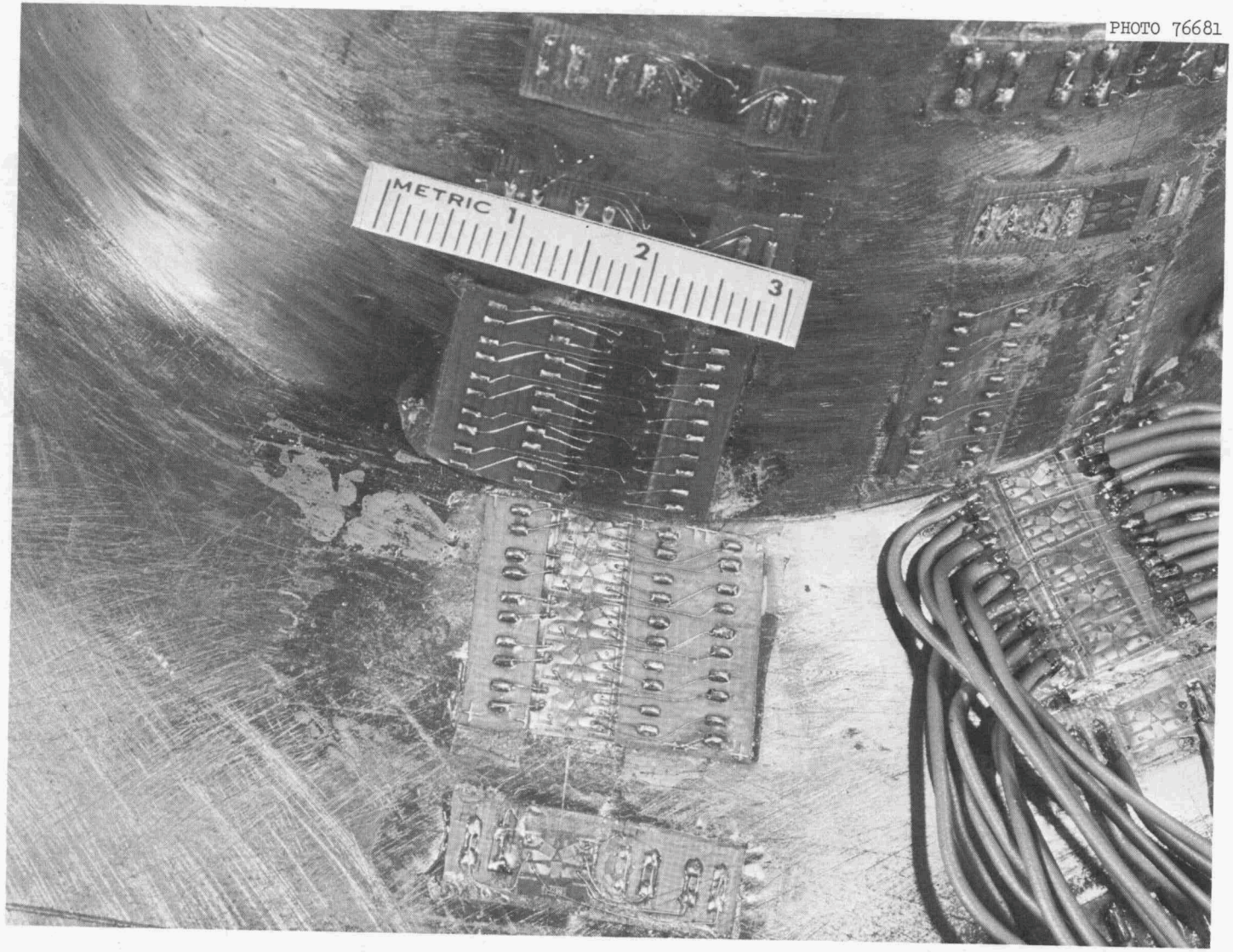

Fig. 6. Closeup of gages in junction region.

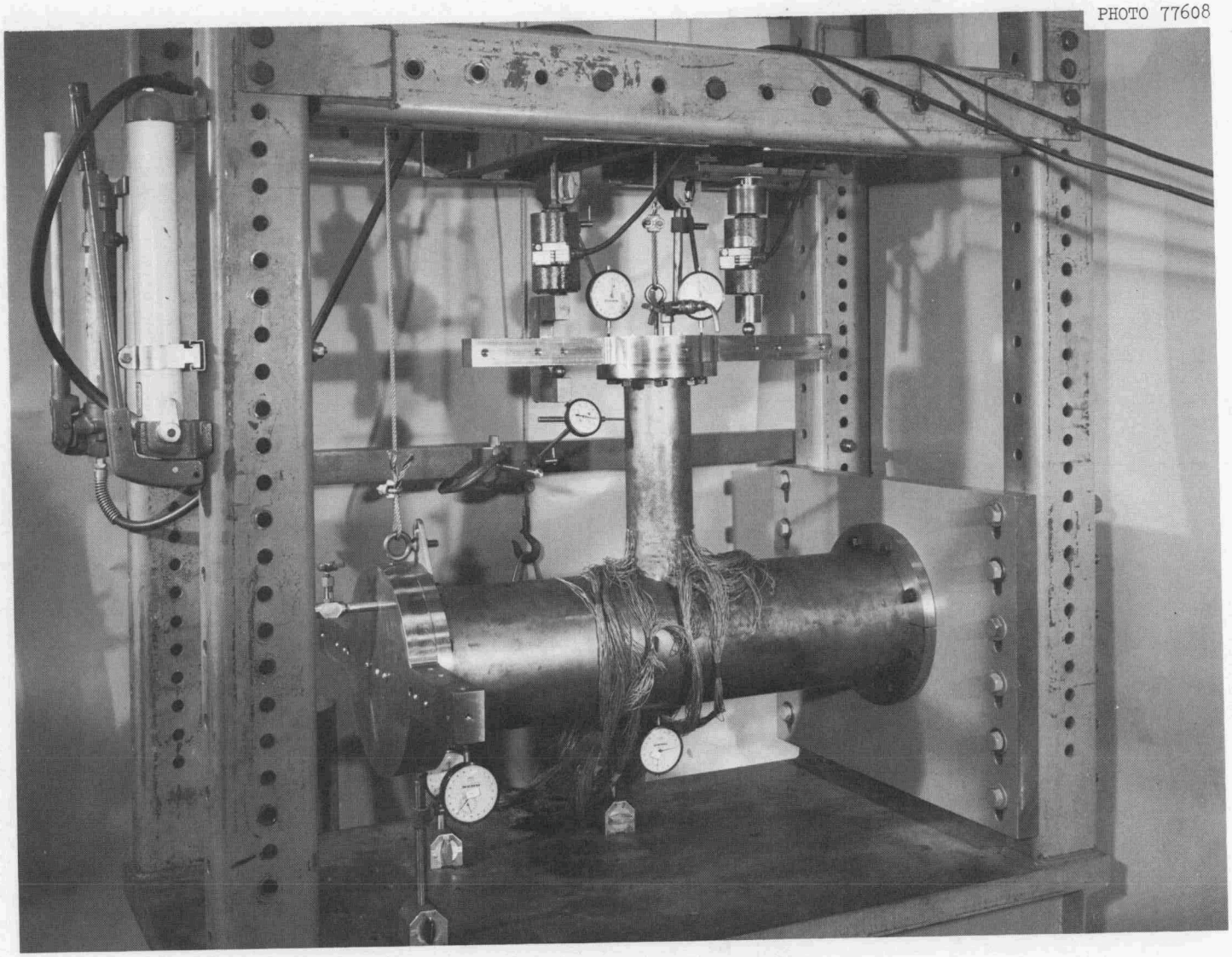

Fig. 7. Instrumented model in test frame being subjected to an in-plane moment loading on the nozzle.

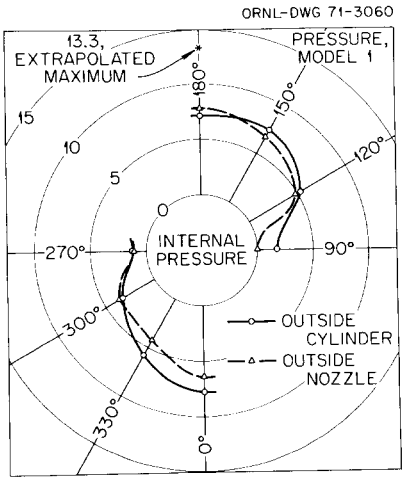

Fig. 8. Variation of maximum principal stress ratios around nozzle-cylinder junction for internal pressure.

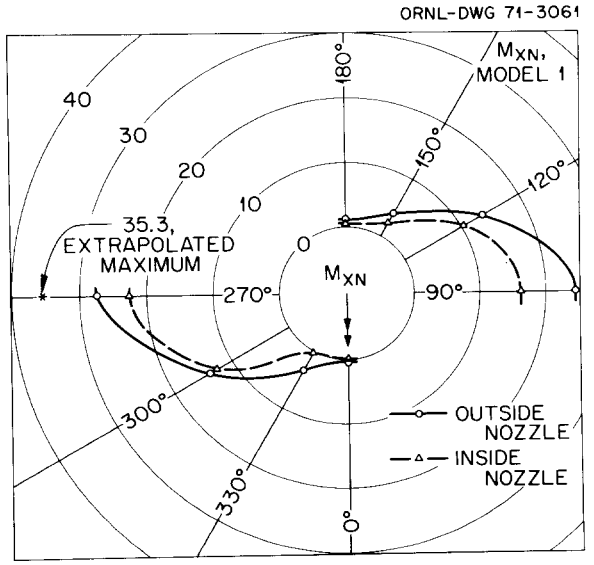

Fig. 9. Variation of maximum principal stress ratios around nozzle-cylinder junction for out-of-plane moment, M_{XN}, on nozzle.

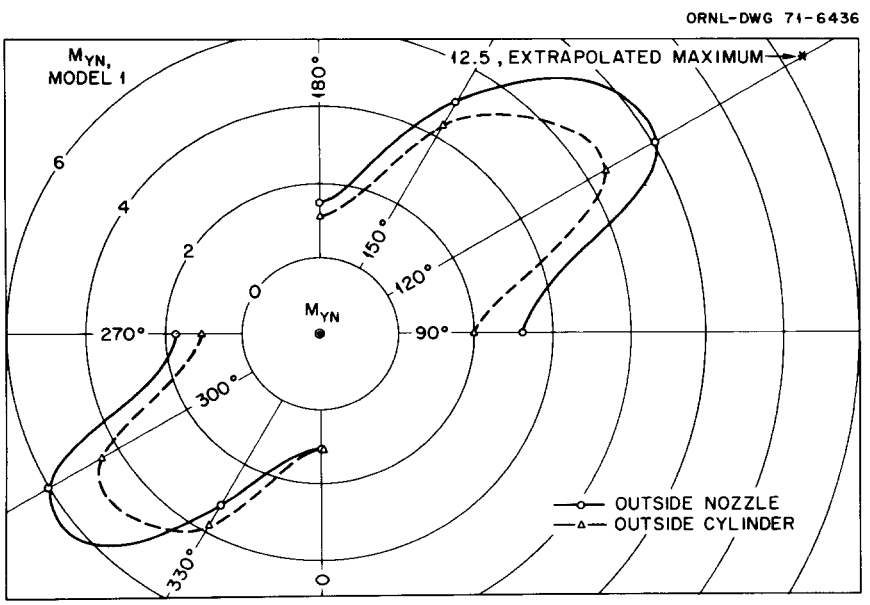

Fig. 10. Variation of maximum principal stress ratios around nozzle-cylinder junction for torsional moment, M_{YN}, on nozzle.

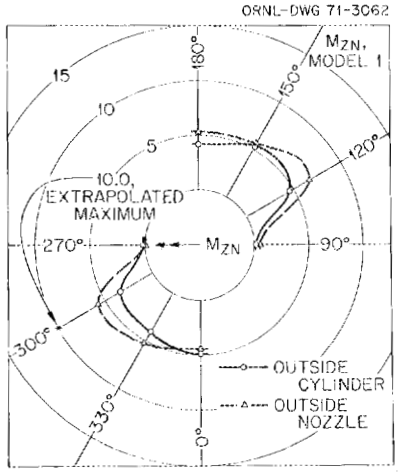

Fig. 11. Variation of maximum principal stress ratios around nozzle-cylinder junction for in-plane moment, M_{ZN}, on nozzle.

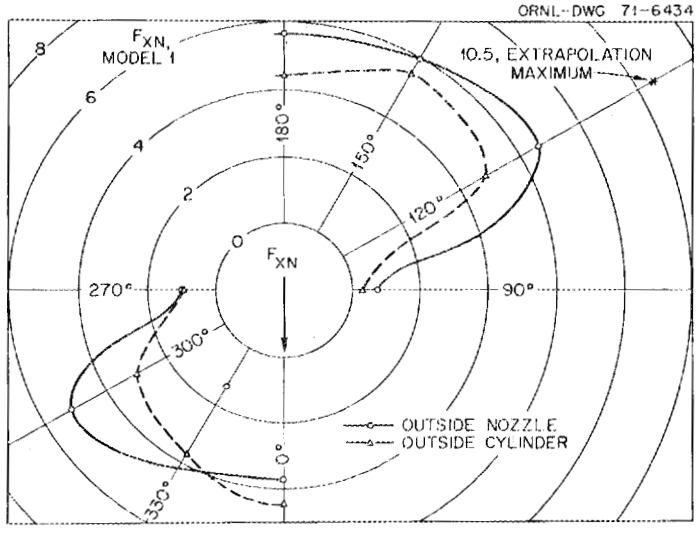

Fig. 12. Variation of maximum principal stress ratios around nozzle-cylinder junction for in-plane force, F_{XN}, on nozzle.

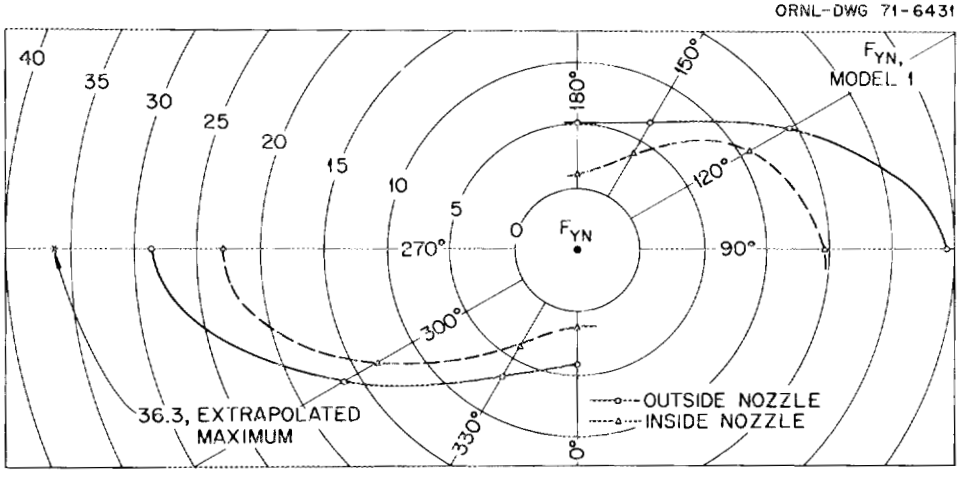

Fig. 13. Variation of maximum principal stress ratios around nozzle-cylinder junction for axial force, F_{YN}, on nozzle.

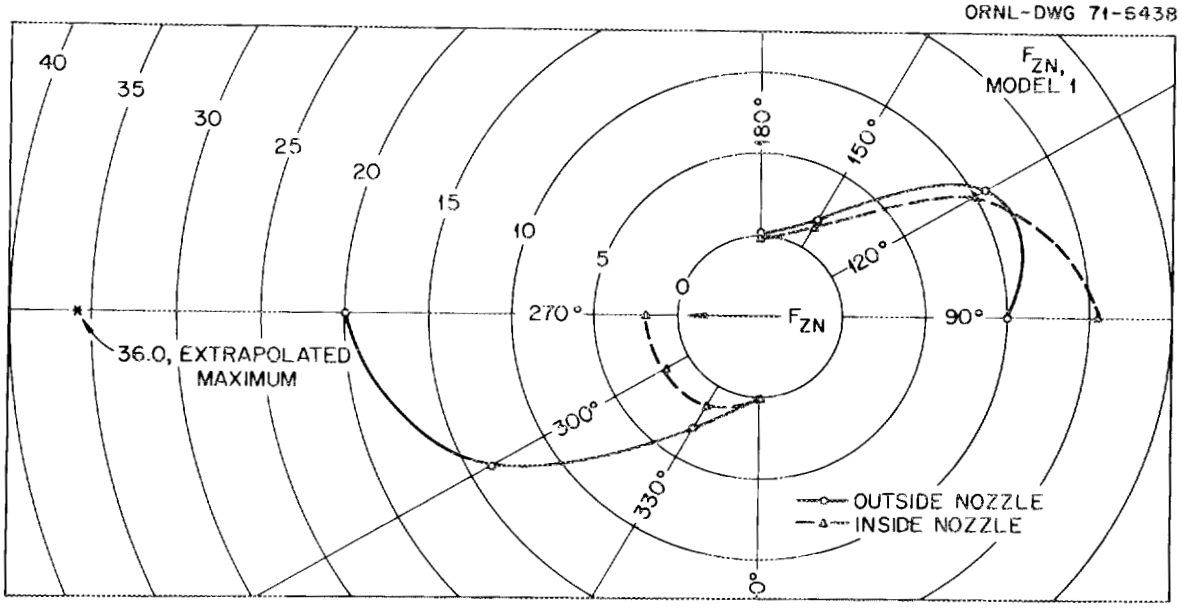

Fig. 14. Variation of maximum principal stress ratios around nozzle-cylinder junction for out-of-plane force, F_{ZN}, on nozzle.

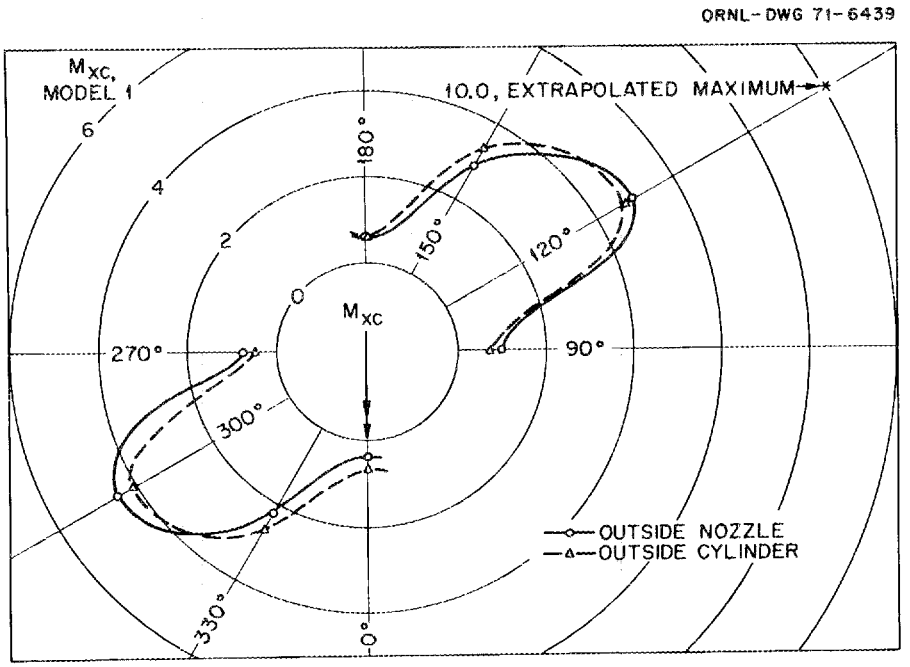

Fig. 15. Variation of maximum principal stress ratios around nozzle-cylinder junction for torsional moment, M_{XC}, on cylinder.

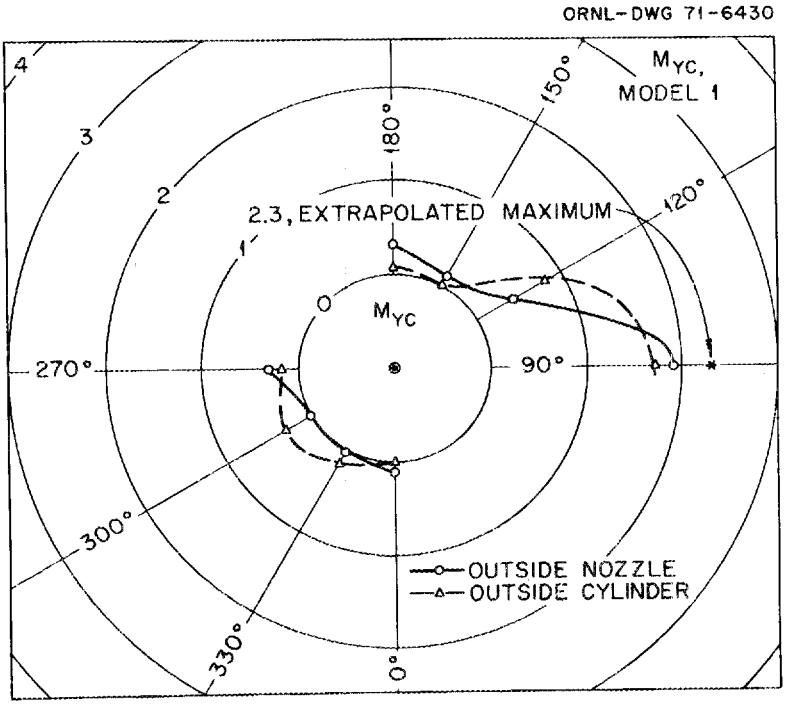

Fig. 16. Variation of maximum principal stress ratios around nozzle-cylinder junction for out-of-plane moment, M_{YC}, on cylinder.

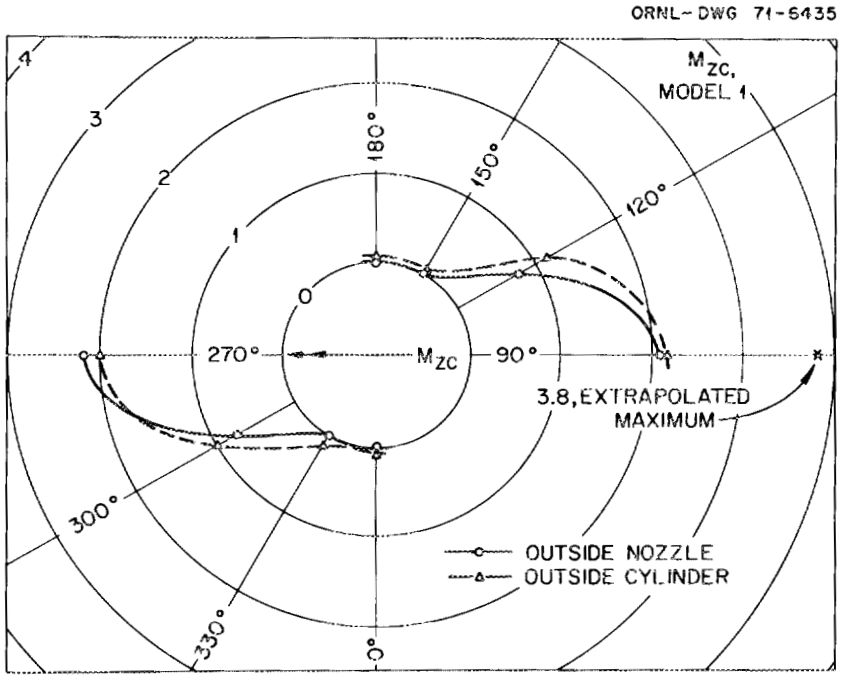

Fig. 17. Variation of maximum principal stress ratios around nozzle-cylinder junction for in-plane moment, M_{ZC}, on cylinder.

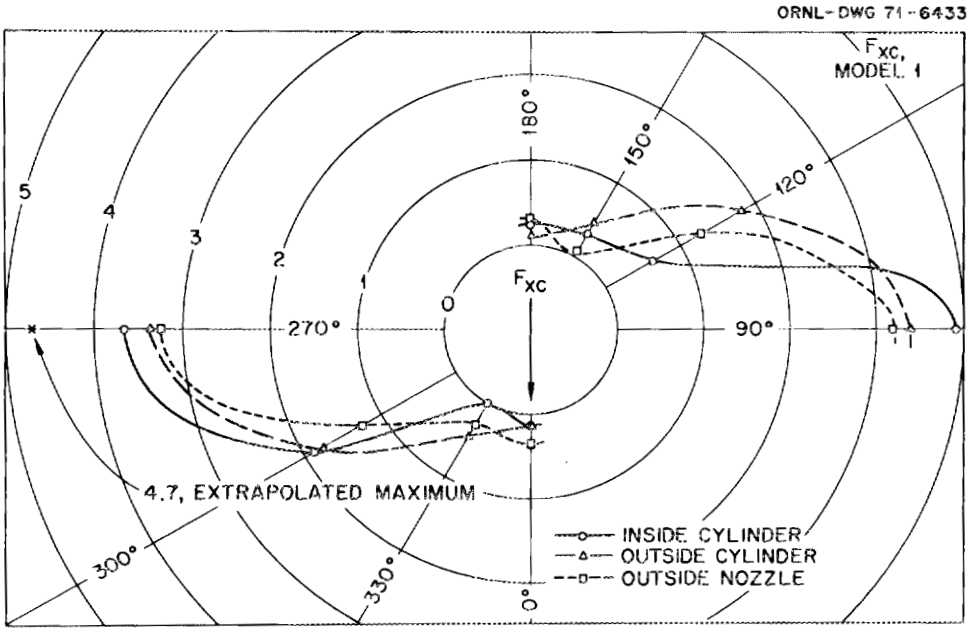

Fig. 18. Variation of maximum principal stress ratios around nozzle-cylinder junction for axial force, F_{XC}, on cylinder.

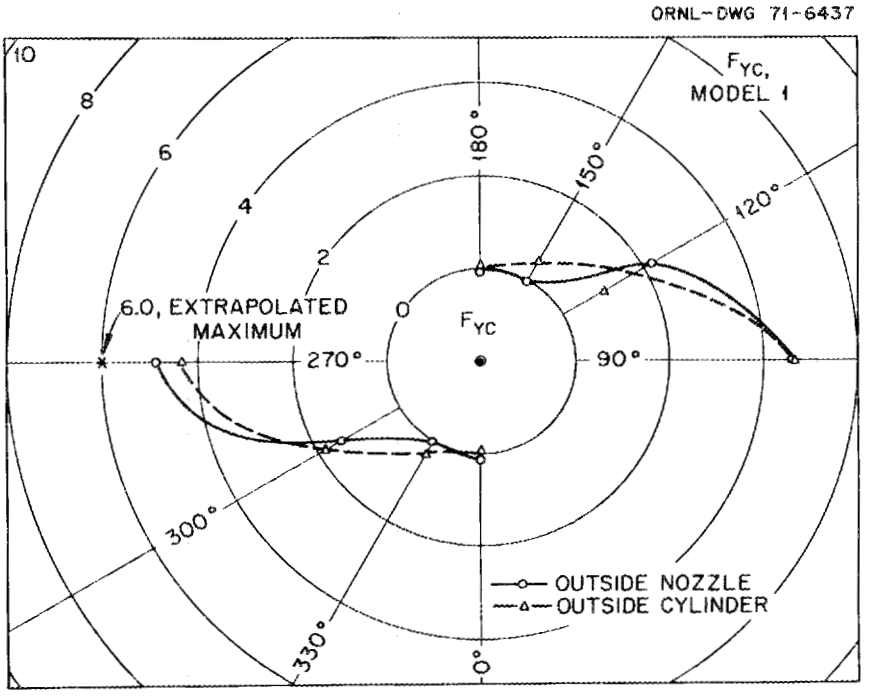

Fig. 19. Variation of maximum principal stress ratios around nozzle-cylinder junction for in-plane force, F_{YC}, on cylinder.

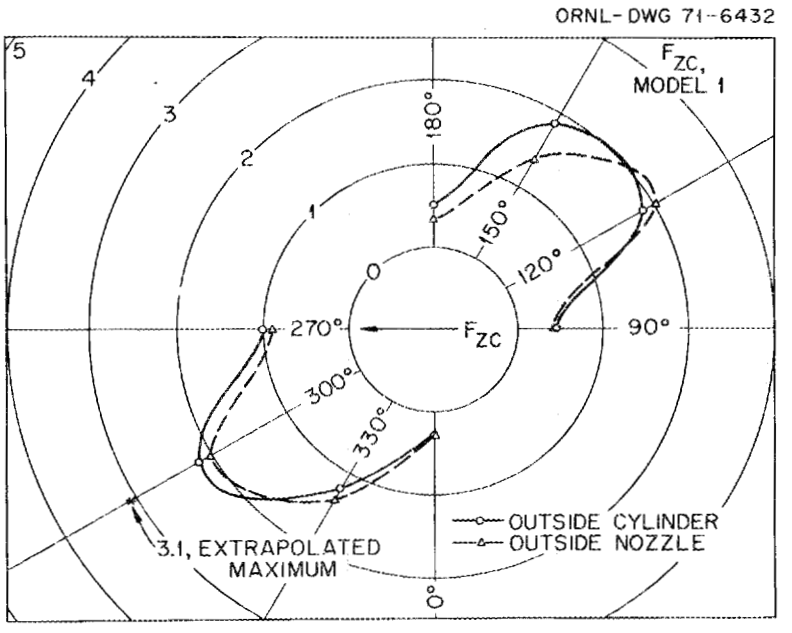

Fig. 20. Variation of maximum principal stress ratios around nozzle-cylinder junction for out-of-plane force, F_{ZC}, on cylinder.

3. FINITE-ELEMENT ANALYSIS

3.1 Background

Thin-shell cylinder-to-cylinder intersection problems have, in recent years, been a favorite with the stress analyst. Their popularity stems not only from the common occurrence of such configurations in practical design, but also from the challenge that they present as a complex shell analysis problem. In addition to their use in piping and pressure vessel configurations, thin-shell cylinder-to-cylinder intersections occur in the petroleum industry, which uses tubular structural members extensively in off-shore oil-drilling towers. Much of the cylinder-to-cylinder intersection research, both experimental and theoretical, that has been done was motivated by the off-shore oil-drilling tower application. The literature associated with the latter application is reviewed in Ref. 6.

Both analytical and numerical analyses have been developed and applied to thin-shell cylinder-to-cylinder intersection problems. Reidelbach,[7] in 1961, developed the first analytical solution for two perpendicularly intersecting cylindrical shells subjected to internal pressure. Eringen[8-11] and his co-workers corrected some errors and approximations in Reidelbach's solutions and formulated a solution in which the intersection curve was approximated by a circle. These solutions consisted of products of Krylov functions and Hankel functions of the first kind. A collocation method was used whereby the boundary conditions were satisfied in a least-squares sense at selected boundary points.

Hansberry and Jones,[12] in 1969, used the method developed by Reidelbach and Eringen et al. to develop a solution for an in-plane bending moment applied to the nozzle of a nozzle-to-cylinder configuration. In 1970, Maye and Eringen[13] developed a solution using Fourier series involving Bessel functions in place of the Krylov functions. As in the case of the earlier solutions, however, the nozzle diameter was limited relative to the cylinder diameter.

In 1967, Bijlaard, Dohrmann, and Wang[14] formulated the problem to include the case where the nozzle and cylinder are of equal diameter.

They indicated a solution in the form given by Flügge for closed cylindrical shells. In 1969, Pan[15] developed a numerical solution to the differential equations of Flügge and Donnell that is applicable to the equal-diameter case. He compared his predictions with the experimental results obtained by Riley[3] for a nozzle-diameter/cylinder-diameter ratio of 1/2. By careful choice of some of the factors used in the solution, he obtained predictions that agreed reasonably well with experiment.

Herrmann and Campbell,[16] in 1968, presented a finite-element shell analysis formulation using flat-plate elements, and as a sample problem they used the 1/2 diameter ratio model tested by Riley.[3] The limited comparisons shown were for internal pressure and indicated reasonably good agreement between theory and experiment. In 1969, Prince and Rashid[17] also presented a flat-plate finite-element shell analysis and used the cylinder-to-cylinder intersection as a sample problem. Their shell analysis program was developed under subcontract to Oak Ridge National Laboratory as a part of the ORNL Prestressed Concrete Reactor Vessel Program. Consequently, the ORNL model described herein was used as their sample problem, and the predictions were compared with preliminary internal pressure results provided by ORNL. The agreement between theory and experiment was reasonably good for the comparisons shown.

3.2 Finite-Element Method

The basic concept of the finite-element method is the idealization of the original structure as an assemblage of discrete structural elements and then assuming some simplified functional representation of displacement behavior for the individual elements. This has proven to be a particularly illusive task for curved-shell structures, and no completely satisfactory formulation exists. Gallagher[18] has recently presented a survey of developments in the finite-element analysis of flat-plate and curved-shell structures, and he concludes that more work is needed in this general area before firm conclusions can be drawn.

Both flat-plate and curved-shell elements have been used for curved-shell structures. These two types of elements are illustrated schematically in Fig. 21. Flat-plate elements have obvious shortcomings. There

is a geometric discretization involved in their use because the true curved surface is represented by a faceted surface. Thus, when flat-plate elements are used for curved-shell structures, two types of approximations are introduced. First, the shell that is actually analyzed differs slightly from the true shell, and second, the stiffness properties of the individual elements are derived on the basis of an assumed set of displacement patterns within the elements; thus constraints are imposed on the manner of deformation of the shell. The errors associated with both types of approximation tend to diminish with reduced mesh sizes in the finite-element idealization.

Curved-shell elements, on the other hand, eliminate the geometric approximation because they can correctly represent the curved-shell surface; however, they are difficult to formulate mathematically. Formulations do exist, but the entire area of curved-shell elements is in a relatively early stage of development, and there are insufficient available numerical comparison data.[18]

Consequently, flat-plate elements have been most widely used in shell analyses to date. The analysis used for this first cylinder-to-cylinder model uses flat-plate elements and was chosen as being representative of currently available and widely used finite-element shell formulations. The program was developed at the University of California, Berkeley, under the direction of Professor R. W. Clough. The original program was written for general shell analysis by Johnson[19,20] and was later modified and adopted by Greste[6,21] for treating the "K" joints of cylindrical shells found in off-shore oil-drilling towers.

The basic elements used in the program are shown in Fig. 22. The elements are nonplanar quadrilaterals that are built up of an assemblage of four component triangles as shown. Within each component triangle, the in-plane displacements u and v are assumed to vary quadratically over the plane of the triangle except that they are constrained to vary linearly along the one exterior edge. The resulting membrane element is referred to as a constrained linear strain triangle (CLST), and it has two degrees of freedom (u and v) at each of the five nodes.

The plate bending portion of the component triangle elements has three degrees of freedom at each of the three corner nodes — two rotations

about axes in the plane of the element and the transverse, or normal, displacement w. The displacement expansion for this element is due to Hsieh, Clough, and Tocher,[22] and the element is referred to as the HCT triangle. Full compatibility of displacements and slopes between triangular element boundaries is achieved by dividing the element into three subtriangles and assuming an independent cubic variation for w within each subtriangle. One of the ten terms of the general cubic is neglected in each subtriangle, so that in the final assembled component triangle the normal slope varies linearly along each exterior edge. It is this feature that ensures slope compatibility in the resulting element system for plate bending problems. The 27 constants in the three cubic expressions for w within the triangular element are reduced to 9 (and related to the 9 nodal degrees of freedom) by internal compatibility considerations. With w varying as a cubic polynomial within each subtriangle, the three components of curvature, and hence the bending and twisting moments, vary linearly.

The total stiffness (membrane plus bending) of the triangular elements that form the components of the quadrilateral is obtained by superposition of the plate bending element and the membrane element. The membrane plus bending stresses vary piecewise linearly over the surface of the resulting triangular element.

The quadrilateral element stiffness is obtained from that of the four component triangles. In general, due to the curvature of the shell that is being discretized, an arbitrary quadrilateral will be nonplanar. This introduces a complication in the transformation of the triangular element stiffness because on the element level only two bending rotations per node are defined. When transformed from the element coordinates to some other coordinate system, a third bending rotation quantity is introduced, and in the transformed system three rotational degrees of freedom should be considered at each node. This consideration regarding the third rotational degree of freedom also arises in the subsequent assembly of the quadrilateral elements into the total structural stiffness, since adjacent elements are in general not coplanar. In his formulation, Johnson[19] chose to retain only two rotations per node in the total element assemblage. He argued that since the element plane in a sufficiently fine

mesh lies close to the shell tangent plane at each node, the rotations could be transformed from the element coordinates (in the plane of the element) to coordinates in the shell tangent plane and the small transformed component of bending rotation about the normal to the shell could be neglected. This is perhaps a reasonable assumption everywhere except at the junction of intersecting shells, as will be discussed later.

The stiffness formulation for the quadrilateral element, as well as for the CLST membrane element and the HCT plate bending element, is summarized by Greste.[6] The quadrilateral element has five degrees of freedom at each node: u, v, w, and the two rotations. In the final assembled structure the five degrees of freedom per node are u, v, w, and the two rotations about the shell tangent coordinates at each node.

The task of the finite-element method is to determine the unknown coefficients of the assumed element displacement functions for u, v, and w. This is done by connecting the quadrilateral elements together at discrete points, the corner nodes, and requiring compatibility of displacements and rotations and equilibrium of forces and moments at these nodes. Unfortunately, when the elements are assembled into a curved-shell structure, compatibility and equilibrium are not completely achieved along the element interfaces. Thus there are inherent small errors involved. Studies by Johnson[19] have shown, however, that these errors are not too significant provided a sufficiently fine element mesh is used.

There is an error in intersecting shell problems, however, which is not diminished by mesh refinement. This error arises from the aforementioned neglect of the rotation about the shell normal. At the junction nodes in the cylinder-to-cylinder intersection problem, there are three nonzero rotational components, but only two of these can be retained as nodal degrees of freedom. Greste[6] chose to define the tangent plane, and hence the two rotational degrees of freedom, at the junction nodes as the cylinder tangent plane. The manner in which he treated the junction nodes thus constrained the normal rotation about the cylindrical shell normal to be zero at the junction. This rotational constraint unrealistically constrains the bending deformation of the adjacent nozzle elements.

The most severe case of this situation is illustrated in Fig. 23. In this case, the rotation of the nozzle elements (adjacent to node A)

about the normal to the cylinder at A is completely constrained. Thus, if in the actual structure the nozzle deforms into the shape shown, the constraint on the idealized structure prevents the rotation θ at A. Greste considered two factors in estimating the magnitude of the constrained rotation and its effects: rigid body displacements and membrane deformations in the cylinder. Because of the relatively small length-to-diameter ratios that are generally considered for the cylinder, Greste reasoned that the rigid body displacements which produce rotations of the type shown in Fig. 23 are small compared with the bending rotations associated with straining of the structure. Therefore, essentially all of the rotation of the type in Fig. 23 can be assumed to be produced by the membrane deformations of the cylinder wall. Greste then further reasoned that in oil-drilling towers the membrane stiffness of the cylinder is very large and the circumferential bending stiffness of the nozzle, or branch as he calls it, is relatively small. Thus the cylinder normal rotations when applied as circumferential bending rotations to the nozzle would be expected to generate only small forces and moments in the nozzle wall. That is, if the rotation θ of Fig. 23 were allowed to take place in the nozzle wall, relatively small additional stresses would be generated.

This argument may be valid for structural joints in off-shore oil-drilling towers, but it does not necessarily remain so for pressure vessel and piping cylinder-to-cylinder configurations in which nozzle and cylinder may be nearly equivalent in stiffness. For these configurations there is, unfortunately, little justification for choosing the cylinder tangent plane as the reference plane for junction nodes. A better choice might have been some average or mean tangent plane at junction nodes giving partial bending constraint to both nozzle and cylinder. Johnson[19] used this latter approach to analyze a folded-plate structure and found that the results agreed well with an elasticity solution.

In conclusion, the error introduced in the junction region by the neglect of the sixth degree of freedom at the junction nodes and by the associated constraint on the bending deformations of the elements adjacent to those nodes is not believed to be a large factor, but it is

present and it is not reduced by mesh refinement. This error will be discussed in Chapter 4, where the theoretical predictions are compared with the experimentally determined stress distributions.

3.3 Finite-Element Idealization of Model

The finite-element representation chosen for the model is depicted in Fig. 24, which shows developed views of one-half of the nozzle, cylinder, and end plates. It was necessary to consider only one-half of the structure because of symmetry considerations. This mesh layout was developed manually and was arranged so that lines of nodes corresponded to the lines of strain gages in the experimental model. There were 649 nodes, resulting in approximately 3000 linear algebraic simultaneous equations to be solved for the unknown displacement parameters. There were 25 nodes along the (half) junction line between nozzle and cylinder. All 13 loading cases considered experimentally were analyzed using this mesh, and the theoretical predictions were compared with the experimentally determined stresses and are given in Chapter 4.

Seven of the 13 loadings — pressure, axial forces on cylinder and nozzle, and in-plane moments and forces on cylinder and nozzle — produce behavior that is theoretically symmetric about the longitudinal plane of symmetry of the model. For these symmetric loadings, it is correct to consider just one-half of the model in the finite-element representation. The boundary conditions on nodal displacements and rotations are those commonly associated with symmetry conditions.

For the remaining six loadings — out-of-plane moments and forces on cylinder and nozzle and torsional moments on cylinder and nozzle — asymmetric conditions exist, and to consider just one-half of the model in the finite-element representation requires assumptions, or approximations, in establishing nodal displacement and rotational boundary conditions. Basically, the boundary conditions used were based on the assumption that the projection on the X-Y plane (see Fig. 2) of the boundary remained fixed in the X-Y plane. In other words, the displacements in the X and Y directions and the rotation about the Z axis were assumed to be zero for the nodes along the boundary in the X-Y plane. Although these conditions

are obviously not strictly correct, they nonetheless seem to be reasonable assumptions that are useful for reducing the size of the problem to be solved.

To investigate the effects of mesh fineness and to verify that the mesh in Fig. 24 was sufficiently fine, analyses were performed on the model using two additional mesh layouts, one coarse and one extra fine. The coarse mesh had the same general arrangement as shown in Fig. 24, but only 219 nodes were used, which resulted in approximately 1000 simultaneous equations. There were only 13 nodes along the (half) junction line between nozzle and cylinder. All 13 loading cases were examined with the coarse mesh.

For the extra-fine mesh layout only one-quarter of the model was considered, and because of the restrictions imposed by the resulting symmetry considerations, only an internal pressure loading was examined. An expanded version of the original University of California program was used, so that it was possible to quadruple the number of elements. Again, the same general arrangement as in Fig. 24 was used. There were 1199 nodes, with 25 nodes being located along the (quarter) junction between nozzle and cylinder.

The results of these coarse and extra-fine mesh analyses can be briefly summarized as follows. The coarse mesh predictions were completely inadequate, while the extra-fine mesh predictions demonstrated no consistent improvement over the predictions based on the fine mesh of Fig. 24. It was concluded therefore that the degree of mesh refinement was sufficient, in the fine-mesh layout, to adequately represent the cylinder-to-cylinder model.

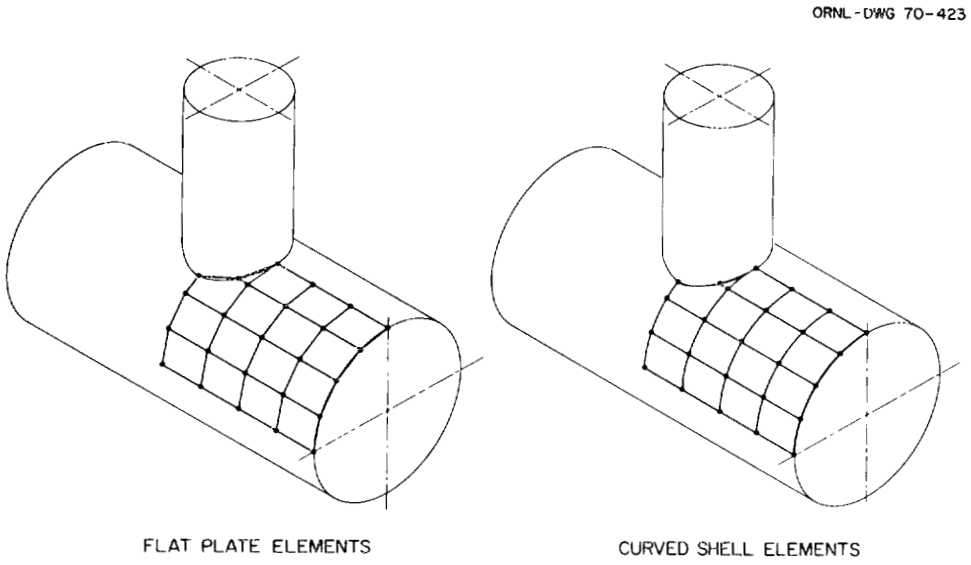

Fig. 21. Flat-plate and curved-shell finite-element idealizations.

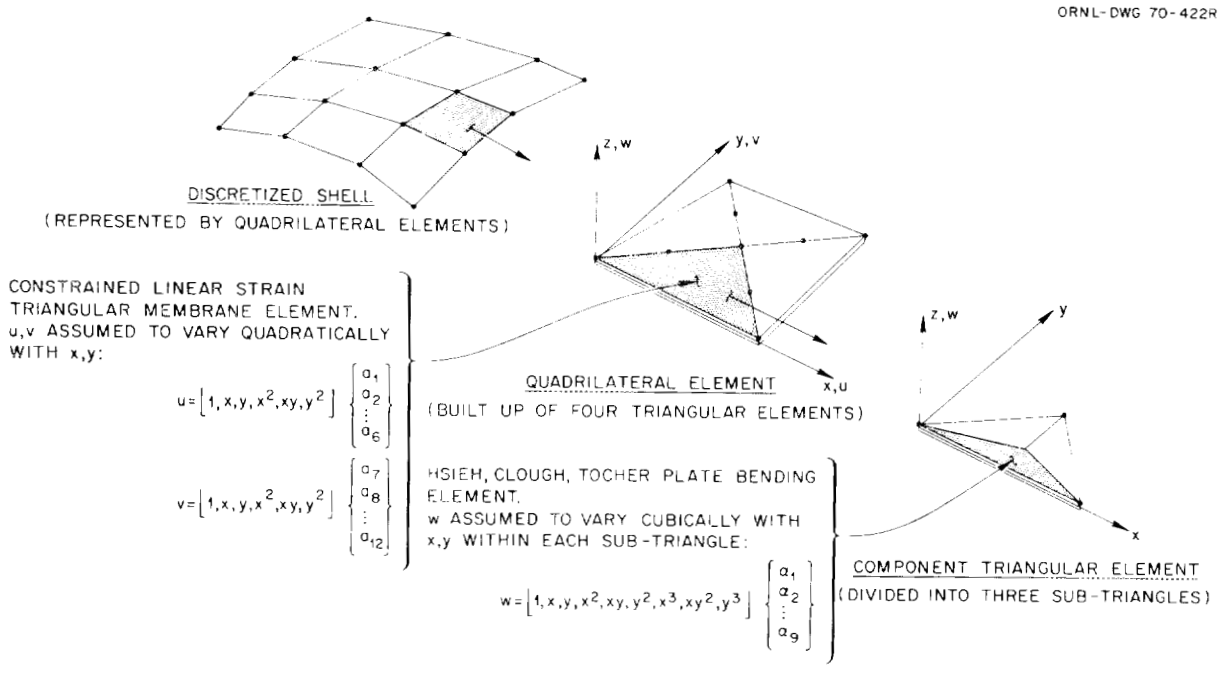

Fig. 22. Quadrilateral element and component triangles.

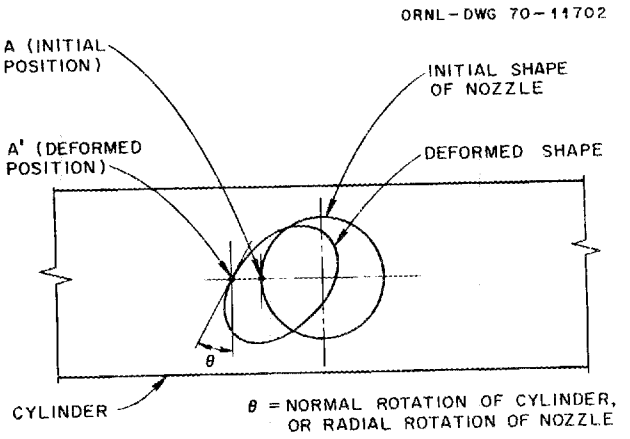

Fig. 23. Constraint at junction nodes.

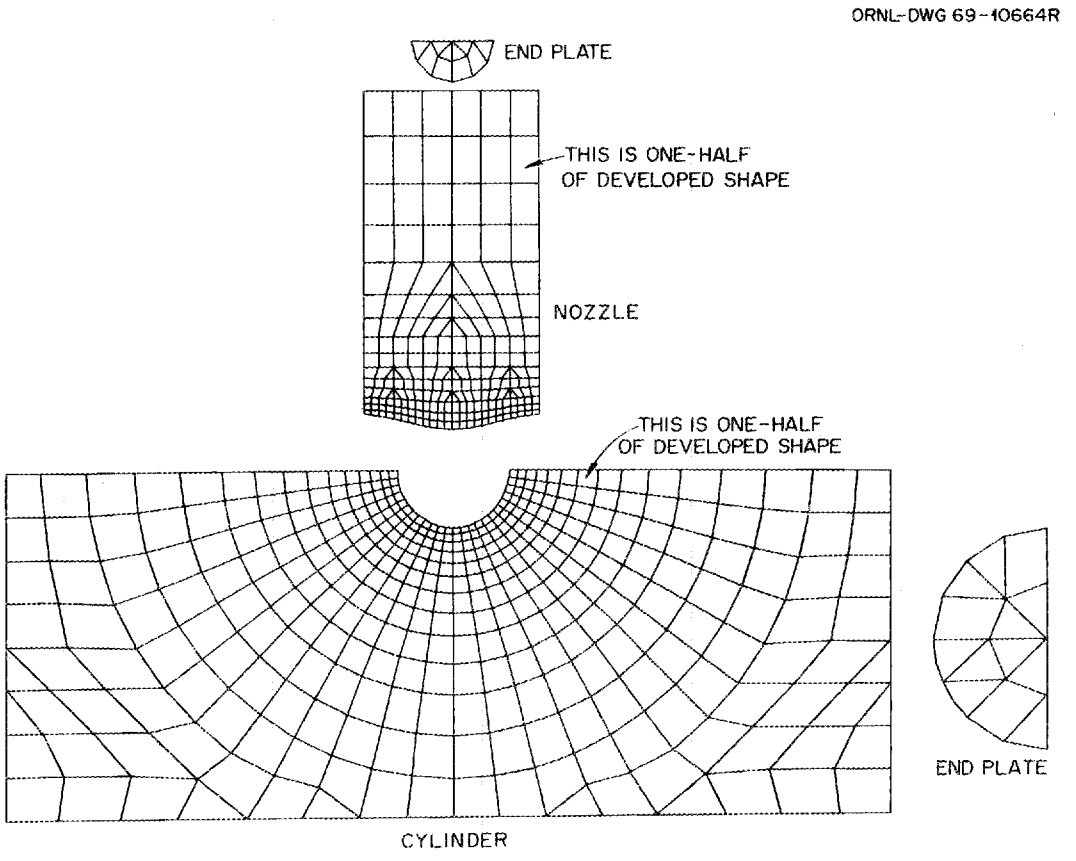

Fig. 24. Finite-element idealization of model.

4. COMPARISON OF THEORY AND EXPERIMENT

The theoretical predictions, based on the fine-mesh element layout shown in Fig. 24, are compared in this chapter with experimentally determined stress distributions for all 13 loading cases. For each loading, the theoretical and experimental stress distributions along the eight gage lines on cylinder and nozzle (see Fig. 3) are presented. The stresses shown are always those parallel (longitudinal) to the gage lines and those perpendicular (transverse) to the gage lines.

4.1 Internal Pressure

An internal pressure of 50 psi was applied to the model, and the measured and predicted stress distributions determined for this value are shown in Figs. 25 through 32. Figure 25 shows the measured and predicted stress distributions on the outside and inside surfaces of the cylinder and on the outside and inside surfaces of the nozzle along the 0° gage line, which is in the longitudinal plane of symmetry (see Fig. 3). The stresses are shown as a function of distance from the junction of nozzle and cylinder midsurfaces. The heavy lines are the predicted stresses, while the fine lines through the experimental points show the measured distributions. The solid lines in each case represent the transverse stresses, which are perpendicular to the gage lines. The dashed lines represent the longitudinal stresses, which are parallel to the gage lines. We can compare, then, the solid lines with each other and the dashed lines with each other.

The agreement between theory and experiment is good in Fig. 25, except that the stresses at the junction, which is where the maximums occur, are at times underestimated somewhat by the finite-element predictions. The general shape and distribution of the stresses are, however, well predicted by theory.

The remaining internal pressure comparisons, Figs. 26 through 32, are arranged to facilitate ready comparison of comparable results. Figure 26 shows the stresses along the 180° gage line, which is opposite the 0° gage line in the longitudinal plane of symmetry. Because of symmetry,

the 180° gage line results should theoretically be the same as those along the 0° gage line, shown in Fig. 25. Comparison of the two figures shows excellent agreement between results for opposite sides of the nozzle in the longitudinal plane of symmetry.

The results for gage lines 30° around from the longitudinal plane of symmetry (see Fig. 3) are shown in Figs. 27 and 28. Figure 27 shows the results for the 330° gage line, which is in the fourth quadrant. Results for the 150° gage line, which is in the second quadrant opposite 330°, are shown in Fig. 28. Agreement between theory and experiment is not as good here as for the previous two figures. Note in particular the large disagreement in the shape of the measured and predicted edge effect on the outer surface of the nozzle along the 330° gage line. The analogous second quadrant results in Fig. 28 show excellent agreement on the outer surface of the nozzle. The maximum measured stresses in Figs. 27 and 28 are both on the outer surface of the cylinder, but the value in the second quadrant is more than 25% greater than the fourth quadrant value.

These measured differences in stresses in quadrants which should yield exactly the same results are, at least partially, associated with minor geometric variations in the model. A careful dimensional inspection of the machined model indicated that, despite the care taken in machining, there were wall thickness variations in both nozzle and cylinder, with the nozzle thickness being as much as 15% greater (0.007 to 0.008 in. compared with the nominal 0.050 in.) in the fourth quadrant than in the second. This helps explain the observed differences in stresses in the two quadrants. The edge effect is damped out less rapidly and has a longer wavelength in a thicker shell than in a thinner one. Also, stresses in the thicker regions of the model would generally be expected to be less than in thinner regions.

The results for gage lines 60° around from the longitudinal plane of symmetry are shown in Figs. 29 and 30. The 300° gage line is in the fourth quadrant while the 120° gage line is opposite it in the second quadrant. The agreement between theory and experiment is reasonably good in Fig. 29. The maximum measured stress is on the outer surface of the cylinder and is almost 9000 psi. In Fig. 30, however, we see that the

analogous maximum stress in the second quadrant is 13,000 psi. These differences in stresses, which should be the same, are pointed out to emphasize that even in a costly and carefully made model, geometric variations inevitably exist and have a significant influence on behavior. These ever-present effects and their implications must always be recognized when comparing theory and experiment.

The internal pressure results for the 270 and 90° gage lines, in the transverse plane of symmetry, are shown in Figs. 31 and 32 respectively. Here on the transverse plane the agreement between theory and experiment is relatively poor. The stresses are, however, very low, so the disagreement is perhaps not too significant.

The overall agreement between theory and experiment, although generally good, is judged to be poorer for the internal pressure case than for any of the 12 external force and moment loading cases. Also, the disagreement between experimental results that should be identical is greater.

The method used to determine the estimated maximum experimental stresses and stress ratios was described in Section 2.5. The maximum theoretically predicted stresses were obtained in the same manner; that is, they were taken as the largest absolute values of the principal stresses. To match the experimental maximums, the search for the theoretical maximums was limited to the gage lines only.

The maximum experimentally determined stress occurred on the outer surface of the nozzle at 180°, and the maximum stress ratio was 13.3. The theoretical maximum stress was also on the outer surface of the nozzle, with the values at 0 and 180° being identical; the maximum stress ratio was 10.2.

4.2 Out-of-Plane Moment Loading, M_{XN}, on Nozzle

An out-of-plane moment loading of 600 in.-lb was applied to the nozzle of the model, and the measured and predicted stress distributions are shown in Figs. 33 through 40. Results for the eight gage lines are arranged here in the same manner as for the internal pressure case, although

the fourth and second quadrant results are not, in this case, theoretically the same.

The results in Figs. 33 and 34 are for 0 and 180°, respectively, in the longitudinal plane of symmetry. As expected, the stresses are small since these locations are somewhat analogous to the neutral axis of a beam in bending. The results for the 330 and 150° gage lines, which are 30° around from the longitudinal plane of symmetry, are shown in Figs. 35 and 36 respectively. At these locations the stresses are larger, and the agreement between theory and experiment is reasonably good.

The results along the 300 and 120° gage lines, which are 60° around from the longitudinal plane of symmetry, are shown in Figs. 37 and 38 respectively. The agreement between theory and experiment is good here. Finally, the results for the 270 and 90° gage lines, which are located in the transverse plane of symmetry, are shown in Figs. 39 and 40 respectively. Here, on the transverse plane, the stresses are a maximum, and the agreement between theory and experiment is very good. The maximum stress is on the outer surface of the nozzle and is closely predicted by the analysis.

The maximum experimentally determined principal stress ratio was 35.3, with the maximum stress occurring on the outer surface of the nozzle at the junction. The theoretical maximum was at the same location, and the maximum stress ratio was 37.2.

4.3 Torsional Moment Loading, M_{YN}, on Nozzle

A torsional moment loading of 2000 in.-lb was applied to the nozzle of the model, and the measured and predicted stress distributions for this value are shown in Figs. 41 through 48. As in the previous case, the fourth and second quadrant results are not theoretically the same. Here the stresses in the longitudinal and transverse planes of symmetry are low and rise to their maximum levels on the intermediate gage lines. Figures 43 and 44 show the results for the 330 and 150° gage lines, respectively, which are 30° around from the longitudinal plane of symmetry. The agreement between theory and experiment is fair at these locations but the peak stresses near the junction are underestimated by the analysis.

The results for the 300 and 120° gage lines, which are 60° around from the longitudinal plane of symmetry, are shown in Figs. 45 and 46 respectively. Again, the agreement is fair, but the analysis underestimates the peak stresses in the junction region. The maximum stress occurs at this location.

The relatively poor quantitative agreement between theory and experiment in this loading case may be traceable to the neglect of the sixth degree of freedom for nodes along the junction in the finite-element formulation. The degree of freedom that was neglected is that corresponding to the nozzle rotation that would be produced by a torsional moment. The consequences of this neglect were discussed in the previous chapter and depicted in Fig. 23.

The maximum experimentally determined stress ratio was 12.5, with the maximum stress located on the outer surface of the nozzle, at the junction, and on the 120° gage line. The maximum theoretical stress was also on the outer surface of the nozzle, at the junction, but on the 300° gage line. The maximum theoretical stress ratio was 5.1.

4.4 In-Plane Moment Loading, M_{ZN}, on Nozzle

An in-plane moment loading of 2400 in.-lb was applied to the nozzle of the model, and the measured and predicted stress distributions are shown in Figs. 49 through 56. Here the stresses are large in the longitudinal plane of symmetry, as shown in Figs. 49 and 50, but the maximum does not occur here. The agreement between theory and experiment is good for the gage lines in the longitudinal plane of symmetry.

The peak stresses are larger along the gage lines 30 and 60° around from the longitudinal plane of symmetry. In the transverse plane of symmetry the stresses are very low, as shown in Figs. 55 and 56. For this loading the transverse plane is somewhat similar to the neutral axis of a beam.

The maximum experimentally determined stress ratio was 10.0, with the maximum stress occurring on the outer surface of the nozzle, at the junction, and along the 300° gage line. The maximum theoretical stress

also occurred on the outer nozzle surface, at the junction, and along the 300° gage line. The stress ratio was 10.9.

4.5 In-Plane Force, F_{XN}, on Nozzle

The in-plane force applied to the nozzle had a value of 200 lb. The comparisons of theory and experiment for the eight gage lines are shown in Figs. 57 through 64. The results here are very similar to the previous case of the in-plane bending moment on the nozzle, and the overall agreement between theory and experiment is very good.

The maximum experimentally determined stress occurred on the outer surface of the nozzle, at the junction, and on the 120° gage line. The maximum ratio was 10.5. The maximum theoretical stress also occurred on the outer surface of the nozzle, at the junction, but on the 330° gage line. The maximum theoretical stress ratio was 11.4.

4.6 Axial Force, F_{YN}, on Nozzle

The axial force applied to the nozzle had a value of 300 lb. The comparisons of theory and experiment are presented in Figs. 65 through 72. The agreement between theory and experiment is reasonably good for this loading, particularly as the larger stress levels are approached on the transverse plane of symmetry (Figs. 71 and 72).

Both the experimentally determined and the theoretically determined maximum stress occurred on the outer surface of the nozzle, at the junction, and on the 270° gage line. The maximum experimental stress ratio was 36.3, while the maximum theoretical stress ratio was 36.0.

4.7 Out-of-Plane Force, F_{ZN}, on Nozzle

The out-of-plane force applied to the nozzle had a value of 100 lb. The comparisons of theory and experiment are presented in Figs. 73 through 80. The results here are very similar to the previous case of the out-of-plane moment on the nozzle, and the overall agreement between theory and experiment is again very good.

Unlike any of the other 12 loading cases, both the experimentally determined and the theoretically determined maximum stress occurred on the inner surface of the nozzle rather than the outer surface. The maximums were at the junction and on the 270° gage line. The maximum experimental stress ratio was 36.0, while the maximum theoretical stress ratio was 32.6.

4.8 Torsional Moment Loading, M_{XC}, on Cylinder

The torsional moment applied to the cylinder had a value of 20,000 in.-lb. The comparisons of theory and experiment are presented in Figs. 81 through 88. As was the case for the torsional moment applied to the nozzle, the stresses are low in the longitudinal and transverse planes of symmetry and rise to their maximum levels on the intermediate gage lines. The agreement between theory and experiment is qualitatively satisfactory on these intermediate lines. The analysis is seen to generally overestimate the peak stresses in the junction region.

Both the experimentally determined and the theoretical maximum stress occurred on the outer surface of the nozzle, at the junction, and on the 120° gage line. The experimental maximum stress ratio was 10.0, while the theoretical maximum stress ratio was 13.0.

4.9 Out-of-Plane Moment Loading, M_{YC}, on Cylinder

The out-of-plane moment loading applied to the cylinder had a value of 20,000 in.-lb. The comparisons of theory and experiment are presented in Figs. 89 through 96. Here, the 0 and 180° gage lines on the longitudinal plane of symmetry are analogous to the neutral axis of a beam in bending, and the stresses are thus low. However, the stresses are not very large anywhere in the model. The maximum stress ratios for this case were the lowest of all 13 loading cases. As a result of the relatively low stress levels, stress distributions are not too well defined, and the agreement between theory and experiment appears to be relatively poor.

Both the experimentally determined and the theoretical maximum stress occurred on the outside surface of the nozzle, at the junction. The experimental maximum, however, occurred on the 90° gage line, while the theoretical maximum occurred at 0°. The experimental maximum stress ratio was only 2.3, and the theoretical ratio was 2.7.

4.10 In-Plane Moment Loading, M_{ZC}, on Cylinder

The in-plane moment loading applied to the cylinder had a value of 20,000 in.-lb. The comparisons of theory and experiment are presented in Figs. 97 through 104. Here the stress levels are a maximum in the transverse plane of symmetry, as shown in Figs. 103 and 104. Where the stress levels are lower along the other gage lines, the apparent agreement between theory and experiment is poorer.

The experimentally determined and the theoretical maximum stress each occurred on the outer surface of the nozzle at the junction. The experimental maximum was on the 90° gage line, while the theoretical maximum occurred on both the 270 and 90° gage lines. The maximum experimental stress ratio was 3.8, and the maximum theoretical ratio was 5.7.

4.11 Axial Force, F_{XC}, on Cylinder

The axial force applied to the cylinder had a value of 5000 lb. The comparisons of theory and experiment for the eight gage lines are presented in Figs. 105 through 112. Considering the relatively low stresses, the agreement between theory and experiment is reasonably good throughout. The agreement between theory and experiment is very good for the 270 and 90° gage lines, as shown in Figs. 111 and 112.

Both the experimentally determined and the theoretically predicted maximum stress occurred on the outer surface of the nozzle, at the junction, and on the 270° gage line. The experimental maximum stress ratio was 4.7, while the theoretical was 5.6.

4.12 In-Plane Force, F_{YC}, on Cylinder

The in-plane force applied to the cylinder had a value of 2000 lb. The comparisons between theory and experiment are shown in Figs. 113 through 120. The agreement between theory and experiment is very good for this loading case.

Both the experimentally determined and the theoretically determined maximum stress occurred on the outer surface of the nozzle, at the junction, and on the 270° gage line. The maximum experimental stress ratio was 6.0, and the maximum theoretical ratio was 5.7.

4.13 Out-of-Plane Force, F_{ZC}, on Cylinder

The value of the out-of-plane force applied to the cylinder was 1200 lb. The comparisons of theory and experiment are shown in Figs. 121 through 128. The 0 and 180° gage lines, in the longitudinal plane of symmetry, are analogous, in this case, to the neutral axis of a beam, so that the stresses are low along these gage lines. They build up, however, for the other gage lines, and the agreement between theory and experiment is very good for this loading case.

Both the experimentally determined maximum stress and the theoretical maximum occurred on the outside surface of the nozzle, at the junction, and along the 300° gage line. The maximum experimental stress ratio was 3.1, while the maximum theoretical ratio was 3.5.

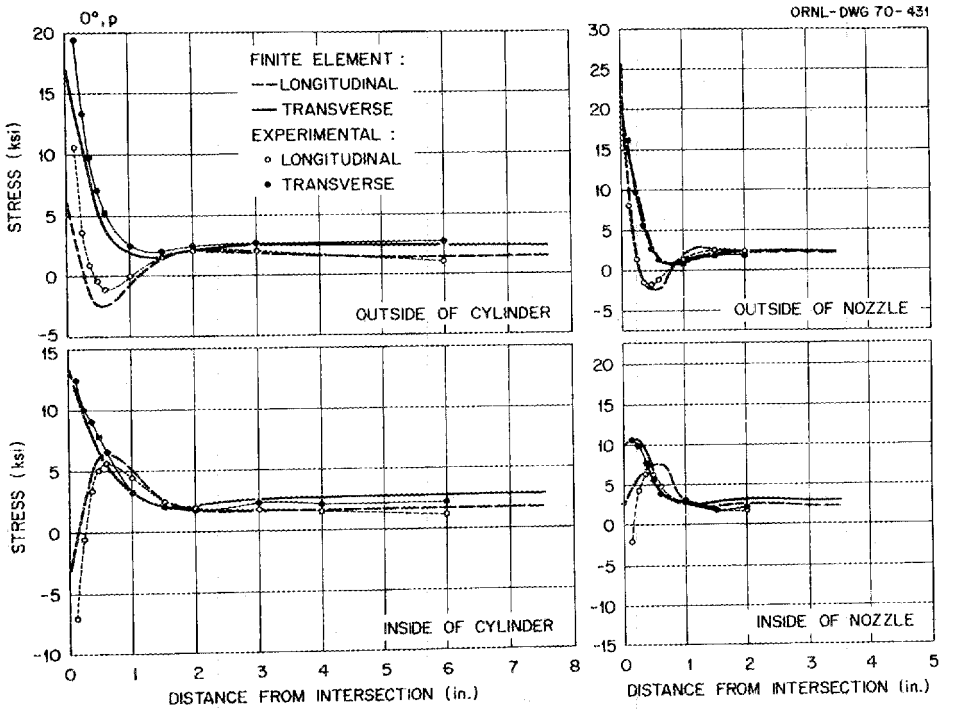

Fig. 25. Measured and predicted stress distributions at 0° for internal pressure of 50 psi.

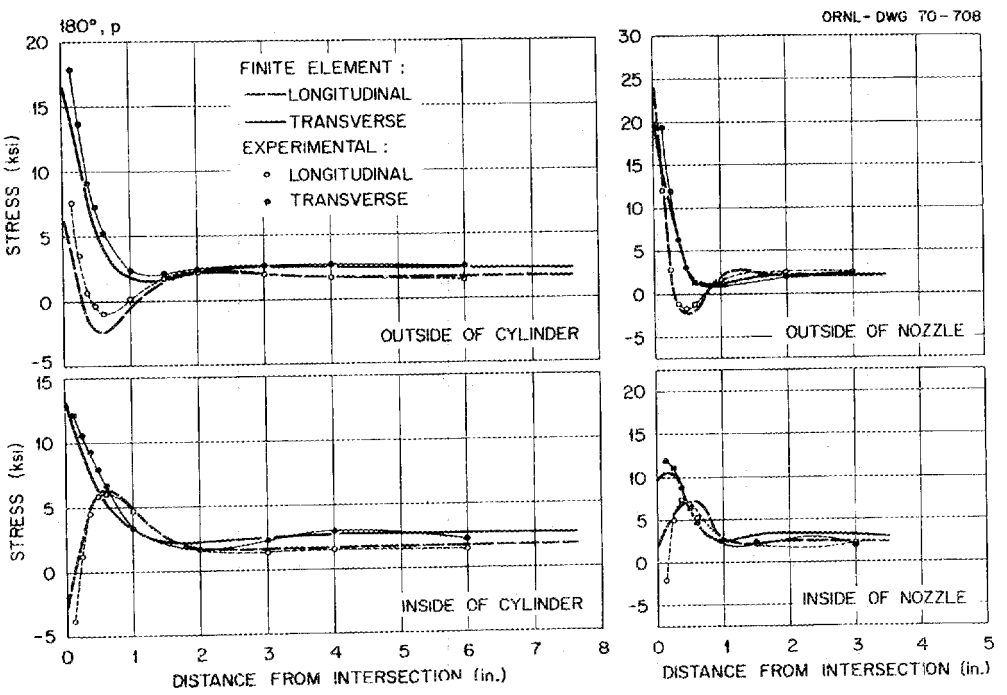

Fig. 26. Measured and predicted stress distributions at 180° for internal pressure of 50 psi.

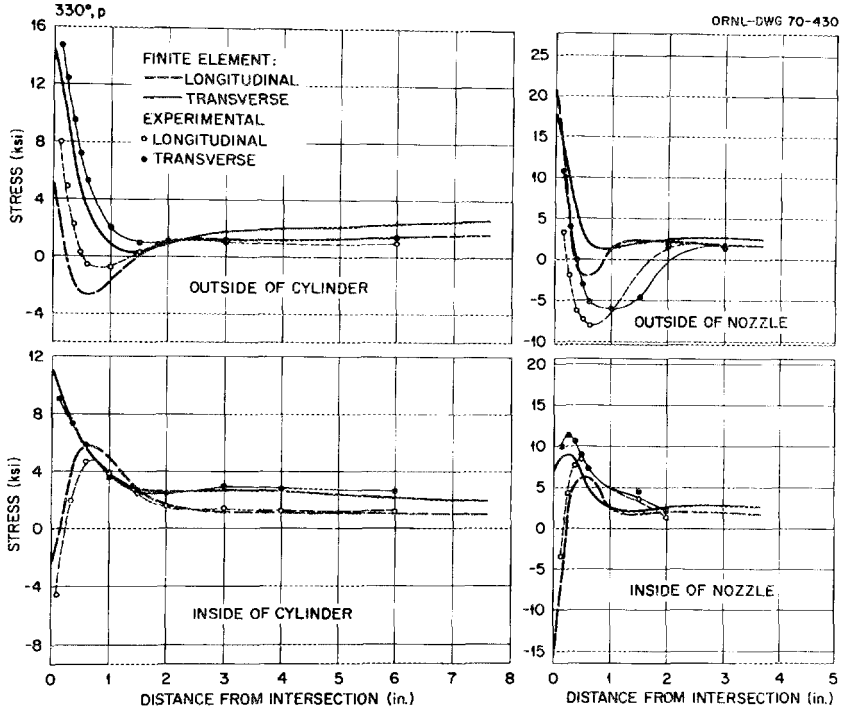

Fig. 27. Measured and predicted stress distributions at 330° for internal pressure of 50 psi.

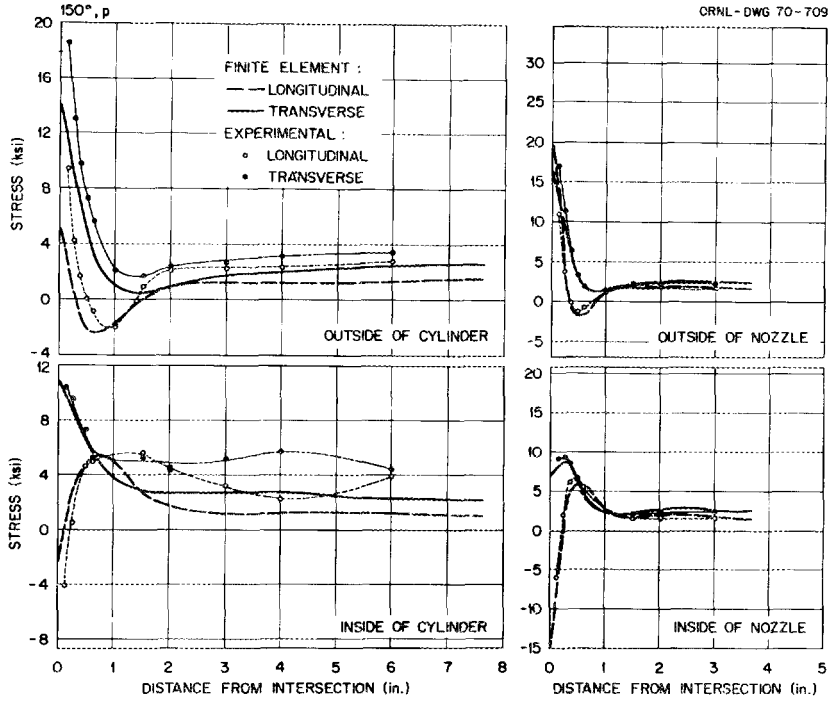

Fig. 28. Measured and predicted stress distributions at 150° for internal pressure of 50 psi.

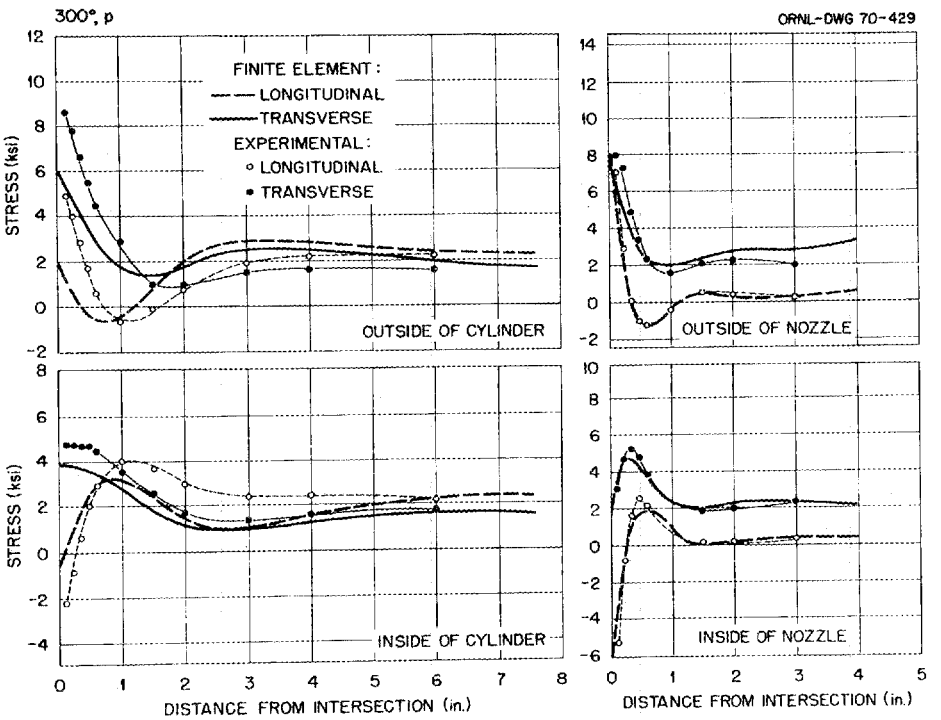

Fig. 29. Measured and predicted stress distributions at 300° for internal pressure of 50 psi.

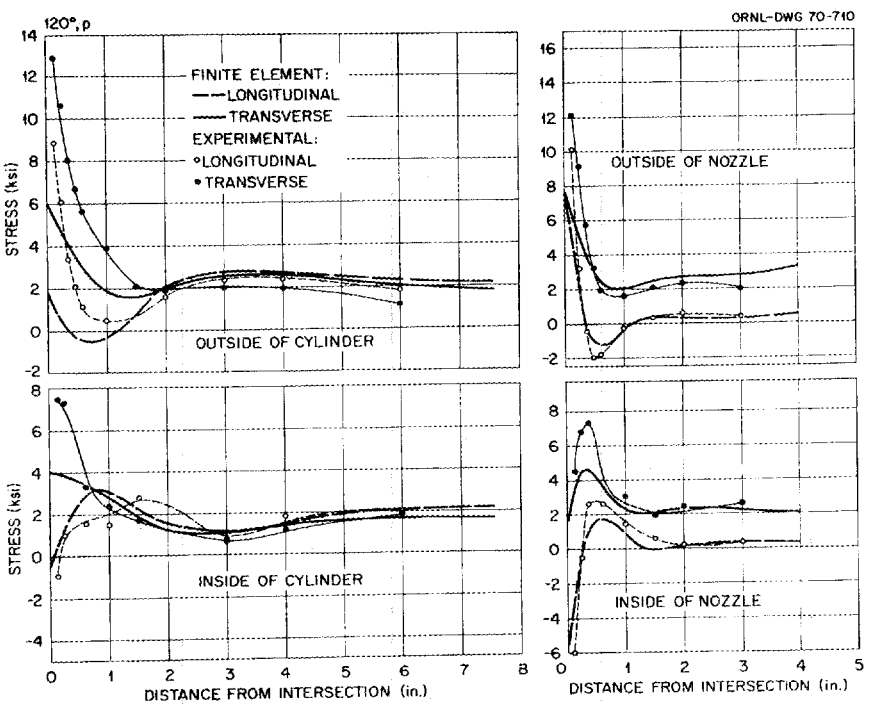

Fig. 30. Measured and predicted stress distributions at 120° for internal pressure of 50 psi.

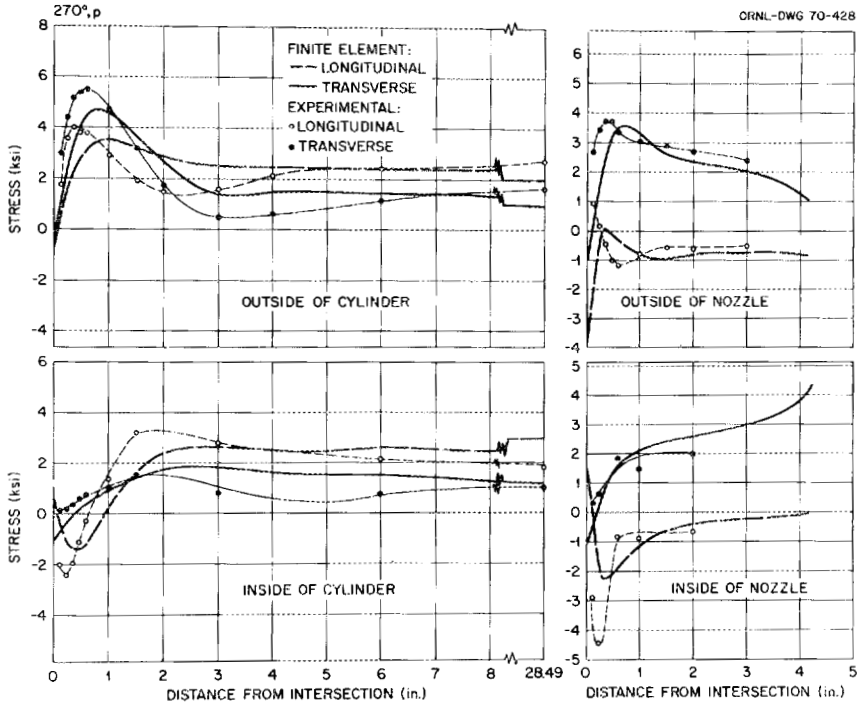

Fig. 31. Measured and predicted stress distributions at 270° for internal pressure of 50 psi.

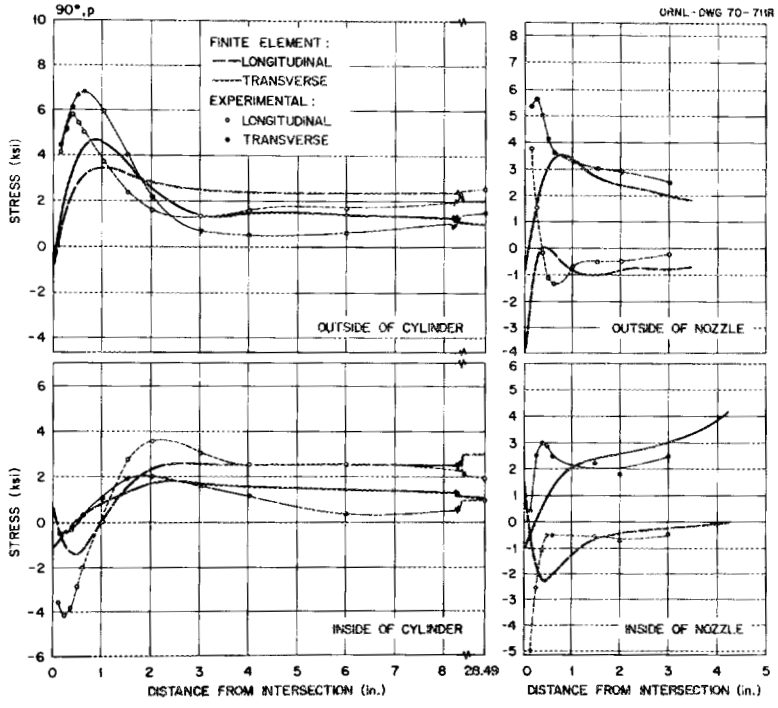

Fig. 32. Measured and predicted stress distributions at 90° for internal pressure of 50 psi.

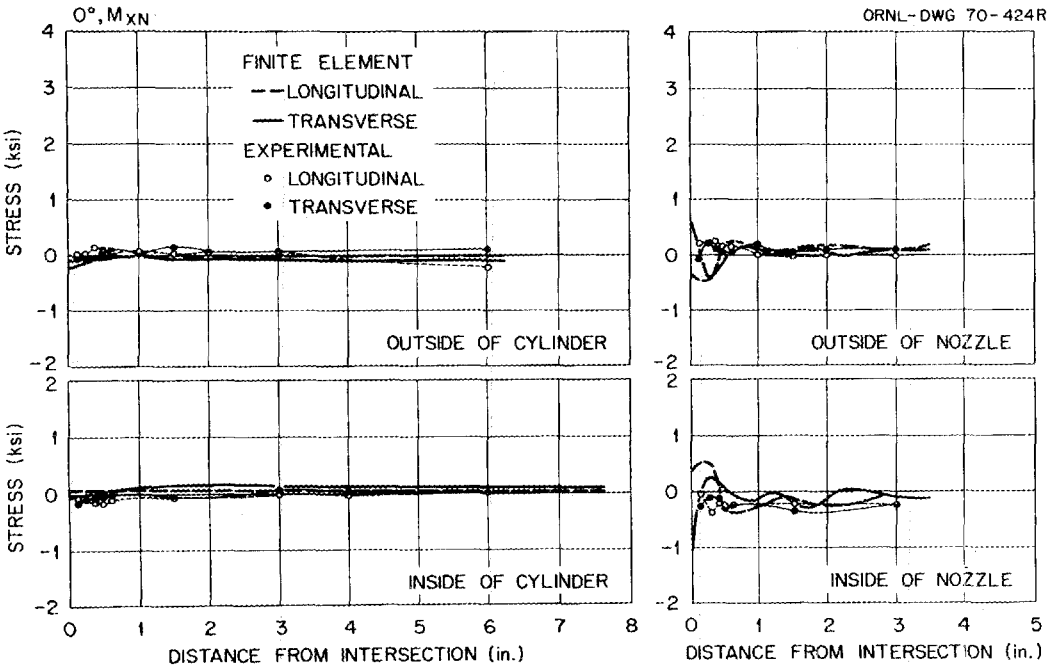

Fig. 33. Measured and predicted stress distributions at 0° for out-of-plane moment, M_{XN}, on nozzle.

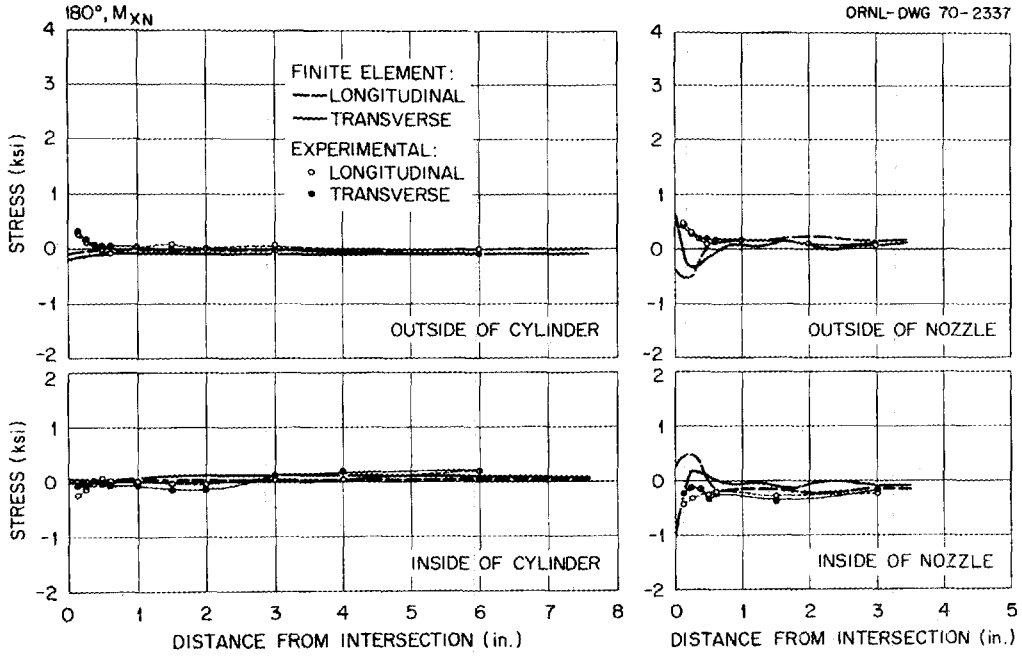

Fig. 34. Measured and predicted stress distributions at 180° for out-of-plane moment, M_{XN}, on nozzle.

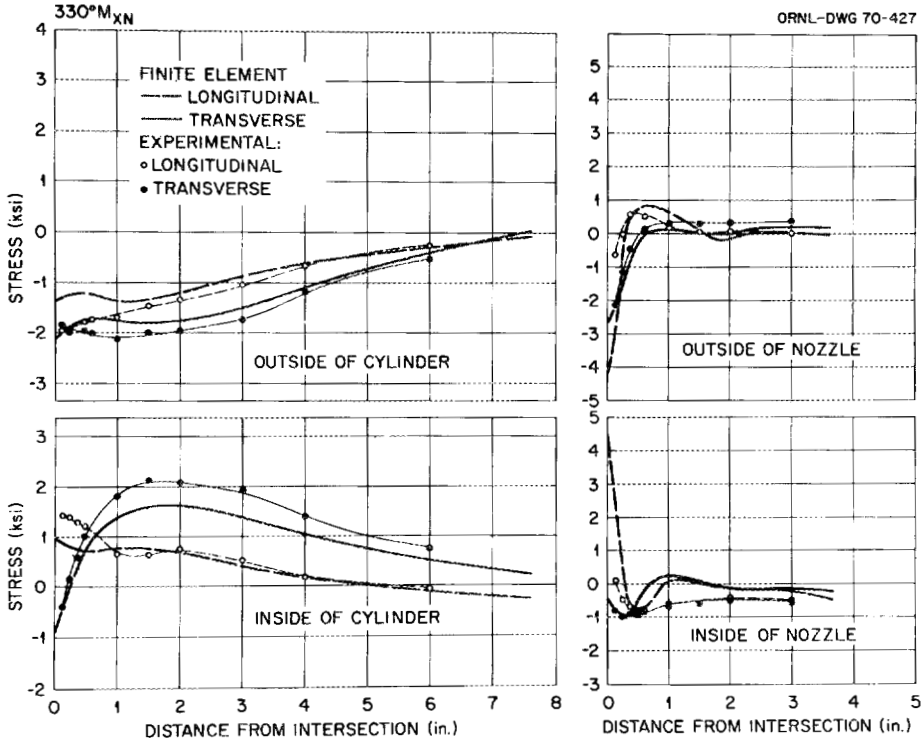

Fig. 35. Measured and predicted stress distributions at 330° for out-of-plane moment, M_{XN}, on nozzle.

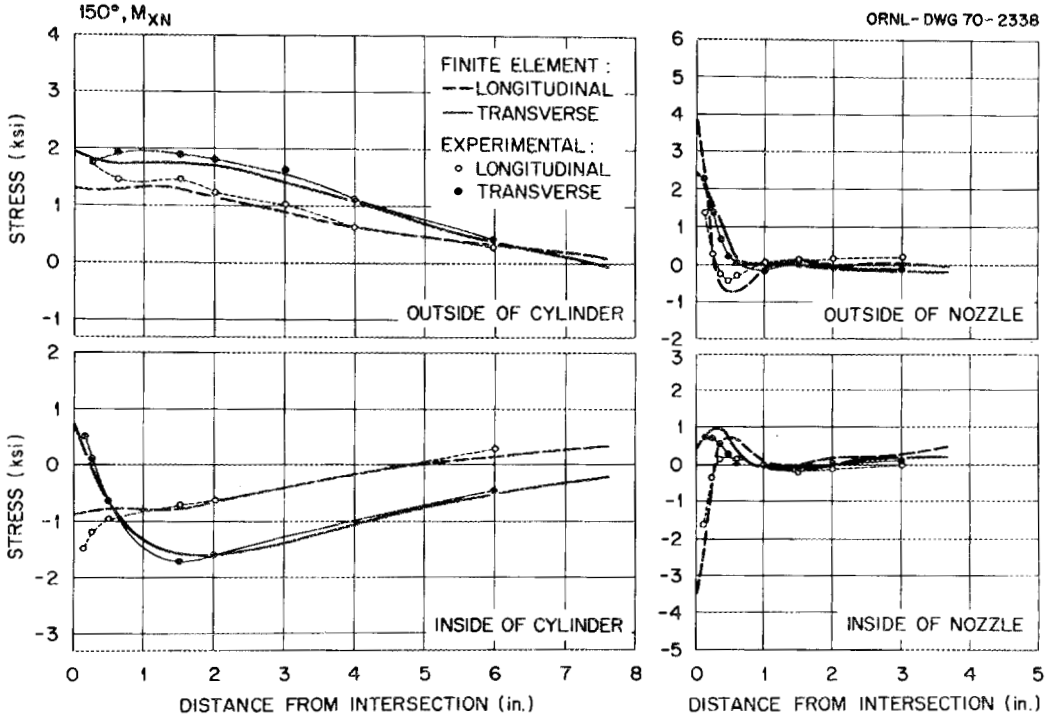

Fig. 36. Measured and predicted stress distributions at 150° for out-of-plane moment, M_{XN}, on nozzle.

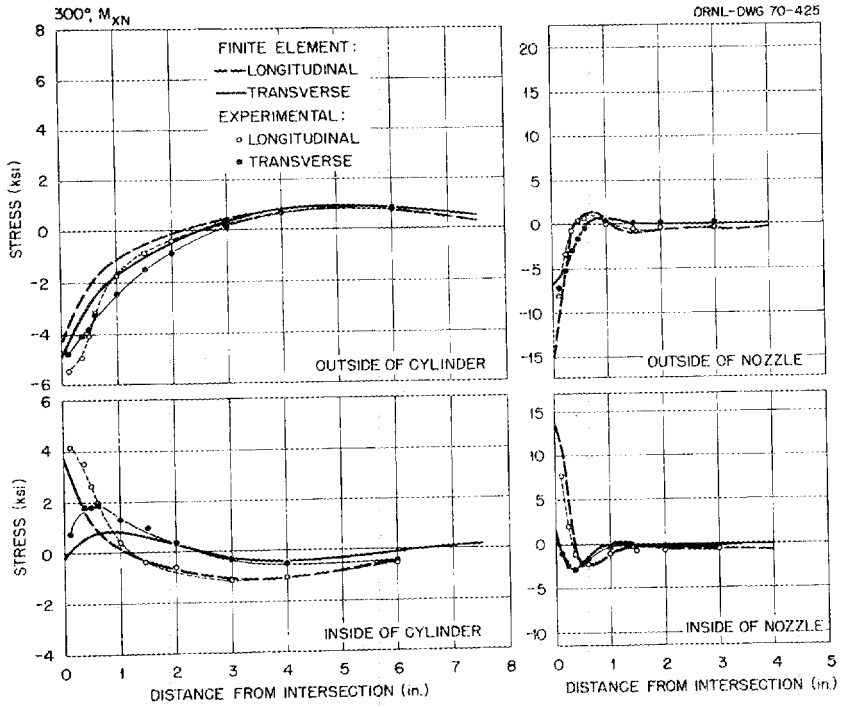

Fig. 37. Measured and predicted stress distributions at 300° for out-of-plane moment, M_{XN}, on nozzle.

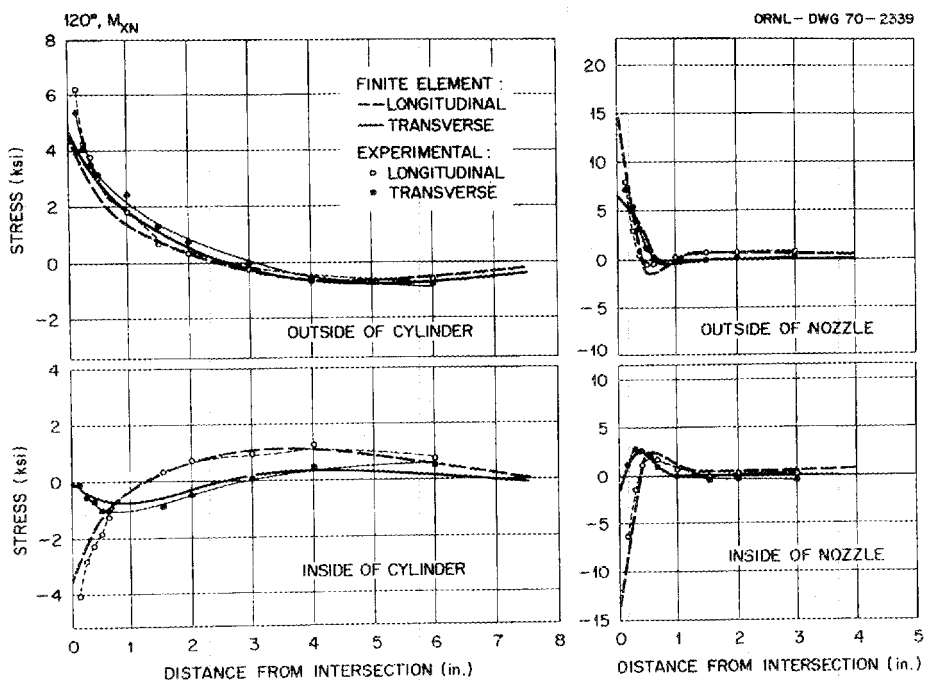

Fig. 38. Measured and predicted stress distributions at 120° for out-of-plane moment, M_{XN}, on nozzle.

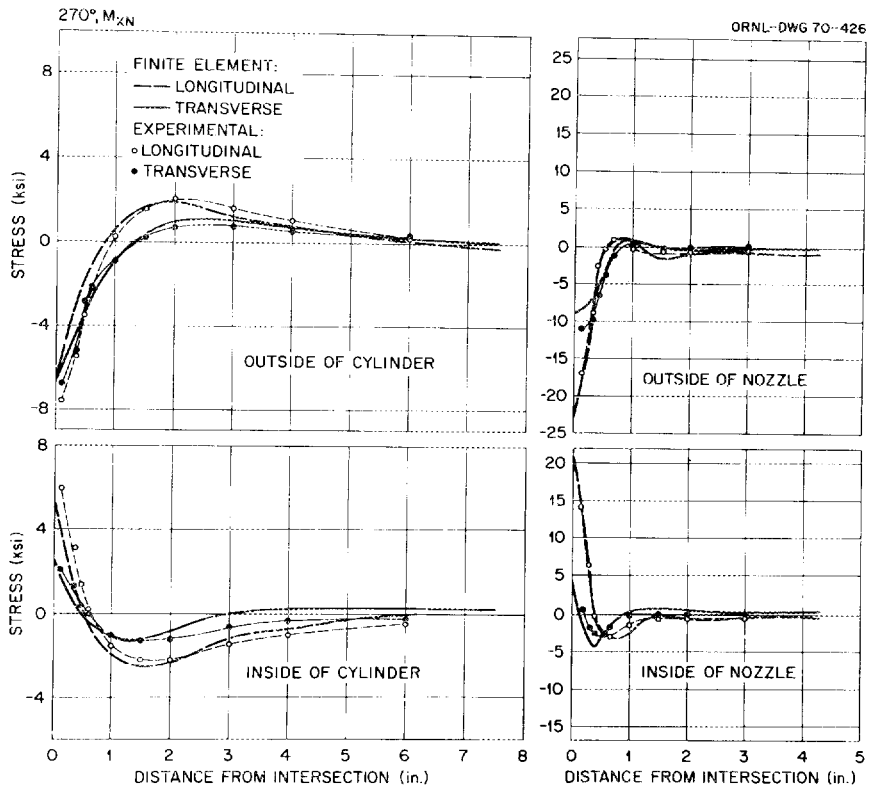

Fig. 39. Measured and predicted stress distributions at 270° for out-of-plane moment, M_{XN}, on nozzle.

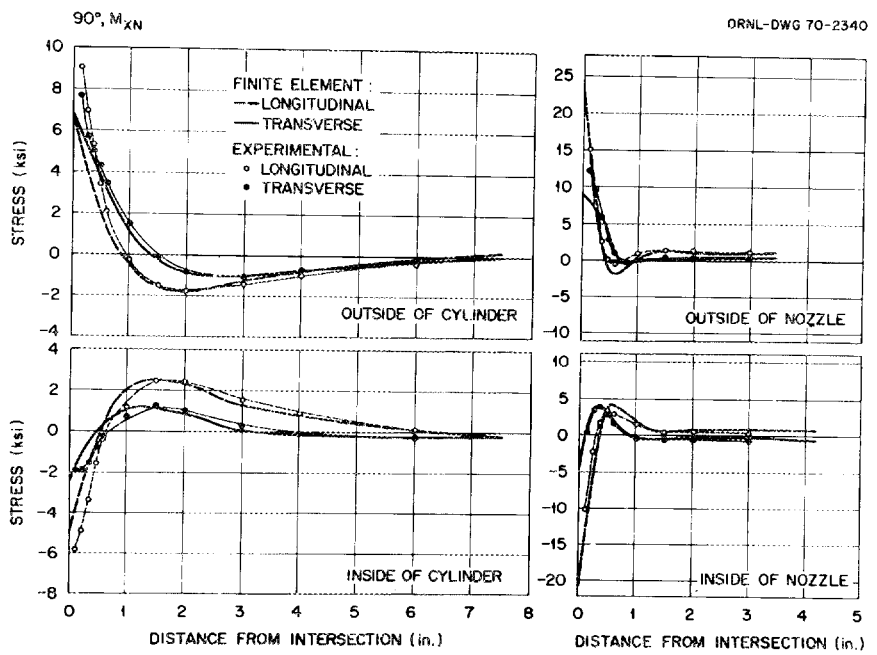

Fig. 40. Measured and predicted stress distributions at 90° for out-of-plane moment, M_{XN}, on nozzle.

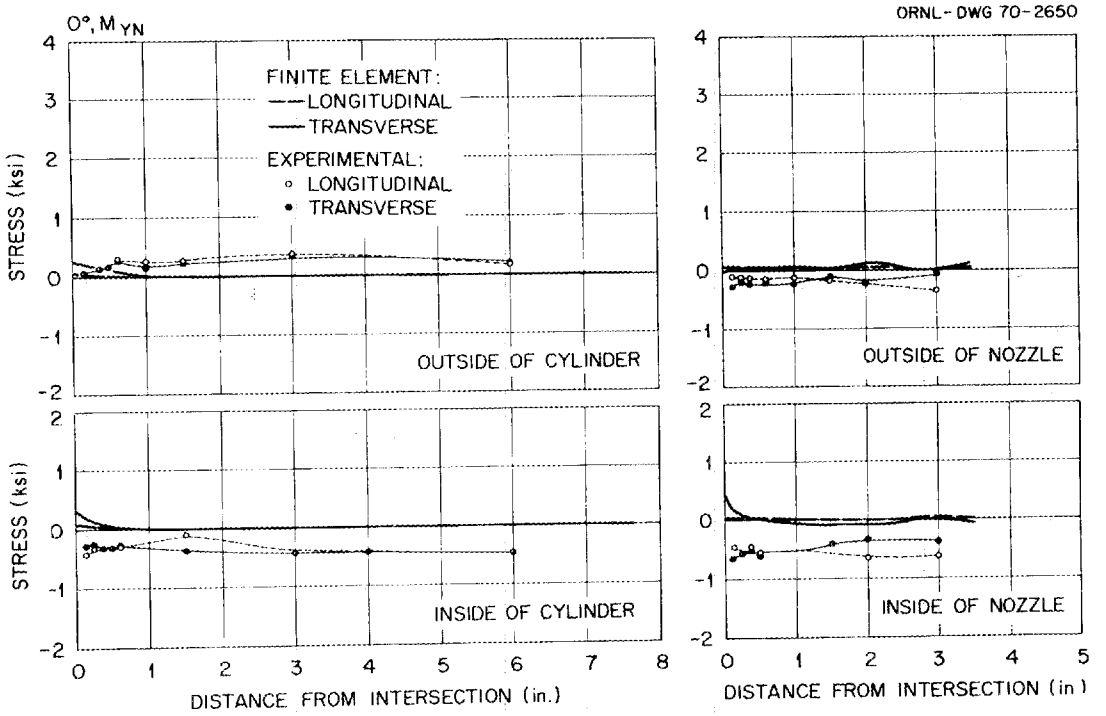

Fig. 41. Measured and predicted stress distributions at 0° for torsional moment, M_{YN}, on nozzle.

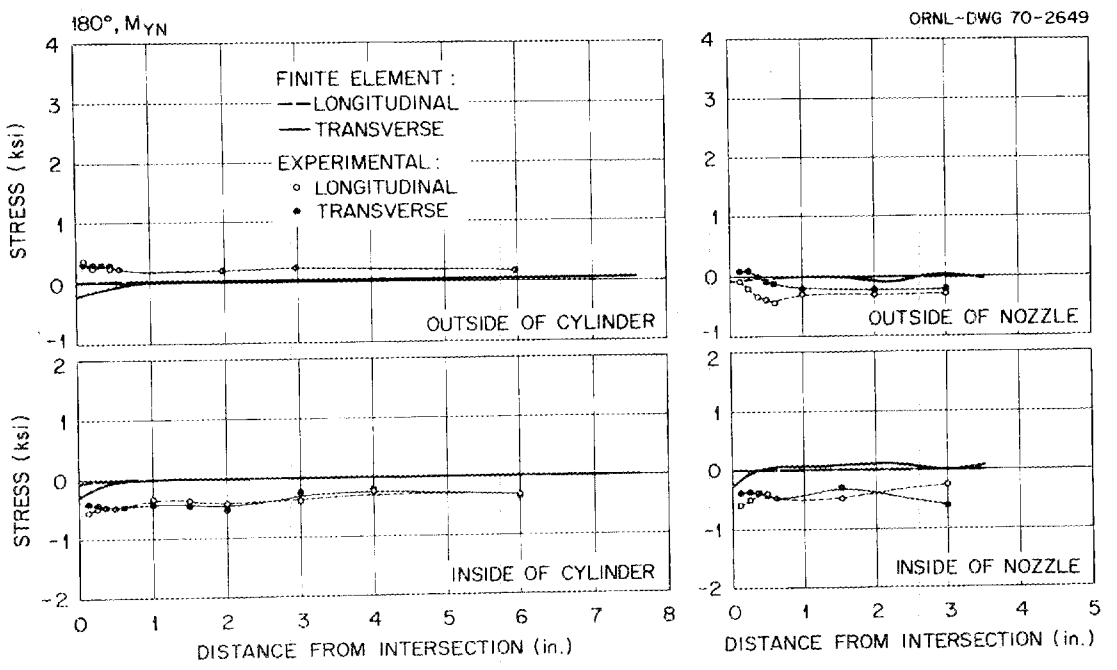

Fig. 42. Measured and predicted stress distributions at 180° for torsional moment, M_{YN}, on nozzle.

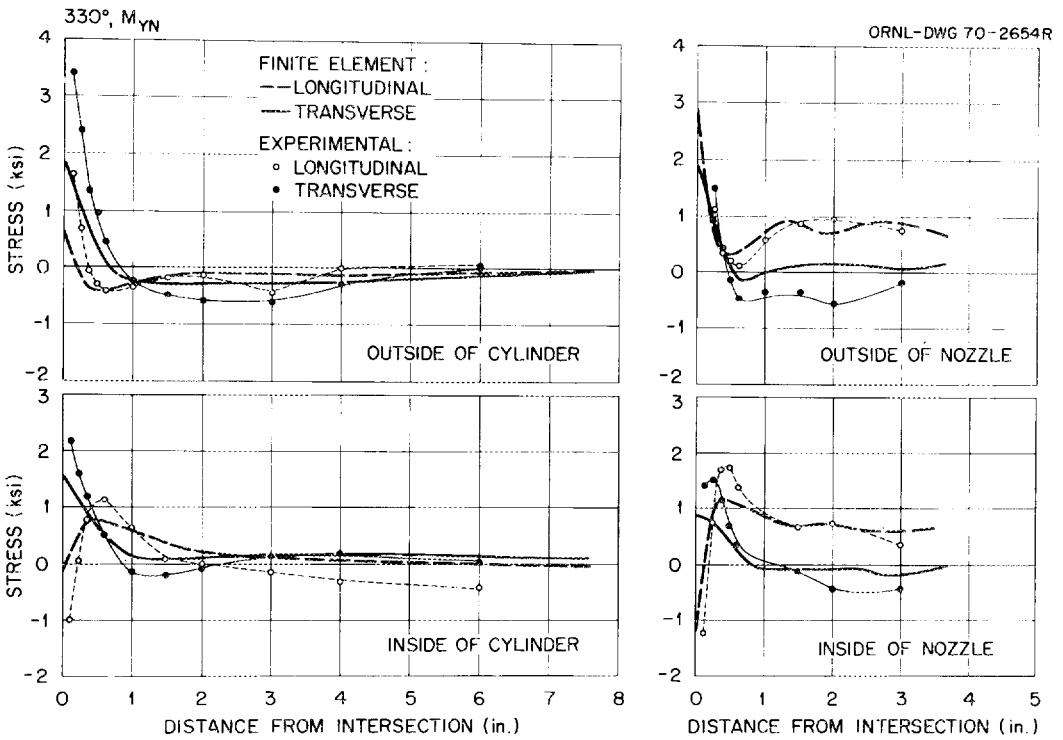

Fig. 43. Measured and predicted stress distributions at 330° for torsional moment, M_{YN}, on nozzle.

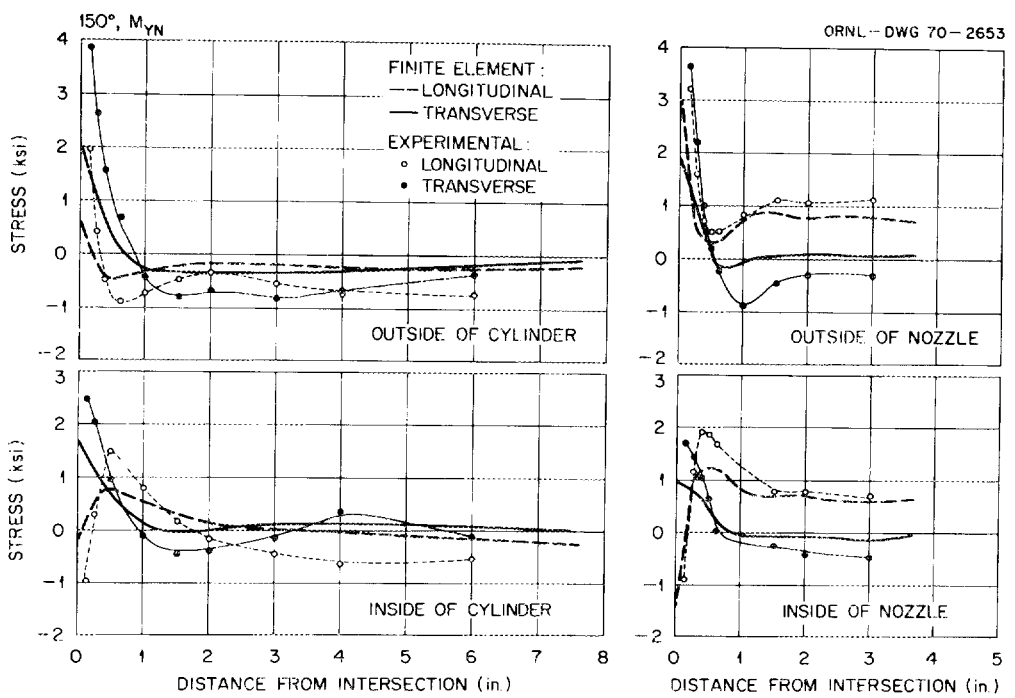

Fig. 44. Measured and predicted stress distributions at 150° for torsional moment, M_{YN}, on nozzle.

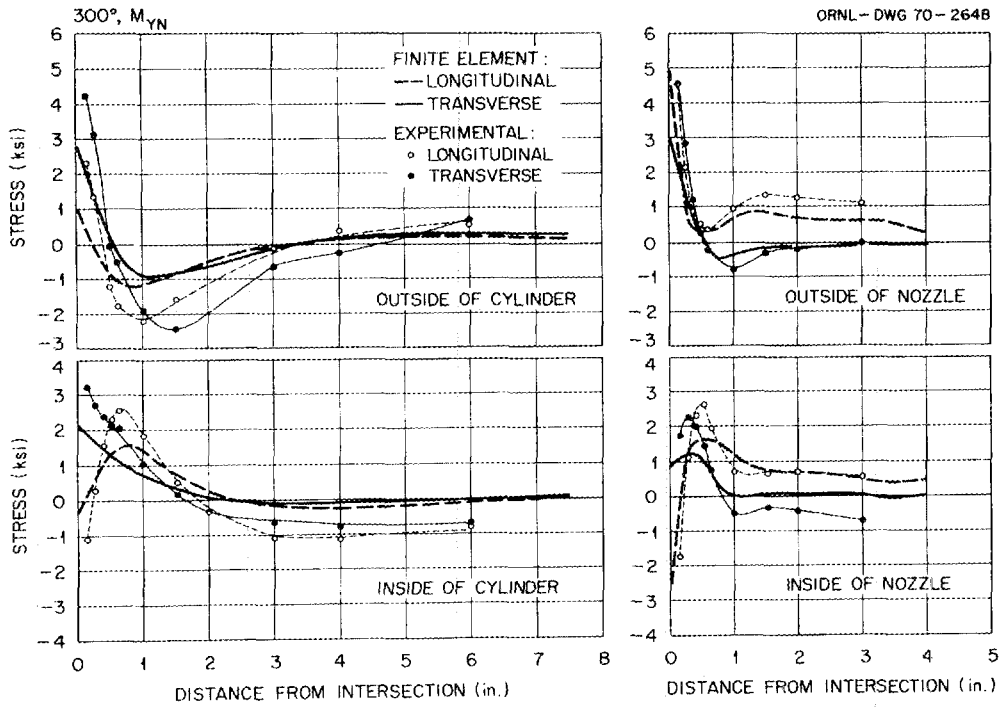

Fig. 45. Measured and predicted stress distributions at 300° for torsional moment, M_{YN}, on nozzle.

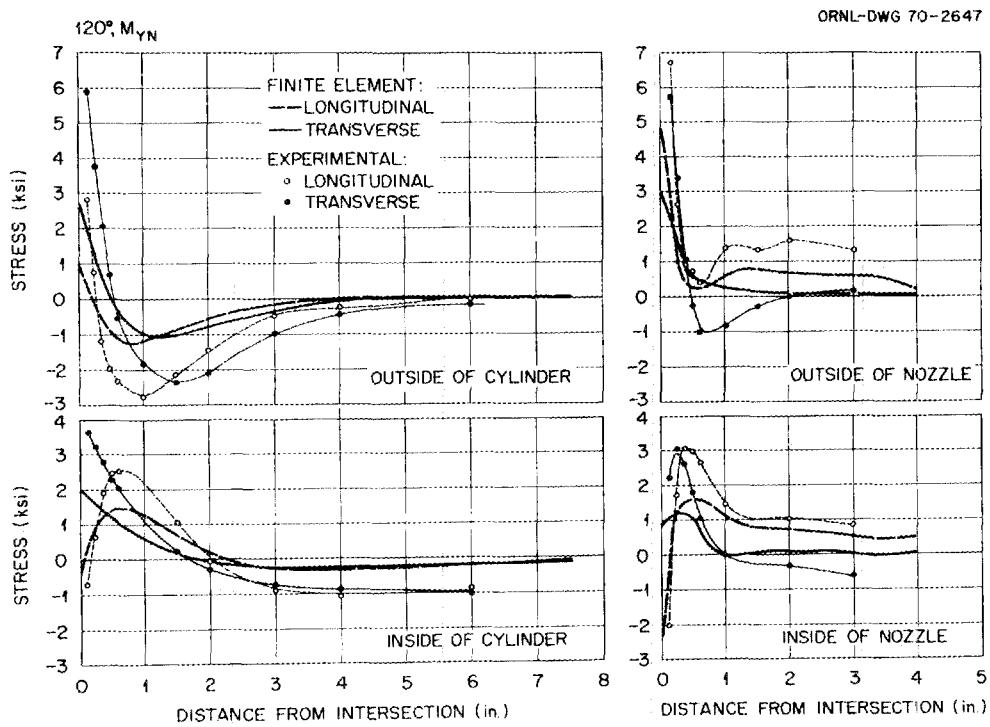

Fig. 46. Measured and predicted stress distributions at 120° for torsional moment, M_{YN}, on nozzle.

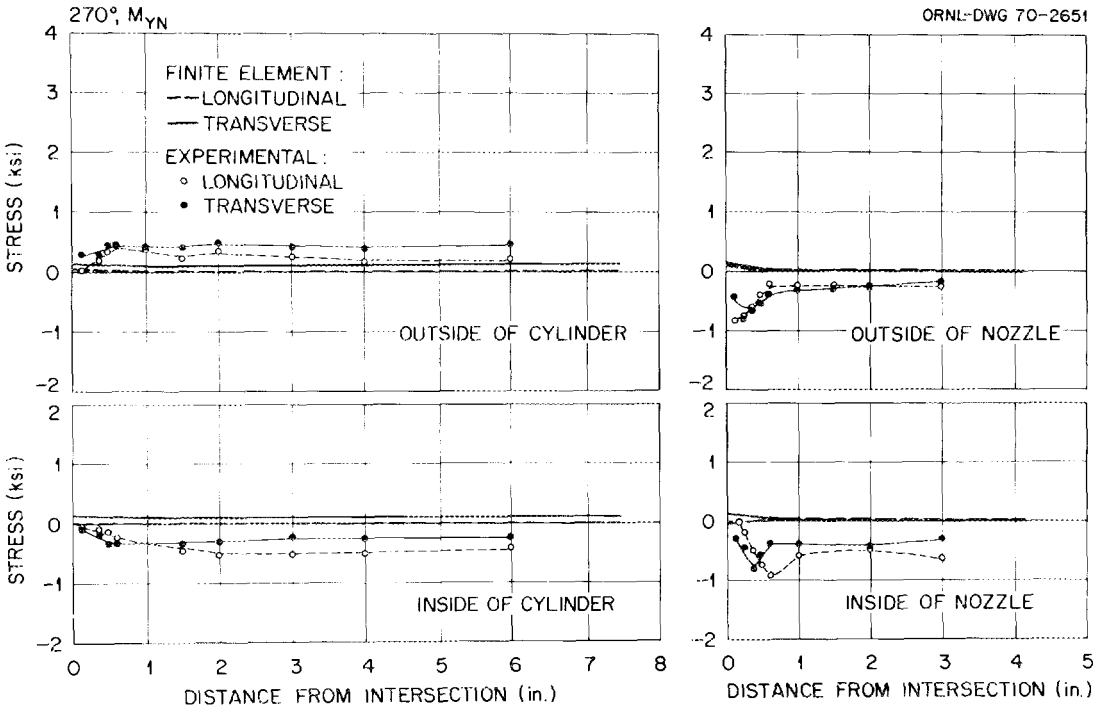

Fig. 47. Measured and predicted stress distributions at 270° for torsional moment, M_{YN}, on nozzle.

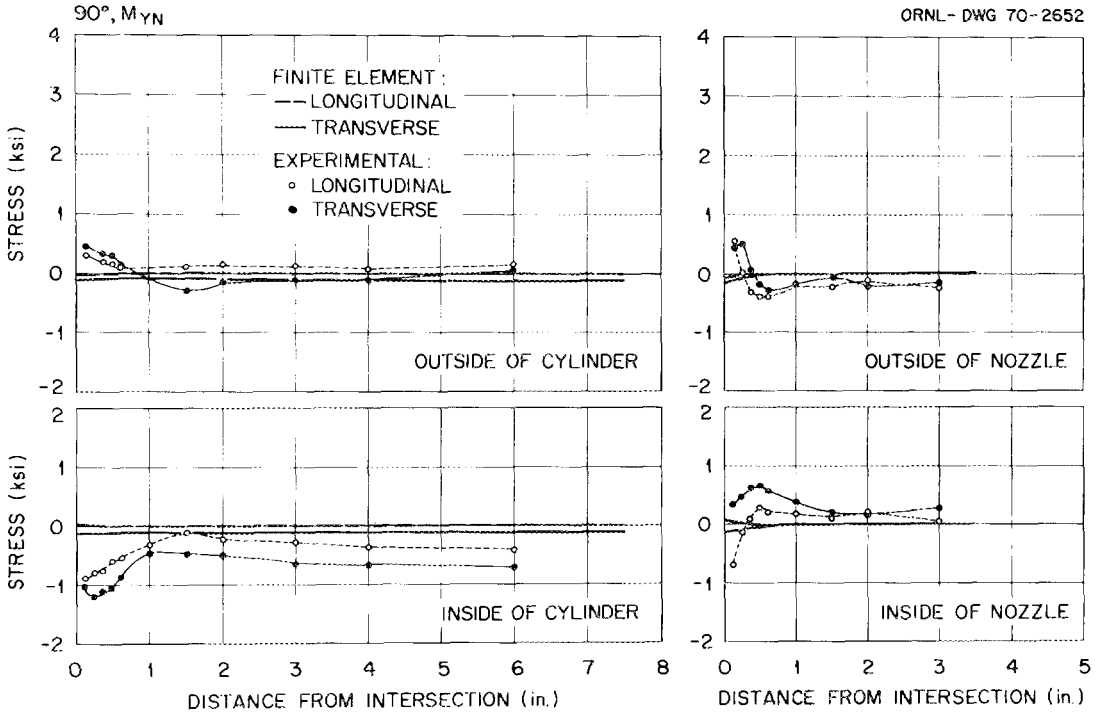

Fig. 48. Measured and predicted stress distributions at 90° for torsional moment, M_{YN}, on nozzle.

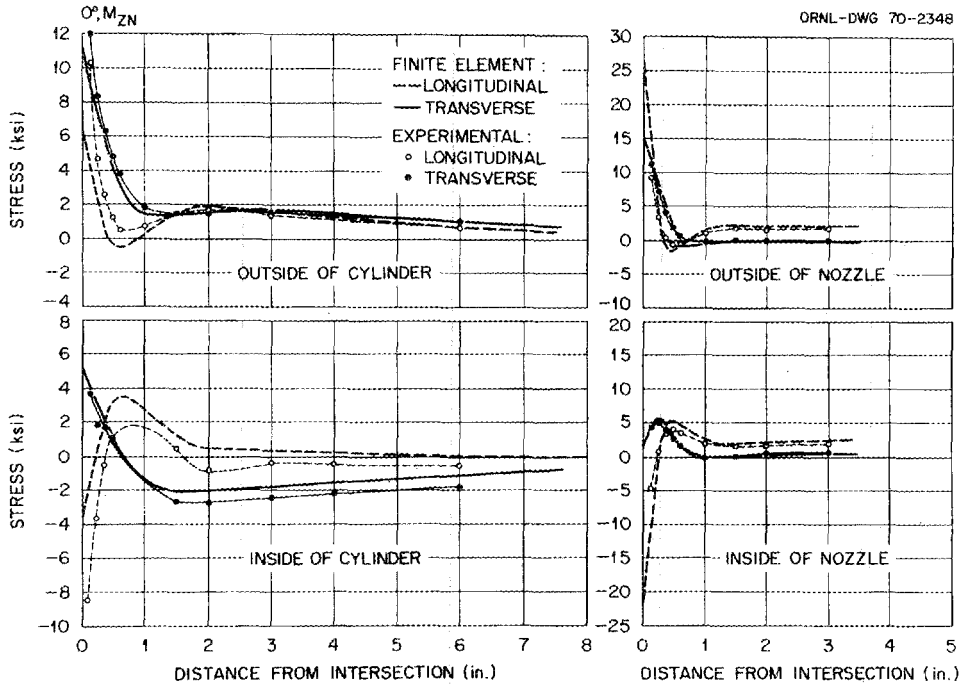

Fig. 49. Measured and predicted stress distributions at 0° for in-plane moment, M_{ZN}, on nozzle.

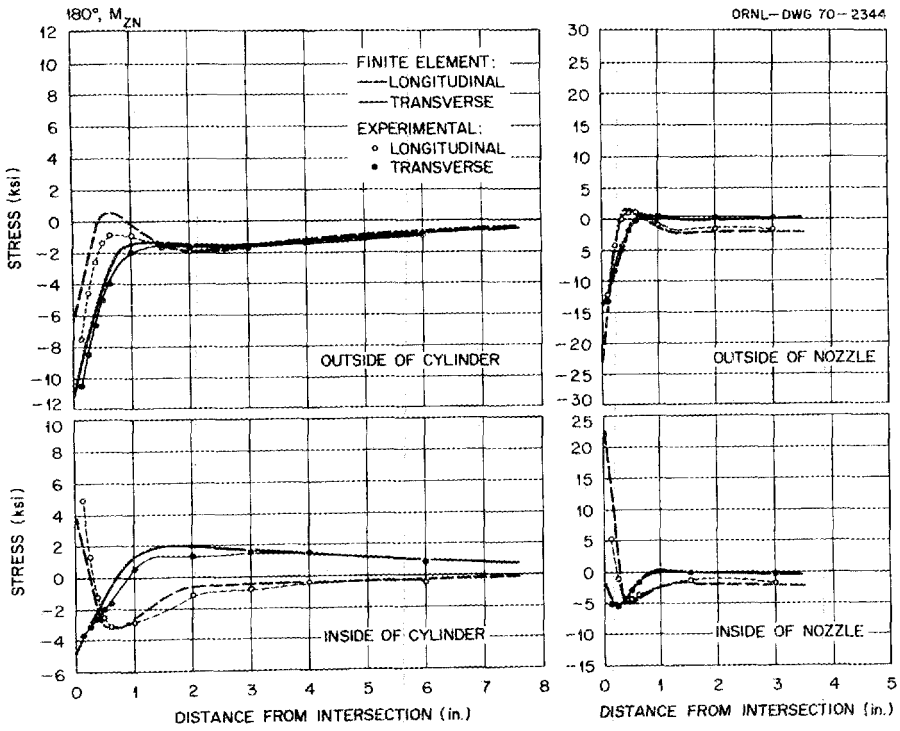

Fig. 50. Measured and predicted stress distributions at 180° for in-plane moment, M_{ZN}, on nozzle.

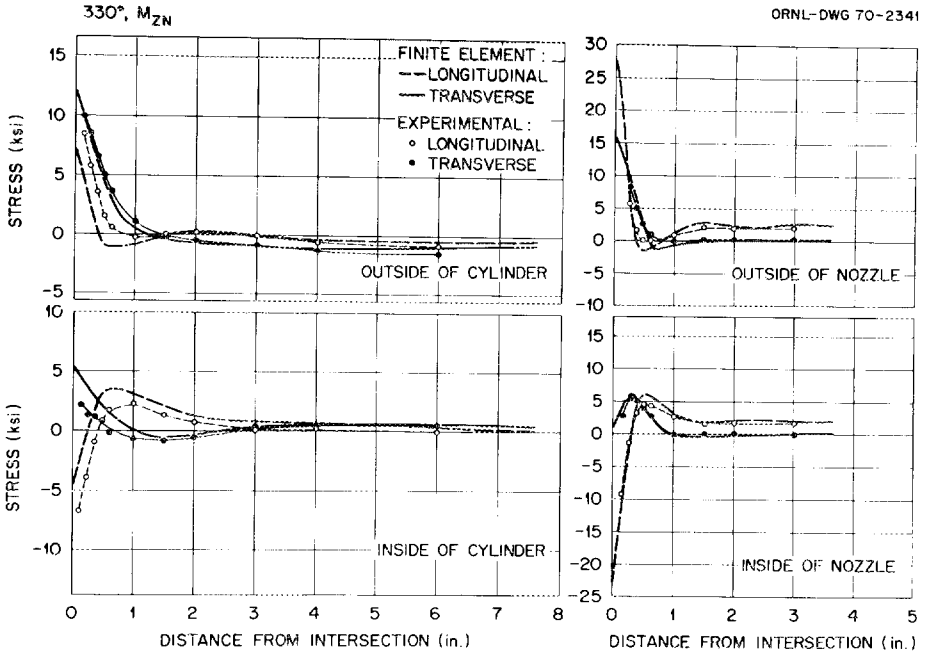

Fig. 51. Measured and predicted stress distributions at 330° for in-plane moment, M_{ZN}, on nozzle.

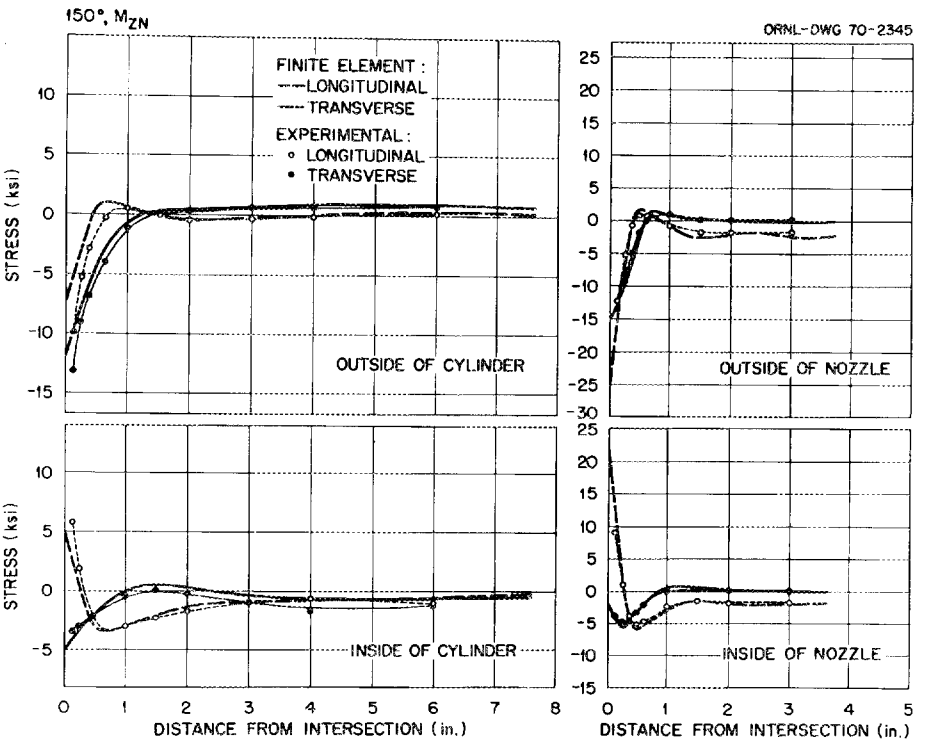

Fig. 52. Measured and predicted stress distributions at 150° for in-plane moment, M_{ZN}, on nozzle.

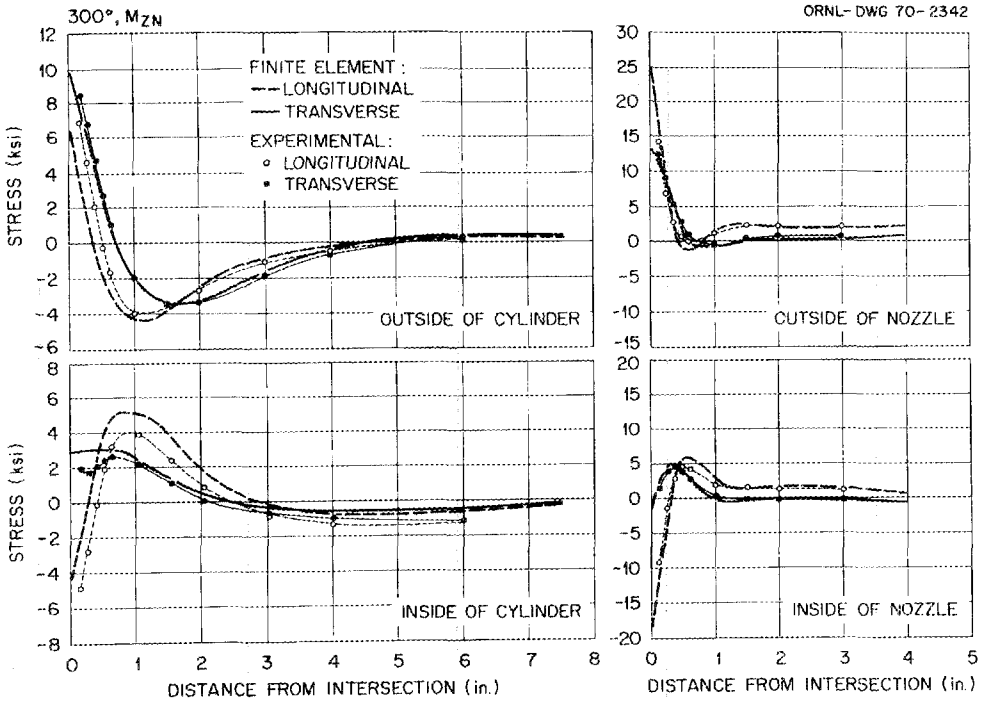

Fig. 53. Measured and predicted stress distributions at 300° for in-plane moment, M_{ZN}, on nozzle.

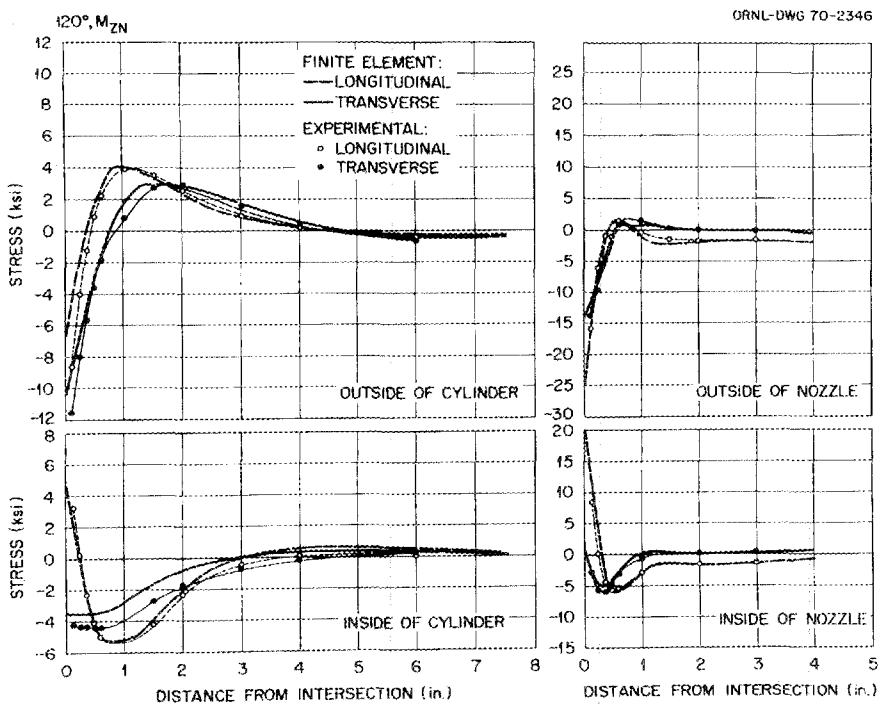

Fig. 54. Measured and predicted stress distributions at 120° for in-plane moment, M_{ZN}, on nozzle.

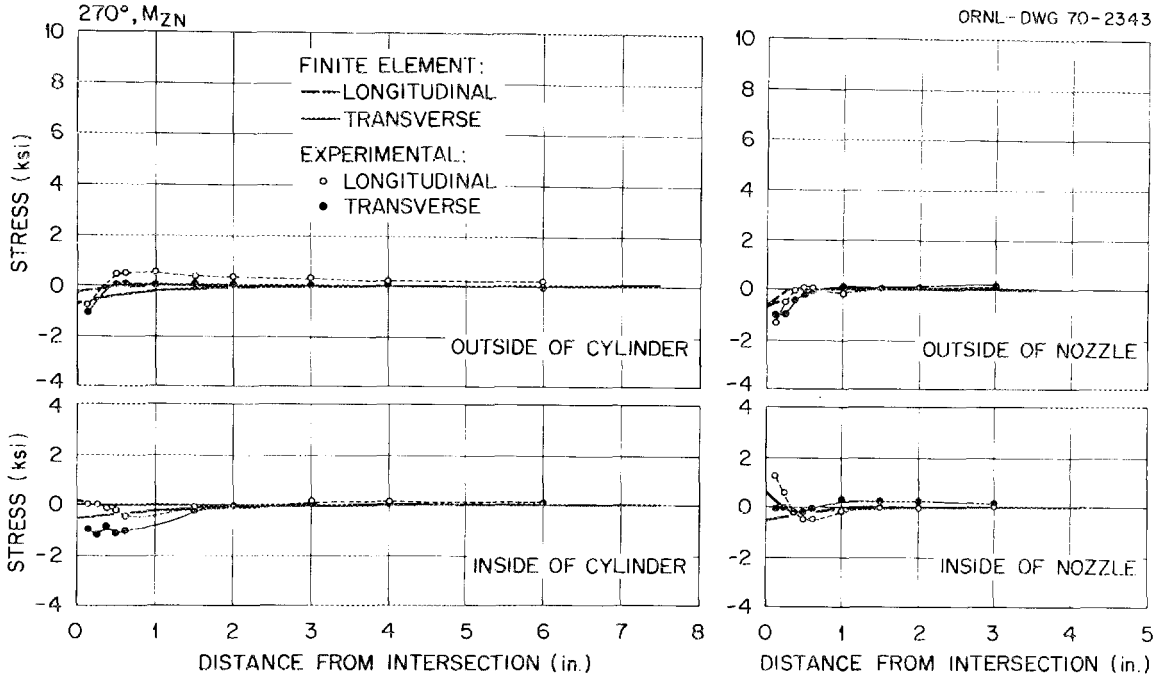

Fig. 55. Measured and predicted stress distributions at 270° for in-plane moment, M_{ZN}, on nozzle.

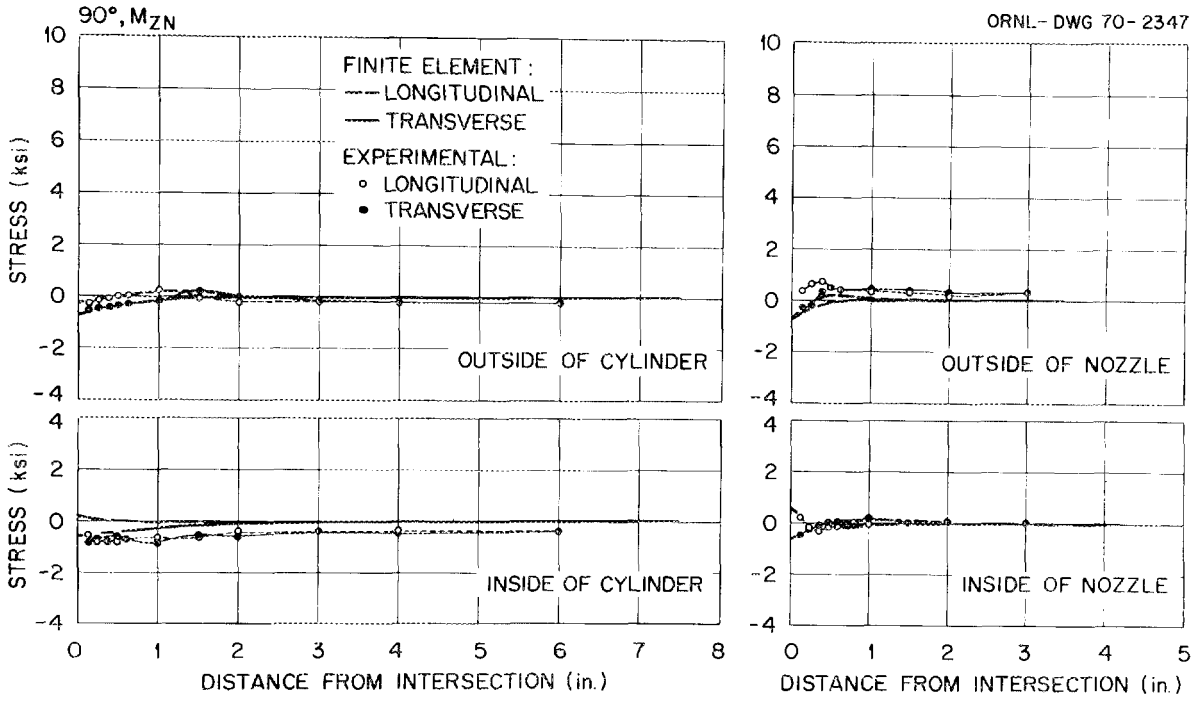

Fig. 56. Measured and predicted stress distributions at 90° for in-plane moment, M_{ZN}, on nozzle.

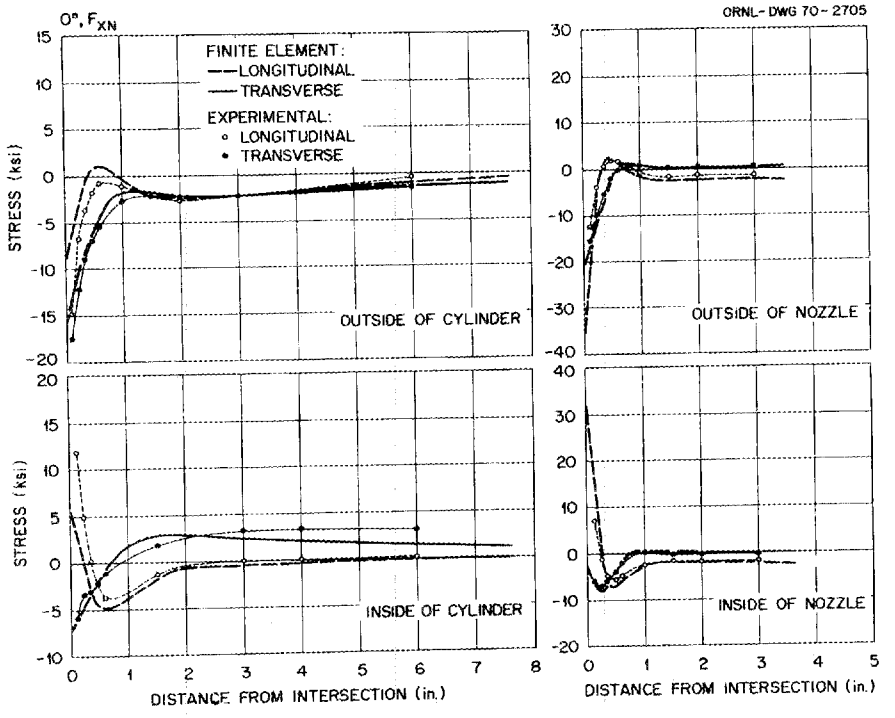

Fig. 57. Measured and predicted stress distributions at 0° for in-plane force, F_{XN}, on nozzle.

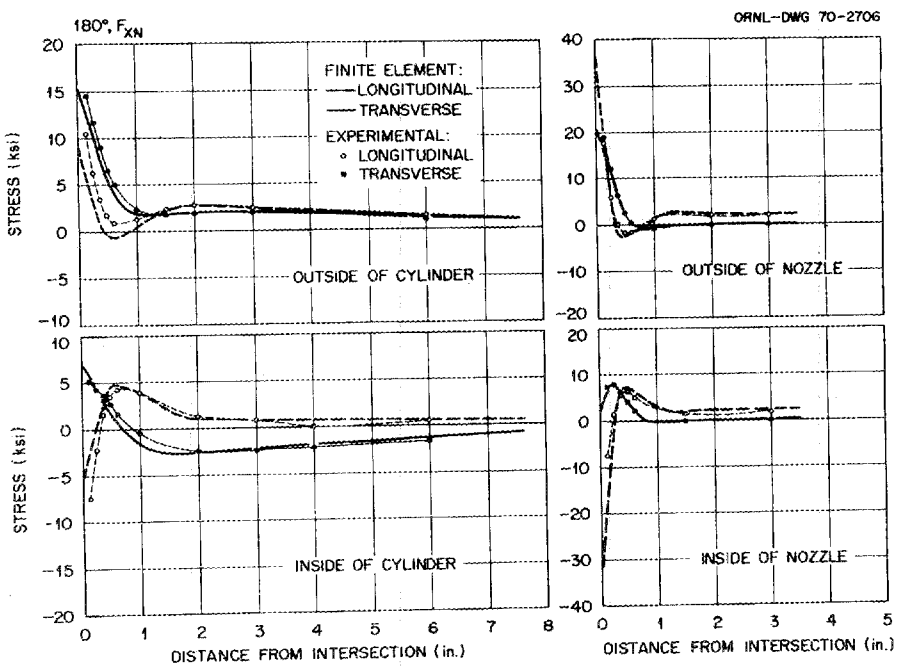

Fig. 58. Measured and predicted stress distributions at 180° for in-plane force, F_{XN}, on nozzle.

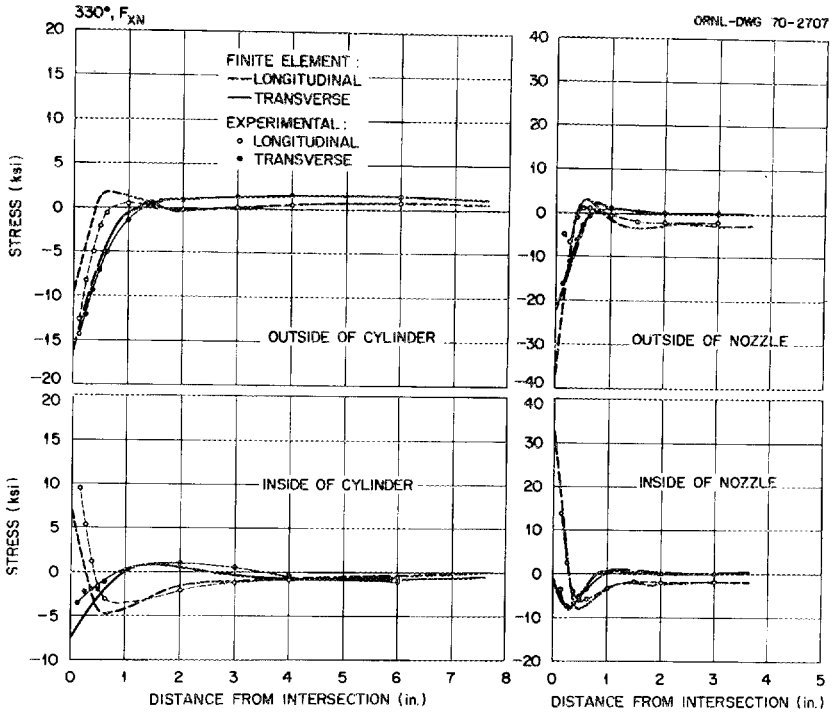

Fig. 59. Measured and predicted stress distributions at 330° for in-plane force, F_{XN}, on nozzle.

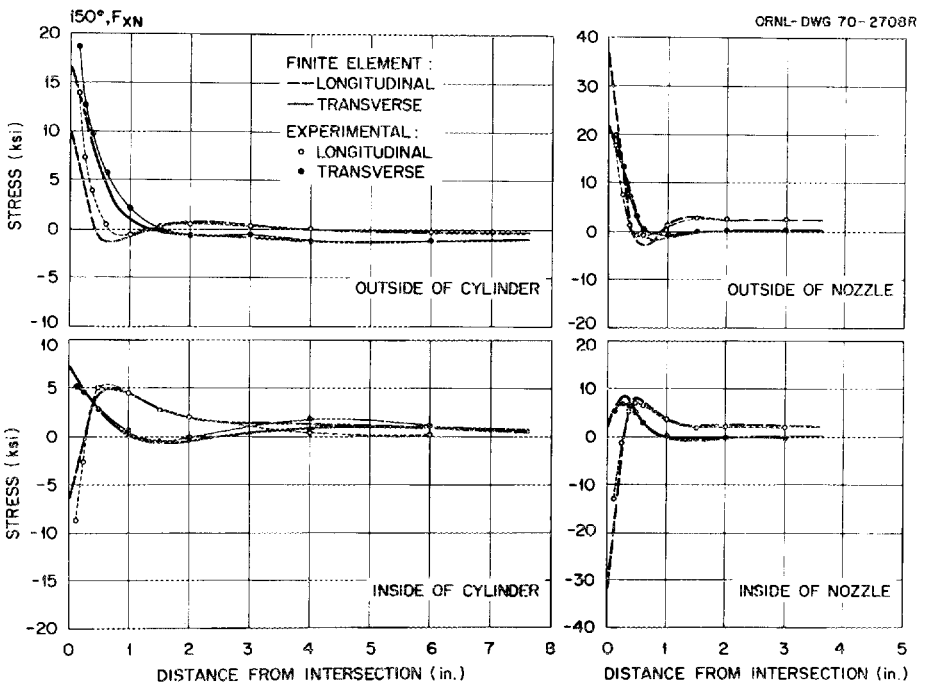

Fig. 60. Measured and predicted stress distributions at 150° for in-plane force, F_{XN}, on nozzle.

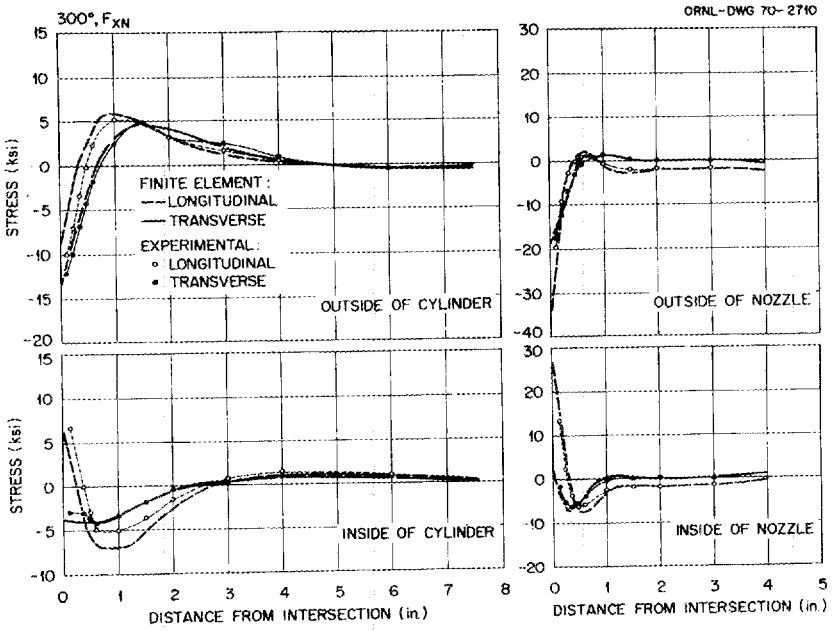

Fig. 61. Measured and predicted stress distributions at 300° for in-plane force, F_{XN}, on nozzle.

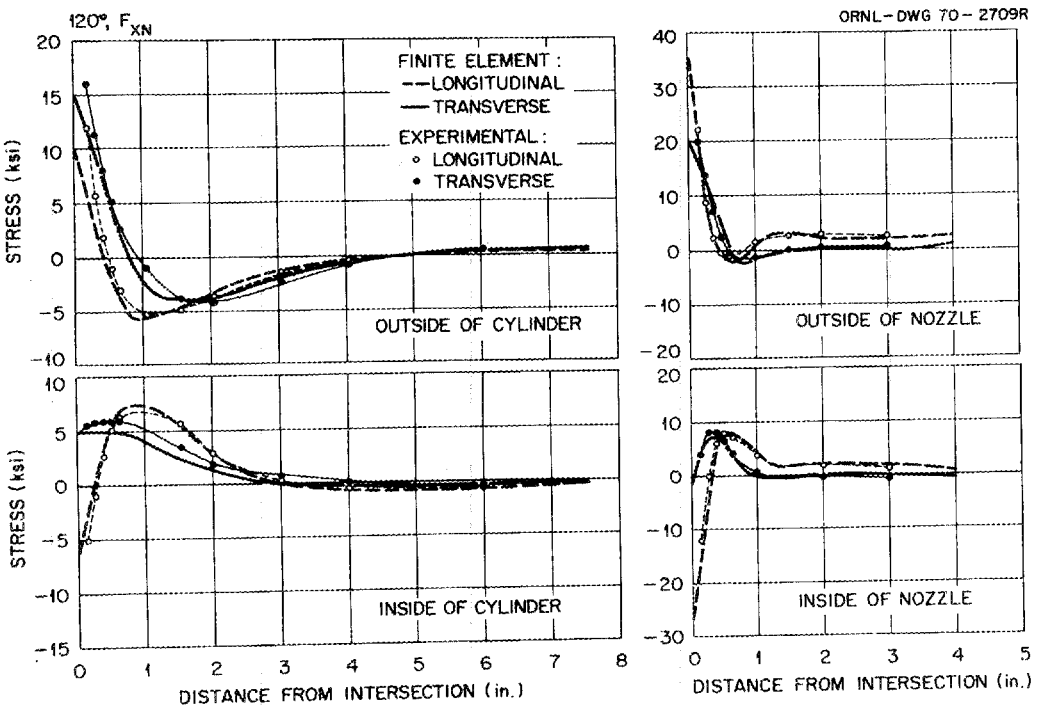

Fig. 62. Measured and predicted stress distributions at 120° for in-plane force, F_{XN}, on nozzle.

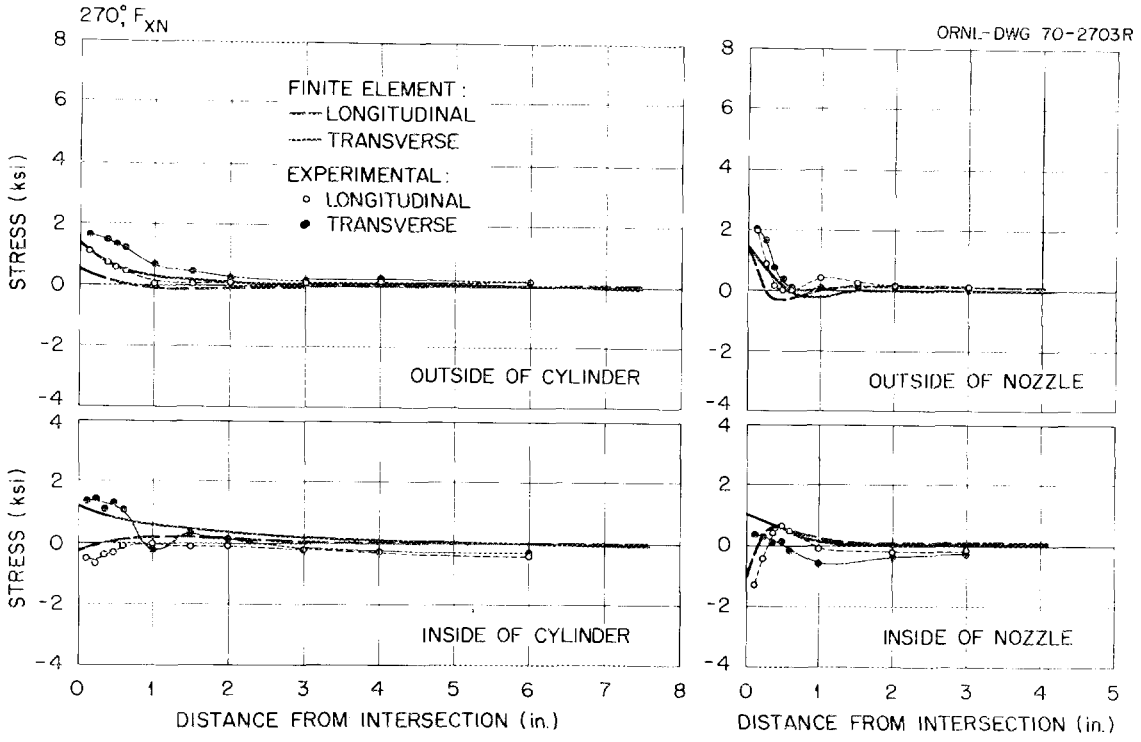

Fig. 63. Measured and predicted stress distributions at 270° for in-plane force, F_{XN}, on nozzle.

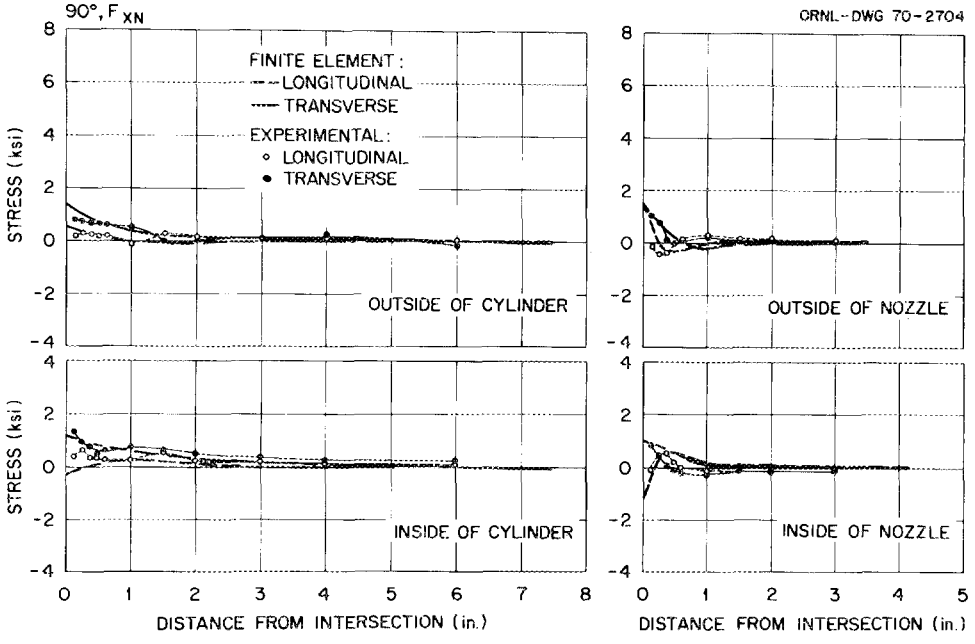

Fig. 64. Measured and predicted stress distributions at 90° for in-plane force, F_{XN}, on nozzle.

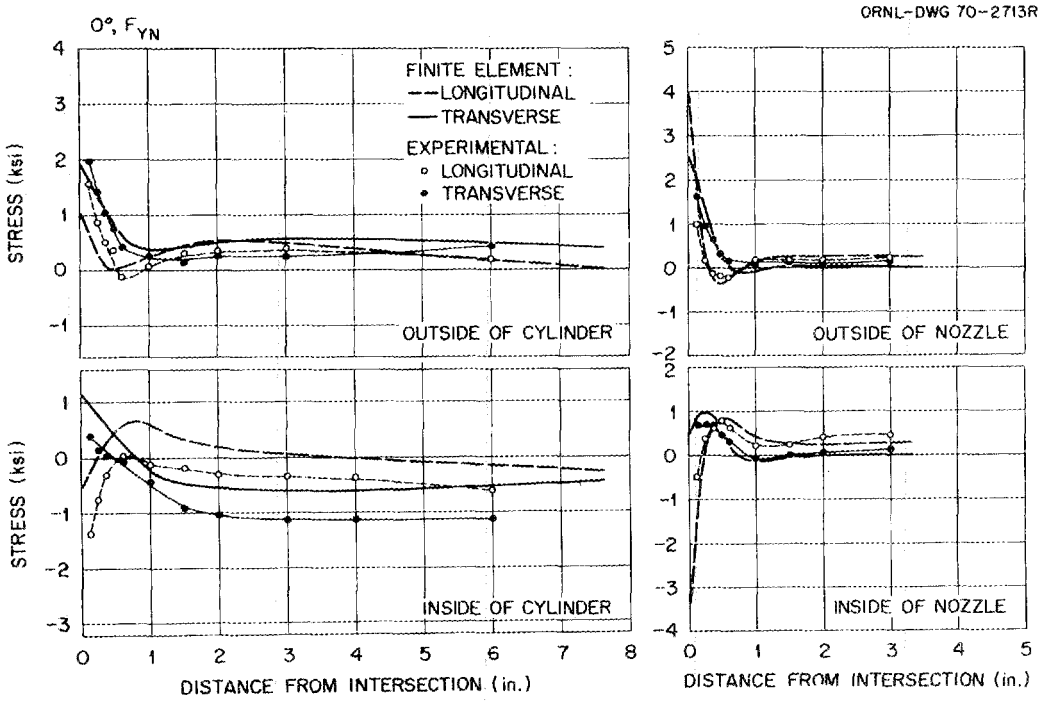

Fig. 65. Measured and predicted stress distributions at 0° for axial force, F_{YN}, on nozzle.

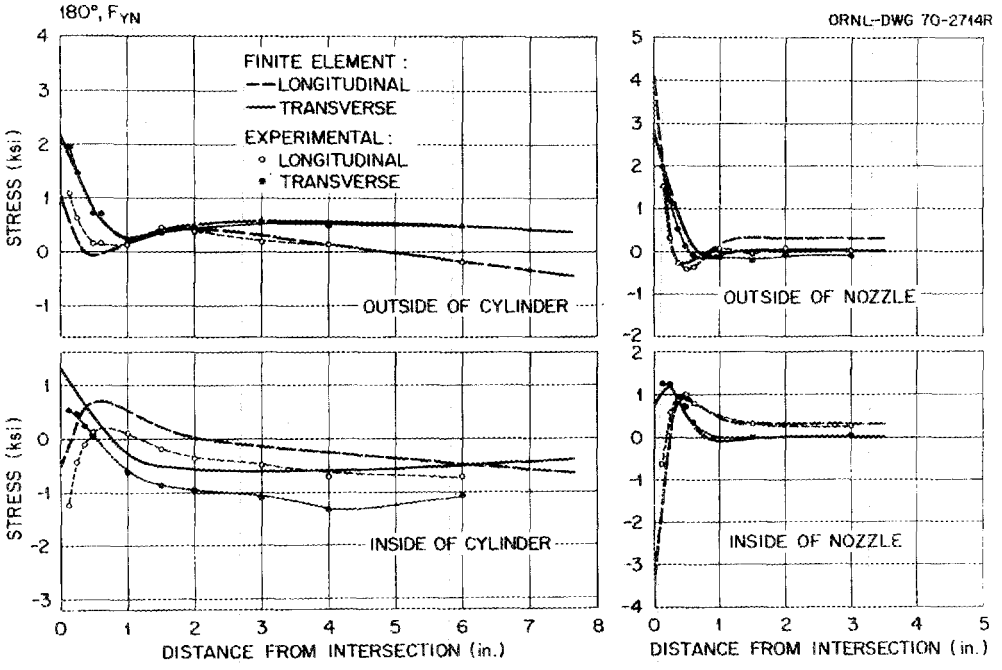

Fig. 66. Measured and predicted stress distributions at 180° for axial force, F_{YN}, on nozzle.

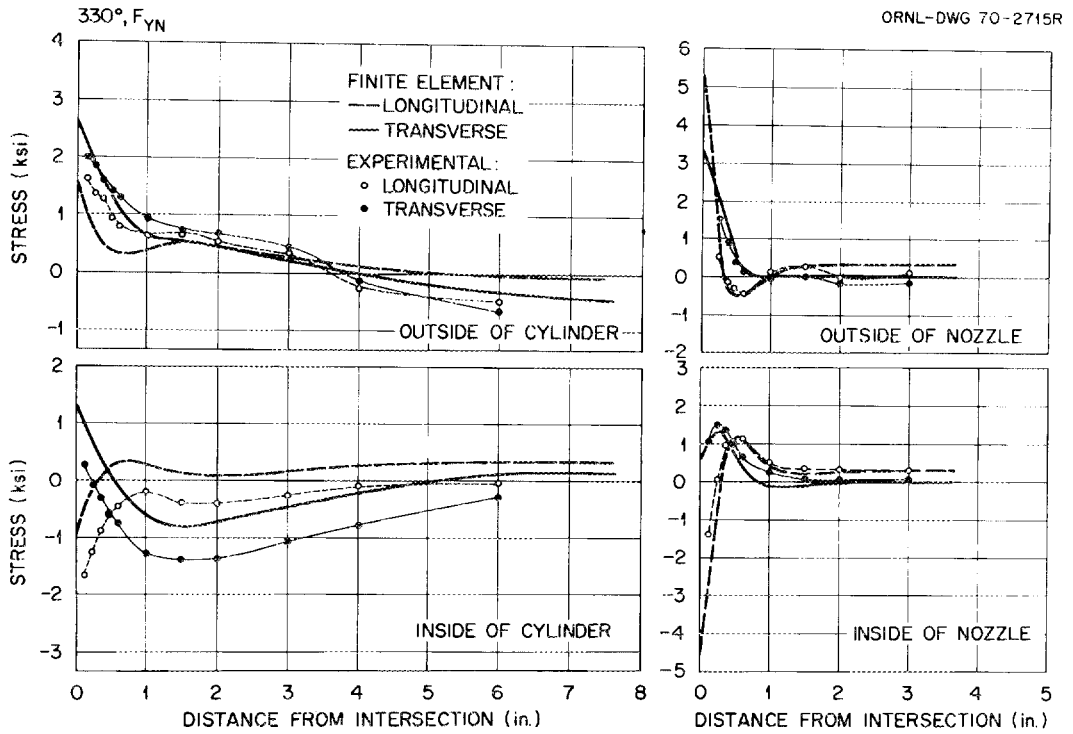

Fig. 67. Measured and predicted stress distributions at 330° for axial force, F_{YN}, on nozzle.

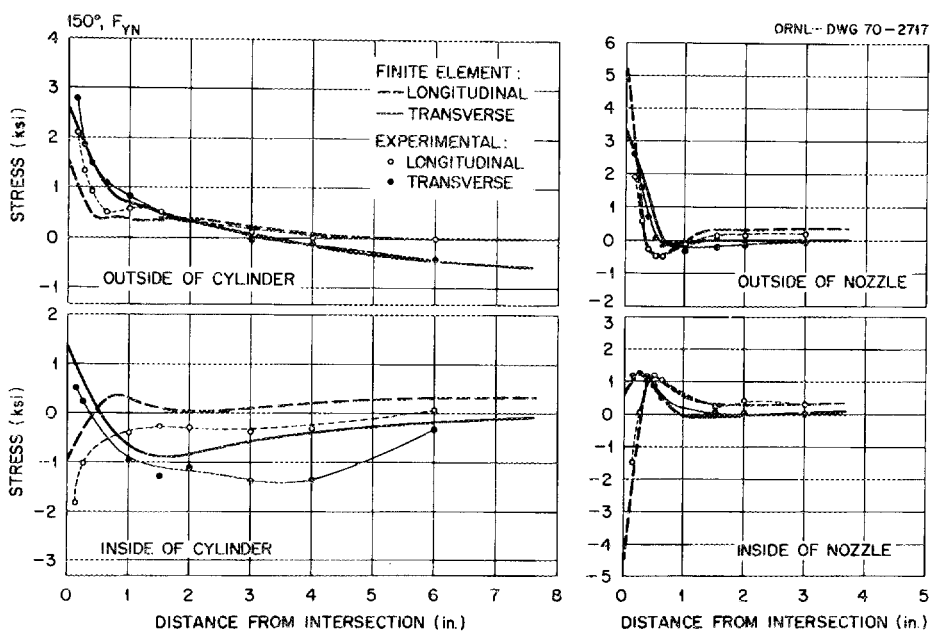

Fig. 68. Measured and predicted stress distributions at 150° for axial force, F_{YN}, on nozzle.

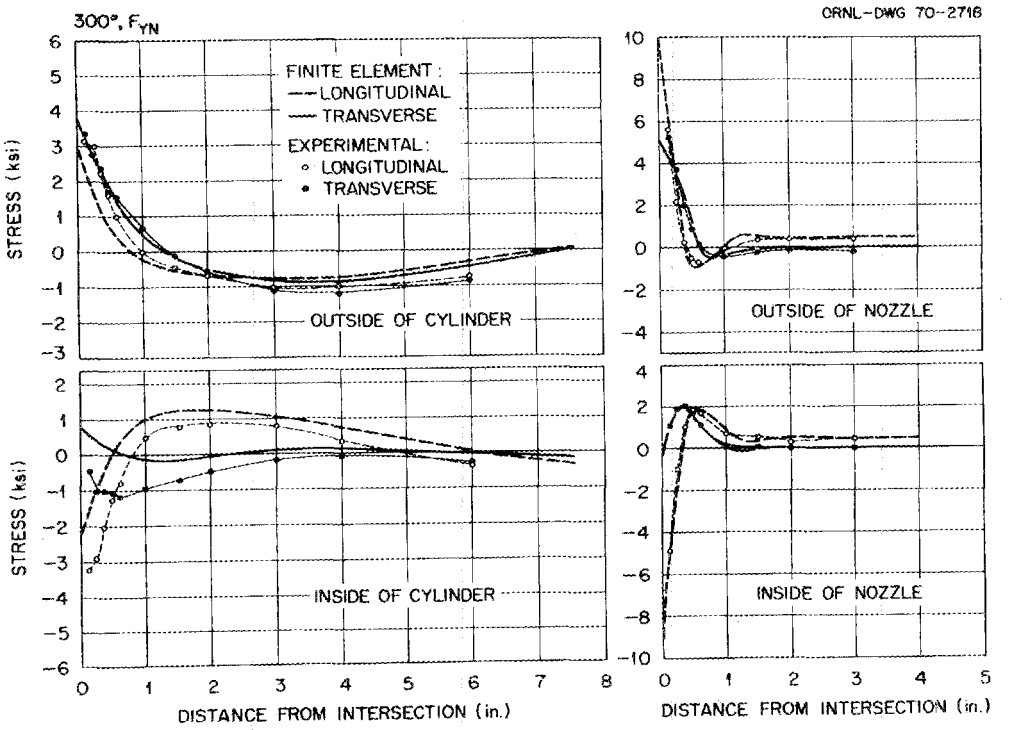

Fig. 69. Measured and predicted stress distributions at 300° for axial force, F_{YN}, on nozzle.

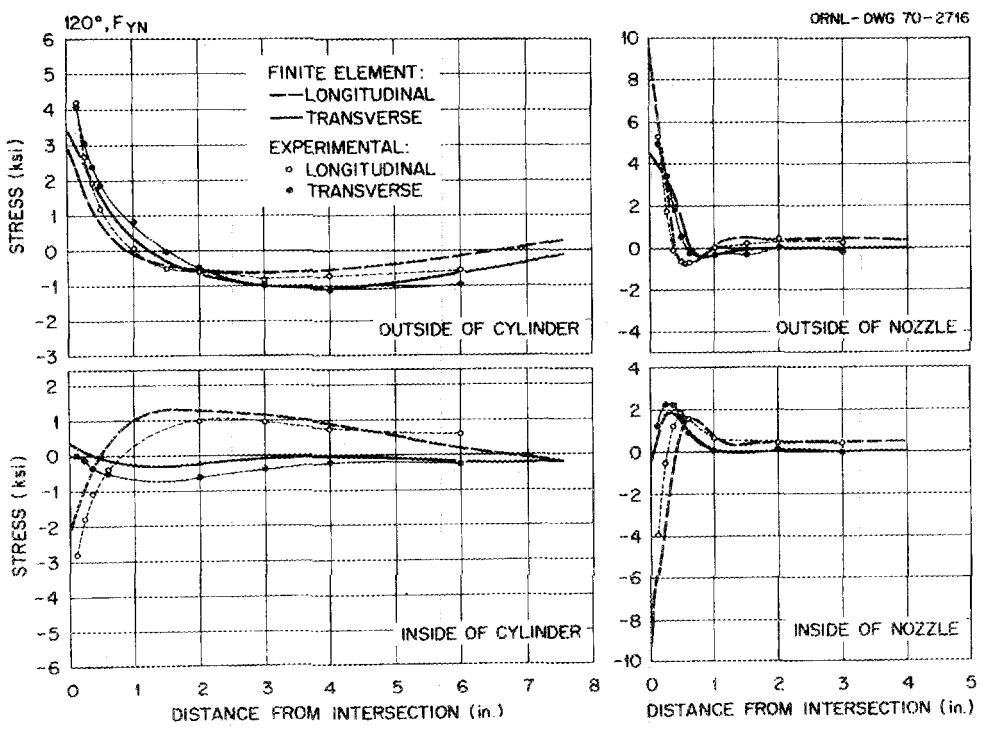

Fig. 70. Measured and predicted stress distributions at 120° for axial force, F_{YN}, on nozzle.

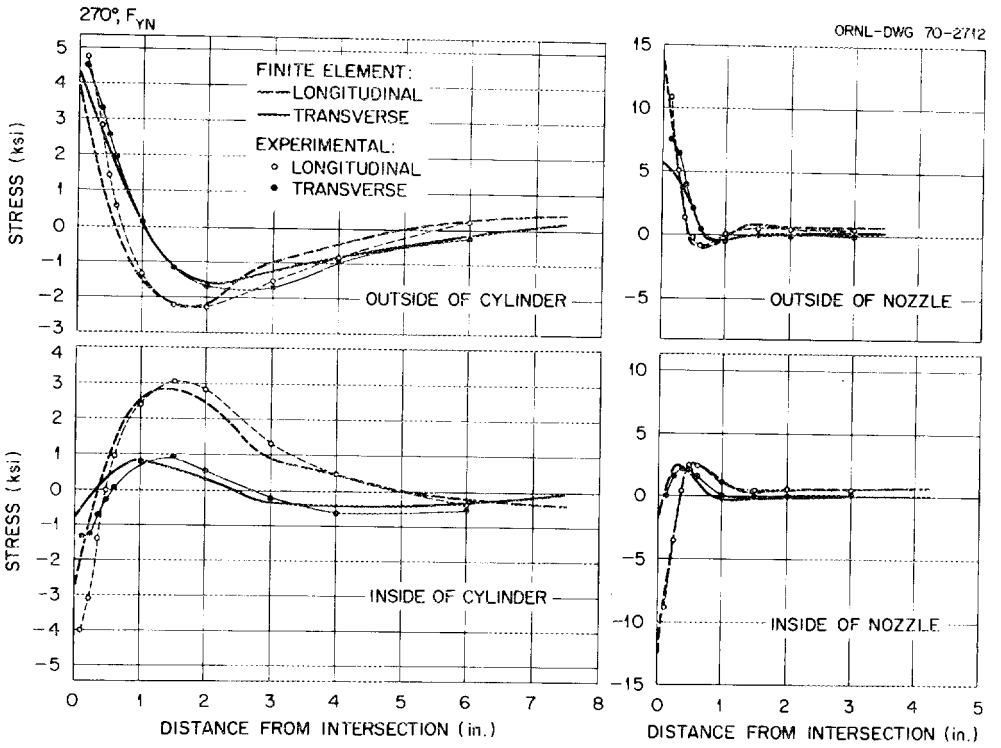

Fig. 71. Measured and predicted stress distributions at 270° for axial force, F_{YN}, on nozzle.

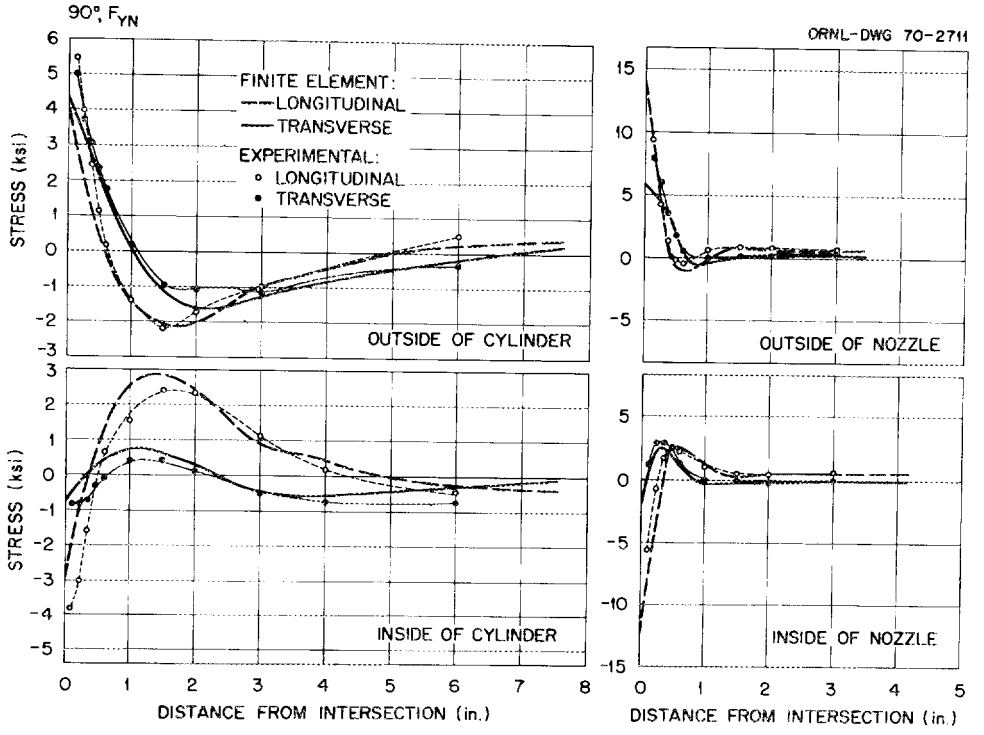

Fig. 72. Measured and predicted stress distributions at 90° for axial force, F_{YN}, on nozzle.

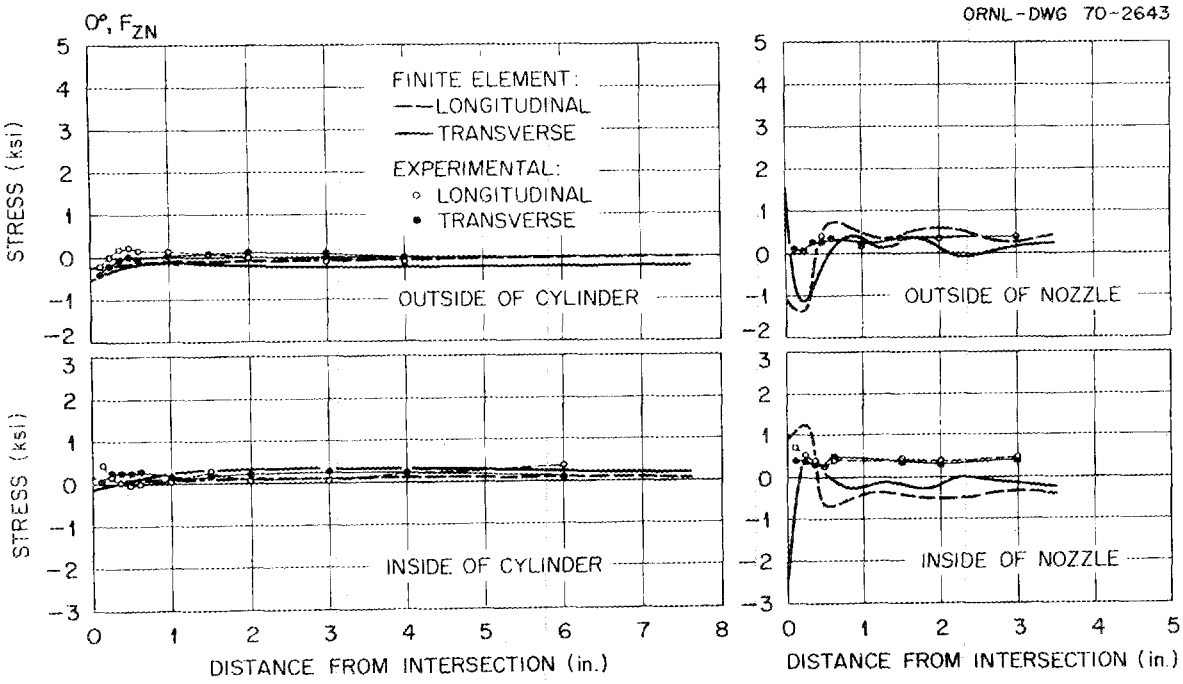

Fig. 73. Measured and predicted stress distributions at 0° for out-of-plane force, F_{ZN}, on nozzle.

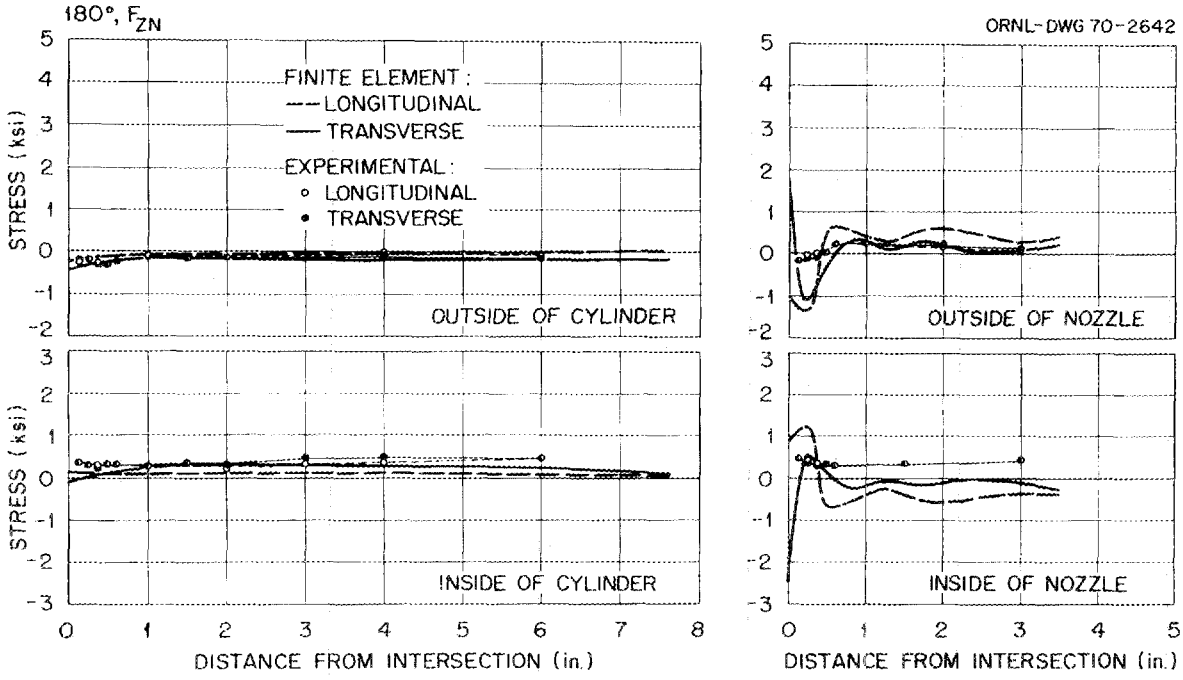

Fig. 74. Measured and predicted stress distributions at 180° for out-of-plane force, F_{ZN}, on nozzle.

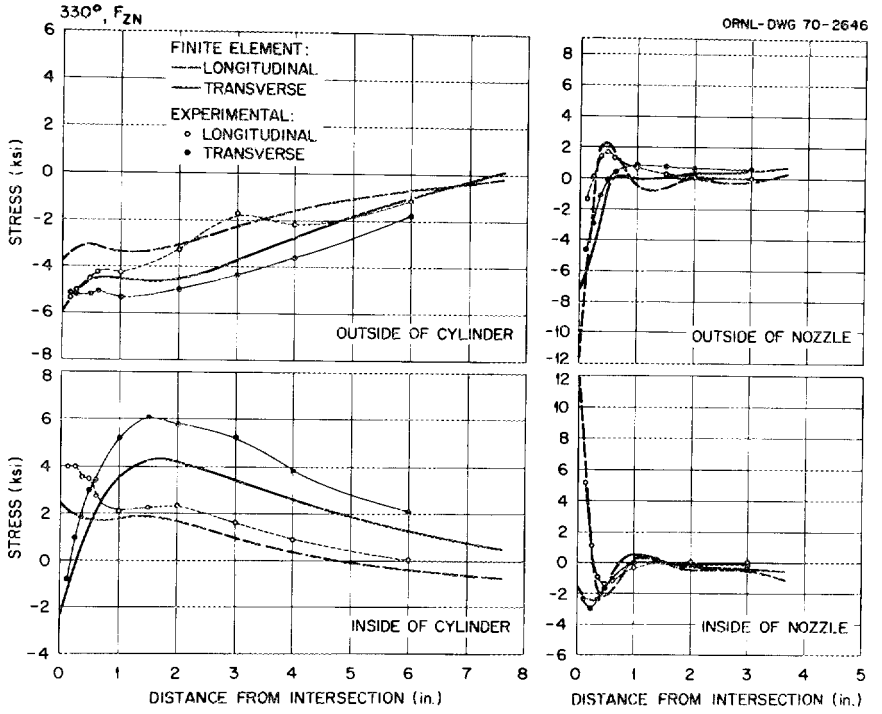

Fig. 75. Measured and predicted stress distributions at 330° for out-of-plane force, F_{ZN}, on nozzle.

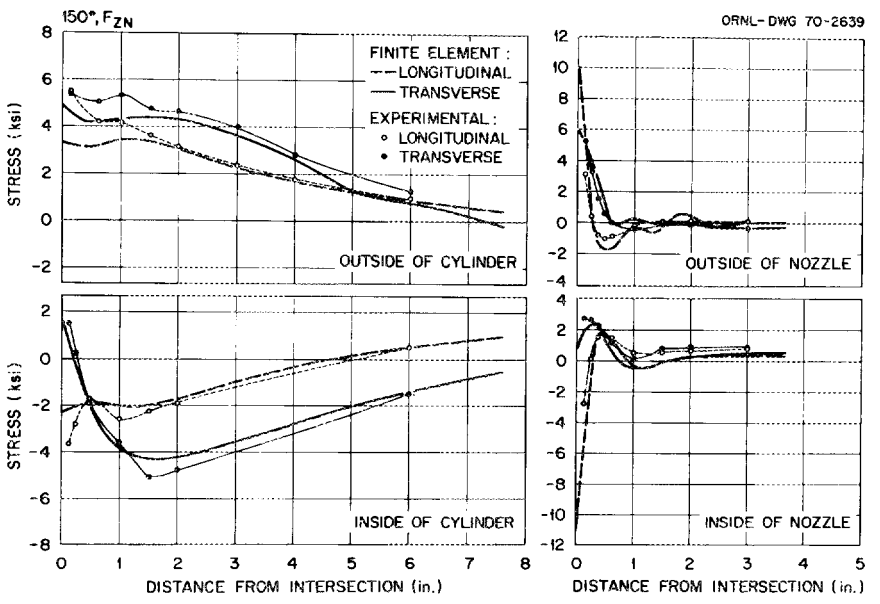

Fig. 76. Measured and predicted stress distributions at 150° for out-of-plane force, F_{ZN}, on nozzle.

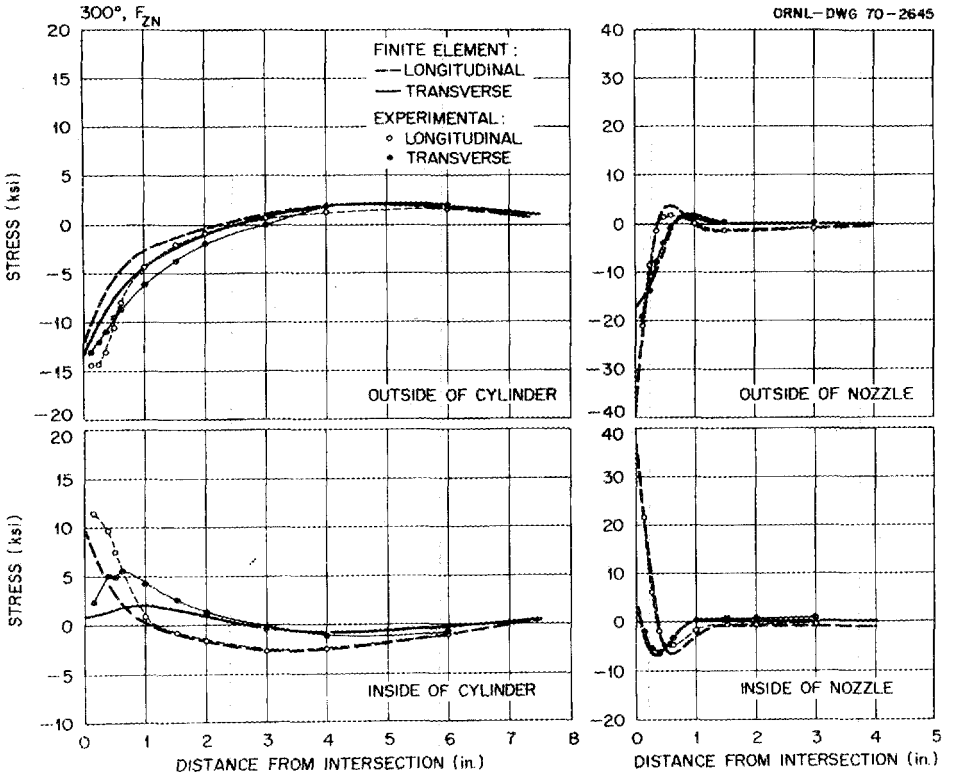

Fig. 77. Measured and predicted stress distributions at 300° for out-of-plane force, F_{ZN}, on nozzle.

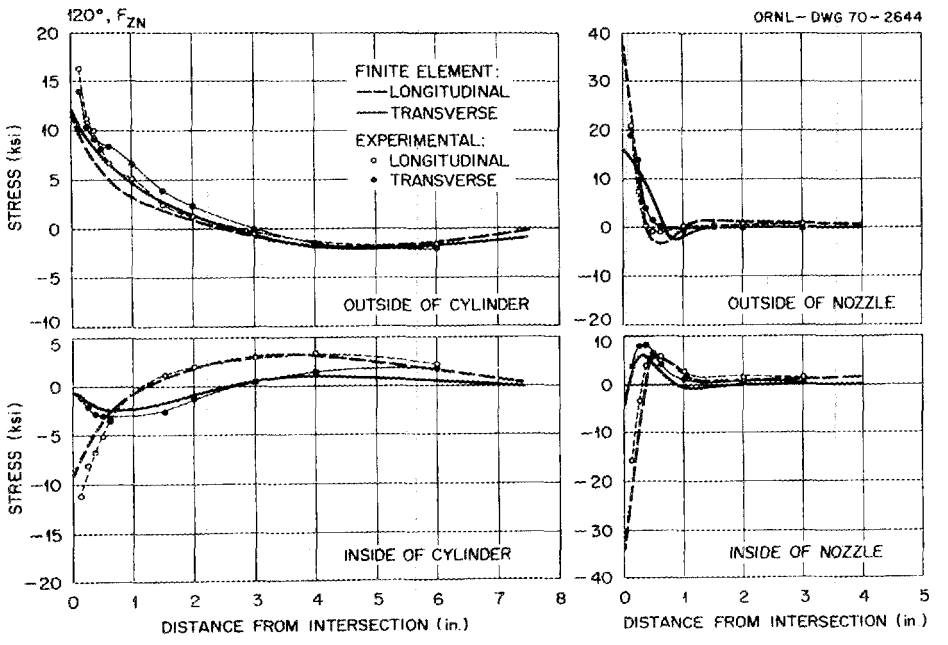

Fig. 78. Measured and predicted stress distributions at 120° for out-of-plane force, F_{ZN}, on nozzle.

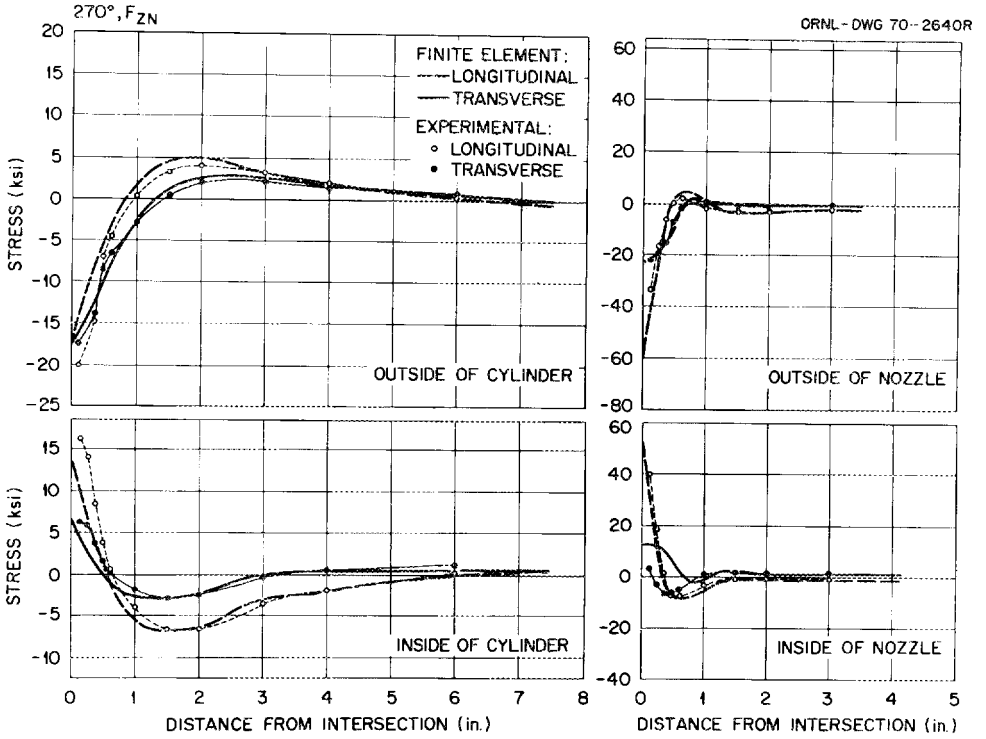

Fig. 79. Measured and predicted stress distributions at 270° for out-of-plane force, F_{ZN}, on nozzle.

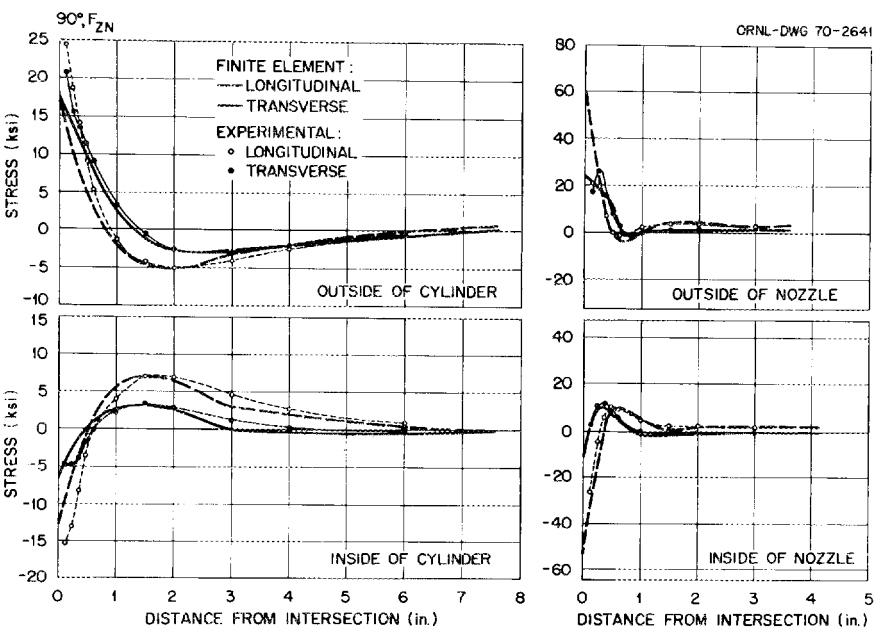

Fig. 80. Measured and predicted stress distributions at 90° for out-of-plane force, F_{ZN}, on nozzle.

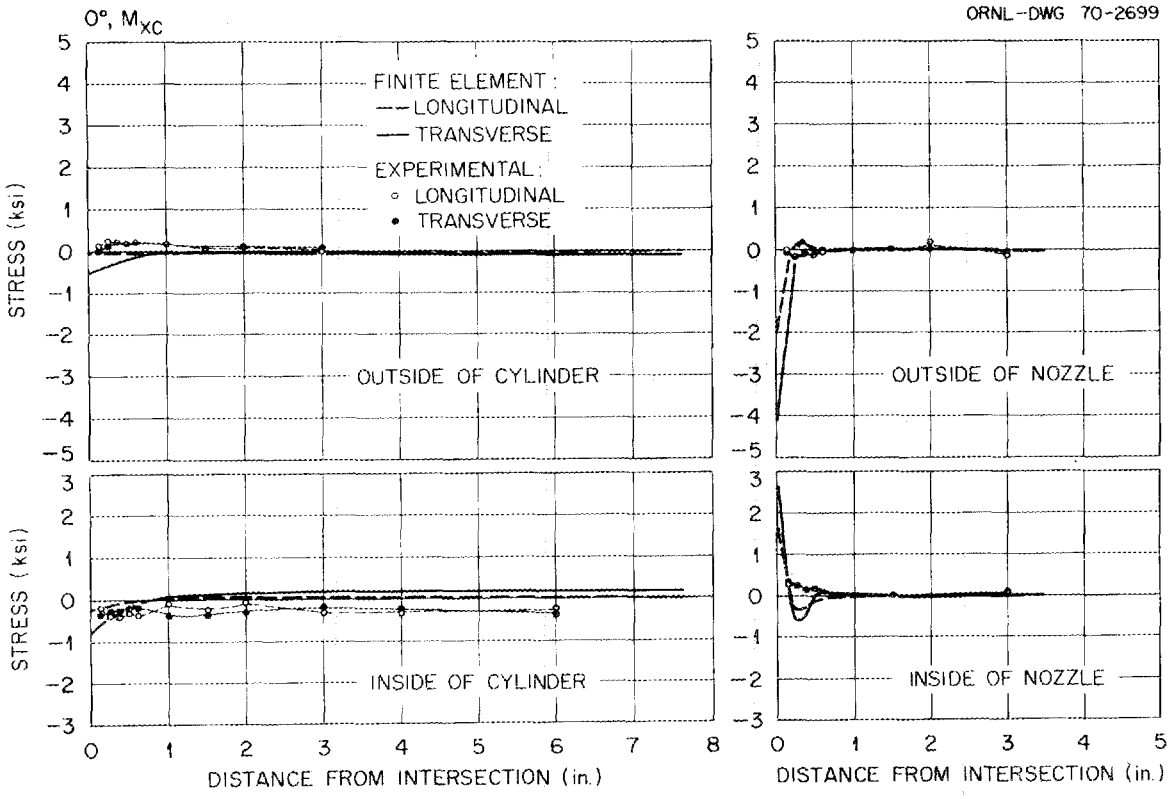

Fig. 81. Measured and predicted stress distributions at 0° for torsional moment, M_{XC}, on cylinder.

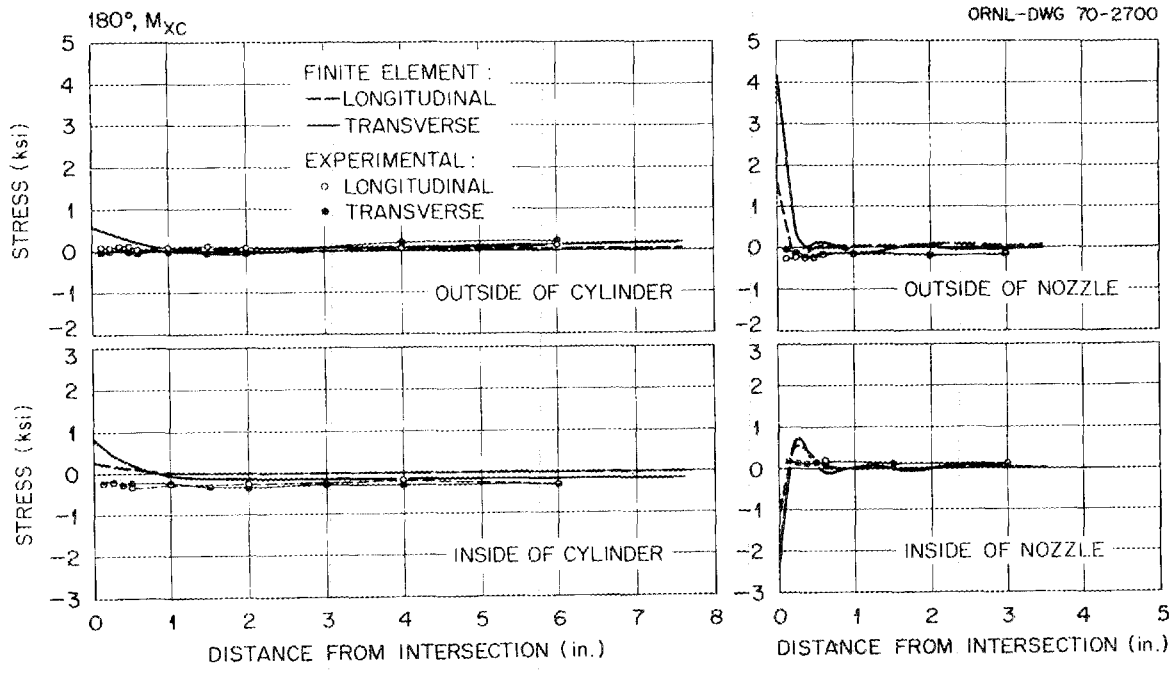

Fig. 82. Measured and predicted stress distributions at 180° for torsional moment, M_{XC}, on cylinder.

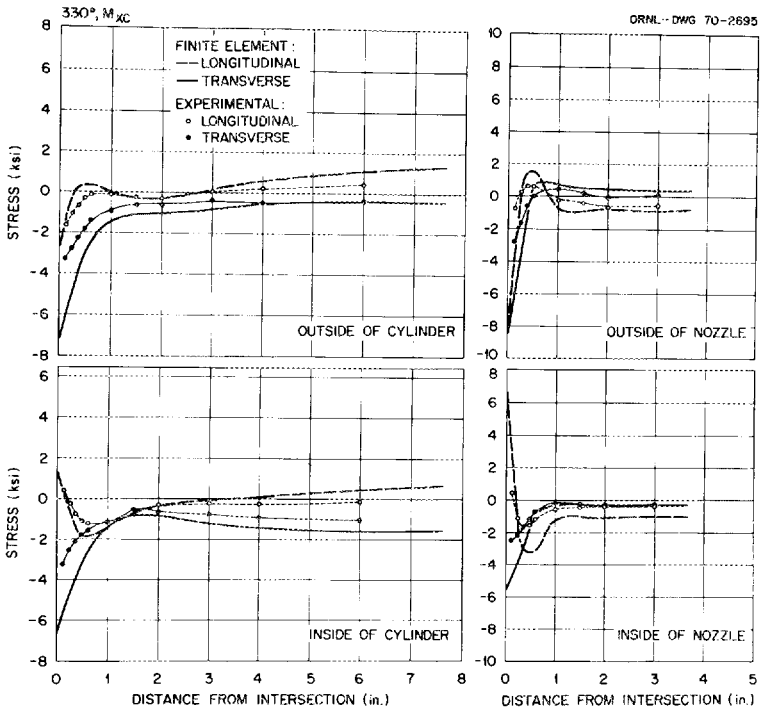

Fig. 83. Measured and predicted stress distributions at 330° for torsional moment, M_{XC}, on cylinder.

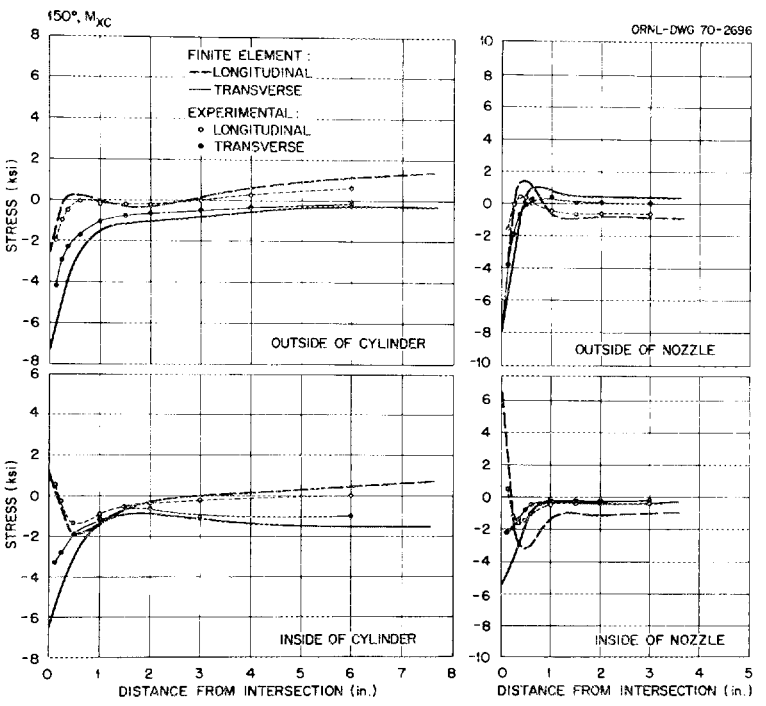

Fig. 84. Measured and predicted stress distributions at 150° for torsional moment, M_{XC}, on cylinder.

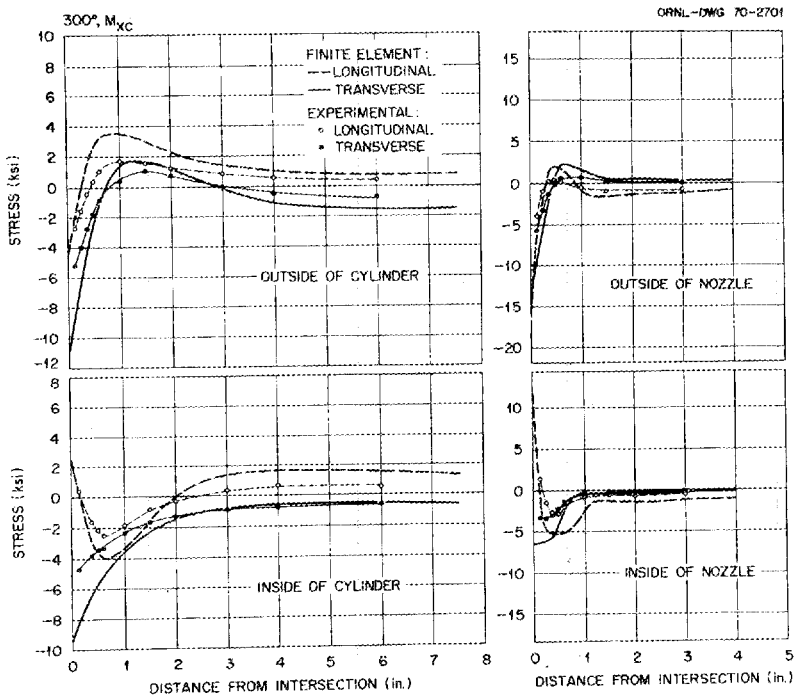

Fig. 85. Measured and predicted stress distributions at 300° for torsional moment, M_{XC}, on cylinder.

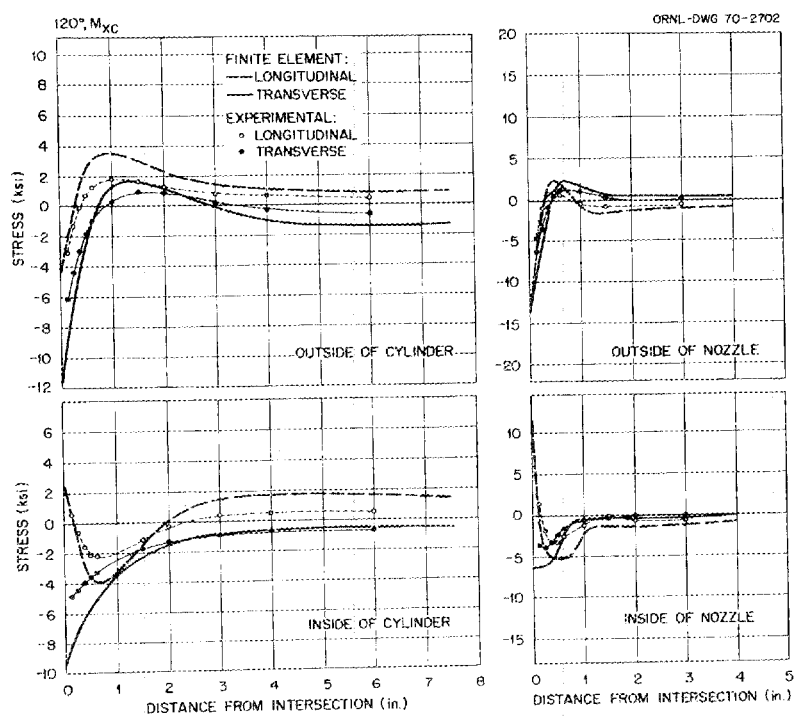

Fig. 86. Measured and predicted stress distributions at 120° for torsional moment, M_{XC}, on cylinder.

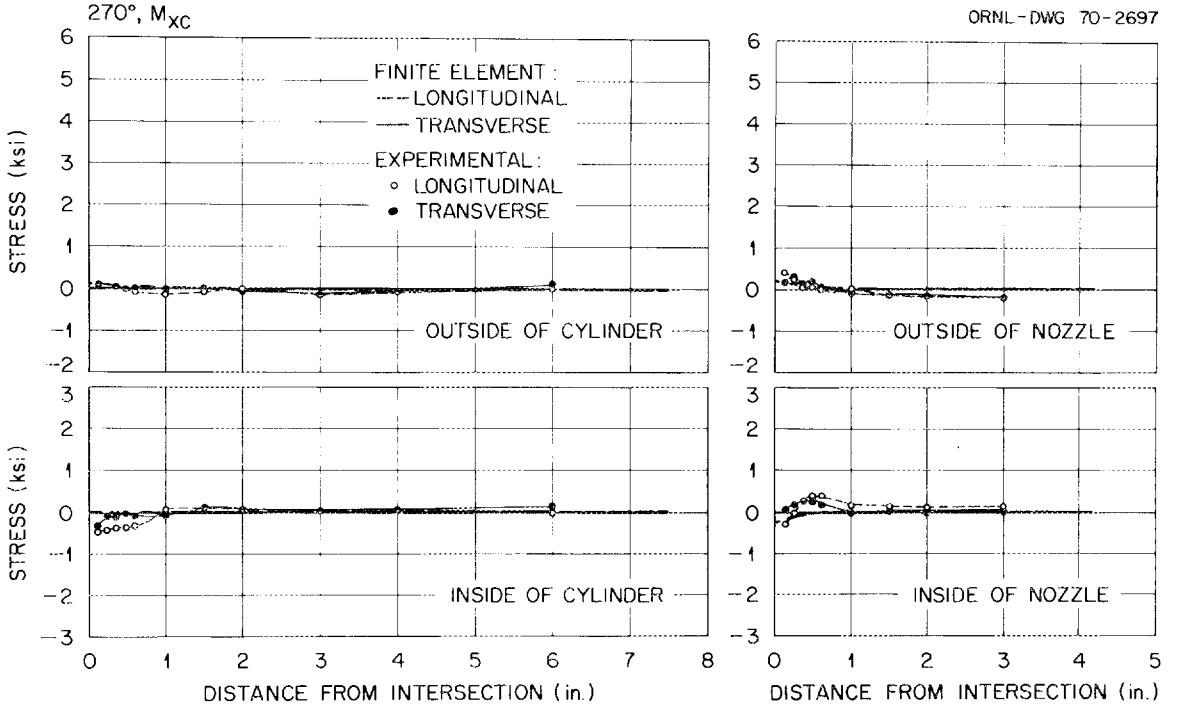

Fig. 87. Measured and predicted stress distributions at 270° for torsional moment, M_{XC}, on cylinder.

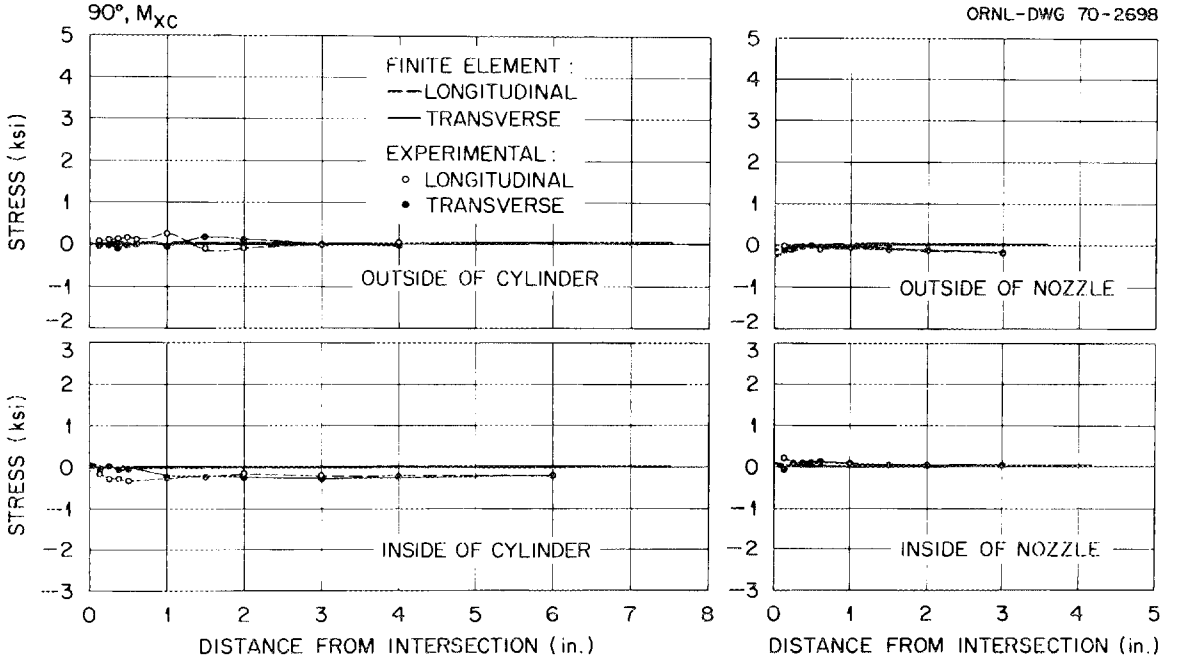

Fig. 88. Measured and predicted stress distributions at 90° for torsional moment, M_{XC}, on cylinder.

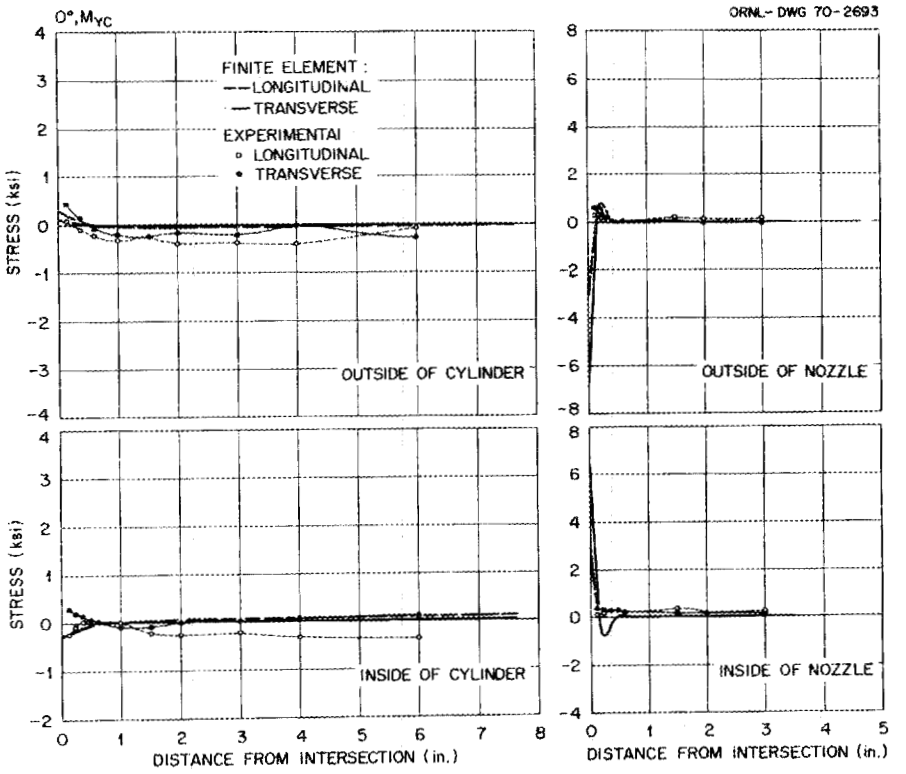

Fig. 89. Measured and predicted stress distributions at 0° for out-of-plane moment, M_{YC}, on cylinder.

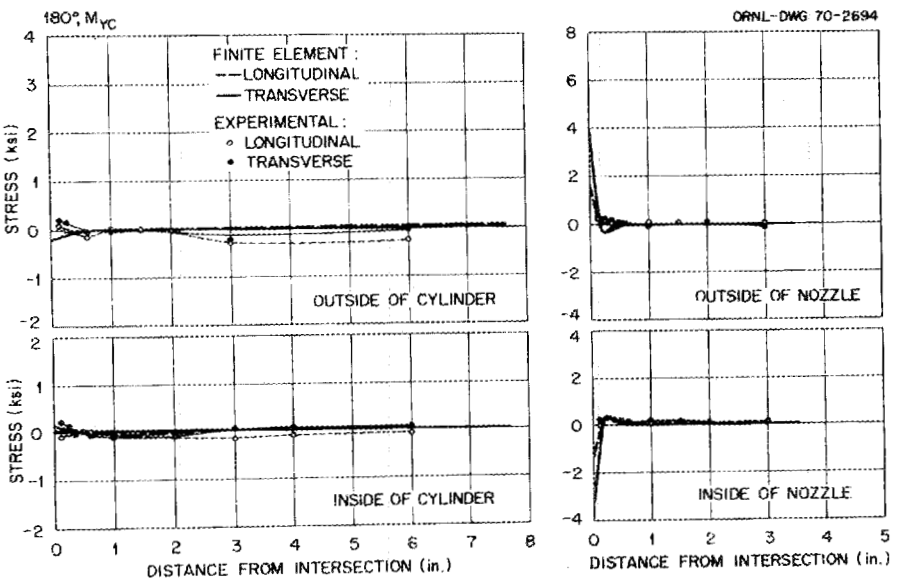

Fig. 90. Measured and predicted stress distributions at 180° for out-of-plane moment, M_{YC}, on cylinder.

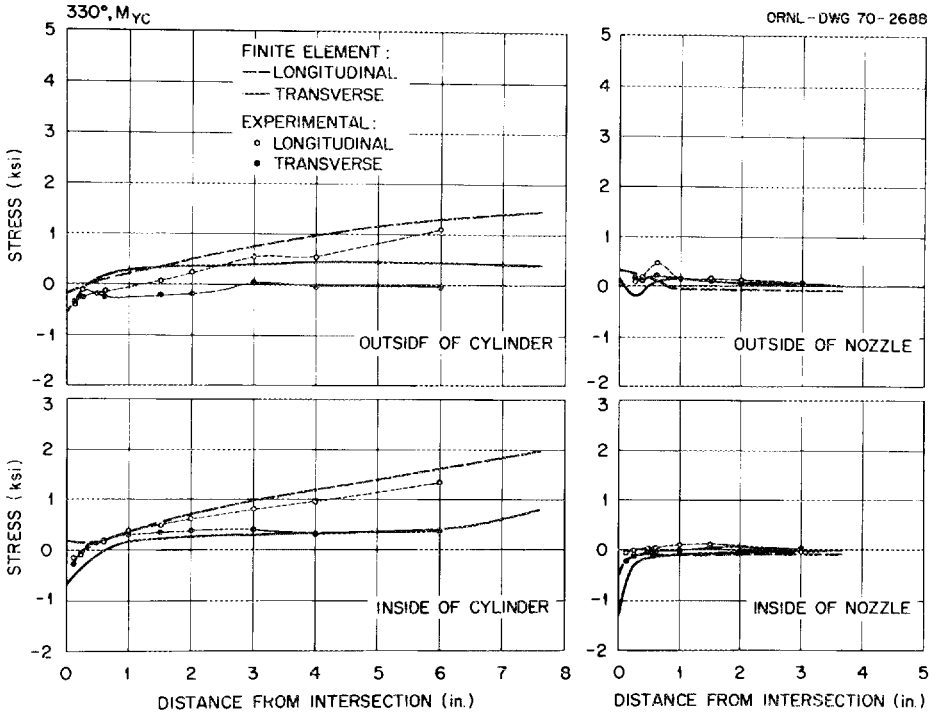

Fig. 91. Measured and predicted stress distributions at 330° for out-of-plane moment, M_{YC}, on cylinder.

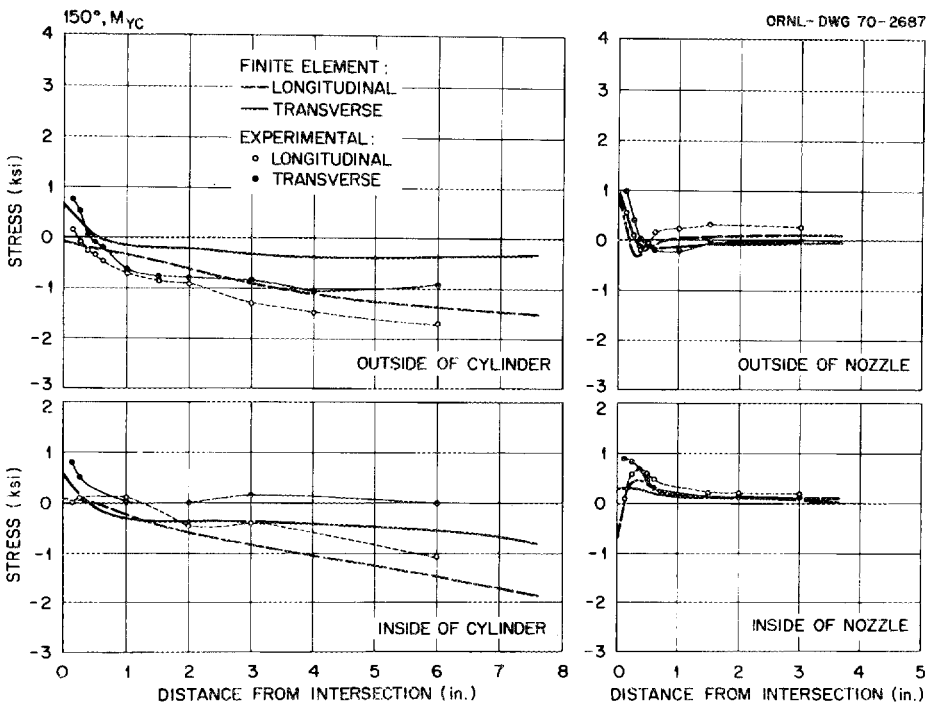

Fig. 92. Measured and predicted stress distributions at 150° for out-of-plane moment, M_{YC}, on cylinder.

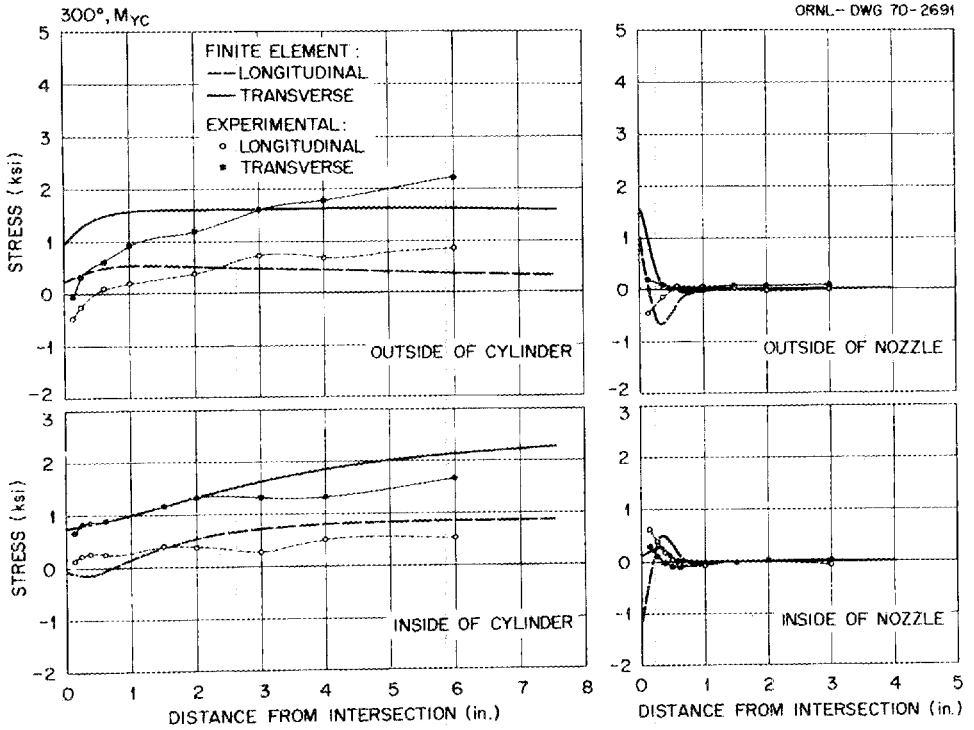

Fig. 93. Measured and predicted stress distributions at 300° for out-of-plane moment, M_{YC}, on cylinder.

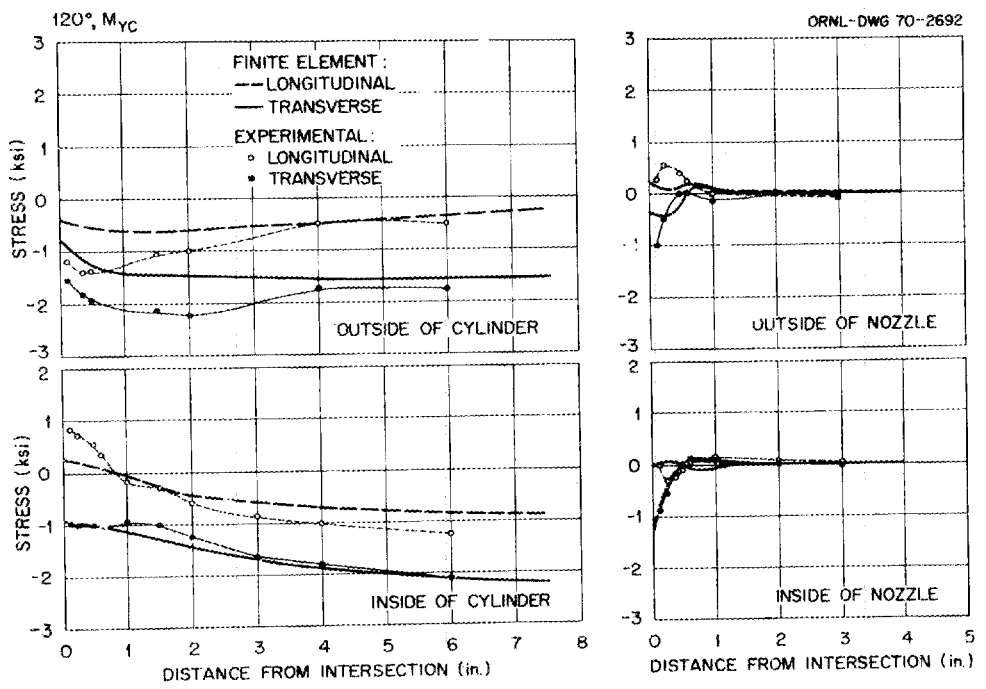

Fig. 94. Measured and predicted stress distributions at 120° for out-of-plane moment, M_{YC}, on cylinder.

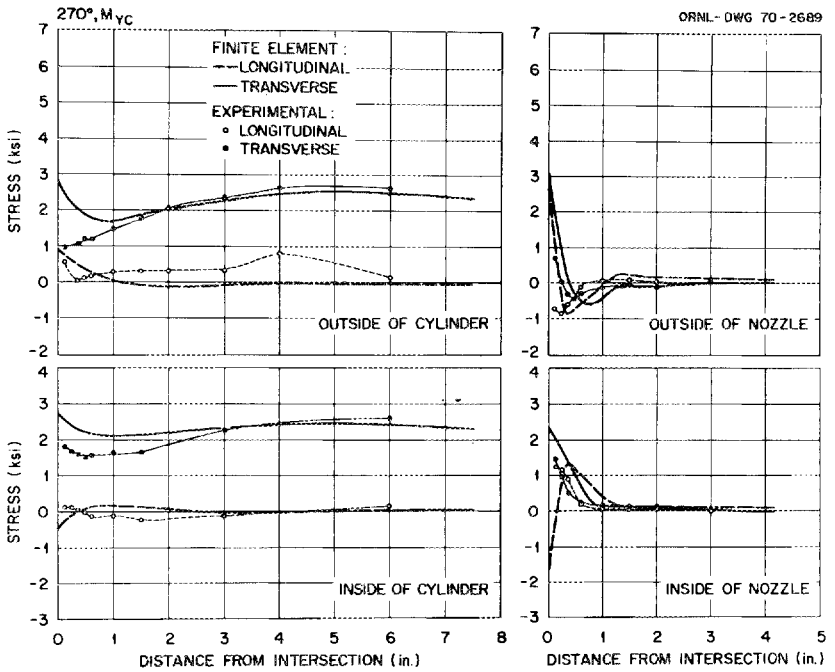

Fig. 95. Measured and predicted stress distributions at 270° for out-of-plane moment, M_{YC}, on cylinder.

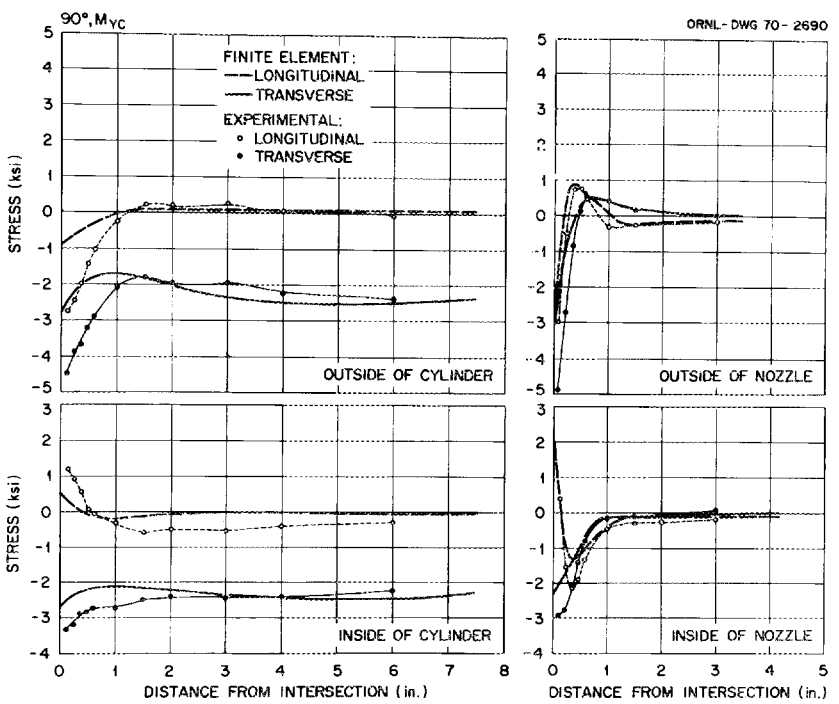

Fig. 96. Measured and predicted stress distributions at 90° for out-of-plane moment, M_{YC}, on cylinder.

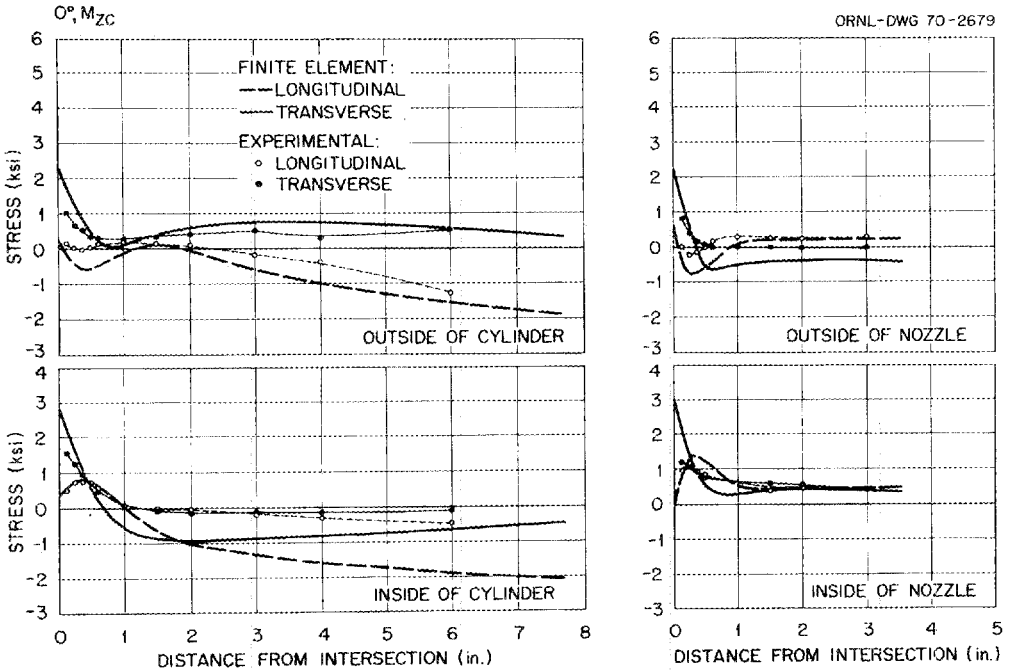

Fig. 97. Measured and predicted stress distributions at 0° for in-plane moment, M_{ZC}, on cylinder.

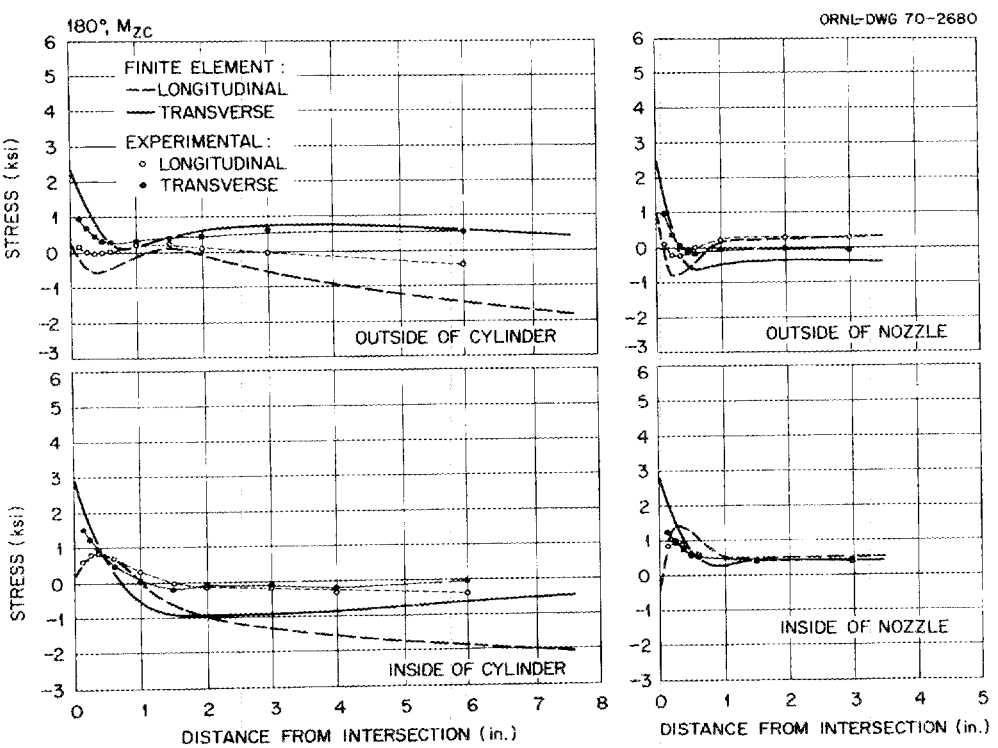

Fig. 98. Measured and predicted stress distributions at 180° for in-plane moment, M_{ZC}, on cylinder.

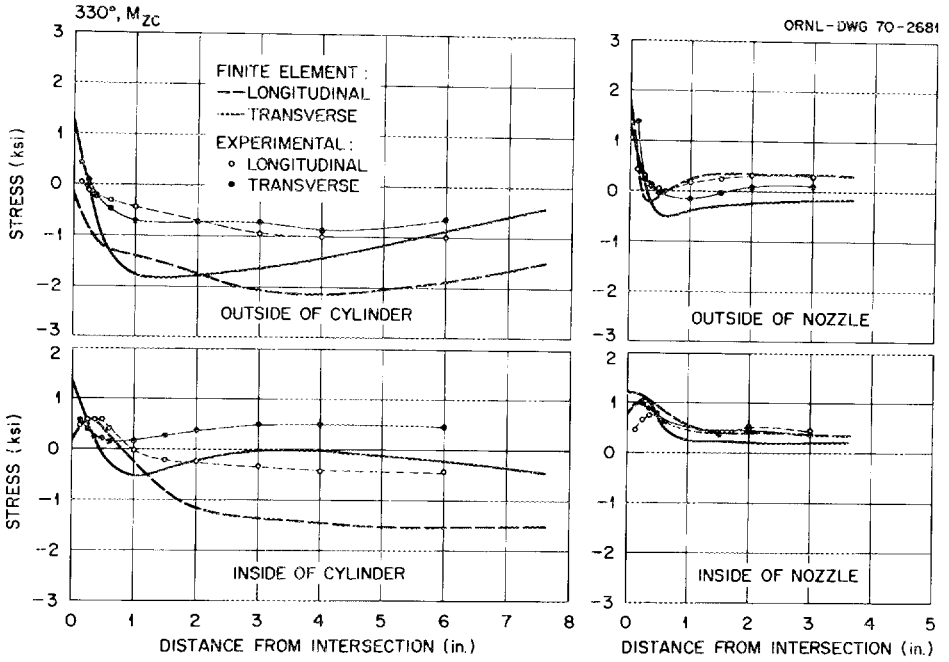

Fig. 99. Measured and predicted stress distributions at 330° for in-plane moment, M_{ZC}, on cylinder.

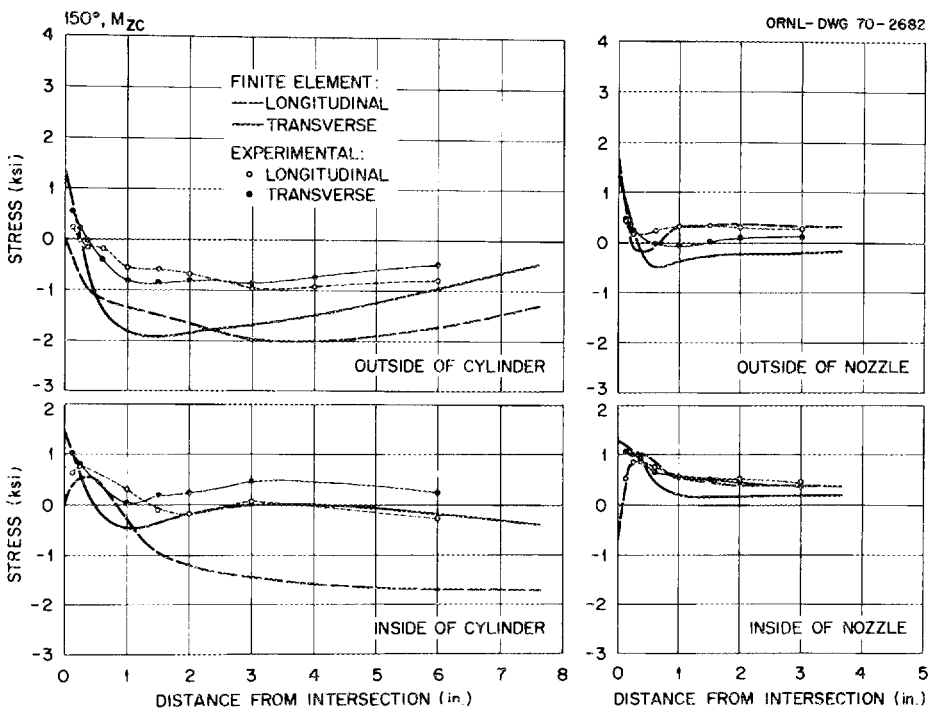

Fig. 100. Measured and predicted stress distributions at 150° for in-plane moment, M_{ZC}, on cylinder.

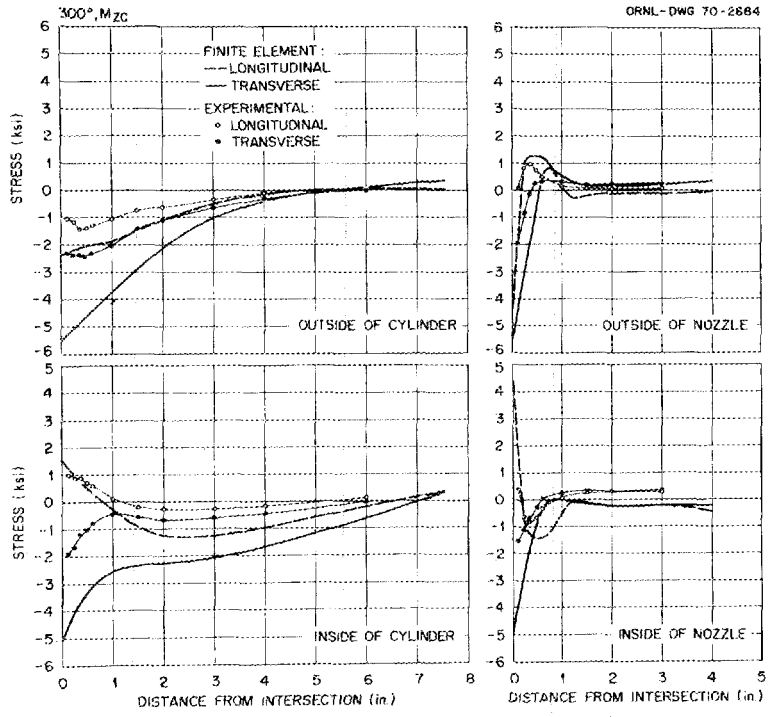

Fig. 101. Measured and predicted stress distributions at 300° for in-plane moment, M_{ZC}, on cylinder.

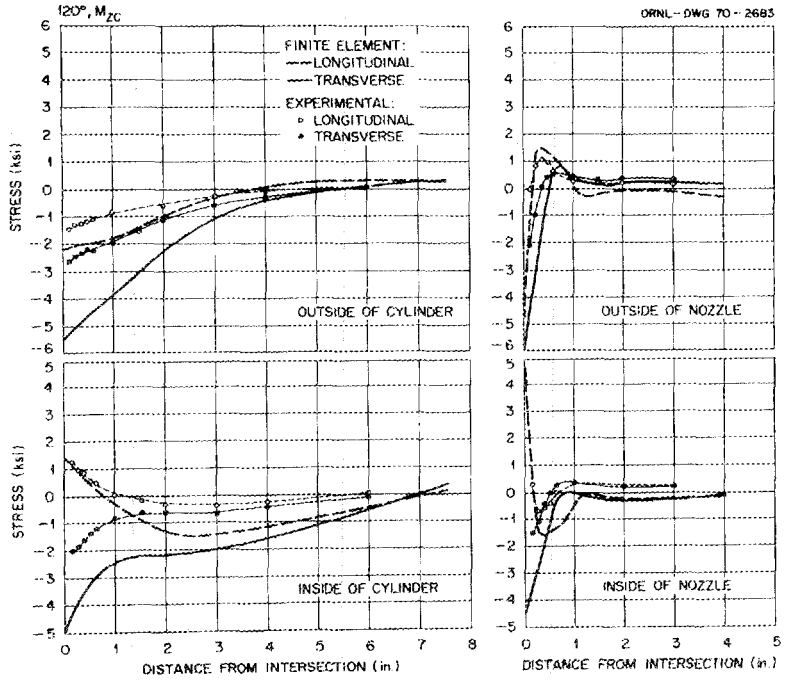

Fig. 102. Measured and predicted stress distributions at 120° for in-plane moment, M_{ZC}, on cylinder.

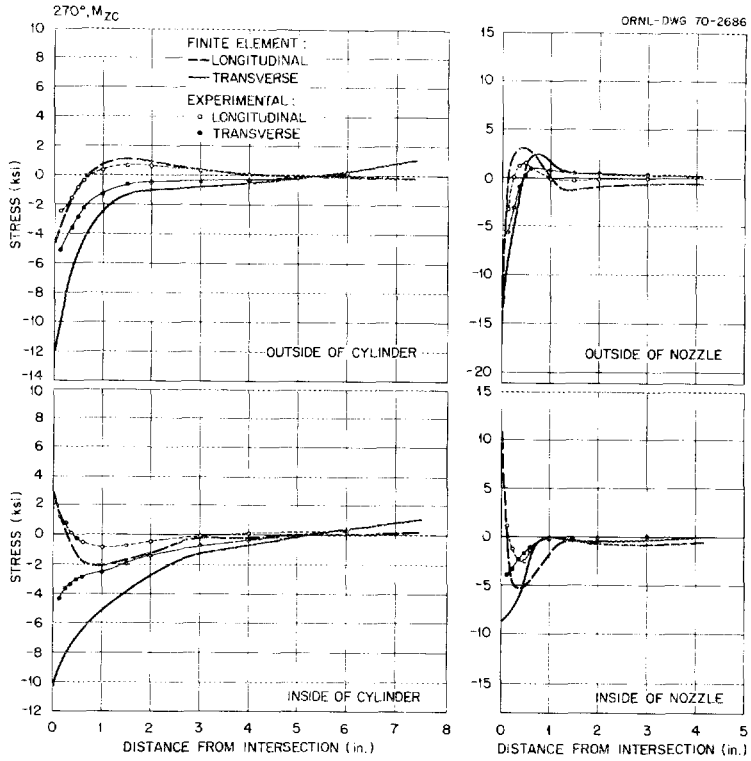

Fig. 103. Measured and predicted stress distributions at 270° for in-plane moment, M_{ZC}, on cylinder.

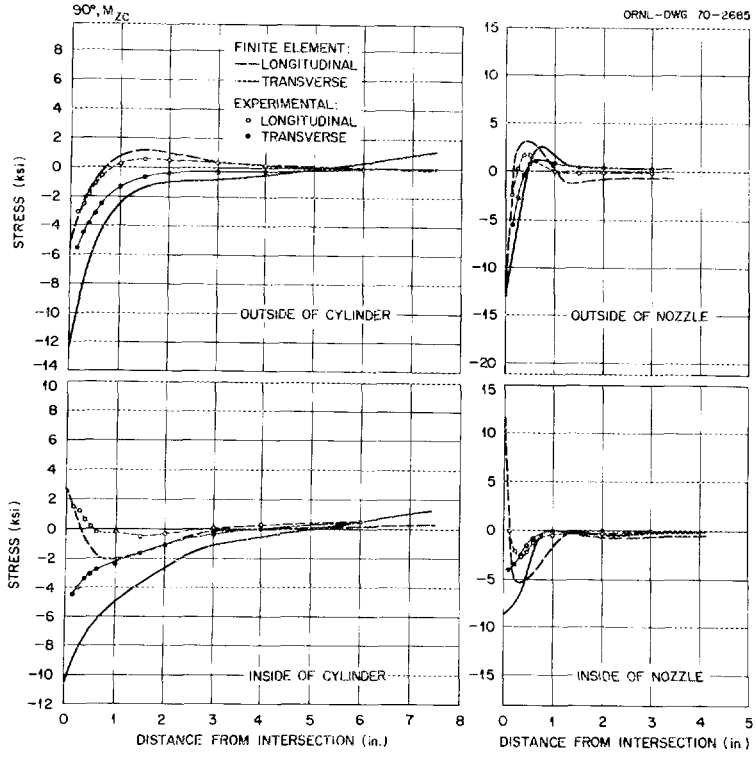

Fig. 104. Measured and predicted stress distributions at 90° for in-plane moment, M_{ZC}, on cylinder.

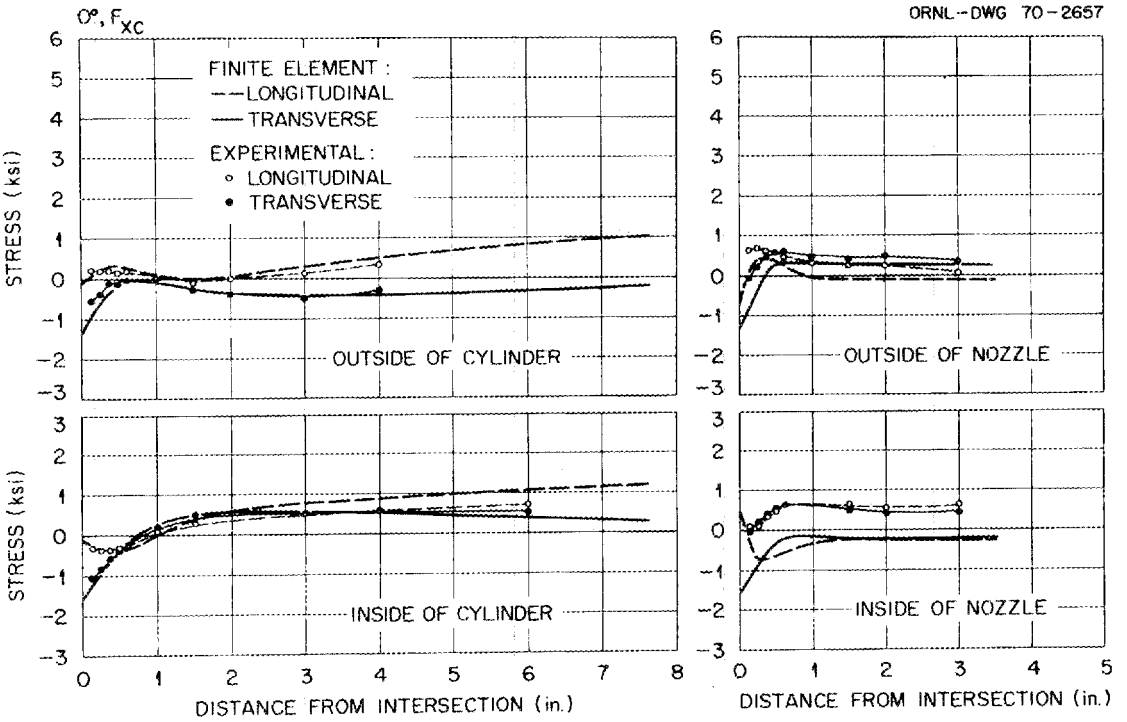

Fig. 105. Measured and predicted stress distributions at 0° for axial force, F_{XC}, on cylinder.

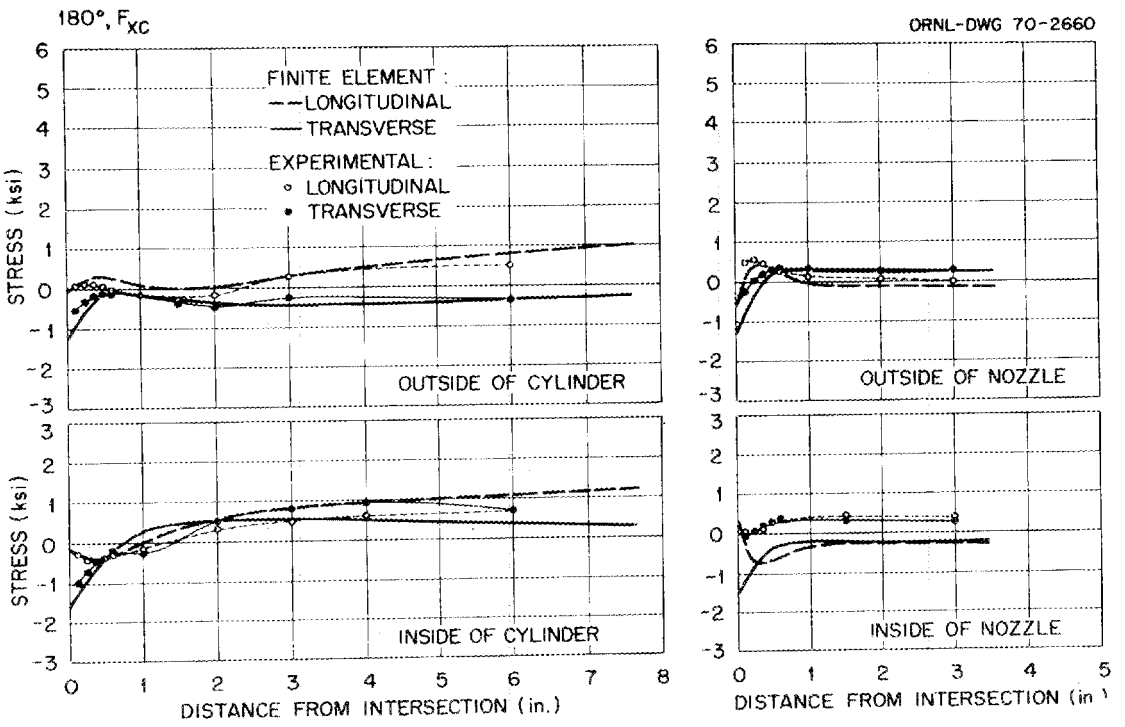

Fig. 106. Measured and predicted stress distributions at 180° for axial force, F_{XC}, on cylinder.

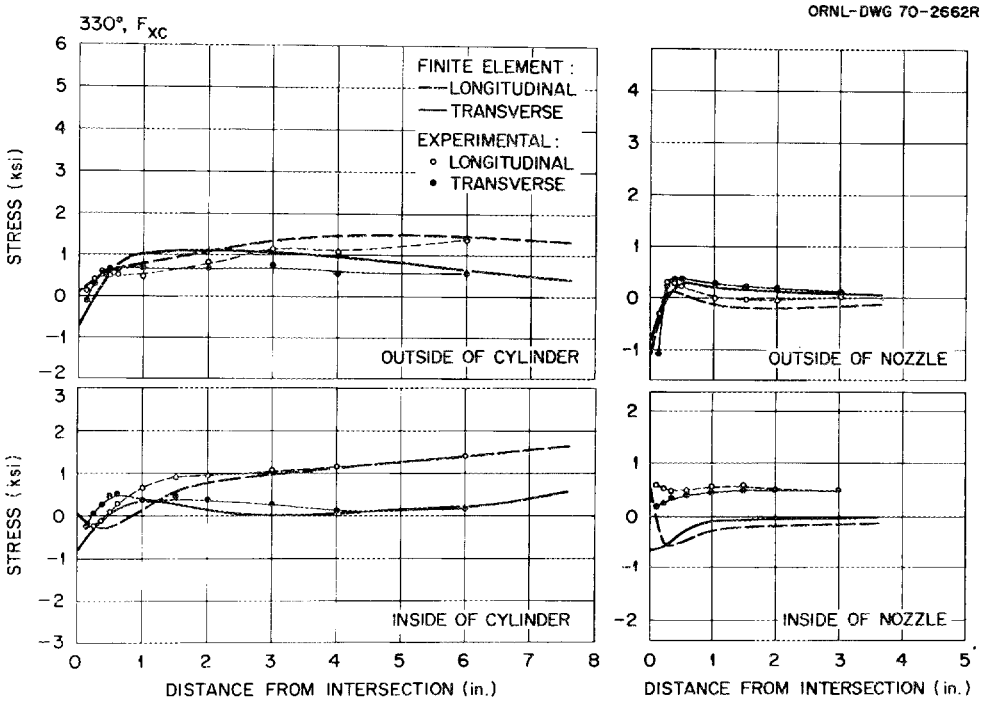

Fig. 107. Measured and predicted stress distributions at 330° for axial force, F_{XC}, on cylinder.

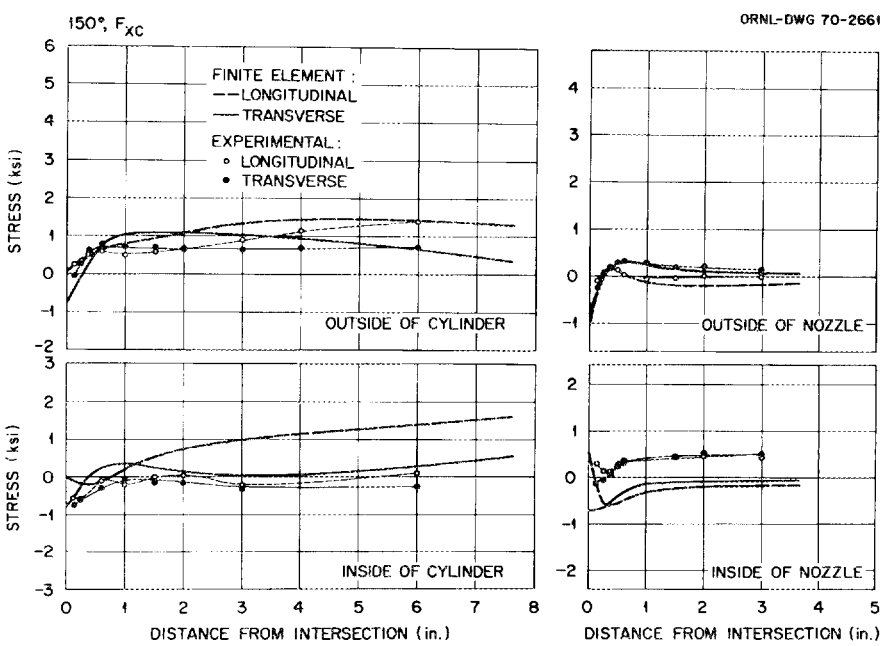

Fig. 108. Measured and predicted stress distributions at 150° for axial force, F_{XC}, on cylinder.

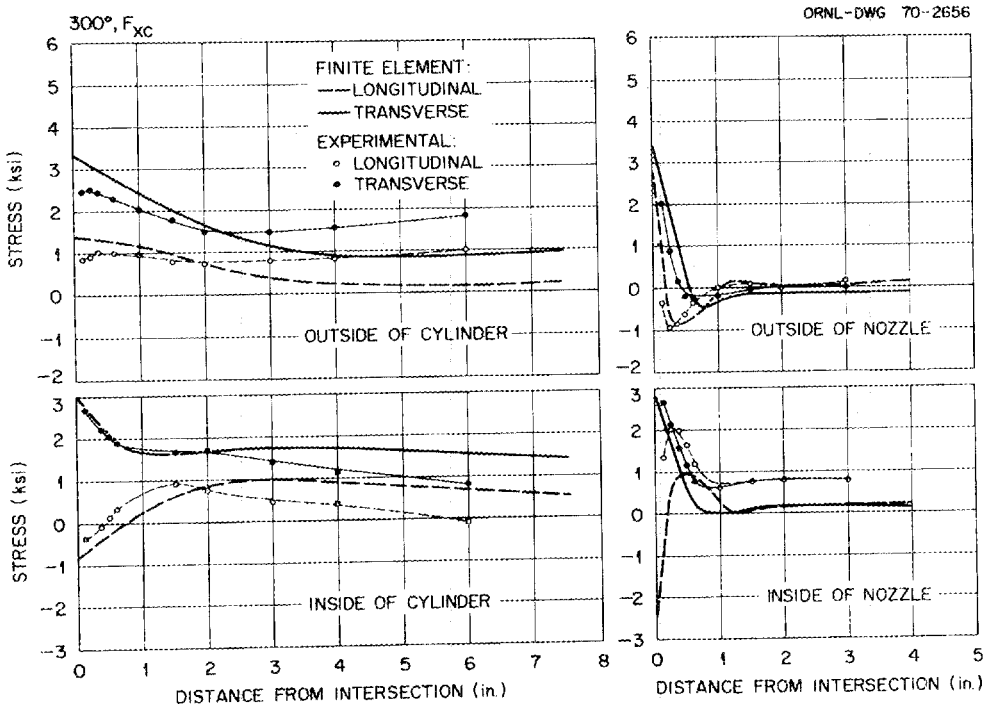

Fig. 109. Measured and predicted stress distributions at 300° for axial force, F_{XC}, on cylinder.

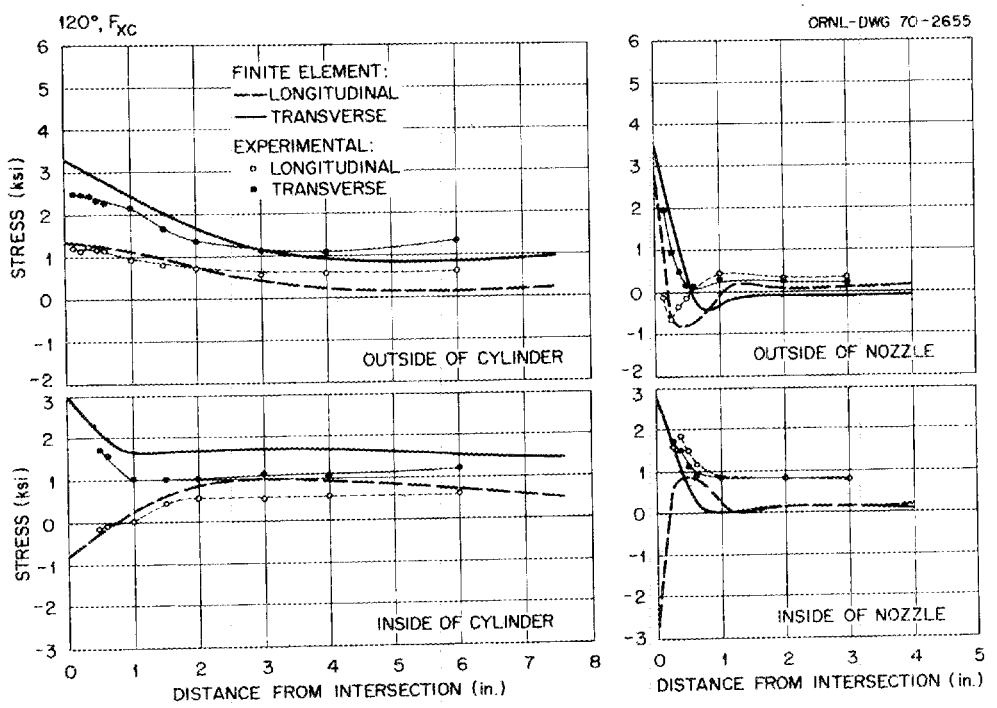

Fig. 110. Measured and predicted stress distributions at 120° for axial force, F_{XC}, on cylinder.

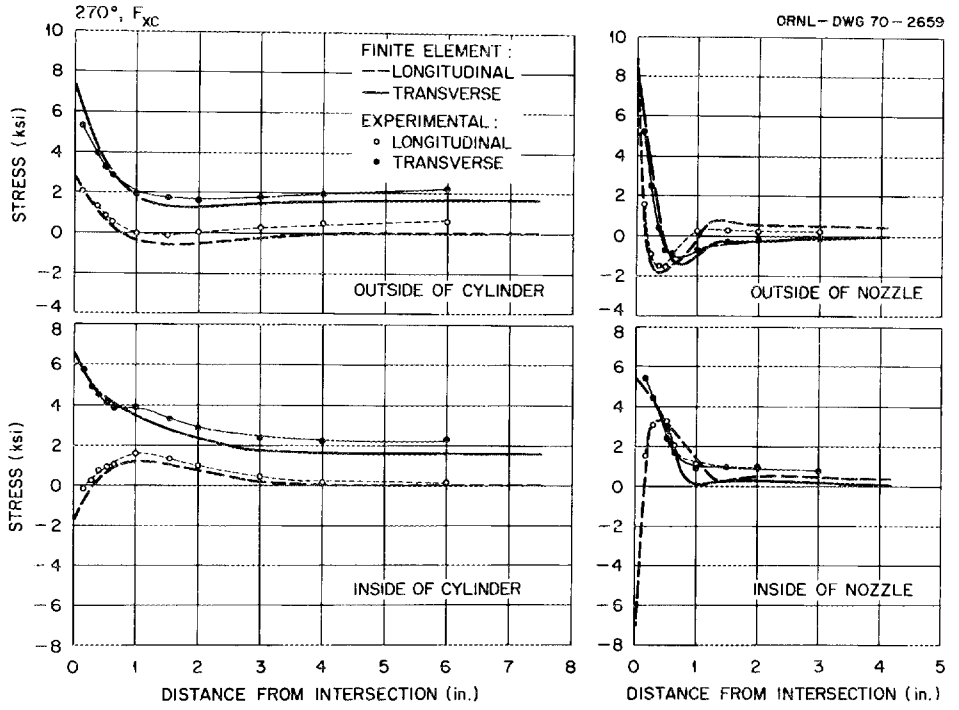

Fig. 111. Measured and predicted stress distributions at 270° for axial force, F_{XC}, on cylinder.

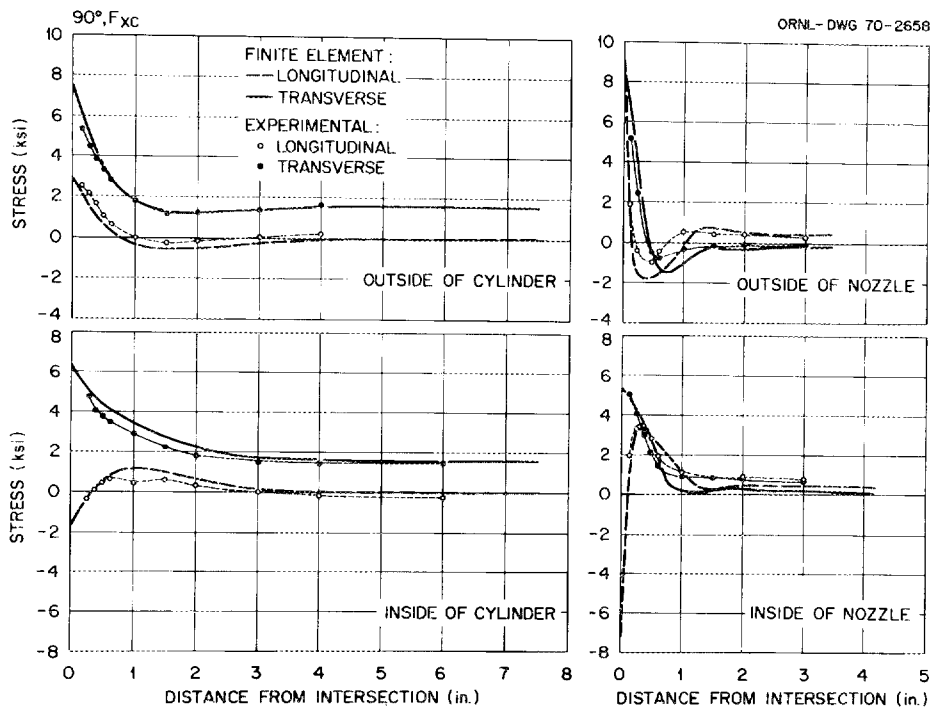

Fig. 112. Measured and predicted stress distributions at 90° for axial force, F_{XC}, on cylinder.

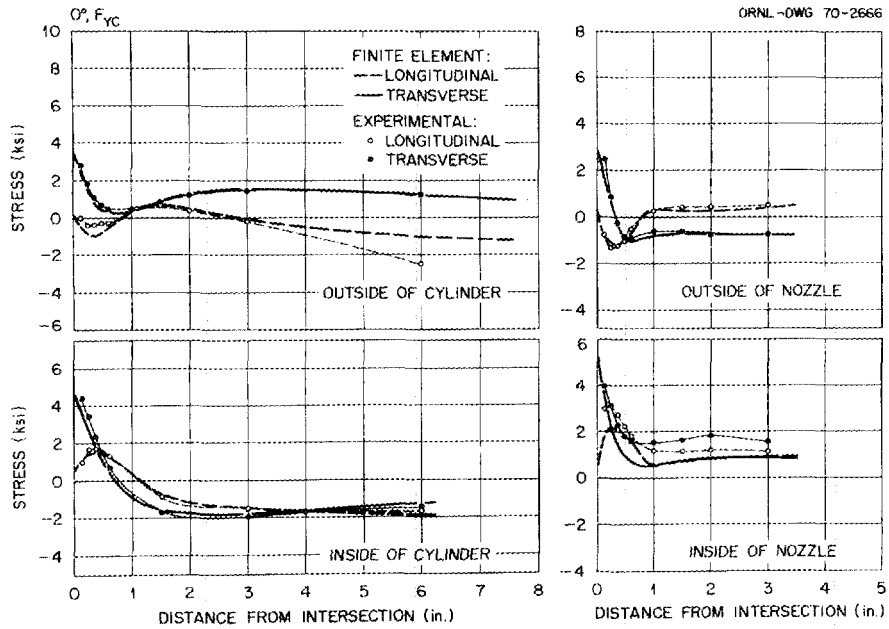

Fig. 113. Measured and predicted stress distributions at 0° for in-plane force, F_{YC}, on cylinder.

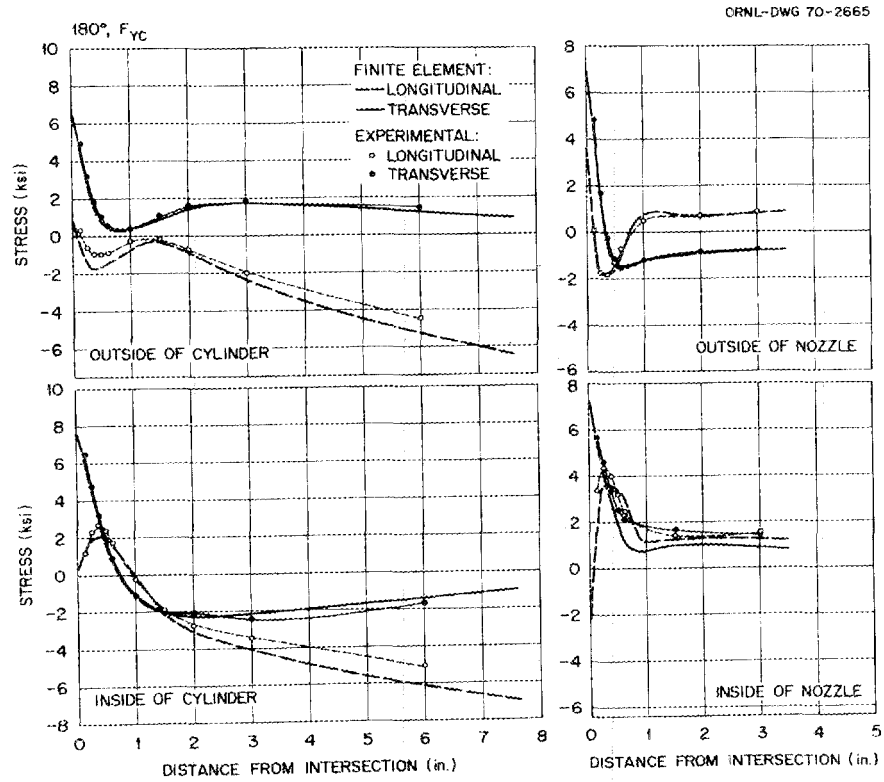

Fig. 114. Measured and predicted stress distributions at 180° for in-plane force, F_{YC}, on cylinder.

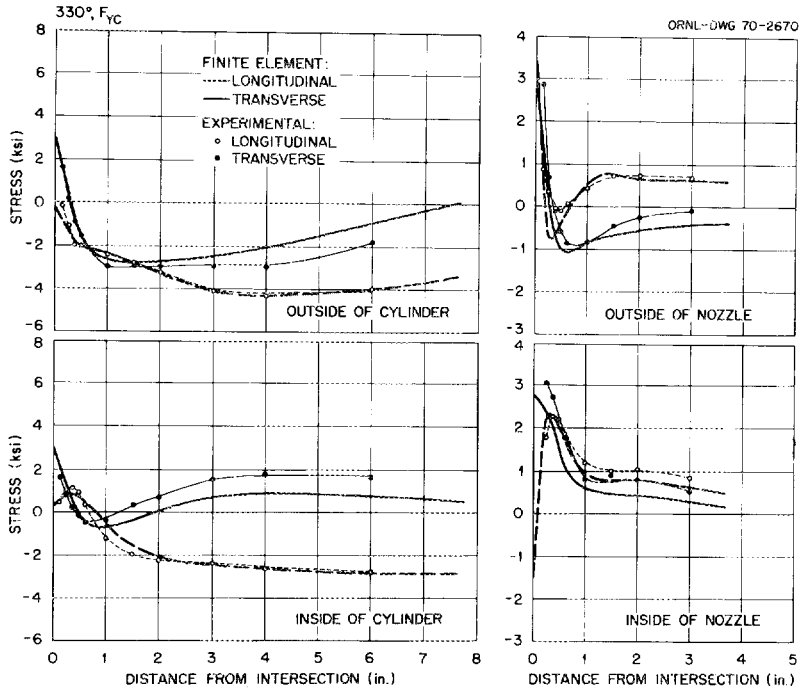

Fig. 115. Measured and predicted stress distributions at 330° for in-plane force, F_{YC}, on cylinder.

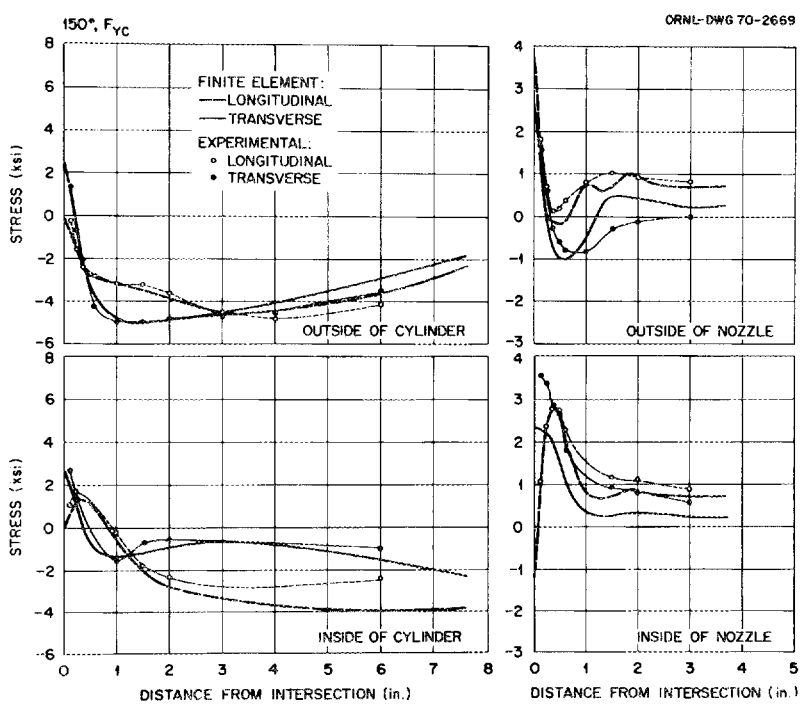

Fig. 116. Measured and predicted stress distributions at 150° for in-plane force, F_{YC}, on cylinder.

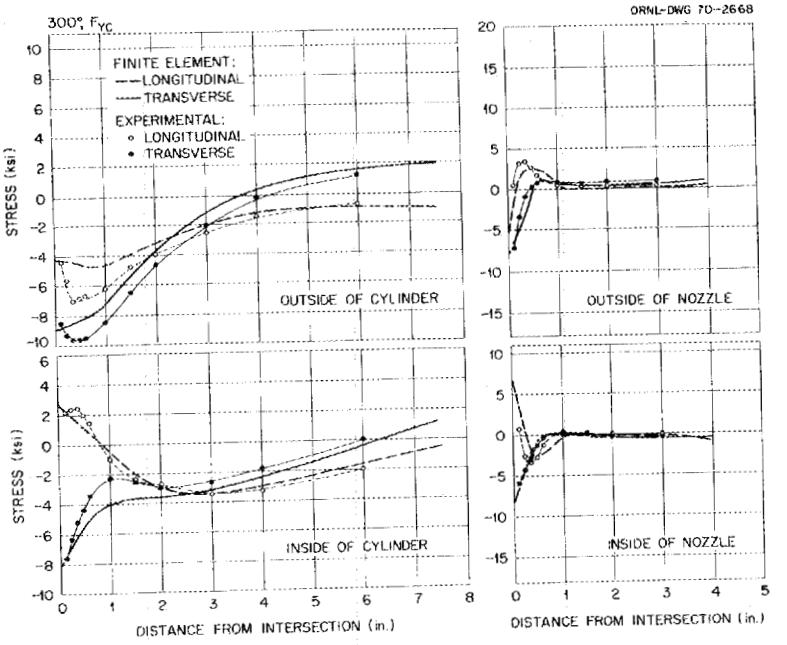

Fig. 117. Measured and predicted stress distributions at 300° for in-plane force, F_{YC}, on cylinder.

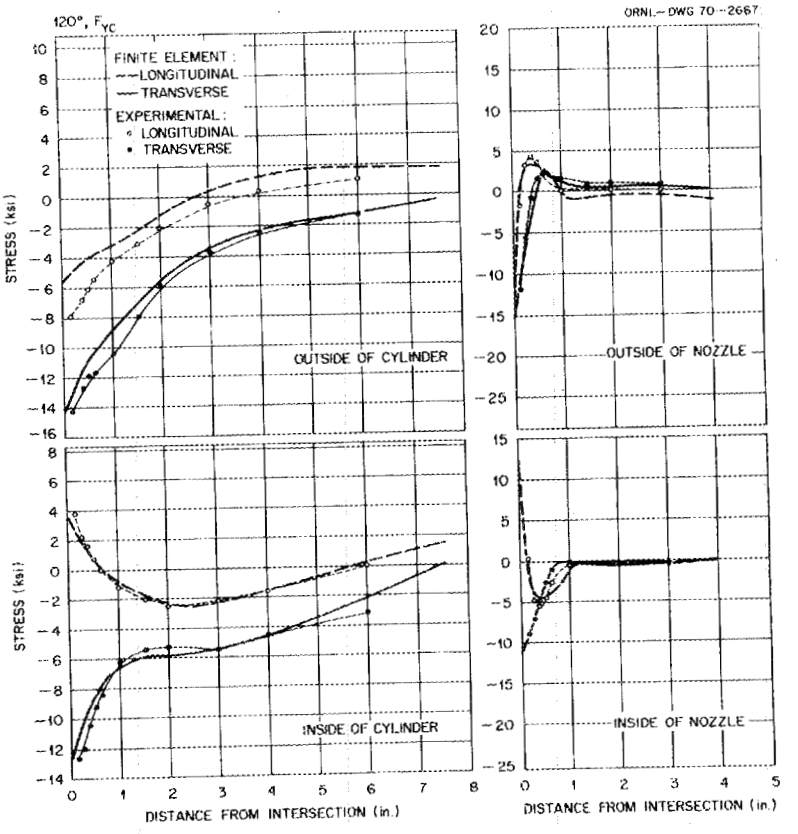

Fig. 118. Measured and predicted stress distributions at 120° for in-plane force, F_{YC}, on cylinder.

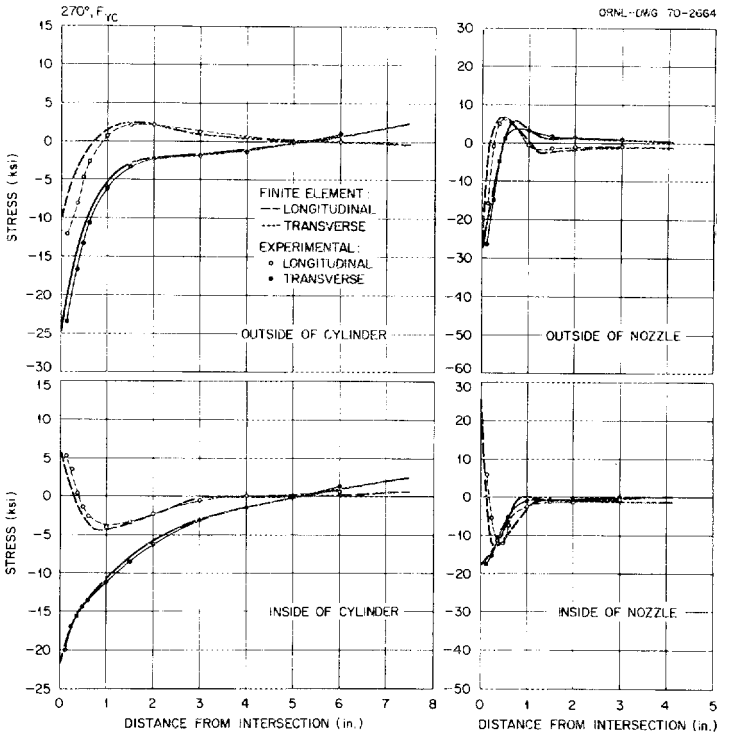

Fig. 119. Measured and predicted stress distributions at 270° for in-plane force, F_{YC}, on cylinder.

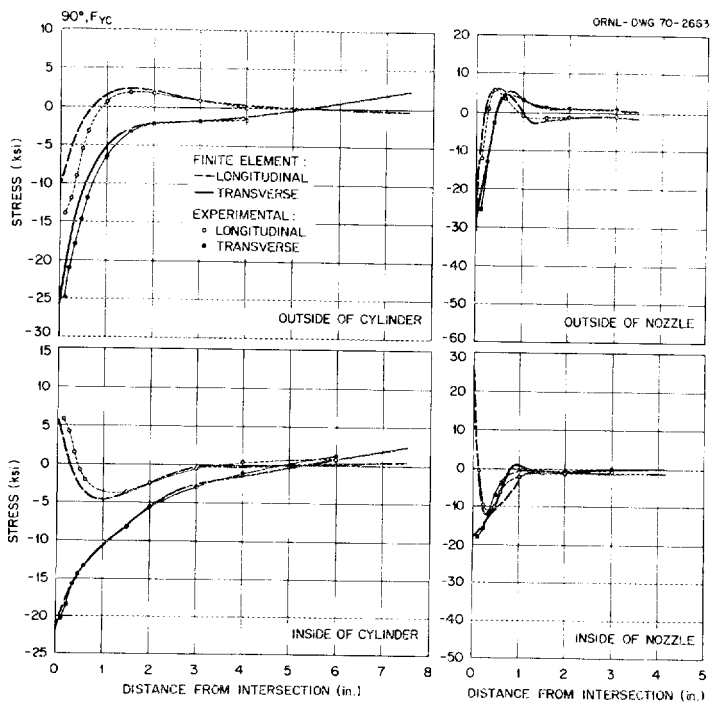

Fig. 120. Measured and predicted stress distributions at 90° for in-plane force, F_{YC}, on cylinder.

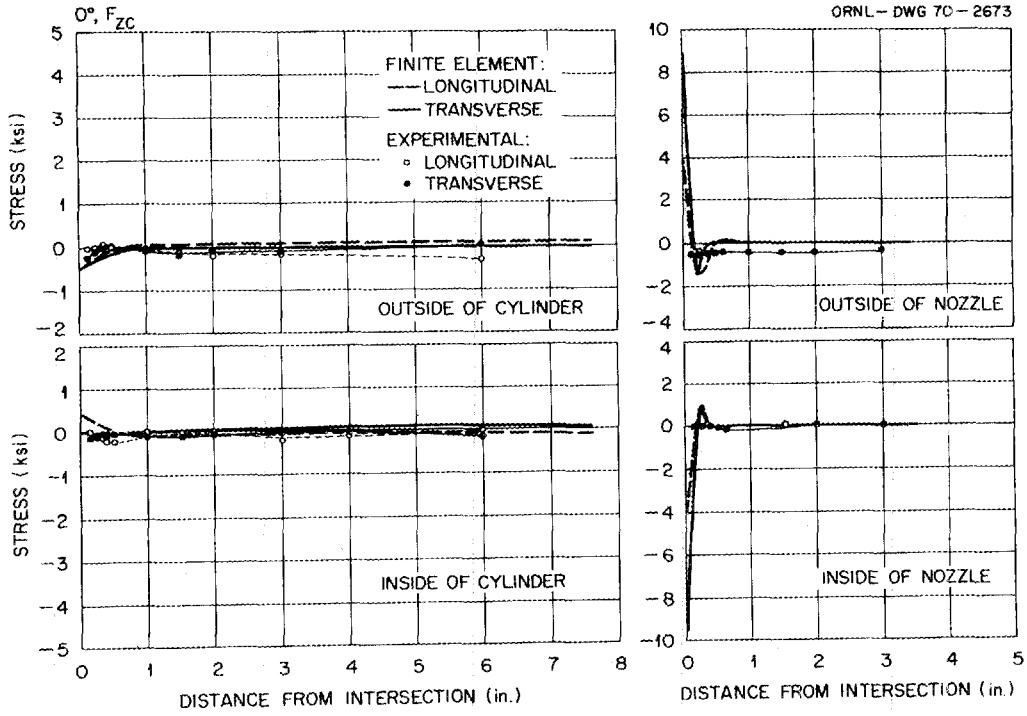

Fig. 121. Measured and predicted stress distributions at 0° for out-of-plane force, F_{ZC}, on cylinder.

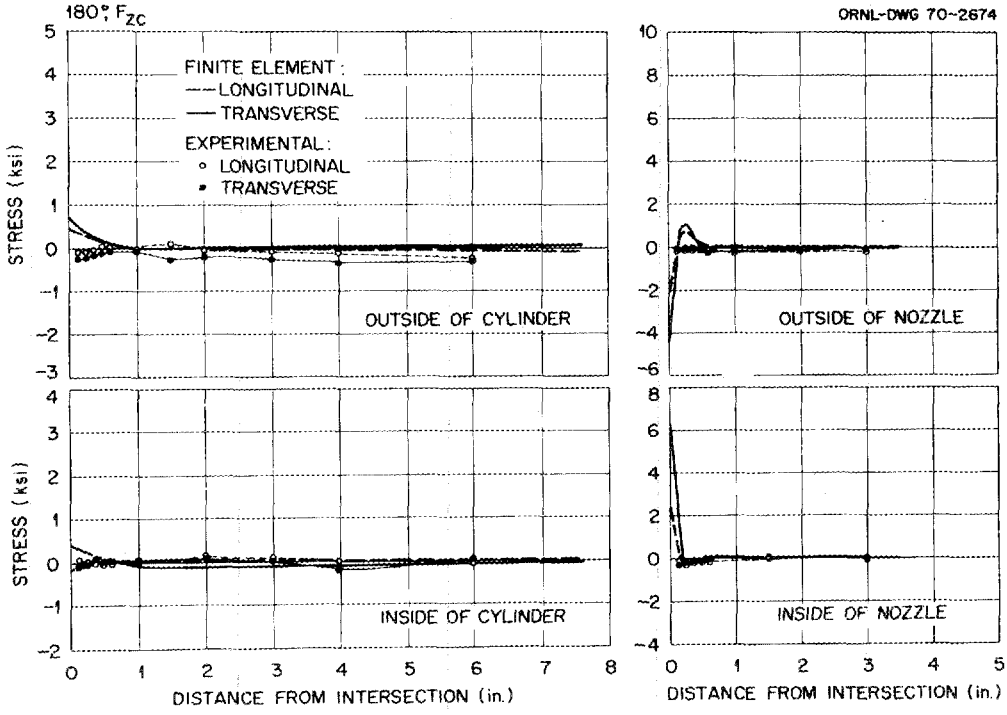

Fig. 122. Measured and predicted stress distributions at 180° for out-of-plane force, F_{ZC}, on cylinder.

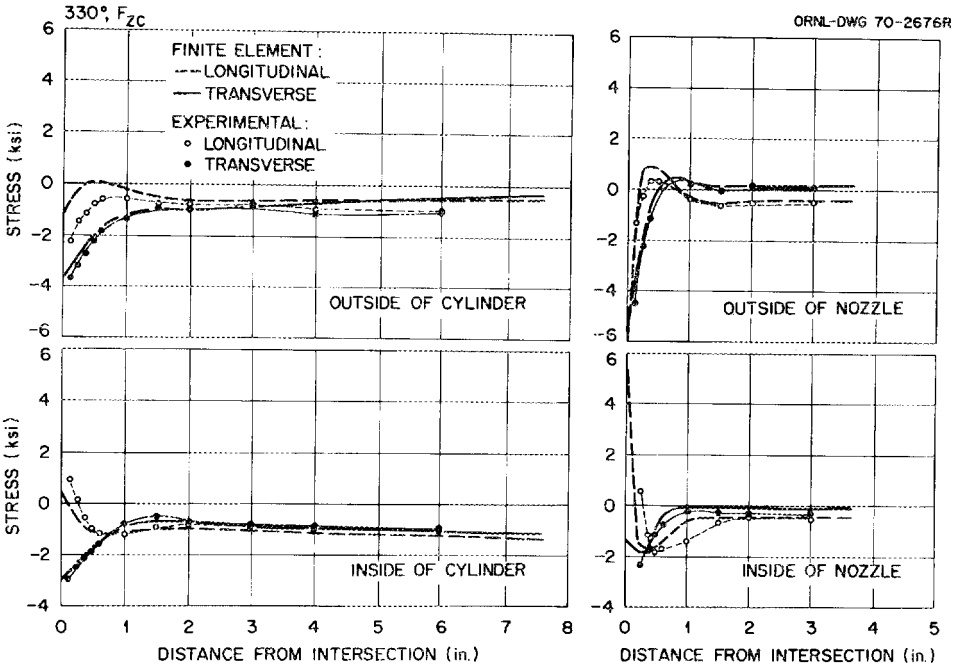

Fig. 123. Measured and predicted stress distributions at 330° for out-of-plane force, F_{ZC}, on cylinder.

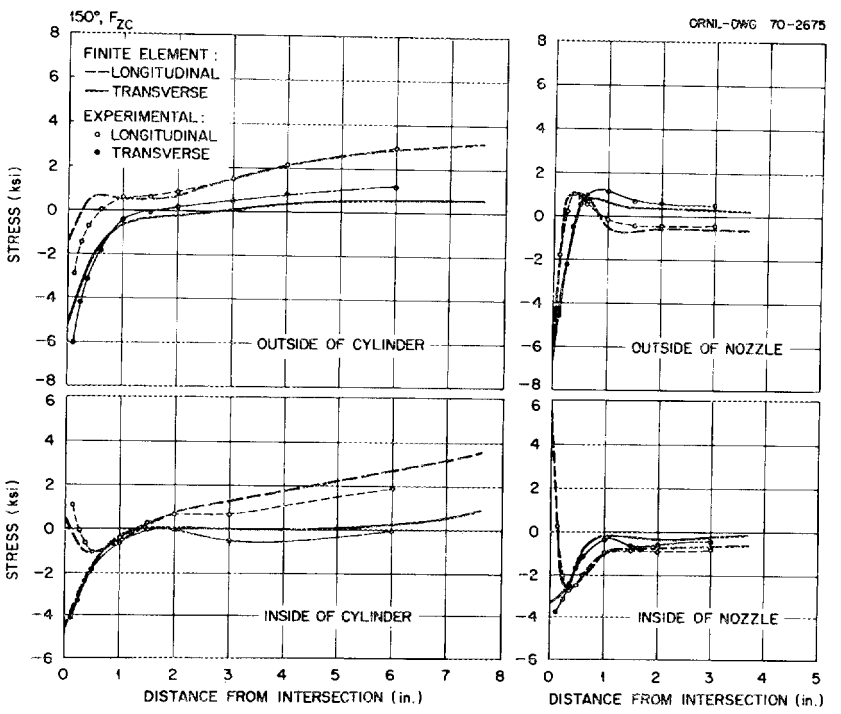

Fig. 124. Measured and predicted stress distributions at 150° for out-of-plane force, F_{ZC}, on cylinder.

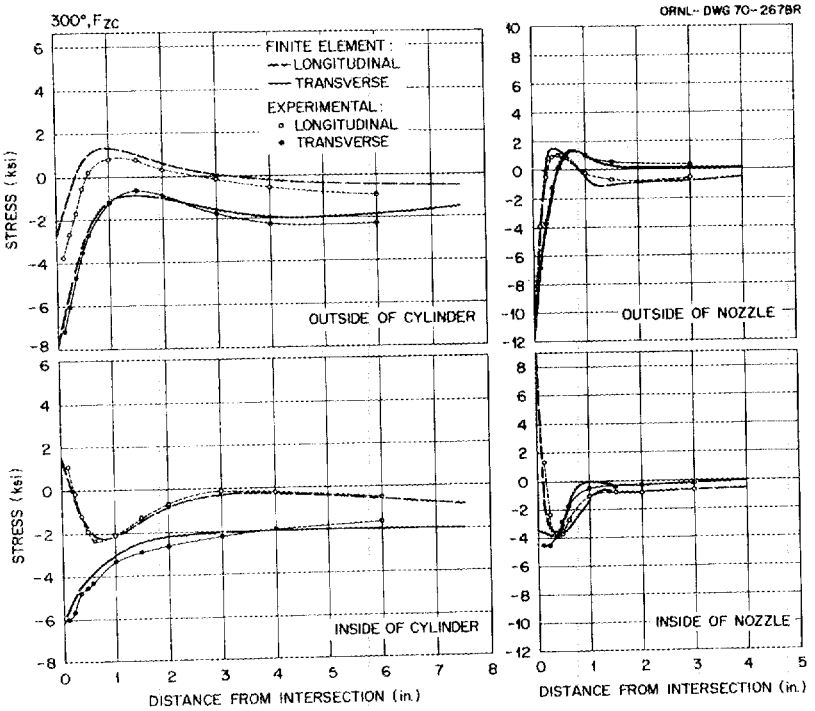

Fig. 125. Measured and predicted stress distributions at 300° for out-of-plane force, F_{ZC}, on cylinder.

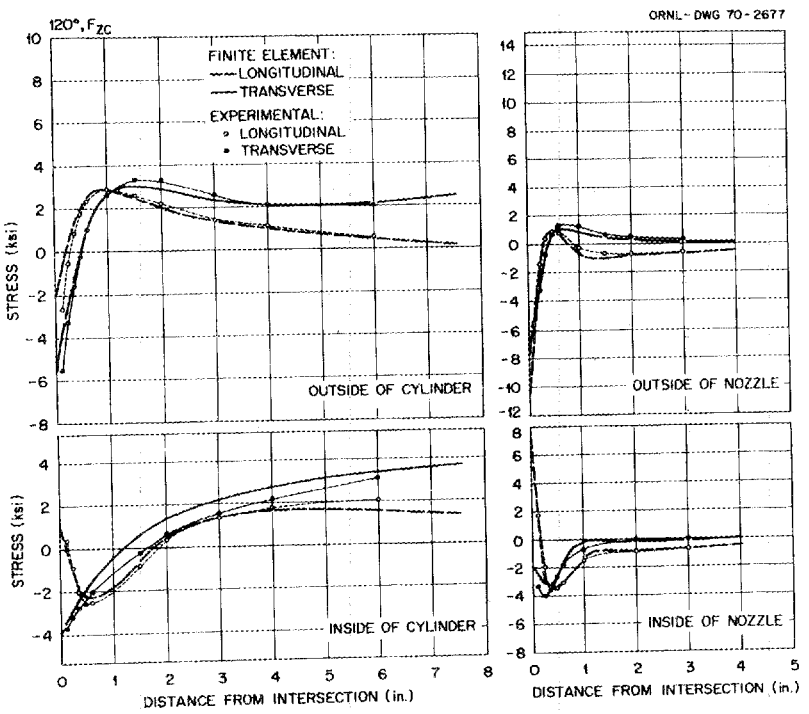

Fig. 126. Measured and predicted stress distributions at 120° for out-of-plane force, F_{ZC}, on cylinder.

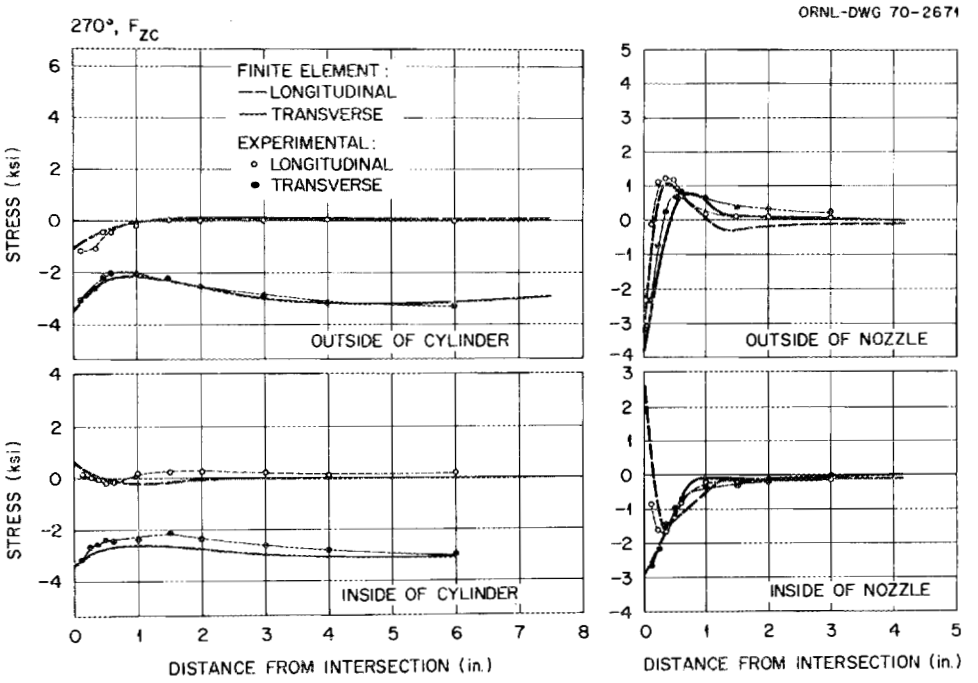

Fig. 127. Measured and predicted stress distributions at 270° for out-of-plane force, F_{ZC}, on cylinder.

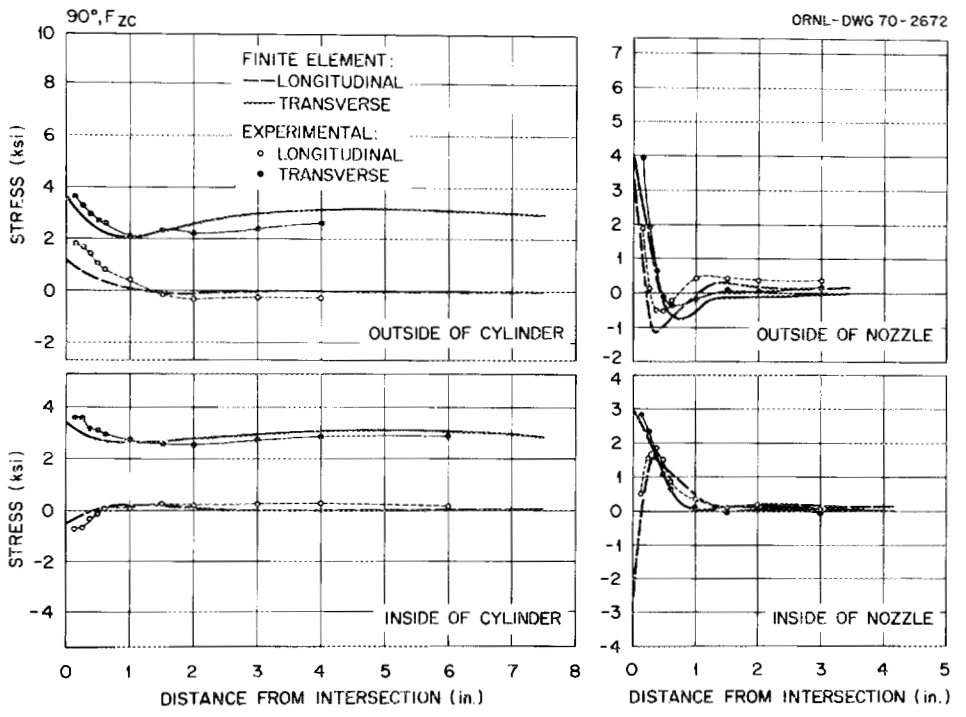

Fig. 128. Measured and predicted stress distributions at 90° for out-of-plane force, F_{ZC}, on cylinder.

5. CONCLUSIONS

An attempt has been made in Table 2 to summarize, concisely, the principal findings of this study in terms of maximum principal stress ratios, locations of maximum principal stresses, and the relative overall agreement between theory and experiment for each loading case. The maximum stress ratios are based on the stresses, either measured or predicted, along the eight lines of strain gages only and were determined by dividing the maximum absolute principal stress value by a nominal membrane stress value as previously described. The maximum experimental principal stresses were determined by extrapolating the experimentally determined stress distributions to the peak stresses at the junction.

The relative overall agreement between the finite-element predictions and the experimental results is rated in Table 2 as excellent, good, fair, or poor. These ratings are, of course, a matter of opinion, but an attempt was made to make an unbiased evaluation by basing them on both the overall qualitative agreement along all the gage lines and on the quantitative agreement in areas where the stresses were relatively high. For the internal pressure case and the case of an axial loading on the cylinder, the relative rating is listed as good, poor. In these cases the agreement was good in regions where the stress levels were relatively high, but poor in regions where they were relatively low.

Table 2 indicates that generally the experimentally determined maximum stress ratios and those based on finite-element predictions are in surprisingly good agreement. Furthermore, the degree of agreement between stress ratios generally correlates well with the relative rating of the overall agreement between theory and experiment. Generally, the agreement was best for those cases involving loadings on the nozzle. The torsional moment on the nozzle was, however, an exception. There the agreement was qualitatively acceptable but was poor quantitatively. This lack of quantitative agreement may be traced to the neglect of the sixth degree of freedom for nodes along the junction in the finite-element formulation. The degree of freedom that was neglected corresponds to the nozzle rotation that would be produced by a torsional moment. The consequences of this neglect were discussed in Chapter 3 and shown in Fig. 23.

Table 2. Summary of maximum stress ratios and maximum stress locations

Loading case	Experimentally determined maximum stress[a]		Theoretical maximum stress		Overall agreement between theory and experiment
	Stress ratio[b]	Location[c]	Stress ratio[b]	Location[c]	
Internal pressure	13.3	Outside nozzle, 180°	10.2	Outside nozzle, 0°	Good, poor
M_{XN}, out-of-plane moment on nozzle	35.3	Outside nozzle, 270°	37.2	Outside nozzle, 270°	Excellent
M_{YN}, torsional moment on nozzle	12.5	Outside nozzle, 120°	5.1	Outside nozzle, 300°	Fair
M_{ZN}, in-plane moment on nozzle	10.0	Outside nozzle, 300°	10.9	Outside nozzle, 300°	Excellent
F_{XN}, in-plane force on nozzle	10.5	Outside nozzle, 120°	11.4	Outside nozzle, 330°	Excellent
F_{YN}, axial force on nozzle	36.3	Outside nozzle, 270°	36.0	Outside nozzle, 270°	Excellent
F_{ZN}, out-of-plane force on nozzle	36.0	Inside nozzle, 270°	32.6	Inside nozzle, 270°	Good
M_{XC}, torsional moment on cylinder	10.0	Outside nozzle, 120°	13.0	Outside nozzle, 120°	Good
M_{YC}, out-of-plane moment on cylinder	2.3	Outside nozzle, 90°	2.7	Outside nozzle, 0°	Fair
M_{ZC}, in-plane moment on cylinder	3.8	Outside nozzle, 90°	5.7	Outside nozzle, 270°	Fair
F_{XC}, axial force on cylinder	4.7	Outside nozzle, 270°	5.6	Outside nozzle, 270°	Good, poor
F_{YC}, in-plane force on cylinder	6.0	Outside nozzle, 270°	5.7	Outside nozzle, 270°	Excellent
F_{ZC}, out-of-plane force on cylinder	3.1	Outside nozzle, 300°	3.5	Outside nozzle, 300°	Good

[a]Based on extrapolation of experimental distributions to maximum at junction.

[b]Ratio of maximum absolute principal stress value to nominal stress value.

[c]Maximums all occurred at the junction.

In every loading case except one, the maximum stress occurred on the outside surface of the nozzle at the junction of nozzle and cylinder. In the one exception, which was the case of an out-of-plane force F_{ZN} on the nozzle, the maximum occurred on the inner surface of the nozzle at the junction. The stresses on the outer surface of the nozzle were, however, almost as high as those on the inner surface.

In 6 of the 13 cases, the maximum values occurred in the transverse plane of symmetry. Both of the torsional moments, the in-plane moment and force on the nozzle, and the out-of-plane force and moment on the cylinder produced maximums at points intermediate to the two planes of symmetry. Only the internal pressure case produced a maximum stress in the longitudinal plane of symmetry.

The maximum stress ratios for the 13 loadings fall into three groups. Three of the loadings — an out-of-plane moment and force on the nozzle and an axial load on the nozzle — produced maximum stress ratios between 35.3 and 36.3, determined experimentally. For each of these three cases the maximum was on the transverse plane of symmetry. For five other cases — internal pressure, an in-plane moment and force on the nozzle, and torsional moments on the nozzle and cylinder — the maximum stress ratios were in the range 10.0 to 13.3. For the five remaining cases, which were loadings on the cylinder, the ratios were 6 and less.

Finally, it should be pointed out that, as would be expected, the out-of-plane moment and force loadings on the nozzle produced quite similar results, and the in-plane moment and force loadings produced similar results. The stress distributions were very similar for each pair, and the maximum stress ratios were very close.

In conclusion, the comparison of these particular finite-element predictions with the experimental results shows reasonably good general agreement. It is felt that this analysis would be satisfactory for most engineering purposes.

There is, however, room for improvement, particularly in four or five specific loading cases, including internal pressure and the nozzle torsional moment. As was discussed in Chapter 3, a finer element mesh does not appear to provide any overall degree of improvement. For the

finite-element analysis, therefore, improvements would have to come from improved finite-element formulations. Further developments and improvements in element formulations for shell structures can be, and are being, made. In particular, inclusion of the sixth degree of freedom, at least in the junction region, might noticeably improve the predictions. Also, curved-shell elements, which would better represent the curved-shell geometry, might, if properly formulated, give improved predictions.

Analytical solutions of the type discussed in the introduction to Chapter 3 also show promise. Development of these analytical procedures is continuing at Oak Ridge National Laboratory. A new internal pressure formulation has been finished, and the formulations for in-plane and out-of-plane nozzle moments on the nozzle are under way. These analyses will also be compared with experimental data as they become available.

Perfect agreement between theory and experiment, however, can never be expected. Small geometric variations and imperfections are inevitable, even in a very carefully machined model, and these slight imperfections can, in a thin shell, markedly affect the measured stress distributions.

ACKNOWLEDGMENTS

The planning and execution of the analytical and experimental study reported herein would not have been possible without the assistance and cooperation of many individuals, both within ORNL and outside. The authors are thus deeply indebted to these people for their contributions.

Special thanks are due J. W. Bryson, ORNL, who was responsible for reducing the experimental data and preparing computer plots of the experimental results and comparisons of these results with predictions. J. P. Rudd performed the very painstaking task of instrumenting the model.

The finite-element computer program used in the analysis was developed at the University of California, Berkeley, and the actual analyses used in this report were performed there. The authors wish to acknowledge the help and advice of Professor R. W. Clough of the University of California, Berkeley, and of Ojars Greste, a former graduate student at Berkeley.

Finally, the support and encouragement of J. L. Mershon, Division of Reactor Development and Technology, U.S. Atomic Energy Commission, is gratefully acknowledged.

REFERENCES

1. D. E. Hardenbergh, S. Y. Zamrik, and A. J. Edmondson, "Experimental Investigation of Stresses in Nozzles in Cylindrical Pressure Vessels," Welding Research Council Bulletin 89, July 1963.

2. D. E. Hardenbergh and S. Y. Zamrik, "Effects of External Loadings on Large Outlets in a Cylindrical Pressure Vessel," Welding Research Council Bulletin 96, May 1964.

3. W. F. Riley, Experimental Determination of Stress Distributions in Thin Walled Cylindrical and Spherical Pressure Vessels with Circular Nozzles, IIT Research Institute Report No. M6053 (March 1965).

4. C. E. Taylor and N. C. Lind, "Photoelastic Study of the Stresses near Openings in Pressure Vessels," Welding Research Council Bulletin 113, April 1966.

5. M. M. Leven, "Photoelastic Determination of Stresses in Reinforced Openings in Pressure Vessels," Welding Research Council Bulletin 113, April 1966.

6. Ojars Greste, Finite Element Analysis of Tubular K Joints, Report UCSESM 70-11, University of California, Berkeley (June 1970).

7. W. Reidelbach, "The State of Stress at the Perpendicular Intersection of Two Right Circular Tubes," Ingenieur-Archiv. 30(5), 293–316 (1961).

8. A. C. Eringen, A. K. Naghdi, and C. C. Thiel, "State of Stress in a Circular Cylindrical Shell with a Circular Hole," Welding Research Council Bulletin 102, January 1965.

9. A. K. Naghdi and A. C. Eringen, "Stress Distribution in a Circular Cylindrical Shell with a Circular Cut-Out," Ingenieur-Archiv. 34(3), 161–72 (1965).

10. A. C. Eringen and E. S. Suhubi, "Stress Distribution at Two Normally Intersecting Shells," Nucl. Struct. Eng. 2(3), 253–70 (1965).

11. A. C. Eringen et al., "Stress Concentrations in Two Normally Intersecting Cylindrical Shells Subject to Internal Pressure," Welding Research Council Bulletin 139, April 1969.

12. J. W. Hansberry and N. Jones, "A Theoretical Study of the Elastic Behavior of Two Normally Intersecting Cylindrical Shells," Trans. ASME, J. Eng. Ind. 91B(3), 563–72 (1969).

13. R. F. Maye and A. C. Eringen, "Further Analysis of Two Normally Intersecting Cylindrical Shells Subjected to Internal Pressure," Nucl. Eng. Des. 12(3), 457–74 (1970).

14. P. P. Bijlaard, R. J. Dohrmann, and I. C. Wang, "Stresses in Junction of Nozzle to Cylinder Pressure Vessel for Equal Diameter of Vessel and Nozzle," Nucl. Eng. Des. 5(3), 349–66 (1967).

15. K. C. Pan and R. E. Beckett, "Stress and Displacement Analysis of a Shell Intersection," Trans. ASME, J. Eng. Ind. 92B(3), 303–8 (May 1970).

16. L. R. Herrmann and D. M. Campbell, "A Finite-Element Analysis for Thin Shells," AIAA J. 6(10), 1842–47 (1968).

17. N. Prince and Y. R. Rashid, "Structural Analysis of Shell Intersections," presented at First International Conference on Pressure Vessels and Piping, Sept. 29–Oct. 2, 1969, Delft, The Netherlands.

18. R. H. Gallagher, "Analysis of Plate and Shell Structures," pp. 155–205 in Proceedings of Symposium on Application of Finite Element Methods in Civil Engineering, Vanderbilt University, Nov. 13–14, 1969, American Society of Civil Engineers.

19. C. P. Johnson, The Analysis of Thin Shells by a Finite Element Procedure, Report 67-22, Department of Civil Engineering, University of California, Berkeley (September 1967).

20. C. P. Johnson and P. G. Smith, A Computer Program for the Analysis of Thin Shells, Report 69-5, Department of Civil Engineering, University of California, Berkeley (August 1967).

21. Ojars Greste, A Computer Program for the Analysis of Tubular K Joints, Report 69-19, Department of Civil Engineering, University of California, Berkeley (November 1969).

22. R. W. Clough and J. L. Tocher, "Finite Element Stiffness Matrices for the Analysis of Plate Bending," Proceedings of Conference on Matrix Methods in Structural Mechanics, Report AFFDL-TR-66-80, Wright-Patterson Air Force Base (November 1966).

Appendix

TABULATION OF EXPERIMENTAL DATA

For the benefit of the reader who may want to use the experimental data presented herein to prepare comparisons with his own analysis techniques, the experimental data on which the various plots in this report were based are tabulated here. For each loading case, a set of data is tabulated for each operable rosette. These data were obtained from the several sets of data taken in each case by the procedures described in Section 2.4.

The rosette listings are grouped according to gage lines. For each rosette, the three strain readings are first listed, followed by the normal stress transverse (perpendicular) to the gage line, the normal stress longitudinal (parallel) to the gage line, the shear stress (referred to the gage line as a coordinate axis), and finally the maximum and minimum stresses. The strains are given in microinches per inch and the stresses are in pounds per square inch.

The nomenclature used to identify and locate each rosette can be explained by considering the following sample designation:

$$\underline{I}\ \ \underline{120}\ \ \underline{N} - \underline{E}\ .$$

The letter I designates that the rosette is located on the inner surface of nozzle or cylinder; O denotes an outside rosette. The number 120 indicates that the rosette is located on the 120° gage line (see Fig. 3 for the gage line designations). The letter N indicates that the rosette is on the nozzle; C designates a rosette on the cylinder; and E designates the location of the rosette along the gage line according to the following convention:

Rosette designation	Distance from nozzle-cylinder intersection (see Fig. 3) (in.)
A	1/8
B	1/4
C	3/8
D	1/2
E	5/8
F	1
G	1 1/2
H	2
J	3
K	4
L	6
M	~28.49

In every case, the rosettes were positioned on the gage lines so that the leg of the Y lay along the gage line and pointed away from the nozzle-cylinder junction. The convention used can be understood by referring to Fig. 6. The leg of the Y is designated as gage 1 in the tabulations, with gages 2 and 3 being numbered from 1 in the counterclockwise direction.

Finally, in those cases where nonlinearity or drift was excessive, or where an individual gage or circuit was otherwise obviously malfunctioning, the rosette of which the gage was a part was not used in the final results plotted in this report for the specific loading under consideration. Nonetheless, these data are listed in the tabulations, but they are marked by an asterisk beside the rosette number.

A.1 Internal Pressure

INTERNAL PRESSURE (50 PSI)

	MICRO-STRAIN			STRESSES			PRIN STRESSES	
ROSETTE	GAGE1	GAGE2	GAGE3	TRANS	LONG	SHEAR	SIGMX	SIGMN
I-O-C-A	-361	306	239	12380	-7122	905	12420	-7164
I-O-C-B	-121	254	193	9960	-633	804	10020	-694
I-O-C-C	19	224	188	9044	3284	481	9084	3244
I-O-C-D	90	195	162	7755	5035	443	7825	4965
I-O-C-E	122	165	138	6540	5612	361	6664	5488
I-O-C-F	114	85	66	3185	4377	247	4426	3136
I-O-C-G	60	54	34	1866	2370	272	2489	1747
I-O-C-H	43	48	31	1697	1792	222	1971	1518
I-O-C-J	34	62	41	2240	1684	279	2355	1568
I-O-C-K	26	52	37	1935	1365	203	1999	1300
I-O-C-L	14	49	42	1990	1010	101	2000	1000
O-O-C-A	159	429	463	19430	10590	-462	19450	10570
O-O-C-B	-16	299	311	13420	3541	-158	13420	3538
O-O-C-C	-68	214	224	9705	859	-127	9706	857
O-O-C-D	-86	152	164	7029	-457	-165	7032	-461
O-O-C-E	-90	113	119	5206	-1147	-82	5207	-1148
O-O-C-F	-26	51	58	2430	-41	-101	2434	-45
O-O-C-G	29	42	50	1994	1468	-101	2013	1449
O-O-C-H	43	52	59	2386	2013	-95	2409	1990
O-O-C-J	38	58	65	2663	1939	-95	2675	1927
O-O-C-K*	34	61	0	1310	1419	817	2183	546
O-O-C-L	6	59	66	2740	993	-82	2744	989
I-O-N-A	-177	233	240	10610	-2135	-95	10610	-2136
I-O-N-B	42	220	230	9865	4228	-133	9868	4225
I-O-N-C	134	173	184	7707	6332	-139	7721	6318
I-O-N-D	153	125	138	5618	6276	-177	6320	5573
I-O-N-E	119	84	98	3880	4728	-190	4769	3839
I-O-N-F	60	0	142	3046	2724	-1887	4779	992
I-O-N-G	37	36	49	1839	1664	-177	1949	1554
I-O-N-H	38	39	57	2068	1747	-241	2197	1618
I-O-N-J*	114	115	130	5264	5001	-190	5363	4901
O-O-N-A	108	368	370	16100	8066	-32	16100	8066
O-O-N-B	-57	222	219	9754	1230	51	9754	1229
O-O-N-C	-108	119	121	5403	-1615	-25	5403	-1615
O-O-N-D	-89	57	53	2532	-1921	57	2532	-1921
O-O-N-E	-55	26	24	1157	-1307	19	1157	-1307
O-O-N-F	33	17	16	695	1192	13	1193	695
O-O-N-G	61	39	35	1562	2308	51	2311	1558
O-O-N-H	56	39	38	1652	2163	13	2164	1651
O-O-N-J*	-49	-69	-80	-3226	-2436	152	-2408	-3254

INTERNAL PRESSURE (50 PSI)

	MICRO-STRAIN			STRESSES			PRIN STRESSES	
ROSETTE	GAGE1	GAGE2	GAGE3	TRANS	LONG	SHEAR	SIGMX	SIGMN
I-90C-A	-114	-29	0	-511	-3589	-399	-460	-3640
I-90C-B	-135	-33	6	-457	-4186	-519	-387	-4257
I-90C-C	-125	-31	9	-354	-3855	-538	-273	-3936
I-90C-D	-96	-19	15	12	-2890	-450	80	-2958
I-90C-E	-70	-13	24	307	-2004	-494	408	-2105
I-90C-F	-10	10	39	1076	38	-393	1207	-94
I-90C-G	73	44	48	1935	2776	-57	2780	1931
I-90C-H	98	54	43	2033	3547	146	3561	2020
I-90C-J	86	42	35	1607	3077	95	3083	1601
I-90C-K	74	31	25	1151	2569	89	2575	1145
I-90C-L	82	-2	23	359	2574	-336	2624	309
O-90C-A	93	105	102	4451	4130	38	4456	4125
O-90C-B	122	115	124	5130	5203	-127	5298	5034
O-90C-C	133	139	148	6151	5837	-120	6192	5796
O-90C-D	114	147	162	6663	5420	-190	6692	5392
O-90C-E	100	151	162	6783	5029	-152	6796	5016
O-90C-F	65	139	134	5924	3716	63	5926	3714
O-90C-G	40	102	84	4040	2409	247	4076	2373
O-90C-H	31	57	45	2201	1601	165	2243	1559
O-90C-J	38	18	15	679	1344	44	1347	676
O-90C-K	48	12	13	511	1607	-13	1607	511
O-90C-L	50	12	19	624	1698	-82	1704	617
I-90N-A	-171	-3	12	396	-4999	-203	404	-5007
I-90N-B	-109	71	38	2512	-2525	437	2549	-2563
I-90N-C	-67	84	48	2967	-1120	475	3021	-1175
I-90N-D	-45	77	49	2828	-506	367	2868	-546
I-90N-E	-40	67	39	2373	-486	374	2421	-534
I-90N-F*	-55	-567	22	-11930	-5232	-7851	-46	-17120
I-90N-G	-42	47	52	2208	-606	-70	2210	-608
I-90N-H	-42	48	33	1832	-705	209	1849	-722
I-90N-J	-38	66	40	2370	-415	336	2410	-455
O-90N-A	71	132	117	5394	3757	190	5416	3735
O-90N-B	-6	133	124	5647	1509	127	5650	1505
O-90N-C	-57	111	115	5033	-186	-63	5034	-187
O-90N-D	-79	88	97	4160	-1133	-114	4163	-1135
O-90N-E	-82	76	86	3651	-1357	-146	3655	-1361
O-90N-F	-56	70	77	3310	-689	-95	3312	-692
O-90N-G	-48	60	75	3018	-520	-203	3030	-532
O-90N-H	-46	62	68	2912	-495	-76	2913	-497
O-90N-J	-33	52	60	2512	-244	-108	2516	-249

INTERNAL PRESSURE (50 PSI)

	MICRO-STRAIN			STRESSES			PRIN STRESSES	
ROSETTE	GAGE1	GAGE2	GAGE3	TRANS	LONG	SHEAR	SIGMX	SIGMN
I120C-A	-105	114	220	7468	-924	-1406	7698	-1153
I120C-B	-40	104	226	7292	976	-1621	7684	584
I120C-C*	12	84	236	7015	2475	-2032	7792	1698
I120C-D*	-10	17	161	3927	879	-1918	4853	-47
I120C-E	19	25	126	3290	1543	-1349	4024	810
I120C-F	26	30	78	2353	1476	-633	2685	1144
I120C-G	76	35	44	1640	2773	-120	2785	1627
I120C-H*	157	75	19	1905	5290	741	5445	1750
I120C-J	14	21	11	695	636	127	795	535
I120C-K	48	14	40	1127	1778	-348	1929	976
I120C-L	48	63	22	1806	1996	545	2454	1348
O120C-A	167	346	247	12860	8876	1323	13260	8477
O120C-B	95	288	198	10590	6028	1203	10890	5730
O120C-C	32	240	127	8049	3370	1507	8492	2926
O120C-D	2	219	85	6661	2069	1785	7273	1457
O120C-E	-19	220	34	5598	1109	2482	6700	7
O120C-F	-24	181	-7	3859	445	2501	5180	-876
O120C-G	0	116	-22	2078	624	1842	3332	-630
O120C-H	33	92	-7	1833	1534	1323	3015	352
O120C-J	58	73	20	1983	2334	709	2889	1428
O120C-K	60	64	27	1919	2372	494	2689	1602
O120C-L	48	43	11	1127	1792	424	1999	921
I120N-A	-247	-20	213	4512	-6060	-3115	5361	-6909
I120N-B	-85	99	206	6798	-498	-1418	7064	-764
I120N-C	15	161	174	7336	2643	-177	7343	2636
I120N-D*	57	161	-51	2339	2427	2824	5207	-441
I120N-E*	50	84	86	3694	2619	-32	3695	2618
I120N-F	18	84	55	3019	1448	386	3109	1358
I120N-G	0	30	56	1901	570	-342	1984	488
I120N-H	-18	61	50	2464	197	152	2474	187
I120N-J	-15	61	57	2607	326	63	2609	324
O120N-A	215	303	258	12110	10090	595	12270	9928
O120N-B	15	256	162	9154	3188	1254	9406	2935
O120N-C	-74	162	94	5700	-500	899	5828	-628
O120N-D	-99	91	50	3201	-2019	545	3257	-2076
O120N-E	-81	50	32	1896	-1855	247	1912	-1871
O120N-F	-25	21	49	1573	-269	-380	1648	-345
O120N-G	-10	29	64	2048	315	-462	2163	199
O120N-H	-4	37	68	2312	580	-424	2411	481
O120N-J	-7	32	57	1971	378	-329	2037	312

INTERNAL PRESSURE (50 PSI)

	MICRO-STRAIN			STRESSES			PRIN STRESSES	
ROSETTE	GAGE1	GAGE2	GAGE3	TRANS	LONG	SHEAR	SIGMX	SIGMN
I150C-A	-243	198	262	10380	-4186	-861	10430	-4237
I150C-B	-79	188	241	9529	478	-709	9584	423
I150C-C*	25	168	0	3669	1856	2241	5181	345
I150C-D	82	149	186	7273	4648	-500	7365	4556
I150C-E	0	125	152	6110	1833	-361	6140	1803
I150C-F*	111	86	157	5225	4903	-950	6027	4101
I150C-G	133	121	126	5284	5591	-63	5604	5272
I150C-H	99	89	122	4518	4335	-437	4872	3980
I150C-J	52	103	135	5175	3121	-437	5264	3032
I150C-K	16	119	142	5716	2199	-310	5743	2172
I150C-L	85	82	124	4418	3877	-557	4767	3528
O150C-A	130	447	404	18550	9472	570	18590	9436
O150C-B	10	348	242	12970	4191	1412	13190	3969
O150C-C	-42	274	166	9718	1646	1431	9964	1400
O150C-D	-74	219	108	7267	-44	1469	7551	-328
O150C-E	-86	182	67	5577	-893	1539	5924	-1240
O150C-F	-89	88	0	2030	-2057	1171	2342	-2369
O150C-G	13	69	6	1636	890	836	2178	348
O150C-H	44	80	28	2333	2012	696	2887	1458
O150C-J	47	88	36	2664	2196	696	3165	1696
O150C-K	46	95	48	3093	2297	614	3427	1963
O150C-L	56	104	56	3458	2720	640	3827	2350
I150N-A	-295	55	342	9045	-6139	-3818	9951	-7045
I150N-B	-26	133	286	9240	2002	-2026	9768	1474
I150N-C	119	175	215	8444	6097	-526	8556	5985
I150N-D	154	156	151	6567	6589	70	6649	6508
I150N-E	137	123	100	4748	5530	310	5638	4640
I150N-F*	31	56	52	2336	1642	44	2339	1639
I150N-G	31	38	56	2033	1551	-241	2133	1451
I150N-H	29	44	60	2255	1560	-222	2320	1496
I150N-J	27	46	63	2362	1521	-222	2417	1466
O150N-A	195	407	380	17070	10980	361	17090	10960
O150N-B	9	308	209	11350	3677	1330	11580	3453
O150N-C	-75	187	100	6401	-318	1159	6595	-512
O150N-D	-80	98	47	3274	-1427	690	3373	-1526
O150N-E	-47	50	24	1681	-907	342	1725	-952
O150N-F	24	26	33	1279	1097	-95	1320	1056
O150N-G	45	41	54	2039	1966	-177	2184	1822
O150N-H	38	45	58	2214	1819	-177	2282	1751
O150N-J	30	46	56	2192	1556	-133	2218	1529

INTERNAL PRESSURE (50 PSI)

	MICRO-STRAIN			STRESSES			PRIN STRESSES	
ROSETTE	GAGE1	GAGE2	GAGE3	TRANS	LONG	SHEAR	SIGMX	SIGMN
I180C-A	-254	281	259	12150	-3981	285	12160	-3986
I180C-B	-66	247	228	10510	1184	260	10510	1177
I180C-C	56	219	207	9296	4471	152	9301	4466
I180C-D	116	189	178	7924	5870	146	7935	5860
I180C-E	134	159	148	6600	6000	139	6630	5969
I180C-F	124	80	76	3290	4693	51	4695	3288
I180C-G*	62	53	-74	-527	1695	1684	2602	-1434
I180C-H	38	39	35	1587	1617	51	1655	1549
I180C-J	21	61	41	2232	1311	266	2304	1240
I180C-K	20	76	57	2892	1466	247	2933	1425
I180C-L	24	57	44	2187	1383	165	2220	1351
O180C-A	71	412	406	17900	7507	82	17900	7506
O180C-B	-23	319	305	13730	3420	190	13730	3416
O180C-C	-71	239	166	8977	555	962	9085	446
O180C-D	-87	167	156	7208	-461	146	7211	-463
O180C-E	-87	118	113	5172	-1072	63	5172	-1072
O180C-F	-20	46	57	2267	81	-146	2277	72
O180C-G	34	44	48	1999	1626	-57	2007	1618
O180C-H	48	51	57	2319	2121	-70	2341	2099
O180C-J	38	58	60	2549	1891	-25	2550	1890
O180C-K	28	58	61	2591	1618	-44	2593	1616
O180C-L	23	52	59	2408	1421	-95	2417	1412
I180N-A	-191	256	276	11890	-2179	-266	11890	-2184
I180N-B	52	237	269	11070	4888	-424	11090	4859
I180N-C	154	189	218	8781	7253	-386	8873	7161
I180N-D	166	140	159	6377	6888	-253	6992	6272
I180N-E	129	98	116	4569	5234	-234	5308	4494
I180N-F*	603	46	65	1781	18640	-253	18640	1777
I180N-G	45	45	62	2301	2030	-222	2425	1906
I180N-H*	0	41	67	2371	711	-348	2441	641
I180N-J	52	36	55	1927	2132	-253	2303	1757
O180N-A	206	454	440	19430	12000	177	19430	12000
O180N-B	-28	263	277	11880	2738	-184	11890	2735
O180N-C	-104	130	152	6308	-1244	-298	6320	-1256
O180N-D	-90	58	73	2992	-1797	-196	3000	-1805
O180N-E	-57	24	29	1222	-1344	-70	1224	-1346
O180N-F	40	26	21	979	1505	63	1513	972
O180N-G*	0	10	36	1003	301	-342	1142	162
O180N-H	58	48	41	1899	2323	101	2346	1876
O180N-J	57	58	49	2298	2386	114	2464	2220

INTERNAL PRESSURE (50 PSI)

	MICRO-STRAIN			STRESSES			PRIN STRESSES	
ROSETTE	GAGE1	GAGE2	GAGE3	TRANS	LONG	SHEAR	SIGMX	SIGMN
I270C-A	-69	-14	14	76	-2044	-367	138	-2106
I270C-B	-83	-14	17	164	-2431	-412	228	-2495
I270C-C	-69	-10	21	316	-1972	-424	392	-2048
I270C-D	-44	-4	28	581	-1137	-424	680	-1236
I270C-E	-18	2	30	730	-309	-380	854	-433
I270C-F	35	15	33	1006	1357	-241	1479	883
I270C-G	92	33	40	1508	3204	-101	3210	1502
I270C-H*	109	0	36	664	3464	-475	3542	585
I270C-J	85	39	1	805	2793	507	2915	683
I270C-K*	0	19	14	731	219	63	739	212
I270C-L	64	23	14	734	2131	120	2141	724
I270C-M	48	27	27	1127	1778	6	1778	1127
O270C-A	28	67	69	2956	1728	-38	2957	1727
O270C-B	75	101	103	4398	3572	-19	4398	3571
O270C-C	81	119	119	5154	3984	0	5154	3984
O270C-D	72	126	122	5372	3779	51	5374	3777
O270C-E	71	130	124	5499	3774	76	5503	3771
O270C-F	49	110	106	4708	2895	51	4710	2894
O270C-G	32	78	68	3182	1910	127	3194	1897
O270C-H	32	43	38	1730	1474	70	1748	1456
O270C-J	48	13	11	479	1598	32	1599	479
O270C-K	65	15	16	597	2118	-13	2118	597
O270C-L	69	26	29	1135	2422	-38	2423	1134
I270N-A	-100	7	1	287	-2908	70	289	-2909
I270N-B	-154	-13	33	619	-4448	-614	692	-4521
I270N-C*	-90	21	-76	-1113	-3028	1292	-463	-3678
I270N-D*	-53	52	-165	-2417	-2308	2893	532	-5256
I270N-E	-47	49	31	1827	-849	241	1848	-871
I270N-F	-44	41	24	1469	-885	228	1491	-907
I270N-G*	-49	44	-19	597	-1289	836	914	-1606
I270N-H	-42	53	36	1989	-672	228	2008	-692
I270N-J*	-392	48	32	2195	-11090	222	2199	-11090
O270N-A	4	65	57	2680	918	108	2686	912
O270N-B	-29	78	77	3427	144	19	3427	144
O270N-C	-53	84	83	3734	-462	13	3734	-462
O270N-D	-71	81	85	3723	-1021	-57	3724	-1022
O270N-E	-73	74	75	3349	-1191	-19	3349	-1191
O270N-F	-57	66	69	3040	-813	-44	3040	-814
O270N-G	-48	60	70	2904	-583	-133	2910	-588
O270N-H	-48	55	66	2706	-628	-152	2712	-635
O270N-J	-41	47	61	2416	-515	-184	2428	-527

INTERNAL PRESSURE (50 PSI)

	MICRO-STRAIN			STRESSES			PRIN STRESSES	
ROSETTE	GAGE1	GAGE2	GAGE3	TRANS	LONG	SHEAR	SIGMX	SIGMN
I300C-A	-123	39	172	4782	-2243	-1766	5201	-2662
I300C-B	-77	22	191	4774	-877	-2248	5559	-1662
I300C-C	-26	13	199	4686	636	-2482	5864	-542
I300C-D	18	14	200	4690	1949	-2476	6149	490
I300C-E	54	24	181	4453	2947	-2102	5933	1467
I300C-F	100	30	135	3514	4048	-1399	5206	2357
I300C-G	96	28	95	2578	3667	-893	4168	2077
I300C-H	82	23	57	1685	2972	-456	3117	1540
I300C-J	66	13	51	1337	2383	-513	2592	1128
I300C-K	64	15	59	1559	2392	-583	2692	1259
I300C-L	55	22	58	1695	2148	-481	2453	1389
0300C-A	77	211	184	8615	4894	361	8650	4859
0300C-B	55	211	146	7783	3989	867	7972	3800
0300C-C	28	201	102	6633	2817	1330	7050	2399
0300C-D	1	186	63	5472	1670	1646	6085	1056
0300C-E	-25	165	36	4435	589	1722	5093	-69
0300C-F	-45	117	-16	2285	-669	1773	3115	-1499
0300C-G	-15	75	-32	946	-172	1425	1917	-1143
0300C-H	15	62	-19	913	730	1083	1908	-265
0300C-J	48	62	8	1483	1885	715	2427	940
0300C-K	57	61	14	1578	2170	627	2567	1180
0300C-L	58	58	15	1545	2203	583	2543	1205
I300N-A	-208	-62	190	3049	-5330	-3356	4227	-6508
I300N-B	-75	50	159	4688	-832	-1450	5045	-1190
I300N-C	1	105	133	5231	1598	-361	5267	1562
I300N-D	38	121	95	4711	2539	348	4765	2485
I300N-E	32	109	66	3818	2115	576	3995	1938
I300N-F*	-711	-60	-664	-15130	-25880	8041	-10840	-30180
I300N-G	-15	42	40	1823	105	19	1823	105
I300N-H	-16	49	37	1919	91	165	1933	76
I300N-J	-16	54	47	2221	196	95	2225	191
0300N-A	155	239	133	7997	7047	1406	9005	6038
0300N-B	24	201	132	7305	2919	924	7492	2732
0300N-C	-45	143	77	4875	108	874	5030	-47
0300N-D	-68	93	57	3375	-1040	481	3427	-1092
0300N-E	-66	57	44	2307	-1275	177	2316	-1284
0300N-F	-29	24	46	1577	-382	-291	1619	-425
0300N-G	-5	30	62	2042	470	-424	2149	363
0300N-H	-11	39	61	2216	337	-285	2258	295
0300N-J	-14	34	53	1927	150	-260	1964	113

INTERNAL PRESSURE (50 PSI)

	MICRO-STRAIN			STRESSES			PRIN STRESSES	
ROSETTE	GAGE1	GAGE2	GAGE3	TRANS	LONG	SHEAR	SIGMX	SIGMN
I330C-A	-245	222	175	9011	-4653	627	9040	-4681
I330C-B*	-119	173	179	7870	-1203	-82	7870	-1204
I330C-C	-9	149	184	7331	1943	-462	7370	1903
I330C-D*	63	164	178	7461	4134	-184	7471	4124
I330C-E	97	105	165	5836	4673	-804	6246	4262
I330C-F	96	56	111	3561	3934	-741	4511	2983
I330C-G	54	35	91	2698	2434	-747	3325	1807
I330C-H	29	29	85	2465	1595	-753	2900	1160
I330C-J	18	36	100	2968	1418	-861	3351	1034
I330C-K	14	30	96	2762	1256	-874	3163	856
I330C-L	16	28	92	2615	1255	-861	3032	838
O330C-A	119	366	308	14690	7971	779	14780	7882
O330C-B	39	309	258	12420	4894	690	12480	4831
O330C-C	-21	249	181	9486	2204	899	9595	2095
O330C-D	-64	200	122	7151	221	1051	7307	65
O330C-E	-73	160	75	5229	-627	1133	5441	-838
O330C-F	-46	85	2	1972	-777	1102	2359	-1164
O330C-G	0	51	-10	909	273	804	1455	-274
O330C-H	21	47	2	1052	957	602	1608	401
O330C-J	21	53	0	1136	968	703	1760	344
O330C-K*	12	1602	4	35290	10940	21290	47640	-1405
O330C-L	17	57	5	1350	904	703	1864	390
I330N-A	-216	53	385	9867	-3526	-4419	11190	-4853
I330N-B	29	179	338	11320	4266	-2121	11910	3677
I330N-C	148	216	275	10630	7621	-779	10820	7432
I330N-D	190	208	210	8992	8400	-32	8994	8398
I330N-E	174	177	163	7287	7404	177	7532	7159
I330N-F*	114	-521	-829	-29790	-5500	4103	-4826	-30460
I330N-G	73	96	111	4463	3534	-196	4502	3494
I330N-H	24	39	55	2052	1328	-209	2108	1272
I330N-J*	15	40	-172	-2920	-420	2836	1430	-4770
O330N-A	0	266	224	10760	3227	557	10800	3186
O330N-B	-106	142	31	3918	-2004	1482	4268	-2354
O330N-C	-208	32	-48	-126	-6282	1064	52	-6461
O330N-D	-214	-43	-107	-3076	-7338	855	-2911	-7503
O330N-E	-217	-104	-143	-5203	-8076	526	-5110	-8169
O330N-F	-143	-145	-141	-6141	-6133	-57	-6080	-6194
O330N-G	-107	-116	-105	-4749	-4647	-152	-4537	-4858
O330N-H	35	36	43	1696	1549	-101	1747	1498
O330N-J	31	33	44	1668	1427	-146	1737	1359

A.2 Out-of-Plane Moment Loading, M_{XN}, on Nozzle

OUT-OF-PLANE MOMENT LOADING, MXN, ON NOZZLE (600 IN-LB)

	MICRO-STRAIN			STRESSES			PRIN STRESSES	
ROSETTE	GAGE1	GAGE2	GAGE3	TRANS	LONG	SHEAR	SIGMX	SIGMN
I-O-C-A	-1	-3	-5	-176	-96	19	-91	-180
I-O-C-B	-3	-8	2	-111	-133	-133	11	-256
I-O-C-C	-5	-13	9	-99	-172	-291	158	-429
I-O-C-D	-6	-15	12	-46	-185	-361	252	-483
I-O-C-E	-4	-15	14	-27	-122	-386	314	-464
I-O-C-F*	0	-21	21	0	0	-557	557	-557
I-O-C-G	-2	-21	18	-61	-75	-519	451	-587
I-O-C-H*	0	-19	17	-52	-16	-488	454	-522
I-O-C-J	-1	-18	20	64	-24	-507	529	-488
I-O-C-K	-2	-14	15	23	-50	-393	381	-408
I-O-C-L	1	-13	9	-95	0	-285	241	-336
O-O-C-A	1	16	-20	-85	3	481	442	-524
O-O-C-B	1	15	-18	-64	9	431	405	-459
O-O-C-C	4	12	-15	-67	108	355	386	-345
O-O-C-D	2	15	-12	61	75	355	423	-287
O-O-C-E	0	12	-10	63	19	291	333	-251
O-O-C-F	1	9	-9	-2	42	241	262	-221
O-O-C-G	-1	9	-2	137	13	146	233	-84
O-O-C-H	0	4	-2	42	13	76	105	-50
O-O-C-J	0	3	1	104	45	25	113	36
O-O-C-K*	-2	-1	0	-29	-66	-19	-21	-74
O-O-C-L	-10	-1	5	84	-260	-82	102	-279
I-O-N-A	1	-1	-10	-252	-47	127	13	-312
I-O-N-B	-5	-1	-10	-235	-227	108	-123	-339
I-O-N-C	-4	1	-11	-225	-196	165	-45	-376
I-O-N-D	-8	0	-11	-242	-301	139	-129	-414
I-O-N-E	-6	-1	-10	-234	-241	120	-117	-358
I-O-N-F*	-7	0	0	8	-212	0	8	-212
I-O-N-G	-7	-7	-6	-274	-296	-6	-273	-298
I-O-N-H*	-7	-2	-6	-160	-248	51	-137	-271
I-O-N-J	-13	-11	-12	-497	-548	6	-496	-549
O-O-N-A	5	13	-16	-57	125	386	431	-363
O-O-N-B	3	14	-8	143	143	291	434	-149
O-O-N-C	6	11	-8	56	202	253	393	-135
O-O-N-D	4	6	-5	17	119	139	216	-80
O-O-N-E	3	8	-4	80	124	152	255	-52
O-O-N-F	-1	7	-1	117	-8	108	179	-70
O-O-N-G	-3	4	-3	24	-78	89	75	-130
O-O-N-H	1	3	1	93	56	19	101	48
O-O-N-J	-1	5	-1	85	-3	76	129	-47

OUT-OF-PLANE MOMENT LOADING, MXN, ON NOZZLE (600 IN-LB)

	MICRO-STRAIN			STRESSES			PRIN STRESSES	
ROSETTE	GAGE1	GAGE2	GAGE3	TRANS	LONG	SHEAR	SIGMX	SIGMN
I-90C-A	-176	-49	-48	-1937	-5856	-25	-1937	-5856
I-90C-B	-144	-48	-45	-1899	-4903	-44	-1898	-4904
I-90C-C	-95	-43	-32	-1556	-3318	-146	-1544	-3330
I-90C-D	-44	-22	-17	-797	-1565	-70	-791	-1571
I-90C-E	-8	-10	-4	-304	-334	-76	-242	-396
I-90C-F	31	18	17	718	1156	13	1157	717
I-90C-G	72	33	27	1237	2524	89	2530	1231
I-90C-H	72	29	24	1069	2488	63	2491	1067
I-90C-J	48	7	10	302	1545	-38	1546	301
I-90C-K	31	-3	-1	-129	902	-19	903	-129
I-90C-L	8	-4	-6	-228	160	19	161	-229
O-90C-A	225	196	166	7721	9074	399	9183	7612
O-90C-B	175	137	133	5750	6971	44	6973	5749
O-90C-C	126	119	115	5000	5292	51	5300	4991
O-90C-D	69	97	102	4310	3374	-63	4314	3370
O-90C-E	34	77	82	3461	2065	-57	3463	2062
O-90C-F	-26	30	34	1449	-349	-51	1451	-351
O-90C-G	-50	-3	-8	-185	-1552	57	-183	-1555
O-90C-H	-52	-20	-21	-862	-1827	13	-862	-1827
O-90C-J	-40	-27	-25	-1095	-1526	-19	-1094	-1527
O-90C-K	-26	-17	-15	-671	-985	-19	-670	-987
O-90C-L	-5	-8	-6	-297	-246	-19	-240	-303
I-90N-A	-343	28	-30	324	-10180	766	380	-10240
I-90N-B	-110	89	62	3431	-2264	361	3454	-2287
I-90N-C	19	90	85	3833	1706	70	3836	1704
I-90N-D	81	65	71	2888	3290	-82	3306	2872
I-90N-E	79	35	42	1594	2859	-95	2866	1587
I-90N-F	48	-19	-1	-492	1307	-241	1338	-524
I-90N-G	19	-18	-11	-658	359	-82	365	-664
I-90N-H	23	-16	-10	-590	522	-89	529	-597
I-90N-J	21	-20	-11	-712	414	-114	425	-724
O-90N-A	385	303	271	12190	15210	431	15270	12130
O-90N-B	144	228	218	9627	7222	133	9635	7215
O-90N-C	27	126	144	5903	2569	-241	5920	2552
O-90N-D	-28	55	68	2746	-17	-177	2758	-29
O-90N-E	-29	13	25	868	-624	-165	886	-642
O-90N-F	29	-1	-2	-106	852	6	852	-106
O-90N-G	38	10	12	439	1272	-25	1273	438
O-90N-H	38	9	11	407	1263	-32	1264	406
O-90N-J	33	10	9	371	1095	19	1096	371

OUT-OF-PLANE MOMENT LOADING, MXN, ON NOZZLE (600 IN-LB)

	MICRO-STRAIN			STRESSES			PRIN STRESSES	
ROSETTE	GAGE1	GAGE2	GAGE3	TRANS	LONG	SHEAR	SIGMX	SIGMN
I120C-A	-138	66	-81	-193	-4192	1956	605	-4990
I120C-B	-91	57	-90	-631	-2926	1950	484	-4041
I120C-C	-71	57	-96	-789	-2375	2045	612	-3775
I120C-D	-54	50	-103	-1090	-1938	2039	569	-3596
I120C-E	-33	48	-100	-1092	-1311	1975	777	-3180
I120C-F*	13	29	-99	-1539	-63	1709	1061	-2663
I120C-G	20	19	-62	-952	327	1083	945	-1570
I120C-H	29	15	-36	-502	733	677	1032	-801
I120C-J	31	5	0	81	951	57	955	77
I120C-K	37	1	22	472	1239	-285	1333	377
I120C-L	19	0	26	554	736	-348	1005	285
O120C-A	153	165	88	5388	6207	1026	6902	4693
O120C-B	101	146	42	4035	4247	1387	5532	2750
O120C-C	90	133	30	3504	3760	1374	5012	2252
O120C-D	69	120	25	3109	3014	1273	4335	1788
O120C-E*	50	128	24	3287	2497	1380	4327	1456
O120C-F	35	98	14	2426	1783	1114	3264	945
O120C-G	10	44	18	1357	721	348	1510	567
O120C-H	4	16	21	810	357	-63	819	349
O120C-J	-8	-16	13	-54	-244	-380	242	-541
O120C-K	-12	-31	1	-644	-564	-424	-178	-1030
O120C-L	-13	-29	-8	-800	-639	-279	-430	-1010
I120N-A	-221	-19	62	1172	-6277	-1083	1326	-6431
I120N-B	-78	28	93	2728	-1520	-867	2898	-1690
I120N-C	9	35	81	2549	1036	-614	2767	818
I120N-D	45	34	53	1862	1899	-247	2128	1633
I120N-E	46	19	25	931	1662	-76	1670	923
I120N-F	22	3	-4	-55	639	95	652	-68
I120N-G	0	-14	-5	-418	-125	-127	-78	-465
I120N-H	11	-7	-7	-315	248	-6	248	-316
I120N-J	11	-11	-9	-440	196	-32	197	-442
O120N-A	192	139	196	7152	7905	-753	8371	6686
O120N-B	41	114	132	5344	2829	-241	5367	2806
O120N-C	-18	68	68	3028	367	0	3028	367
O120N-D	-34	33	17	1144	-669	215	1169	-694
O120N-E	-19	13	-7	157	-537	260	244	-624
O120N-F	11	2	-11	-221	262	177	320	-279
O120N-G	21	5	-6	-44	628	139	656	-72
O120N-H	21	5	1	102	672	51	677	97
O120N-J	22	5	3	153	716	32	718	151

OUT-OF-PLANE MOMENT LOADING, MXN, ON NOZZLE (600 IN-LB)

	MICRO-STRAIN			STRESSES			PRIN STRESSES	
ROSETTE	GAGE1	GAGE2	GAGE3	TRANS	LONG	SHEAR	SIGMX	SIGMN
I150C-A	-55	44	-23	510	-1501	893	849	-1840
I150C-B	-41	45	-42	98	-1211	1159	774	-1887
I150C-C*	-36	40	0	927	-805	538	1081	-959
I150C-D	-25	33	-64	-662	-954	1292	492	-2108
I150C-E*	0	33	-64	-668	-201	1292	878	-1747
I150C-F*	-17	22	-74	-1120	-835	1273	303	-2258
I150C-G	-7	-1	-78	-1737	-721	1019	-90	-2368
I150C-H	-5	-5	-69	-1614	-627	855	-133	-2107
I150C-J*	17	-29	-65	-2097	-116	475	-8	-2205
I150C-K*	22	-55	-61	-2573	-102	76	-100	-2575
I150C-L	14	-7	-13	-465	288	82	297	-474
O150C-A*	55	49	62	2384	2355	-177	2547	2191
O150C-B	41	51	30	1741	1748	272	2017	1472
O150C-C*	29	44	17	1305	1247	355	1632	921
O150C-D*	29	0	42	888	1122	-557	1574	435
O150C-E	29	65	25	1932	1435	532	2271	1097
O150C-F*	30	69	33	2213	1562	475	2463	1312
O150C-G	29	63	24	1879	1448	526	2231	1095
O150C-H	23	60	23	1813	1242	494	2098	957
O150C-J	18	52	23	1631	1017	393	1822	825
O150C-K	9	33	18	1108	603	196	1175	536
O150C-L	6	11	7	390	302	51	413	279
I150N-A	-62	13	16	715	-1639	-38	716	-1639
I150N-B	-20	12	19	701	-389	-95	709	-397
I150N-C	0	9	15	523	143	-89	542	123
I150N-D	6	6	6	254	262	-6	265	251
I150N-E	4	1	-1	6	116	32	124	-2
I150N-F	-1	0	0	-9	-45	-6	-8	-46
I150N-G	-7	1	-7	-118	-235	101	-60	-294
I150N-H	-4	3	-3	5	-127	76	39	-162
I150N-J	-2	6	-3	65	-52	114	135	-121
O150N-A	23	39	66	2283	1369	-361	2408	1244
O150N-B	-5	26	38	1405	265	-165	1429	242
O150N-C	-17	10	19	666	-313	-114	679	-326
O150N-D	-18	3	6	228	-459	-38	230	-461
O150N-E	-11	2	-1	23	-335	44	28	-341
O150N-F	2	-4	-4	-180	3	6	3	-180
O150N-G	3	0	0	-14	96	6	96	-14
O150N-H	5	-2	-3	-110	110	13	110	-110
O150N-J	7	-5	-1	-143	157	-57	167	-154

OUT-OF-PLANE MOMENT LOADING, MXN, ON NOZZLE (600 IN-LB)

	MICRO-STRAIN			STRESSES			PRIN STRESSES	
ROSETTE	GAGE1	GAGE2	GAGE3	TRANS	LONG	SHEAR	SIGMX	SIGMN
I180C-A	-8	1	-5	-75	-251	76	-47	-279
I180C-B	-4	5	-9	-79	-138	177	71	-288
I180C-C	-2	13	-11	44	-44	317	320	-320
I180C-D	2	13	-14	-23	50	367	383	-355
I180C-E	1	14	-17	-53	13	412	393	-433
I180C-F	0	15	-18	-63	-5	443	410	-478
I180C-G	0	16	-22	-136	-41	513	427	-603
I180C-H	0	12	-19	-135	-55	412	319	-509
I180C-J	0	19	-15	93	42	462	531	-395
I180C-K	-1	21	-13	179	25	462	570	-367
I180C-L	5	16	-6	204	204	291	495	-88
O180C-A	5	-7	20	298	232	-361	627	-98
O180C-B	2	-10	17	155	103	-348	478	-220
O180C-C	1	-11	15	72	64	-348	416	-280
O180C-D	-1	-10	11	33	-33	-285	287	-287
O180C-E	-4	-10	12	57	-111	-298	282	-336
O180C-F	0	-7	8	10	17	-196	210	-183
O180C-G	2	-5	4	-13	67	-120	154	-100
O180C-H	0	-3	2	-21	-6	-76	63	-90
O180C-J	2	0	-1	-24	64	25	71	-30
O180C-K*	2	7	0	134	97	95	212	19
O180C-L	0	-1	-2	-73	-36	6	-35	-74
I180N-A	-13	-4	-8	-247	-459	44	-238	-468
I180N-B	-10	-3	-4	-135	-340	13	-135	-341
I180N-C	-3	-5	-3	-163	-149	-25	-130	-183
I180N-D	-5	-8	-9	-349	-262	13	-260	-351
I180N-E	-5	-5	-6	-245	-216	13	-212	-250
I180N-F*	0	67	-10	1243	373	1019	1916	-300
I180N-G	-6	-5	-13	-390	-302	101	-236	-457
I180N-H*	0	61	-8	1159	348	918	1757	-250
I180N-J	-6	-2	-6	-171	-237	44	-149	-259
O180N-A	10	-5	24	406	436	-380	801	41
O180N-B	7	-6	18	254	276	-323	588	-58
O180N-C	4	-6	13	153	160	-247	403	-91
O180N-D	1	-3	10	156	75	-171	291	-60
O180N-E	2	-1	8	144	114	-127	256	2
O180N-F	4	0	7	132	154	-95	238	47
O180N-G*	0	9	7	345	103	32	349	99
O180N-H	1	-1	5	92	71	-82	165	-2
O180N-J	0	0	4	83	39	-63	128	-6

OUT-OF-PLANE MOMENT LOADING, MXN, ON NOZZLE (600 IN-LB)

	MICRO-STRAIN			STRESSES			PRIN STRESSES	
ROSETTE	GAGE1	GAGE2	GAGE3	TRANS	LONG	SHEAR	SIGMX	SIGMN
I270C-A	177	49	55	2083	5928	-76	5929	2081
I270C-B*	148	49	49	2009	5051	0	5051	2009
I270C-C	90	34	29	1280	3078	76	3082	1277
I270C-D	41	11	7	342	1328	57	1332	338
I270C-E	5	4	-7	-58	139	146	217	-135
I270C-F	-42	-20	-30	-1050	-1584	133	-1019	-1615
I270C-G	-62	-29	-34	-1321	-2250	70	-1316	-2255
I270C-H	-62	-29	-31	-1268	-2248	25	-1268	-2249
I270C-J	-43	-16	-17	-673	-1499	6	-673	-1499
I270C-K	-32	-11	-8	-383	-1070	-38	-381	-1072
I270C-L	-15	-6	-8	-287	-528	32	-283	-532
I270C-M	-10	-9	-8	-365	-409	-13	-362	-412
O270C-A	-185	-170	-148	-6773	-7578	-291	-6679	-7672
O270C-B*	0	0	-134	-2956	-887	1792	148	-3990
O270C-C	-131	-129	-114	-5193	-5492	-209	-5085	-5600
O270C-D	-75	-103	-90	-4158	-3500	-165	-3461	-4197
O270C-E	-41	-78	-72	-3255	-2217	-76	-2211	-3260
O270C-F	22	-30	-31	-1361	262	13	262	-1361
O270C-G	50	5	8	227	1565	-32	1566	226
O270C-H	59	23	27	1042	2080	-51	2083	1040
O270C-J	44	21	30	1080	1636	-114	1658	1057
O270C-K	27	19	22	868	1073	-38	1080	862
O270C-L	4	9	12	444	262	-44	455	251
I270N-A	463	19	27	514	14050	-101	14050	514
I270N-B	220	-59	-16	-1892	6033	-570	6074	-1933
I270N-C	25	-87	-40	-2837	-110	-627	28	-2974
I270N-D	-78	-79	-58	-2932	-3232	-272	-2771	-3393
I270N-E	-86	-57	-54	-2350	-3271	-38	-2348	-3273
I270N-F	-58	-14	-1	-270	-1834	-177	-250	-1854
I270N-G	-31	-5	2	-28	-949	-89	-20	-958
I270N-H	-29	-5	1	-63	-874	-82	-54	-882
I270N-J	-23	-8	-2	-194	-743	-70	-186	-751
O270N-A	-448	-276	-252	-11100	-16760	-317	-11080	-16780
O270N-B	-184	-220	-233	-9751	-8442	171	-8420	-9773
O270N-C	-23	-137	-150	-6293	-2586	171	-2579	-6301
O270N-D	30	-73	-82	-3448	-136	120	-132	-3452
O270N-E	44	-24	-27	-1155	965	38	966	-1156
O270N-F	-11	10	7	399	-223	44	402	-226
O270N-G	-27	-2	-3	-85	-838	6	-85	-838
O270N-H	-26	-2	-6	-160	-818	51	-156	-822
O270N-J	-22	0	-2	-18	-661	38	-16	-663

OUT-OF-PLANE MOMENT LOADING, MXN, ON NOZZLE (600 IN-LB)

	MICRO-STRAIN			STRESSES			PRIN STRESSES	
ROSETTE	GAGE1	GAGE2	GAGE3	TRANS	LONG	SHEAR	SIGMX	SIGMN
I300C-A	132	-61	101	733	4169	-2165	5215	-313
I300C-B*	121	0	124	2582	4410	-1646	5379	1613
I300C-C	98	-39	126	1803	3492	-2210	5013	282
I300C-D	70	-40	124	1782	2644	-2191	4446	-20
I300C-E	46	-39	127	1892	1936	-2216	4130	-302
I300C-F	0	-25	84	1295	389	-1456	2367	-683
I300C-G	-23	-16	60	986	-403	-1013	1520	-936
I300C-H	-25	-16	31	372	-630	-627	673	-931
I300C-J	-37	-8	-9	-325	-1195	6	-325	-1195
I300C-K	-30	-1	-26	-562	-1081	336	-397	-1246
I300C-L	-15	5	-27	-464	-581	431	-88	-957
O300C-A	-133	-162	-62	-4783	-5427	-1342	-3725	-6485
O300C-B*	-137	-163	-45	-4434	-5450	-1577	-3286	-6598
O300C-C	-123	-149	-43	-4084	-4918	-1418	-3023	-5979
O300C-D	-98	-137	-42	-3819	-4083	-1266	-2678	-5224
O300C-E	-74	-120	-32	-3261	-3188	-1165	-2059	-4390
O300C-F	-33	-84	-28	-2428	-1726	-747	-1252	-2903
O300C-G	-14	-43	-25	-1478	-871	-234	-791	-1558
O300C-H	-5	-14	-26	-883	-407	158	-359	-930
O300C-J	5	21	-14	141	199	469	639	-300
O300C-K	15	31	-3	600	636	462	1080	155
O300C-L	14	25	9	726	645	222	911	460
I300N-A	266	38	-75	-1097	7654	1513	7909	-1351
I300N-B	88	-14	-94	-2468	1911	1057	2153	-2710
I300N-C	-10	-38	-96	-2945	-1169	779	-876	-3238
I300N-D	-56	-40	-72	-2404	-2389	418	-1978	-2814
I300N-E	-60	-36	-47	-1740	-2333	146	-1707	-2367
I300N-F	-33	-13	-8	-423	-1125	-76	-415	-1133
I300N-G	-23	-8	-10	-351	-790	25	-350	-791
I300N-H	-24	-6	-10	-339	-815	57	-333	-821
I300N-J	-20	-9	-10	-385	-729	6	-385	-729
O300N-A	-197	-136	-201	-7199	-8062	861	-6667	-8593
O300N-B	-59	-111	-129	-5219	-3348	241	-3317	-5250
O300N-C	9	-73	-63	-2986	-639	-133	-632	-2993
O300N-D	31	-45	-25	-1570	470	-272	506	-1605
O300N-E	27	-20	2	-427	685	-291	756	-498
O300N-F	-3	3	18	463	53	-203	546	-30
O300N-G	-17	0	9	207	-451	-114	226	-470
O300N-H	-13	0	5	140	-357	-63	148	-365
O300N-J	-13	1	6	171	-348	-70	181	-357

OUT-OF-PLANE MOMENT LOADING, MXN, ON NOZZLE (600 IN-LB)

	MICRO-STRAIN			STRESSES			PRIN STRESSES	
ROSETTE	GAGE1	GAGE2	GAGE3	TRANS	LONG	SHEAR	SIGMX	SIGMN
I330C-A	51	-54	40	-370	1429	-1254	2072	-1013
I330C-B	45	-47	57	170	1391	-1374	2284	-723
I330C-C	37	-39	67	586	1288	-1418	2398	-524
I330C-D	30	-29	78	1032	1208	-1431	2554	-313
I330C-E*	19	-27	81	1159	918	-1437	2481	-404
I330C-F	4	-4	87	1824	661	-1209	2584	-99
I330C-G	0	10	87	2131	625	-1038	2661	95
I330C-H	4	16	79	2084	754	-848	2497	341
I330C-J	-2	23	65	1924	506	-557	2117	313
I330C-K	-9	18	45	1388	160	-367	1489	58
I330C-L	-10	13	19	722	-97	-89	731	-107
O330C-A	-47	-45	-42	-1860	-1969	-32	-1851	-1978
O330C-B	-46	-49	-43	-1976	-1961	-76	-1892	-2045
O330C-C*	-50	-52	-40	-1971	-2102	-165	-1859	-2214
O330C-D	-40	-56	-36	-1972	-1789	-272	-1593	-2168
O330C-E	-38	-61	-33	-2016	-1745	-374	-1483	-2278
O330C-F	-35	-68	-31	-2134	-1695	-494	-1374	-2455
O330C-G	-29	-66	-27	-2005	-1471	-513	-1160	-2316
O330C-H	-25	-63	-28	-1967	-1346	-462	-1099	-2213
O330C-J	-18	-53	-27	-1735	-1048	-355	-898	-1885
O330C-K	-10	-36	-19	-1190	-671	-234	-580	-1280
O330C-L	-3	-10	-15	-529	-259	70	-242	-546
I330N-A	11	-16	-22	-838	91	82	98	-845
I330N-B	-7	-20	-25	-995	-512	63	-504	-1003
I330N-C	-14	-18	-26	-935	-708	108	-665	-978
I330N-D	-23	-18	-25	-915	-959	89	-846	-1028
I330N-E	-18	-17	-23	-847	-796	82	-735	-908
I330N-F	-17	-15	-15	-629	-702	0	-629	-702
I330N-G	-14	-14	-15	-622	-600	19	-589	-633
I330N-H	-11	-10	-15	-521	-484	70	-430	-574
I330N-J	-12	-12	-16	-603	-537	57	-504	-636
O330N-A	0	-40	-57	-2151	-645	228	-612	-2185
O330N-B	10	-19	-32	-1139	-28	177	-1	-1167
O330N-C	23	-5	-15	-454	562	133	580	-471
O330N-D*	21	0	0	-24	635	0	635	-24
O330N-E	16	3	3	118	520	6	520	118
O330N-F	3	6	8	300	176	-19	303	173
O330N-G	-1	5	8	294	45	-38	300	40
O330N-H	-1	8	6	314	66	25	317	63
O330N-J	-4	6	10	359	-6	-51	366	-13

A.3 Torsional Moment Loading, M_{YN}, on Nozzle

TORSIONAL MOMENT LOADING, MYN, ON NOZZLE (2000 IN-LB)

	MICRO-STRAIN			STRESSES			PRIN STRESSES	
ROSETTE	GAGE1	GAGE2	GAGE3	TRANS	LONG	SHEAR	SIGMX	SIGMN
I-O-C-A	-12	-10	-4	-300	-447	-89	-259	-488
I-O-C-B	-9	-6	-7	-262	-335	13	-260	-337
I-O-C-C	-8	-1	-14	-325	-340	165	-168	-497
I-O-C-D	-8	1	-17	-326	-326	241	-85	-566
I-O-C-E	-8	2	-16	-284	-313	241	-58	-540
I-O-C-F*	0	-6	-11	-376	-113	63	-98	-390
I-O-C-G	-10	-12	-9	-459	-437	-44	-402	-494
I-O-C-H*	0	-14	-7	-460	-138	-89	-115	-482
I-O-C-J	-10	-14	-7	-438	-431	-95	-339	-530
I-O-C-K	-11	-15	-8	-479	-472	-95	-380	-570
I-O-C-L	-10	-15	-6	-459	-451	-120	-335	-575
O-O-C-A	1	40	-36	83	53	1013	1081	-945
O-O-C-B*	5	25	-20	99	186	595	739	-454
O-O-C-C	3	18	-12	122	122	393	515	-270
O-O-C-D	4	12	-5	153	160	222	378	-65
O-O-C-E	7	10	1	254	276	120	386	144
O-O-C-F	7	1	6	149	244	-57	271	123
O-O-C-G	6	3	8	223	252	-63	303	173
O-O-C-H*	7	7	30	797	439	-310	976	260
O-O-C-J	9	9	6	325	354	38	380	299
O-O-C-K*	10	5	0	93	342	63	357	78
O-O-C-L	-1	7	2	200	17	70	224	-6
I-O-N-A	-9	-66	35	-659	-468	-1342	782	-1909
I-O-N-B	-14	-74	48	-559	-581	-1627	1057	-2197
I-O-N-C	-11	-74	51	-489	-475	-1659	1177	-2141
I-O-N-D	-13	-76	48	-612	-583	-1646	1049	-2244
I-O-N-E*	-21	-77	47	-635	-818	-1652	929	-2381
I-O-N-F*	-15	0	52	1166	-107	-696	1473	-414
I-O-N-G	-10	-68	49	-417	-439	-1564	1136	-1992
I-O-N-H	-19	-66	49	-345	-674	-1526	1026	-2044
I-O-N-J	-18	-70	52	-388	-644	-1627	1116	-2148
O-O-N-A	-1	45	-59	-323	-125	1387	1166	-1614
O-O-N-B	-3	49	-60	-237	-157	1450	1254	-1647
O-O-N-C	-3	54	-67	-279	-169	1602	1379	-1827
O-O-N-D*	-1	60	-69	-197	-102	1716	1567	-1866
O-O-N-E	-4	62	-73	-236	-185	1792	1581	-2002
O-O-N-F	-3	65	-77	-248	-160	1887	1684	-2091
O-O-N-G	-6	70	-77	-130	-210	1956	1787	-2127
O-O-N-H	-6	67	-78	-244	-244	1925	1680	-2169
O-O-N-J	-11	68	-73	-102	-373	1880	1648	-2123

TORSIONAL MOMENT LOADING, MYN, ON NOZZLE (2000 IN-LB)

	MICRO-STRAIN			STRESSES			PRIN STRESSES	
ROSETTE	GAGE1	GAGE2	GAGE3	TRANS	LONG	SHEAR	SIGMX	SIGMN
I-90C-A	-19	-132	84	-1024	-877	-2874	1925	-3826
I-90C-B	-15	-140	85	-1195	-801	-2988	1997	-3993
I-90C-C	-14	-151	100	-1102	-744	-3337	2418	-4265
I-90C-D	-9	-141	92	-1066	-591	-3096	2277	-3933
I-90C-E	-10	-124	85	-846	-539	-2773	2085	-3470
I-90C-F	-6	-70	49	-453	-321	-1595	1210	-1984
I-90C-G	1	-24	3	-461	-110	-367	122	-692
I-90C-H	-2	2	-25	-488	-218	361	32	-738
I-90C-J	-3	3	-31	-623	-287	456	31	-941
I-90C-K	-5	-10	-21	-673	-359	146	-302	-730
I-90C-L	-6	-19	-13	-703	-396	-76	-379	-721
O-90C-A	6	71	-50	453	307	1621	2003	-1242
O-90C-B*	13	48	-40	173	451	1178	1498	-874
O-90C-C	2	67	-51	332	157	1570	1817	-1328
O-90C-D	2	72	-58	290	144	1735	1954	-1519
O-90C-E	1	70	-65	113	77	1804	1900	-1709
O-90C-F*	-7	67	-86	-410	-323	2026	1660	-2393
O-90C-G	6	60	-73	-299	96	1773	1682	-1886
O-90C-H	6	45	-52	-162	136	1298	1293	-1320
O-90C-J	6	12	-18	-132	132	405	426	-426
O-90C-K	3	-2	-2	-108	53	0	53	-108
O-90C-L	4	2	0	37	139	25	145	31
I-90N-A	-27	-84	98	332	-699	-2425	2296	-2662
I-90N-B	-10	-62	83	470	-144	-1937	2124	-1799
I-90N-C	-3	-54	82	620	86	-1804	2177	-1471
I-90N-D	3	-57	87	655	282	-1931	2408	-1472
I-90N-E	1	-59	85	563	197	-1912	2301	-1541
I-90N-F	3	-62	79	362	194	-1880	2161	-1604
I-90N-G	1	-67	76	207	105	-1899	2056	-1744
I-90N-H	5	-66	73	161	205	-1849	2032	-1666
I-90N-J	-2	-61	74	274	25	-1798	1952	-1653
O-90N-A	13	116	-96	435	530	2817	3300	-2336
O-90N-B	-5	107	-86	475	-60	2564	2813	-2338
O-90N-C	-11	92	-91	23	-335	2438	2288	-2600
O-90N-D	-12	81	-90	-185	-412	2273	1977	-2574
O-90N-E	-11	67	-81	-301	-418	1975	1616	-2336
O-90N-F	-5	55	-64	-193	-201	1589	1392	-1786
O-90N-G	-7	57	-62	-86	-240	1589	1428	-1754
O-90N-H	-2	57	-67	-217	-136	1665	1489	-1842
O-90N-J	-7	58	-66	-159	-262	1659	1449	-1870

TORSIONAL MOMENT LOADING, MYN, ON NOZZLE (2000 IN-LB)

	MICRO-STRAIN			STRESSES			PRIN STRESSES	
ROSETTE	GAGE1	GAGE2	GAGE3	TRANS	LONG	SHEAR	SIGMX	SIGMN
I120C-A	-61	31	133	3670	-724	-1349	4051	-1105
I120C-B	-10	32	113	3206	677	-1076	3602	281
I120C-C	36	19	110	2791	1921	-1222	3653	1059
I120C-D	60	10	97	2273	2492	-1165	3553	1213
I120C-E	64	7	89	2029	2533	-1095	3405	1157
I120C-F*	26	-17	51	734	1004	-905	1784	-46
I120C-G	32	-21	32	215	1034	-709	1443	-194
I120C-H	0	-33	19	-313	-94	-696	501	-909
I120C-J	-24	-37	-1	-799	-953	-475	-395	-1357
I120C-K	-27	-29	-13	-911	-1072	-215	-761	-1221
I120C-L	-20	-25	-21	-991	-896	-57	-869	-1018
C120C-A	36	205	64	5883	2834	1880	6779	1938
C120C-B	-12	136	34	3753	755	1368	4283	225
C120C-C	-60	96	-7	2029	-1187	1368	2532	-1690
C120C-D	-72	56	-29	675	-1965	1133	1095	-2384
C120C-E	-73	29	-59	-578	-2355	1171	4	-2936
C120C-F	-75	-10	-79	-1871	-2799	918	-1307	-3264
C120C-G	-48	-35	-77	-2402	-2160	564	-1705	-2857
C120C-H	-28	-37	-63	-2163	-1476	342	-1335	-2304
C120C-J	-5	-5	-41	-1007	-459	488	-174	-1292
C120C-K	-4	11	-33	-466	-254	589	239	-958
C120C-L	0	9	-16	-167	-50	329	226	-443
I120N-A	-89	-78	174	2218	-2001	-3362	4077	-3860
I120N-B	27	-36	177	3073	1720	-2830	5306	-513
I120N-C	76	-29	152	2621	3067	-2425	5280	409
I120N-D	83	-43	128	1779	3014	-2273	4752	41
I120N-E	79	-51	103	1041	2693	-2051	4078	-345
I120N-F	48	-69	71	-11	1451	-1861	2719	-1280
I120N-G*	0	-176	60	-2548	-765	-3140	1608	-4921
I120N-H	37	-78	63	-364	989	-1880	2311	-1686
I120N-J	35	-80	54	-613	857	-1792	2059	-1814
O120N-A	167	210	59	5738	6725	2007	8299	4165
O120N-B	54	168	-11	3397	2627	2393	5431	584
O120N-C	21	114	-67	1021	948	2406	3391	-1422
O120N-D	26	91	-101	-237	699	2558	2831	-2369
O120N-E	24	62	-107	-1018	407	2260	2065	-2675
O120N-F	55	54	-90	-844	1401	1918	2501	-1944
O120N-G	47	66	-77	-302	1307	1899	2565	-1560
O120N-H	54	72	-70	-18	1620	1899	2869	-1267
O120N-J	41	73	-63	174	1292	1817	2634	-1168

TORSIONAL MOMENT LOADING, MYN, ON NOZZLE (2000 IN-LB)

	MICRO-STRAIN			STRESSES			PRIN STRESSES	
ROSETTE	GAGE1	GAGE2	GAGE3	TRANS	LONG	SHEAR	SIGMX	SIGMN
I150C-A	-57	48	63	2485	-951	-203	2497	-963
I150C-B	-11	54	38	2049	287	209	2073	262
I150C-C*	18	48	0	1045	855	646	1603	298
I150C-D	40	38	7	958	1499	418	1727	731
I150C-E*	0	-18	-1	-418	-125	-228	-1	-542
I150C-F	28	7	-10	-114	793	228	847	-168
I150C-G	10	-15	-5	-450	165	-127	190	-475
I150C-H	-1	-19	1	-385	-158	-272	23	-566
I150C-J	-13	-17	10	-132	-439	-367	113	-683
I150C-K	-26	2	13	362	-661	-139	381	-680
I150C-L	-16	-15	9	-118	-520	-323	61	-699
O150C-A	26	142	36	3877	1947	1406	4617	1207
O150C-B	-13	100	19	2636	406	1083	3075	-33
O150C-C	-22	64	5	1550	-504	779	1812	-766
O150C-D*	-29	0	-10	-188	-912	133	-164	-935
O150C-E	-37	29	-1	656	-901	412	759	-1003
O150C-F	-20	-7	-14	-438	-730	101	-406	-762
O150C-G	-8	-16	-21	-806	-484	76	-467	-823
O150C-H	-5	-17	-15	-684	-362	-25	-360	-686
O150C-J	-10	-20	-19	-845	-567	-25	-565	-847
O150C-K	-18	-11	-22	-712	-741	139	-586	-866
O150C-L	-21	-6	-11	-353	-747	63	-343	-757
I150N-A	-48	-44	120	1724	-923	-2178	2949	-2148
I150N-B	24	-50	117	1446	1147	-2235	3537	-943
I150N-C	54	-54	104	1048	1925	-2115	3646	-673
I150N-D	56	-61	93	649	1863	-2051	3395	-883
I150N-E	56	-71	76	32	1692	-1956	2987	-1263
I150N-F*	29	-70	0	-1567	385	-931	758	-1939
I150N-G	29	-70	60	-251	794	-1741	2089	-1546
I150N-H	28	-77	60	-407	719	-1836	2077	-1764
I150N-J	29	-80	61	-460	718	-1880	2099	-1841
O150N-A	71	150	20	3661	3237	1722	5184	1713
O150N-B	31	130	-29	2201	1601	2115	4037	-235
O150N-C	14	109	-64	988	710	2305	3157	-1460
O150N-D	15	91	-82	182	497	2311	2656	-1977
O150N-E	19	80	-89	-219	504	2248	2419	-2134
O150N-F	36	60	-98	-886	818	2108	2240	-2308
O150N-G	41	67	-85	-453	1104	2020	2490	-1839
O150N-H	38	72	-84	-292	1053	2077	2563	-1803
O150N-J	41	70	-82	-317	1131	2026	2559	-1744

TORSIONAL MOMENT LOADING, MYN, ON NOZZLE (2000 IN-LB)

	MICRO-STRAIN			STRESSES			PRIN STRESSES	
ROSETTE	GAGE1	GAGE2	GAGE3	TRANS	LONG	SHEAR	SIGMX	SIGMN
I180C-A	-15	-10	-10	-443	-575	0	-443	-575
I180C-B	-13	-5	-16	-456	-522	146	-340	-638
I180C-C	-12	-2	-21	-488	-503	253	-242	-749
I180C-D	-11	-2	-22	-510	-495	266	-236	-768
I180C-E	-11	-1	-21	-478	-486	272	-210	-754
I180C-F	-8	-5	-16	-440	-374	146	-258	-557
I180C-G	-9	-9	-13	-471	-399	63	-361	-508
I180C-H	-10	-13	-11	-533	-445	-25	-438	-539
I180C-J	-11	-8	-4	-249	-403	-57	-230	-422
I180C-K	-6	-6	-4	-213	-249	-19	-204	-257
I180C-L	-8	-12	-5	-357	-335	-95	-251	-442
O180C-A	8	40	-26	295	316	880	1186	-575
O180C-B	5	25	-12	266	223	494	739	-250
O180C-C	6	17	-4	286	271	279	557	0
O180C-D	4	11	1	267	194	139	375	87
O180C-E	4	5	5	215	193	-6	216	191
O180C-F*	2	-1	9	175	124	-133	285	14
O180C-G*	3	1	8	205	161	-89	275	92
O180C-H	4	1	6	153	160	-57	213	99
O180C-J	5	5	6	235	213	-19	246	202
O180C-K*	0	6	5	251	75	13	252	74
O180C-L	3	5	2	143	129	38	175	97
I180N-A	-16	-65	46	-410	-608	-1475	969	-1988
I180N-B	-13	-79	60	-393	-517	-1855	1401	-2311
I180N-C	-10	-83	65	-397	-404	-1969	1569	-2370
I180N-D	-10	-83	62	-449	-434	-1925	1483	-2366
I180N-E	-12	-83	59	-509	-509	-1887	1378	-2396
I180N-F*	0	-94	58	-773	-232	-2026	1542	-2546
I180N-G	-13	-73	57	-320	-495	-1735	1330	-2144
I180N-H*	0	8	57	1410	423	-652	1734	99
I180N-J	-2	-86	56	-645	-265	-1887	1441	-2351
O180N-A	-3	59	-56	77	-77	1539	1540	-1540
O180N-B	-8	63	-59	92	-215	1621	1567	-1689
O180N-C	-12	67	-67	-7	-373	1785	1605	-1985
O180N-D	-12	69	-74	-91	-398	1912	1674	-2163
O180N-E	-13	71	-78	-132	-439	1988	1709	-2279
O180N-F	-7	74	-83	-191	-271	2096	1865	-2327
O180N-G*	0	43	-86	-940	-282	1709	1130	-2352
O180N-H	-8	71	-84	-263	-321	2064	1772	-2356
O180N-J	-7	74	-86	-243	-287	2127	1863	-2392

TORSIONAL MOMENT LOADING, MYN, ON NOZZLE (2000 IN-LB)

	MICRO-STRAIN			STRESSES			PRIN STRESSES	
ROSETTE	GAGE1	GAGE2	GAGE3	TRANS	LONG	SHEAR	SIGMX	SIGMN
I270C-A	-1	-124	119	-103	-74	-3229	3141	-3317
I270C-B*	0	-143	128	-324	-83	-3615	3414	-3821
I270C-C	-1	-137	128	-197	-102	-3527	3378	-3676
I270C-D	-1	-127	112	-333	-129	-3178	2949	-3411
I270C-E	-5	-109	94	-329	-241	-2710	2425	-2995
I270C-F*	-15	-65	58	-140	-498	-1640	1331	-1969
I270C-G	-12	-21	5	-342	-473	-342	-59	-756
I270C-H	-15	7	-21	-297	-545	367	-33	-809
I270C-J	-15	10	-21	-234	-526	405	51	-811
I270C-K	-15	-1	-11	-255	-519	139	-195	-579
I270C-L	-12	-9	-2	-237	-442	-89	-204	-475
I270C-M	-11	-7	-11	-385	-443	51	-356	-473
O270C-A	-2	42	-29	285	14	956	1115	-816
O270C-B*	0	0	-48	-1065	-320	646	53	-1438
O270C-C	3	69	-57	268	180	1684	1909	-1461
O270C-D	6	78	-57	453	321	1798	2186	-1412
O270C-E	10	84	-63	449	420	1963	2397	-1528
O270C-F	9	88	-70	388	373	2102	2482	-1722
O270C-G	3	76	-57	404	207	1779	2087	-1476
O270C-H	7	59	-36	504	351	1260	1690	-835
O270C-J	4	24	-4	424	241	374	717	-52
O270C-K	1	11	7	395	161	63	411	145
O270C-L	2	10	11	468	197	-19	469	196
I270N-A	3	-115	102	-296	-3	-2900	2754	-3053
I270N-B	-2	-87	67	-458	-194	-2051	1730	-2381
I270N-C	-9	-71	35	-784	-506	-1406	768	-2057
I270N-D	-19	-67	39	-584	-760	-1406	736	-2080
I270N-E	-28	-69	50	-388	-943	-1583	942	-2272
I270N-F	-16	-74	56	-390	-602	-1728	1236	-2227
I270N-G*	-16	0	58	1302	-80	-779	1652	-430
I270N-H	-12	-79	57	-467	-497	-1823	1341	-2305
I270N-J	-19	-71	56	-313	-664	-1684	1204	-2182
O270N-A	-24	80	-101	-444	-846	2412	1776	-3066
O270N-B	-18	76	-113	-805	-783	2514	1719	-3308
O270N-C	-14	71	-103	-674	-616	2317	1673	-2962
O270N-D	-9	66	-92	-555	-423	2102	1614	-2592
O270N-E	-4	59	-78	-414	-228	1836	1512	-2164
O270N-F	-5	46	-59	-297	-246	1399	1128	-1671
O270N-G	-5	49	-62	-276	-240	1475	1217	-1733
O270N-H	-6	49	-63	-286	-271	1494	1216	-1773
O270N-J	-7	56	-65	-180	-268	1608	1385	-1833

TORSIONAL MOMENT LOADING, MYN, ON NOZZLE (2000 IN-LB)

	MICRO-STRAIN			STRESSES			PRIN STRESSES	
ROSETTE	GAGE1	GAGE2	GAGE3	TRANS	LONG	SHEAR	SIGMX	SIGMN
I300C-A	-70	36	107	3220	-1130	-943	3416	-1325
I300C-B	-18	15	106	2683	263	-1222	3193	-247
I300C-C	28	6	104	2392	1559	-1317	3357	594
I300C-D	56	3	99	2184	2323	-1285	3541	967
I300C-E	65	2	95	2059	2571	-1241	3582	1048
I300C-F	50	-10	58	1010	1814	-912	2408	416
I300C-G	14	-26	34	172	479	-798	1138	-487
I300C-H	-9	-33	15	-398	-376	-640	253	-1027
I300C-J	-31	-27	-5	-676	-1130	-291	-534	-1272
I300C-K	-31	-18	-21	-823	-1173	38	-818	-1177
I300C-L	-20	-8	-25	-699	-808	222	-525	-982
O300C-A	34	137	58	4244	2300	1051	4704	1840
O300C-B	-351	103	22	3143	-9592	1076	3233	-9683
O300C-C*	148	136	75	4474	5790	823	6186	4078
O300C-D	-62	40	-48	-99	-1883	1178	486	-2468
O300C-E	-70	19	-48	-570	-2281	899	-185	-2667
O300C-F	-72	-19	-71	-1915	-2742	690	-1524	-3133
O300C-G	-50	-41	-74	-2472	-2253	443	-1906	-2819
O300C-H*	-27	-136	-55	-4169	-2063	-1089	-1601	-4631
O300C-J	-66	-6	-29	-711	-2181	310	-648	-2244
O300C-K	342	12	-10	-334	10150	291	10160	-342
O300C-L	-134	14	6	586	-3859	114	589	-3861
I300N-A	-76	-86	162	1744	-1758	-3299	3728	-3741
I300N-B	14	-42	145	2251	1089	-2501	4237	-898
I300N-C	57	-28	122	2005	2326	-2001	4173	158
I300N-D	73	-29	98	1444	2629	-1684	3822	251
I300N-E	57	-39	76	751	1950	-1532	2996	-294
I300N-F	29	-62	39	-533	710	-1342	1567	-1391
I300N-G	25	-69	56	-309	649	-1665	1902	-1563
I300N-H	28	-70	52	-428	713	-1633	1873	-1588
I300N-J	26	-75	44	-718	569	-1583	1634	-1783
O300N-A	106	172	42	4593	4571	1728	6311	2854
O300N-B	43	145	-14	2846	2137	2121	4642	341
O300N-C	17	110	-54	1203	874	2184	3229	-1152
O300N-D	14	85	-72	256	504	2089	2473	-1713
O300N-E	14	69	-80	-256	351	1994	2065	-1970
O300N-F	40	45	-80	-806	956	1665	1958	-1809
O300N-G	48	55	-68	-345	1336	1633	2333	-1342
O300N-H	45	57	-65	-237	1269	1621	2303	-1271
O300N-J	36	60	-59	-19	1078	1583	2205	-1146

TORSIONAL MOMENT LOADING, MYN, ON NOZZLE (2000 IN-LB)

	MICRO-STRAIN			STRESSES			PRIN STRESSES	
ROSETTE	GAGE1	GAGE2	GAGE3	TRANS	LONG	SHEAR	SIGMX	SIGMN
I330C-A	-56	58	38	2181	-1014	272	2204	-1037
I330C-B	-14	44	28	1603	53	215	1632	24
I330C-C	14	37	17	1175	780	266	1309	646
I330C-D*	29	28	11	836	1106	222	1230	711
I330C-E	33	19	6	497	1133	171	1176	454
I330C-F	23	-8	2	-151	653	-127	673	-170
I330C-G	6	-16	7	-215	107	-304	290	-398
I330C-H	0	-16	12	-95	-14	-374	321	-430
I330C-J	-7	-11	18	154	-168	-380	406	-419
I330C-K	-13	-8	16	192	-327	-310	337	-472
I330C-L	-14	-6	6	26	-420	-158	77	-470
O330C-A	20	121	36	3424	1640	1127	3969	1095
O330C-B	-2	82	27	2394	661	741	2667	388
O330C-C	-16	46	13	1323	-88	437	1448	-212
O330C-D	-20	36	5	931	-320	412	1054	-443
O330C-E	-19	20	-2	418	-445	291	507	-534
O330C-F	-10	-4	-10	-282	-384	76	-241	-424
O330C-G	-1	-15	-9	-521	-199	-89	-176	-543
O330C-H	0	-17	-11	-606	-168	-76	-155	-619
O330C-J	-10	-17	-12	-637	-476	-63	-454	-659
O330C-K	2	-6	-8	-316	-24	25	-21	-318
O330C-L	1	1	0	9	45	19	54	1
I330N-A	-56	-49	109	1387	-1252	-2108	2555	-2419
I330N-B	10	-38	106	1493	733	-1912	3063	-836
I330N-C	45	-37	91	1142	1683	-1709	3143	-319
I330N-D	50	-43	77	676	1714	-1595	2873	-483
I330N-E	42	-48	67	351	1360	-1532	2468	-758
I330N-F*	36	-57	31	-593	891	-1171	1536	-1237
I330N-G	23	-59	54	-141	656	-1501	1810	-1295
I330N-H	29	-65	46	-460	732	-1475	1727	-1455
I330N-J	16	-64	44	-456	348	-1431	1432	-1541
O330N-A*	0	111	12	2695	808	1317	3371	132
O330N-B	22	96	-27	1501	1106	1646	2961	-355
O330N-C	6	74	-55	411	309	1709	2070	-1350
O330N-D	8	60	-67	-165	179	1703	1719	-1705
O330N-E	8	54	-76	-489	96	1735	1562	-1956
O330N-F	23	61	-77	-370	573	1830	1991	-1788
O330N-G	32	58	-73	-359	862	1754	2108	-1606
O330N-H	38	50	-75	-574	954	1665	2022	-1642
O330N-J	26	64	-72	-196	725	1811	2133	-1604

A.4 In-Plane Moment Loading, M_{ZN}, on Nozzle

IN-PLANE MOMENT LOADING, MZN, ON NOZZLE (2400 IN-LB)

	MICRO-STRAIN			STRESSES			PRIN STRESSES	
ROSETTE	GAGE1	GAGE2	GAGE3	TRANS	LONG	SHEAR	SIGMX	SIGMN
I-O-C-A	-321	91	60	3685	-8532	412	3698	-8546
I-O-C-B	-143	48	27	1817	-3732	285	1832	-3746
I-O-C-C	-34	41	35	1709	-514	76	1711	-516
I-O-C-D	26	25	26	1089	1097	-19	1112	1074
I-O-C-E*	0	8	15	491	147	-95	515	123
I-O-C-F*	0	-38	-35	-1608	-483	-38	-481	-1610
I-O-C-G	44	-59	-59	-2649	517	-6	517	-2649
I-O-C-H	0	-65	-59	-2715	-815	-76	-812	-2718
I-O-C-J	12	-61	-50	-2457	-381	-152	-370	-2468
I-O-C-K	8	-53	-47	-2192	-415	-82	-411	-2195
I-O-C-L	0	-37	-43	-1755	-526	76	-522	-1759
O-O-C-A	223	271	289	12070	10320	-234	12100	10290
O-O-C-B	70	191	192	8330	4609	-19	8330	4609
O-O-C-C	22	143	143	6284	2555	-45	6284	2555
O-O-C-D	-8	107	108	4750	1197	-13	4750	1197
O-O-C-E	-23	85	86	3764	445	-13	3764	445
O-O-C-F	5	40	42	1802	683	-32	1802	682
O-O-C-G	33	32	35	1437	1415	-44	1471	1380
O-O-C-H	39	33	36	1481	1628	-38	1637	1472
O-O-C-J	30	34	34	1460	1350	6	1460	1350
O-O-C-K*	22	34	0	728	874	456	1263	339
O-O-C-L	10	22	24	1012	617	-25	1014	616
I-O-N-A	-203	92	95	4317	-4792	-38	4317	-4792
I-O-N-B	-23	111	108	4840	768	44	4840	767
I-O-N-C	73	96	88	3972	3387	101	3989	3370
I-O-N-D	108	65	62	2659	4048	38	4049	2658
I-O-N-E	100	38	38	1551	3459	-6	3459	1551
I-O-N-F	65	0	0	-71	1918	0	1918	-71
I-O-N-G	48	5	2	93	1482	38	1483	92
I-O-N-H	48	11	10	418	1551	19	1551	417
I-O-N-J	55	12	16	566	1824	-51	1826	564
O-O-N-A	193	254	262	11140	9130	-108	11150	9124
O-O-N-B	39	167	162	7184	3338	76	7185	3337
O-O-N-C	-33	91	92	4068	223	-13	4068	222
O-O-N-D	-45	40	40	1814	-796	6	1814	-796
O-O-N-E	-29	10	12	512	-716	-25	513	-717
O-O-N-F	31	-7	-4	-275	859	-44	860	-276
O-O-N-G	56	3	2	43	1695	13	1695	43
O-O-N-H	52	0	-1	-78	1531	13	1531	-78
O-O-N-J	58	2	-1	-43	1726	38	1727	-44

IN-PLANE MOMENT LOADING, MZN, ON NOZZLE (2400 IN-LB)

	MICRO-STRAIN			STRESSES			PRIN STRESSES	
ROSETTE	GAGE1	GAGE2	GAGE3	TRANS	LONG	SHEAR	SIGMX	SIGMN
I-90C-A	-11	162	-200	-834	-578	4818	4114	-5526
I-90C-B	-21	180	-213	-708	-840	5230	4456	-6004
I-90C-C	-19	198	-238	-857	-813	5799	4965	-6635
I-90C-D	-22	193	-223	-634	-846	5553	4814	-6294
I-90C-E	-17	178	-211	-712	-727	5179	4459	-5899
I-90C-F	-13	116	-155	-842	-652	3609	2863	-4357
I-90C-G	-17	44	-72	-597	-692	1539	894	-2184
I-90C-H	-8	-11	-15	-577	-401	51	-388	-590
I-90C-J	-9	-35	14	-450	-406	-659	231	-1087
I-90C-K	-8	-24	4	-430	-357	-367	-25	-763
I-90C-L	-9	-8	-12	-429	-385	51	-352	-463
O-90C-A	-5	-4	-24	-600	-337	266	-172	-765
O-90C-B	-2	19	-43	-520	-213	836	483	-1216
O-90C-C	0	-1	-21	-491	-147	272	3	-641
O-90C-D	3	-12	-7	-431	-44	-70	-32	-444
O-90C-E	3	-25	9	-358	-22	-456	296	-676
O-90C-F	9	-64	54	-229	188	-1564	1557	-1598
O-90C-G	-5	-71	79	193	-85	-2001	2060	-1951
O-90C-H	-8	-68	66	-44	-241	-1779	1639	-1924
O-90C-J	-4	-33	24	-194	-186	-766	576	-956
O-90C-K	-6	-10	-1	-234	-241	-120	-117	-358
O-90C-L	-5	-8	-3	-245	-216	-63	-166	-296
I-90N-A	11	73	-94	-483	197	2222	2106	-2391
I-90N-B	-5	10	-22	-256	-219	437	200	-675
I-90N-C	-11	-21	14	-134	-382	-469	227	-743
I-90N-D	-6	-29	27	-45	-199	-753	635	-880
I-90N-E	-4	-28	29	15	-124	-753	702	-811
I-90N-F	-3	-6	12	150	-55	-241	309	-214
I-90N-G	0	2	-1	10	3	44	51	-38
I-90N-H	0	0	2	52	16	-32	71	-3
I-90N-J	1	0	1	30	38	-19	53	15
O-90N-A	12	-63	50	-296	282	-1513	1534	-1547
O-90N-B	22	-66	55	-264	577	-1602	1812	-1500
O-90N-C	20	-42	57	291	700	-1317	1828	-837
O-90N-D	12	-17	37	426	484	-709	1165	-255
O-90N-E	8	2	17	409	365	-203	591	183
O-90N-F	6	23	-8	328	270	405	705	-108
O-90N-G	6	19	-2	359	279	285	607	31
O-90N-H	1	14	-2	271	110	215	420	-40
O-90N-J	6	12	1	286	257	152	424	119

IN-PLANE MOMENT LOADING, MZN, ON NOZZLE (2400 IN-LB)

	MICRO-STRAIN			STRESSES			PRIN STRESSES	
ROSETTE	GAGE1	GAGE2	GAGE3	TRANS	LONG	SHEAR	SIGMX	SIGMN
I120C-A	150	-26	-158	-4207	3243	1766	3640	-4604
I120C-B	50	-28	-167	-4337	210	1849	867	-4994
I120C-C	-35	-19	-181	-4348	-2345	2165	-961	-5732
I120C-D	-94	-21	-186	-4451	-4144	2203	-2089	-6506
I120C-E	-122	-27	-182	-4451	-4985	2070	-2631	-6806
I120C-F*	-77	-10	-143	-3258	-3273	1773	-1493	-5038
I120C-G	-117	-16	-115	-2744	-4330	1323	-1994	-5080
I120C-H	-59	1	-85	-1763	-2297	1146	-853	-3206
I120C-J	-9	12	-45	-701	-467	760	185	-1353
I120C-K	7	9	-17	-185	144	336	353	-394
I120C-L	4	-2	9	132	154	-146	289	-3
O120C-A	-171	-304	-231	-11570	-8590	-975	-8299	-11860
O120C-B	-53	-199	-169	-8025	-4004	-393	-3956	-8063
O120C-C	17	-142	-114	-5627	-1175	-374	-1144	-5658
O120C-D	66	-92	-66	-3539	906	-355	934	-3568
O120C-E	94	-52	-25	-1795	2284	-367	2317	-1828
O120C-F	122	16	30	879	3913	-196	3926	867
O120C-G	90	66	67	2804	3550	-13	3550	2804
O120C-H	57	74	66	3008	2613	114	3038	2583
O120C-J	17	34	42	1642	1006	-108	1660	988
O120C-K	6	-3	26	495	334	-380	802	26
O120C-L	-8	-26	-1	-587	-404	-336	-148	-843
I120N-A	313	116	-226	-2767	8550	4559	10160	-4374
I120N-B	61	-31	-229	-5770	108	2634	1116	-6777
I120N-C	-88	-101	-176	-6002	-4452	1000	-3962	-6493
I120N-D	-143	-104	-114	-4636	-5696	146	-4616	-5716
I120N-E	-148	-84	-62	-3033	-5358	-291	-2997	-5394
I120N-F	-89	-26	-3	-529	-2825	-304	-489	-2864
I120N-G*	0	1	0	21	6	13	28	-1
I120N-H	-53	6	8	350	-1477	-25	351	-1478
I120N-J	-49	9	11	492	-1321	-38	493	-1321
O120N-A	-384	-319	-326	-13760	-15660	101	-13760	-15670
O120N-B	-106	-261	-177	-9502	-6030	-1121	-5700	-9833
O120N-C	10	-147	-56	-4471	-1028	-1222	-638	-4861
O120N-D	40	-68	23	-1026	904	-1216	1491	-1613
O120N-E	36	-12	60	1015	1388	-969	2188	215
O120N-F	-31	29	40	1549	-476	-158	1561	-489
O120N-G	-52	3	10	360	-1460	-95	365	-1465
O120N-H	-61	-2	0	15	-1820	-19	15	-1821
O120N-J	-51	-6	0	-69	-1560	-89	-64	-1566

IN-PLANE MOMENT LOADING, MZN, ON NOZZLE (2400 IN-LB)

	MICRO-STRAIN			STRESSES			PRIN STRESSES	
ROSETTE	GAGE1	GAGE2	GAGE3	TRANS	LONG	SHEAR	SIGMX	SIGMN
I150C-A	233	-89	-62	-3588	5923	-361	5937	-3602
I150C-B	90	-97	-41	-3138	1767	-753	1880	-3252
I150C-C*	7	-89	0	-1971	-378	-1190	258	-2607
I150C-D	-52	-81	-18	-2104	-2199	-842	-1309	-2995
I150C-E*	0	-69	-10	-1734	-520	-798	-125	-2129
I150C-F	-102	-38	14	-420	-3191	-703	-252	-3359
I150C-G	-78	-6	6	76	-2330	-158	86	-2340
I150C-H	-55	-1	-14	-274	-1736	177	-253	-1757
I150C-J	-24	-4	-42	-997	-1012	507	-498	-1511
I150C-K	-7	-38	-44	-1789	-736	89	-729	-1796
I150C-L	-24	-16	-44	-1290	-1100	367	-816	-1574
O150C-A	-199	-314	-299	-13240	-9946	-196	-9935	-13260
O150C-B	-86	-246	-171	-9065	-5286	-994	-5040	-9311
O150C-C	-28	-189	-126	-6904	-2898	-836	-2731	-7072
O150C-D*	12	0	-92	-2029	-238	1222	381	-2649
O150C-E	31	-116	-64	-3992	-271	-703	-143	-4120
O150C-F	29	-32	-16	-1087	544	-209	570	-1113
O150C-G	-4	8	-1	161	-80	120	211	-130
O150C-H	-16	19	-2	383	-370	272	471	-458
O150C-J	-15	25	3	633	-266	285	716	-349
O150C-K	-7	27	8	770	17	247	844	-57
O150C-L	0	28	11	856	257	228	933	180
I150N-A	343	40	-199	-3876	9130	3185	9868	-4614
I150N-B	80	-33	-182	-4829	946	1988	1564	-5447
I150N-C	-82	-83	-138	-4756	-3893	734	-3473	-5176
I150N-D	-140	-75	-87	-3418	-5217	165	-3403	-5232
I150N-E	-138	-60	-41	-2062	-4767	-253	-2039	-4791
I150N-F	-85	-5	0	-11	-2541	-63	-10	-2543
I150N-G	-55	4	2	196	-1595	19	197	-1595
I150N-H	-57	-2	2	63	-1692	-51	64	-1693
I150N-J	-59	0	2	118	-1747	-32	118	-1747
O150N-A	-277	-305	-328	-13610	-12410	317	-12330	-13680
O150N-B	-84	-243	-180	-9213	-5287	-842	-5114	-9386
O150N-C	27	-150	-68	-4823	-649	-1083	-385	-5087
O150N-D	46	-70	-4	-1690	876	-880	1149	-1963
O150N-E	26	-26	26	-39	758	-690	1157	-437
O150N-F	-35	6	36	947	-757	-399	1036	-845
O150N-G	-62	-2	11	266	-1773	-184	283	-1790
O150N-H	-61	-6	10	161	-1777	-209	183	-1799
O150N-J	-60	0	7	223	-1730	-95	227	-1734

IN-PLANE MOMENT LOADING, MZN, ON NOZZLE (2400 IN-LB)

	MICRO-STRAIN			STRESSES			PRIN STRESSES	
ROSETTE	GAGE1	GAGE2	GAGE3	TRANS	LONG	SHEAR	SIGMX	SIGMN
I180C-A	202	-86	-72	-3700	4949	-196	4953	-3704
I180C-B	75	-76	-65	-3163	1303	-146	1308	-3168
I180C-C	-15	-65	-57	-2657	-1239	-101	-1232	-2665
I180C-D	-66	-51	-44	-2016	-2586	-89	-2003	-2600
I180C-E	-91	-32	-48	-1644	-3216	209	-1617	-3244
I180C-F	-103	11	8	531	-2934	51	532	-2935
I180C-G*	-82	0	32	801	-2226	-431	861	-2286
I180C-H	-52	28	32	1384	-1153	-57	1385	-1154
I180C-J	-41	37	34	1612	-757	38	1613	-757
I180C-K	-28	34	36	1555	-360	-25	1555	-361
I180C-L	-23	24	15	882	-434	114	892	-444
O180C-A	-146	-241	-243	-10470	-7518	25	-7518	-10470
O180C-B	-67	-197	-191	-8449	-4545	-76	-4543	-8450
O180C-C	-19	-157	-146	-6642	-2577	-139	-2572	-6647
O180C-D	4	-119	-109	-5018	-1377	-139	-1372	-5023
O180C-E	10	-92	-86	-3928	-865	-82	-863	-3930
O180C-F	-12	-43	-46	-1940	-938	44	-936	-1942
O180C-G	-41	-36	-36	-1542	-1703	0	-1542	-1703
O180C-H	-48	-37	-42	-1680	-1958	76	-1661	-1978
O180C-J	-40	-40	-41	-1752	-1737	13	-1730	-1759
O180C-K*	0	-36	-38	-1629	-489	25	-488	-1630
O180C-L	-20	-23	-23	-1001	-913	0	-913	-1001
I180N-A	229	-114	-111	-5202	5311	-51	5311	-5202
I180N-B	18	-122	-132	-5597	-1137	127	-1134	-5600
I180N-C*	-89	-101	-114	-4633	-4070	171	-4022	-4681
I180N-D	-119	-70	-74	-3024	-4471	51	-3022	-4473
I180N-E	-110	-42	-41	-1697	-3802	-13	-1697	-3802
I180N-F*	0	18	-2	355	107	266	524	-63
I180N-G	-45	-2	-4	-87	-1366	19	-86	-1366
I180N-H*	0	-10	-6	-345	-103	-44	-96	-353
I180N-J	-57	-10	-4	-251	-1786	-76	-247	-1790
O180N-A	-274	-311	-289	-12900	-12080	-291	-11990	-12990
O180N-B	-51	-187	-184	-8101	-3956	-44	-3955	-8101
O180N-C	47	-89	-100	-4197	138	146	143	-4202
O180N-D	59	-29	-40	-1569	1311	152	1319	-1577
O180N-E	46	3	-3	-40	1371	82	1376	-45
O180N-F	-29	17	16	752	-630	19	752	-630
O180N-G*	0	7	6	282	85	19	284	83
O180N-H	-48	8	7	377	-1341	19	377	-1341
O180N-J	-56	9	8	417	-1557	13	417	-1557

IN-PLANE MOMENT LOADING, MZN, ON NOZZLE (2400 IN-LB)

	MICRO-STRAIN			STRESSES			PRIN STRESSES	
ROSETTE	GAGE1	GAGE2	GAGE3	TRANS	LONG	SHEAR	SIGMX	SIGMN
I270C-A	9	-227	181	-1022	-50	-5439	4924	-5997
I270C-B	10	-253	198	-1222	-67	-6002	5385	-6675
I270C-C	3	-246	205	-902	-171	-6015	5490	-6562
I270C-D	2	-238	185	-1161	-291	-5629	4919	-6372
I270C-E	-6	-215	167	-1059	-489	-5090	4324	-5872
I270C-F*	-8	-138	137	-22	-249	-3666	3532	-3803
I270C-G	-1	-63	51	-260	-121	-1513	1325	-1705
I270C-H	0	-6	1	-93	-42	-95	30	-166
I270C-J	2	24	-22	40	69	608	662	-554
I270C-K	2	13	-11	39	83	329	391	-269
I270C-L	4	0	3	58	132	-38	148	42
I270C-M	-1	5	7	263	36	-19	264	34
O270C-A	-15	-72	23	-1060	-760	-1260	359	-2178
O270C-B*	0	0	0	10	3	-6	14	-1
O270C-C*	-1	-19	-19	-834	-293	-13	-293	-834
O270C-D	18	7	-21	-333	442	367	588	-480
O270C-E	18	28	-30	-82	503	772	1036	-616
O270C-F	17	68	-62	118	534	1741	2079	-1428
O270C-G	10	84	-73	219	365	2089	2383	-1799
O270C-H	10	74	-61	272	367	1792	2111	-1473
O270C-J	7	32	-23	191	271	728	960	-498
O270C-K	6	8	-4	88	197	158	310	-25
O270C-L	5	2	5	161	205	-38	227	139
I270N-A	42	-119	117	-99	1239	-3147	3787	-2647
I270N-B	19	-41	41	-31	547	-1095	1391	-875
I270N-C	-7	4	-16	-254	-276	272	8	-537
I270N-D	-17	26	-36	-191	-556	823	470	-1216
I270N-E	-17	27	-30	-54	-530	753	498	-1082
I270N-F	-9	13	1	312	-163	158	360	-211
I270N-G	-4	1	10	245	-55	-108	280	-89
I270N-H	-4	3	5	182	-60	-32	186	-64
I270N-J	-1	4	1	106	3	38	118	-9
O270N-A	-35	21	-71	-1048	-1369	1228	30	-2447
O270N-B	-8	45	-91	-1005	-530	1804	1053	-2587
O270N-C	3	47	-67	-442	-47	1507	1275	-1764
O270N-D	4	30	-40	-214	64	937	873	-1022
O270N-E	1	12	-13	-33	33	336	337	-337
O270N-F	-6	-12	17	111	-138	-380	386	-413
O270N-G	-1	-10	14	106	3	-317	375	-266
O270N-H	0	-5	10	114	49	-209	293	-130
O270N-J	1	-2	10	187	85	-165	308	-37

IN-PLANE MOMENT LOADING, MZN, ON NOZZLE (2400 IN-LB)

	MICRO-STRAIN			STRESSES			PRIN STRESSES	
ROSETTE	GAGE1	GAGE2	GAGE3	TRANS	LONG	SHEAR	SIGMX	SIGMN
I300C-A	-184	-15	96	1978	-4938	-1469	2277	-5237
I300C-B	-110	-39	113	1750	-2768	-2026	2525	-3544
I300C-C	-25	-37	131	2085	-130	-2235	3472	-1517
I300C-D	39	-31	145	2464	1908	-2343	4545	-173
I300C-E	81	-22	151	2742	3246	-2298	5306	682
I300C-F	108	-18	125	2241	3923	-1912	5171	993
I300C-G	68	-29	86	1178	2406	-1545	3455	130
I300C-H	28	-46	52	106	859	-1298	1833	-869
I300C-J	-20	-45	16	-615	-783	-817	122	-1520
I300C-K	-34	-36	-10	-976	-1319	-336	-770	-1524
I300C-L	-26	-20	-31	-1089	-1111	146	-954	-1246
O300C-A	143	211	186	8584	6866	336	8648	6803
O300C-B	87	179	134	6786	4659	589	6939	4507
O300C-C	20	131	83	4677	2016	633	4820	1873
O300C-D	-35	86	35	2691	-248	684	2843	-399
O300C-E	-70	45	-3	1006	-1794	640	1145	-1933
O300C-F	-113	-33	-63	-1975	-3985	399	-1899	-4062
O300C-G	-84	-77	-86	-3480	-3553	127	-3385	-3648
O300C-H	-57	-72	-80	-3279	-2695	114	-2673	-3301
O300C-J	-24	-31	-58	-1927	-1291	361	-1128	-2090
O300C-K	-12	5	-36	-666	-556	538	-70	-1152
O300C-L	2	19	-9	238	129	374	561	-194
I300N-A	-321	-163	204	1251	-9262	-4900	3181	-11190
I300N-B	-85	-15	180	3717	-1422	-2590	4795	-2501
I300N-C	48	63	147	4553	2806	-1121	5100	2258
I300N-D	114	86	98	3916	4596	-171	4637	3876
I300N-E	113	75	54	2717	4194	279	4245	2666
I300N-F	62	22	-10	182	1922	431	2023	82
I300N-G	48	-5	-3	-220	1374	-25	1374	-220
I300N-H	48	-5	-4	-241	1382	-13	1382	-241
I300N-J	42	-7	-7	-339	1167	0	1167	-339
O300N-A	349	285	296	12390	14180	-146	14190	12380
O300N-B	137	244	168	8914	6794	1013	9321	6388
O300N-C	35	167	66	5089	2582	1349	5677	1994
O300N-D	-6	103	14	2586	591	1184	3137	40
O300N-E	-15	52	-17	790	-219	912	1327	-757
O300N-F	35	-5	-22	-633	851	234	887	-670
O300N-G	67	6	7	208	2087	-6	2087	208
O300N-H	61	11	12	444	1972	-6	1972	444
O300N-J	57	14	15	563	1894	-13	1894	563

IN-PLANE MOMENT LOADING, MZN, ON NOZZLE (2400 IN-LB)

	MICRO-STRAIN			STRESSES			PRIN STRESSES	
ROSETTE	GAGE1	GAGE2	GAGE3	TRANS	LONG	SHEAR	SIGMX	SIGMN
I330C-A	-249	101	-18	2101	-6840	1589	2375	-7114
I330C-B	-144	68	-21	1203	-3959	1190	1464	-4220
I330C-C	-46	58	-10	1105	-1051	918	1443	-1389
I330C-D	18	48	-10	805	783	766	1560	28
I330C-E	58	0	-10	-294	1651	139	1661	-303
I330C-F	81	-11	-18	-715	2209	89	2212	-718
I330C-G	48	-29	-12	-951	1155	-215	1176	-973
I330C-H	28	-28	1	-605	645	-386	755	-714
I330C-J	0	-14	23	209	63	-494	635	-364
I330C-K	2	-11	31	436	202	-557	888	-250
I330C-L	-7	-7	27	456	-63	-450	716	-322
O330C-A	182	258	200	9889	8427	772	10220	8094
O330C-B	106	214	174	8416	5704	526	8514	5606
O330C-C	52	170	131	6544	3517	519	6630	3430
O330C-D	-2	136	90	4984	1438	614	5087	1335
O330C-E	-20	105	57	3594	479	646	3722	351
O330C-F	-21	38	6	984	-346	431	1111	-473
O330C-G	0	-4	-9	-272	-81	63	-62	-291
O330C-H	12	-14	-12	-588	180	-32	182	-589
O330C-J	5	-26	-15	-893	-125	-146	-99	-920
O330C-K	-8	-41	-22	-1381	-642	-247	-567	-1456
O330C-L	-14	-38	-30	-1468	-854	-101	-838	-1484
I330N-A	-341	-82	183	2589	-9445	-3533	3549	-10410
I330N-B	-100	40	188	5133	-1454	-1969	5677	-1998
I330N-C	53	78	150	4955	3069	-962	5359	2665
I330N-D	110	79	101	3827	4441	-291	4557	3711
I330N-E	115	60	61	2526	4222	-13	4222	2526
I330N-F	85	8	-11	-167	2502	247	2525	-189
I330N-G	51	0	2	-4	1538	-32	1539	-5
I330N-H	55	4	2	65	1673	25	1674	64
I330N-J	56	1	4	43	1681	-38	1682	42
O330N-A*	0	286	309	13080	3923	-304	13090	3913
O330N-B	104	220	162	8273	5590	779	8482	5380
O330N-C	-1	149	74	4910	1430	1000	5177	1163
O330N-D	-29	85	23	2414	-160	823	2654	-401
O330N-E	-16	47	-12	780	-237	779	1201	-658
O330N-F	29	10	-25	-345	752	469	925	-518
O330N-G	66	14	-5	126	2005	247	2037	94
O330N-H	59	9	0	133	1822	120	1830	125
O330N-J	63	11	-2	119	1918	177	1935	102

A.5 In-Plane Force, F_{XN}, on Nozzle

IN-PLANE FORCE LOADING, FXN, ON NOZZLE (200 LB)

	MICRO-STRAIN			STRESSES			PRIN STRESSES	
ROSETTE	GAGE1	GAGE2	GAGE3	TRANS	LONG	SHEAR	SIGMX	SIGMN
I-O-C-A	454	-149	-103	-6024	11820	-614	11840	-6045
I-O-C-B	194	-89	-55	-3368	4820	-456	4846	-3393
I-O-C-C	36	-75	-65	-3120	133	-133	139	-3126
I-O-C-D	-51	-53	-53	-2273	-2207	6	-2207	-2274
I-O-C-E	-112	-27	-35	-1234	-3735	114	-1229	-3740
I-O-C-F*	0	43	38	1765	530	70	1769	526
I-O-C-G	-77	72	72	3249	-1335	6	3249	-1335
I-O-C-H*	0	79	73	3342	1003	89	3345	999
I-O-C-J	-30	77	61	3062	6	215	3077	-9
I-O-C-K	-27	64	57	2682	6	89	2685	3
I-O-C-L	-13	34	48	1811	144	-190	1832	123
O-O-C-A	-321	-401	-421	-17730	-14940	260	-14920	-17750
O-O-C-B	-102	-280	-279	-12190	-6722	-13	-6722	-12190
O-O-C-C	-33	-207	-204	-8997	-3697	-44	-3697	-8998
O-O-C-D	9	-159	-158	-6965	-1833	-13	-1833	-6965
O-O-C-E	31	-126	-124	-5527	-732	-25	-732	-5528
O-O-C-F	-10	-60	-62	-2674	-1087	32	-1087	-2674
O-O-C-G	-54	-48	-52	-2145	-2254	57	-2120	-2279
O-O-C-H	-65	-53	-57	-2342	-2641	44	-2335	-2648
O-O-C-J	-52	-55	-55	-2345	-2272	0	-2272	-2345
O-O-C-K*	-38	-48	0	-1003	-1441	-633	-552	-1892
O-O-C-L	1	-34	-36	-1526	-415	25	-415	-1527
I-O-N-A	296	-136	-140	-6394	6978	57	6978	-6394
I-O-N-B	29	-166	-162	-7260	-1294	-51	-1294	-7260
I-O-N-C	-111	-142	-131	-5884	-5087	-146	-5061	-5909
I-O-N-D	-157	-99	-92	-4016	-5909	-95	-4011	-5914
I-O-N-E	-143	-59	-54	-2318	-4986	-70	-2316	-4988
I-O-N-F	-90	0	0	99	-2679	0	99	-2679
I-O-N-G	-57	-8	-5	-220	-1762	0	-219	-1763
I-O-N-H	-62	-13	-13	-506	-2019	-1	-506	-2019
I-O-N-J	-59	-13	-17	-604	-1949	1	-602	-1951
O-O-N-A	-260	-357	-363	-15560	-12480	82	-12480	-15560
O-O-N-B	-33	-224	-219	-9708	-3910	-57	-3910	-9708
O-O-N-C	69	-118	-121	-5330	483	32	483	-5330
O-O-N-D	81	-45	-44	-2032	1828	-13	1828	-2032
O-O-N-E	57	-4	-5	-261	1632	19	1633	-261
O-O-N-F	-28	24	20	1002	-526	57	1004	-529
O-O-N-G	-60	8	8	411	-1687	6	411	-1687
O-O-N-H	-50	10	8	431	-1368	25	431	-1368
O-O-N-J	-53	10	13	549	-1418	-44	550	-1419

IN-PLANE FORCE LOADING, FXN, ON NOZZLE (200 LB)

	MICRO-STRAIN			STRESSES			PRIN STRESSES	
ROSETTE	GAGE1	GAGE2	GAGE3	TRANS	LONG	SHEAR	SIGMX	SIGMN
I-90C-A	-1	-213	274	1338	373	-6483	7357	-5646
I-90C-B	11	-245	287	907	614	-7091	7853	-6332
I-90C-C	2	-280	315	781	291	-7933	8473	-7401
I-90C-D	6	-275	296	464	310	-7604	7991	-7217
I-90C-E	2	-254	281	603	252	-7129	7559	-6704
I-90C-F	-7	-172	206	749	25	-5033	5433	-4659
I-90C-G	12	-67	97	644	564	-2184	2789	-1580
I-90C-H	3	8	15	498	235	-89	525	208
I-90C-J	3	43	-27	351	205	924	1206	-649
I-90C-K	3	26	-14	258	163	526	738	-317
I-90C-L	1	4	6	228	111	-25	234	106
O-90C-A	-3	-4	38	755	141	-570	1095	-199
O-90C-B	2	-35	67	687	277	-1355	1852	-888
O-90C-C	1	-7	36	647	223	-570	1042	-174
O-90C-D	0	13	17	659	183	-44	663	179
O-90C-E	0	32	-5	595	179	488	917	-143
O-90C-F	-9	90	-67	511	-118	2102	2322	-1929
O-90C-G	10	102	-104	-63	266	2754	2861	-2657
O-90C-H	4	93	-91	27	122	2450	2525	-2376
O-90C-J	2	44	-38	144	114	1089	1218	-960
O-90C-K	1	12	-1	250	103	177	368	-15
O-90C-L	2	-8	0	-169	6	-101	53	-216
I-90N-A	-13	-80	116	819	-154	-2615	2992	-2327
I-90N-B	11	4	15	416	453	-146	581	288
I-90N-C	17	47	-44	55	515	1209	1516	-946
I-90N-D	6	61	-67	-132	146	1697	1709	-1696
I-90N-E	2	55	-67	-264	-8	1614	1484	-1755
I-90N-F	-3	27	-38	-248	-160	861	659	-1066
I-90N-G	-3	14	-20	-133	-125	450	321	-579
I-90N-H	-5	14	-22	-172	-194	488	304	-671
I-90N-J	-3	15	-23	-174	-138	500	344	-657
O-90N-A	-15	88	-42	1019	-136	1735	2270	-1387
O-90N-B	-24	85	-52	747	-503	1830	2056	-1811
O-90N-C	-16	54	-52	59	-453	1418	1244	-1638
O-90N-D	-1	18	-22	-103	-74	532	444	-620
O-90N-E	4	-5	8	48	128	-171	264	-87
O-90N-F	7	-35	44	191	257	-1057	1282	-834
O-90N-G	4	-32	33	17	119	-874	943	-807
O-90N-H	3	-27	30	80	110	-760	855	-665
O-90N-J	2	-24	25	8	60	-652	687	-619

IN-PLANE FORCE LOADING, FXN, ON NOZZLE (200 LB)

	MICRO-STRAIN			STRESSES			PRIN STRESSES	
ROSETTE	GAGE1	GAGE2	GAGE3	TRANS	LONG	SHEAR	SIGMX	SIGMN
I120C-A	-229	34	209	5589	-5209	-2324	6068	-5688
I120C-B	-93	39	225	5898	-1010	-2476	6694	-1806
I120C-C	30	26	243	5878	2662	-2887	7575	965
I120C-D	111	29	246	5904	5107	-2893	8426	2585
I120C-E	151	36	240	5902	6304	-2716	8826	3379
I120C-F*	93	-31	172	3000	3680	-2703	6065	615
I120C-G	153	19	146	3456	5627	-1703	6561	2522
I120C-H	76	-19	106	1838	2832	-1671	4079	591
I120C-J	3	-21	55	748	324	-1013	1571	-499
I120C-K	-18	-16	15	9	-525	-412	233	-748
I120C-L	-15	-3	-22	-526	-614	253	-313	-827
O120C-A	242	410	337	16140	12100	969	16360	11880
O120C-B	78	271	252	11400	5759	253	11410	5747
O120C-C	-18	194	174	8103	1889	266	8115	1878
O120C-D	-85	128	107	5273	-956	279	5286	-968
O120C-E	-124	71	50	2810	-2878	279	2824	-2891
O120C-F	-162	-18	-31	-909	-5120	177	-901	-5127
O120C-G	-122	-90	-85	-3709	-4777	-76	-3704	-4782
O120C-H	-78	-102	-87	-4071	-3573	-190	-3509	-4135
O120C-J	-24	-48	-56	-2240	-1399	108	-1385	-2253
O120C-K	-8	1	-34	-712	-456	475	-92	-1076
O120C-L	8	30	-4	566	398	450	939	25
I120N-A	-449	-154	306	3836	-12340	-6129	5896	-14400
I120N-B	-91	57	304	8027	-315	-3286	9166	-1454
I120N-C	118	149	227	8132	5975	-1045	8555	5552
I120N-D	196	162	137	6375	7786	336	7862	6299
I120N-E	199	130	63	4021	7180	886	7411	3790
I120N-F	114	47	-17	544	3570	848	3792	322
I120N-G*	0	-14	-23	-825	-248	120	-224	-849
I120N-H	57	6	-24	-459	1559	393	1632	-533
I120N-J	50	2	-30	-682	1292	431	1382	-771
O120N-A	537	450	486	19990	22120	-475	22220	19890
O120N-B	148	367	272	13870	8610	1266	14160	8321
O120N-C	-5	212	114	7191	2015	1304	7501	1705
O120N-D	-46	96	7	2327	-685	1190	2741	-1098
O120N-E	-38	24	-44	-407	-1277	905	163	-1846
O120N-F	58	-30	-19	-1139	1397	-146	1406	-1148
O120N-G	84	-10	19	117	2544	-380	2602	59
O120N-H	91	-1	23	391	2840	-323	2882	349
O120N-J	77	6	27	625	2511	-279	2552	585

IN-PLANE FORCE LOADING, FXN, ON NOZZLE (200 LB)

	MICRO-STRAIN			STRESSES			PRIN STRESSES	
ROSETTE	GAGE1	GAGE2	GAGE3	TRANS	LONG	SHEAR	SIGMX	SIGMN
I150C-A	-343	123	90	5055	-8762	443	5070	-8776
I150C-B	-134	140	59	4523	-2663	1070	4679	-2819
I150C-C*	-10	128	0	2820	561	1703	3734	-353
I150C-D	138	114	20	2783	4983	1247	5546	2220
I150C-E*	0	104	8	2444	733	1279	3127	50
I150C-F	143	58	-30	459	4443	1171	4762	140
I150C-G	96	1	-22	-554	2699	310	2729	-583
I150C-H	67	-6	4	-115	1975	-127	1983	-123
I150C-J*	-27	-12	43	708	-586	-741	1045	-922
I150C-K	-8	38	44	1816	302	-70	1819	299
I150C-L	-5	0	50	1123	194	-665	1469	-152
C150C-A	279	432	430	18640	13960	38	18640	13960
C150C-B	114	337	243	12640	7227	1254	12910	6950
C150C-C	33	260	179	9614	3868	1076	9809	3673
C150C-D*	-20	0	133	2947	271	-1773	3830	-612
C150C-E	-47	157	97	5628	291	798	5745	175
C150C-F	-42	39	48	1957	-667	-108	1962	-672
C150C-G	6	-8	7	-28	177	-190	290	-141
C150C-H	23	-36	7	-663	500	-576	737	-900
C150C-J	18	-24	-3	-605	360	-279	435	-679
C150C-K	11	-45	-11	-1234	-42	-450	108	-1385
C150C-L	4	-38	-17	-1195	-230	-279	-156	-1270
I150N-A	-490	-55	272	5312	-13120	-4362	6292	-14100
I150N-B	-115	51	245	6623	-1477	-2583	7377	-2231
I150N-C	111	124	181	6572	5308	-753	6924	4956
I150N-D	188	117	112	4828	7079	76	7082	4825
I150N-E	187	88	45	2729	6436	576	6523	2642
I150N-F	111	12	0	150	3367	165	3375	142
I150N-G	65	-3	-18	-520	1783	196	1799	-537
I150N-H	65	5	-14	-270	1872	247	1900	-298
I150N-J	62	5	-14	-266	1773	247	1803	-296
C150N-A	388	434	485	19770	17580	-671	19960	17390
C150N-B	116	344	268	13330	7479	1007	13500	7311
C150N-C	-33	206	114	7076	1125	1228	7319	881
C150N-D	-60	100	28	2865	-951	962	3094	-1180
C150N-E	-37	36	-17	469	-971	703	755	-1257
C150N-F	50	-11	-28	-911	1223	215	1245	-933
C150N-G	85	2	1	-20	2532	19	2532	-20
C150N-H	78	8	3	154	2398	57	2400	153
C150N-J	73	0	9	119	2217	-108	2222	113

IN-PLANE FORCE LOADING, FXN, ON NOZZLE (200 LB)

	MICRO-STRAIN			STRESSES			PRIN STRESSES	
ROSETTE	GAGE1	GAGE2	GAGE3	TRANS	LONG	SHEAR	SIGMX	SIGMN
I180C-A	-301	121	96	5114	-7490	329	5122	-7498
I180C-B	-116	101	85	4201	-2218	215	4208	-2226
I180C-C	15	87	75	3555	1523	165	3568	1509
I180C-D	89	67	58	2660	3464	114	3480	2644
I180C-E	124	40	39	1597	4200	13	4200	1597
I180C-F	140	-24	-21	-1135	3851	-38	3851	-1136
I180C-G*	79	-158	-60	-4880	902	-1298	1180	-5158
I180C-H	66	-56	-53	-2464	1242	-44	1243	-2465
I180C-J	53	-52	-60	-2523	826	101	829	-2526
I180C-K	25	-48	-52	-2210	78	57	80	-2211
I180C-L	36	-33	-42	-1690	577	114	582	-1696
O180C-A	202	342	337	14710	10470	63	14710	10470
O180C-B	90	277	266	11830	6243	139	11830	6239
O180C-C	22	219	200	9188	3412	241	9198	3402
O180C-D	-10	163	140	6664	1686	310	6684	1666
O180C-E	-24	124	113	5217	838	146	5222	833
O180C-F	16	55	57	2437	1202	-32	2438	1201
O180C-G	57	45	48	1963	2300	-38	2304	1959
O180C-H	70	47	52	2105	2742	-70	2749	2098
O180C-J	57	48	53	2173	2348	-63	2369	2152
O180C-K*	0	43	47	1974	592	-44	1975	591
O180C-L	33	27	33	1290	1371	-82	1422	1239
I180N-A	-329	162	157	7380	-7665	76	7381	-7666
I180N-B	-30	169	185	7825	1435	-215	7832	1428
I180N-C	118	139	155	6335	5450	-222	6387	5398
I180N-D	166	96	101	4162	6224	-63	6226	4160
I180N-E	147	52	51	2115	5040	13	5040	2115
I180N-F*	0	-22	0	-491	-147	-285	14	-652
I180N-G	51	-4	-4	-224	1473	0	1473	-224
I180N-H*	0	3	2	115	34	19	119	30
I180N-J	56	8	0	95	1711	108	1718	88
O180N-A	401	456	423	18890	17690	437	19030	17540
O180N-B	78	278	274	12040	5950	57	12040	5949
O180N-C	-62	134	152	6345	36	-234	6354	27
O180N-D	-81	48	63	2533	-1678	-190	2542	-1686
O180N-E	-60	4	10	369	-1686	-70	371	-1688
O180N-F	42	-17	-17	-777	1021	0	1021	-777
O180N-G*	0	17	2	418	125	203	521	22
O180N-H	65	-1	-3	-155	1892	25	1893	-155
O180N-J	63	-3	-7	-288	1795	57	1797	-290

IN-PLANE FORCE LOADING, FXN, ON NOZZLE (200 LB)

	MICRO-STRAIN			STRESSES			PRIN STRESSES	
ROSETTE	GAGE1	GAGE2	GAGE3	TRANS	LONG	SHEAR	SIGMX	SIGMN
I270C-A	-30	307	-247	1349	-508	7382	7861	-7020
I270C-B	-37	339	-276	1440	-666	8193	8647	-7873
I270C-C	-23	331	-281	1112	-365	8155	8561	-7815
I270C-D	-24	318	-260	1300	-323	7712	8243	-7265
I270C-E	-14	288	-239	1091	-86	7021	7548	-6544
I270C-F	0	187	-195	-178	-39	5084	4976	-5193
I270C-G	-7	86	-72	311	-121	2096	2202	-2012
I270C-H	-4	8	-3	109	-81	139	182	-155
I270C-J	-6	-37	26	-224	-238	-836	605	-1067
I270C-K	-8	-26	12	-294	-331	-500	188	-813
I270C-L	-11	-5	-10	-322	-439	63	-294	-466
I270C-M	-4	-11	-12	-508	-266	6	-266	-508
O270C-A	19	109	-34	1639	1076	1906	3284	-569
O270C-B*	0	0	3	73	22	-44	99	-4
O270C-C	9	40	28	1484	702	171	1520	666
O270C-D	6	16	44	1320	567	-374	1474	413
O270C-E	2	-6	63	1240	443	-918	1843	-159
O270C-F	-5	-71	102	695	66	-2305	2706	-1946
O270C-G	-3	-98	120	484	45	-2900	3173	-2643
O270C-H	1	-88	98	218	94	-2488	2645	-2333
O270C-J	0	-35	42	156	61	-1032	1142	-925
O270C-K	1	2	10	270	124	-101	322	72
O270C-L	4	7	1	163	163	76	239	87
I270N-A	-49	152	-140	325	-1371	3900	3468	-4514
I270N-B	-17	41	-31	238	-442	956	913	-1116
I270N-C	12	-29	35	101	401	-855	1119	-617
I270N-D	20	-62	67	103	630	-1722	2109	-1376
I270N-E	18	-65	57	-197	468	-1614	1784	-1513
I270N-F	2	-42	14	-608	-125	-747	419	-1152
I270N-G*	-2	0	3	65	-38	-38	77	-50
I270N-H	-3	-26	7	-404	-207	-437	142	-753
I270N-J	-3	-24	12	-257	-177	-488	272	-706
O270N-A	45	-1	96	2040	1952	-1304	3301	691
O270N-B	11	-41	117	1669	843	-2108	3404	-893
O270N-C	-3	-49	83	745	124	-1754	2216	-1347
O270N-D	-3	-24	40	369	11	-855	1063	-683
O270N-E	-1	0	3	74	-6	-32	85	-17
O270N-F	13	38	-34	80	409	969	1227	-738
O270N-G	6	37	-30	139	227	886	1071	-704
O270N-H	4	31	-26	110	161	753	890	-618
O270N-J	4	28	-27	6	116	728	791	-669

IN-PLANE FORCE LOADING, FXN, ON NOZZLE (200 LB)

	MICRO-STRAIN			STRESSES			PRIN STRESSES	
ROSETTE	GAGE1	GAGE2	GAGE3	TRANS	LONG	SHEAR	SIGMX	SIGMN
I300C-A	251	6	-129	-2970	6636	1798	6962	-3296
I300C-B*	147	45	0	820	4665	595	4755	730
I300C-C	26	40	-181	-3130	-169	2944	1646	-4945
I300C-D	-66	33	-205	-3709	-3080	3166	-213	-6575
I300C-E	-122	19	-219	-4284	-4935	3172	-1421	-7798
I300C-F	-136	19	-186	-3516	-5146	2741	-1471	-7191
I300C-G	-104	36	-129	-1923	-3685	2197	-437	-5171
I300C-H	-47	58	-80	-429	-1540	1836	934	-2903
I300C-J	17	52	-33	399	633	1140	1662	-630
I300C-K	37	42	4	973	1390	513	1735	628
I300C-L	24	19	17	768	943	38	951	760
O300C-A	-218	-298	-272	-12300	-10220	-348	-10160	-12360
O300C-B	-137	-258	-202	-9970	-7097	-741	-6917	-10150
O300C-C	-44	-188	-127	-6876	-3389	-817	-3207	-7058
O300C-D	38	-132	-63	-4314	-139	-918	54	-4507
O300C-E	96	-71	-9	-1860	2308	-823	2464	-2016
O300C-F	148	43	80	2542	5210	-500	5301	2451
O300C-G	115	104	120	4793	4888	-209	5055	4626
O300C-H	75	36	116	3260	3230	-1064	4309	2181
O300C-J	31	36	80	2503	1692	-589	2813	1383
O300C-K	11	-10	48	824	575	-772	1482	-83
O300C-L	-7	-30	8	-473	-342	-507	103	-918
I300N-A	468	212	-280	-2019	13450	6559	15860	-4426
I300N-B	126	1	-247	-5538	2116	3311	3350	-6772
I300N-C	-64	-105	-199	-6624	-3912	1247	-3425	-7110
I300N-D	-161	-144	-130	-5849	-6588	-196	-5800	-6636
I300N-E	-161	-129	-67	-4136	-6074	-817	-3838	-6372
I300N-F	-88	-51	23	-519	-2807	-981	-156	-3171
I300N-G	-67	-14	12	21	-2004	-348	80	-2062
I300N-H	-66	-13	9	-32	-1977	-291	10	-2020
I300N-J	-57	-17	14	1	-1725	-405	91	-1815
O300N-A	-488	-387	-430	-17410	-19860	570	-17280	-19990
O300N-B	-189	-326	-244	-12310	-9354	-1095	-8993	-12680
O300N-C	-32	-215	-100	-6900	-3025	-1532	-2492	-7432
O300N-D	27	-123	-27	-3320	-183	-1273	268	-3771
O300N-E	34	-48	18	-706	815	-886	1222	-1113
O300N-F	-32	30	24	1215	-591	82	1219	-594
O300N-G	-77	19	-11	252	-2248	393	312	-2308
O300N-H	-66	11	-20	-137	-2008	418	-48	-2097
O300N-J	-60	6	-19	-237	-1867	336	-171	-1934

IN-PLANE FORCE LOADING, FXN, ON NOZZLE (200 LB)

	MICRO-STRAIN			STRESSES			PRIN STRESSES	
ROSETTE	GAGE1	GAGE2	GAGE3	TRANS	LONG	SHEAR	SIGMX	SIGMN
I330C-A	352	-160	15	-3572	9478	-2336	9883	-3977
I330C-B	200	-112	20	-2246	5328	-1760	5717	-2635
I330C-C	59	-97	8	-2029	1173	-1393	1694	-2550
I330C-D	-35	-95	3	-1987	-1651	-1304	-504	-3134
I330C-E	-93	-63	7	-1131	-3119	-924	-767	-3482
I330C-F*	-125	4	-262	-5523	-5420	3546	-1926	-9017
I330C-G*	-80	31	10	996	-2096	272	1020	-2120
I330C-H	-47	32	-15	438	-1280	627	643	-1484
I330C-J	-25	12	-41	-620	-942	709	-54	-1508
I330C-K	-13	6	-54	-1041	-697	804	-47	-1691
I330C-L	-1	1	-52	-1116	-363	715	69	-1548
O330C-A	-279	-369	-298	-14350	-12690	-943	-12260	-14770
O330C-B	-153	-304	-254	-12090	-8218	-659	-8109	-12200
O330C-C	-74	-242	-188	-9360	-5032	-722	-4915	-9477
O330C-D	1	-192	-128	-7041	-2069	-848	-1929	-7182
O330C-E	30	-145	-81	-5015	-606	-855	-446	-5175
O330C-F	30	-52	-8	-1349	494	-595	669	-1524
O330C-G	-1	5	17	471	113	-158	531	53
O330C-H	-15	25	17	936	-176	101	945	-185
O330C-J	-6	40	24	1416	254	209	1453	217
O330C-K	2	42	27	1512	511	209	1554	469
O330C-L	11	39	29	1492	776	127	1514	754
I330N-A	496	112	-257	-3720	13750	4913	15040	-5006
I330N-B	146	-68	-265	-7472	2149	2621	2817	-8139
I330N-C	-72	-121	-206	-7106	-4299	1127	-3902	-7502
I330N-D	-156	-124	-138	-5593	-6368	177	-5555	-6407
I330N-E	-163	-98	-79	-3716	-6005	-260	-3687	-6034
I330N-F	-115	-20	22	158	-3417	-564	245	-3503
I330N-G	-65	-11	2	-117	-1974	-177	-100	-1991
I330N-H	-71	-20	-1	-402	-2259	-253	-368	-2293
I330N-J	-67	-14	-4	-323	-2121	-139	-312	-2132
O330N-A	0	-309	-429	-16210	-4863	1595	-4643	-16430
O330N-B	-111	-286	-223	-11080	-6647	-842	-6493	-11240
O330N-C	29	-176	-101	-6120	-981	-1007	-791	-6310
O330N-D	65	-97	-23	-2724	1136	-988	1374	-2962
O330N-E	47	-43	20	-542	1234	-842	1570	-878
O330N-F	-24	12	38	1112	-379	-342	1187	-454
O330N-G	-69	8	13	535	-1907	-76	538	-1909
O330N-H	-67	5	-1	157	-1949	89	160	-1953
O330N-J	-63	0	1	111	-1863	-13	111	-1863

A.6 Axial Force, F_{YN}, on Nozzle

AXIAL FORCE LOADING, FYN, ON NOZZLE (300 LB)

	MICRO-STRAIN			STRESSES			PRIN STRESSES	
ROSETTE	GAGE1	GAGE2	GAGE3	TRANS	LONG	SHEAR	SIGMX	SIGMN
I-O-C-A	-49	9	6	389	-1366	38	389	-1367
I-O-C-B	-27	5	0	134	-758	76	140	-765
I-O-C-C	-11	2	-1	22	-321	44	28	-327
I-O-C-D*	0	3	3	126	24	0	126	24
I-O-C-E	2	-1	-2	-75	34	19	38	-78
I-O-C-F	0	-8	-12	-439	-132	51	-124	-447
I-O-C-G	3	-21	-20	-922	-191	-13	-191	-922
I-O-C-H	0	-25	-23	-1044	-313	-25	-312	-1045
I-O-C-J	0	-27	-25	-1128	-338	-25	-338	-1129
I-O-C-K	-1	-27	-25	-1127	-367	-25	-366	-1128
I-O-C-L	-9	-23	-29	-1118	-606	76	-595	-1129
O-O-C-A	32	48	43	1960	1543	70	1971	1532
O-O-C-B	14	31	34	1405	849	-38	1407	847
O-C-C-C	6	26	21	1017	476	63	1025	469
O-O-C-D	4	19	15	737	335	44	742	330
O-O-C-E	-9	11	7	396	-152	57	402	-158
O-O-C-F	-1	7	5	252	47	25	255	44
O-O-C-G	9	4	2	126	295	19	297	124
O-O-C-H	9	6	7	262	335	-13	337	260
O-O-C-J	11	5	6	218	393	-13	394	217
O-O-C-K*	10	11	0	229	368	146	460	137
O-O-C-L	2	7	12	416	182	-76	438	159
I-O-N-A	-24	15	15	684	-508	-6	684	-508
I-O-N-B	5	15	17	694	365	-32	697	362
I-O-N-C	13	14	16	654	595	-25	663	586
I-O-N-D	21	12	8	426	755	57	765	417
I-O-N-E	17	9	7	315	608	25	610	313
I-O-N-F	8	0	-4	-92	215	51	223	-101
I-O-N-G	8	-1	1	2	229	-32	233	-2
I-O-N-H	13	0	3	58	417	-32	420	56
I-O-N-J	14	2	4	121	450	-19	451	120
O-O-N-A	17	36	38	1611	982	-38	1613	980
O-O-N-B	-5	19	24	945	141	-63	950	136
O-O-N-C	-11	15	13	628	-139	32	630	-141
O-O-N-D	-10	10	4	303	-208	76	314	-219
O-O-N-E	-10	3	3	146	-241	-6	146	-241
O-O-N-F	5	3	0	78	180	38	193	65
O-O-N-G	4	2	4	132	154	-32	176	109
O-O-N-H	5	2	2	88	183	6	184	88
O-O-N-J	6	4	3	150	230	19	235	146

AXIAL FORCE LOADING, FYN, ON NOZZLE (300 LB)

	MICRO-STRAIN			STRESSES			PRIN STRESSES	
ROSETTE	GAGE1	GAGE2	GAGE3	TRANS	LONG	SHEAR	SIGMX	SIGMN
I-90C-A	-120	-20	-24	-840	-3844	44	-839	-3845
I-90C-B	-91	-25	-19	-861	-2995	-76	-858	-2998
I-90C-C	-45	-18	-19	-755	-1581	6	-755	-1581
I-90C-D	-6	-8	-7	-327	-284	-13	-280	-331
I-90C-E	23	-1	-2	-98	655	19	655	-99
I-90C-F	48	14	7	417	1579	95	1587	409
I-90C-G	77	17	7	448	2444	133	2453	439
I-90C-H	77	9	1	145	2367	101	2372	140
I-90C-J	43	-9	-11	-486	1151	25	1152	-487
I-90C-K	13	-15	-19	-767	169	51	172	-769
I-90C-L	-8	-15	-19	-744	-451	63	-438	-757
O-90C-A	132	125	110	5036	5460	203	5541	4954
O-90C-B	96	84	89	3697	3974	-63	3988	3683
O-90C-C	51	71	72	3077	2463	-13	3077	2462
O-90C-D	14	48	59	2355	1134	-146	2372	1117
O-90C-E	-13	36	43	1748	139	-101	1754	133
O-90C-F	-48	-3	9	179	-1401	-152	193	-1415
O-90C-G	-64	-27	-22	-1005	-2226	-57	-1003	-2229
O-90C-H	-46	-26	-26	-1099	-1698	0	-1099	-1698
O-90C-J	-22	-32	-23	-1177	-1009	0	-946	-1240
O-90C-K*	18	-15	-11	-594	364	-44	366	-596
O-90C-L	19	-16	0	-366	475	-209	524	-415
I-90N-A	-201	41	3	1193	-5687	500	1229	-5723
I-90N-B	-55	76	57	2974	-747	260	2992	-765
I-90N-C	29	69	67	2945	1739	32	2946	1738
I-90N-D	64	54	54	2311	2604	0	2604	2311
I-90N-E	62	30	35	1363	2262	-70	2268	1358
I-90N-F	38	0	2	10	1158	-19	1158	10
I-90N-G	16	-3	1	-49	456	-57	462	-55
I-90N-H	19	-3	-3	-168	534	0	534	-168
I-90N-J	21	-1	1	-13	638	-32	639	-15
O-90N-A	234	198	178	8004	9415	260	9461	7958
O-90N-B	83	146	137	6134	4321	114	6141	4314
O-90N-C	10	81	84	3613	1397	-44	3613	1397
O-90N-D	-22	34	44	1727	-152	-133	1736	-161
O-90N-E	-20	9	15	545	-450	-76	550	-455
O-90N-F	20	0	1	20	605	-13	605	20
O-90N-G	29	5	4	166	934	6	934	166
O-90N-H	27	5	8	252	888	-44	891	249
O-90N-J	19	9	8	344	688	6	688	344

AXIAL FORCE LOADING, FYN, ON NOZZLE (300 LB)

	MICRO-STRAIN			STRESSES			PRIN STRESSES	
ROSETTE	GAGE1	GAGE2	GAGE3	TRANS	LONG	SHEAR	SIGMX	SIGMN
I120C-A	-95	31	-36	-10	-2854	893	247	-3111
I120C-B	-58	29	-39	-166	-1803	899	232	-2200
I120C-C	-34	25	-43	-370	-1123	905	234	-1727
I120C-D*	-8	21	-48	-586	-418	918	420	-1424
I120C-E	6	19	-45	-560	3	855	622	-1178
I120C-F*	23	2	-55	-1184	329	753	640	-1495
I120C-G*	41	-6	-30	-839	989	317	1042	-892
I120C-H	37	-10	-16	-605	931	76	934	-609
I120C-J	29	-22	5	-407	733	-367	841	-515
I120C-K	22	-22	12	-254	580	-456	781	-455
I120C-L	-1	-21	9	-281	-113	-399	211	-605
O120C-A	98	116	75	4090	4178	545	4680	3588
O120C-B	58	97	45	3059	2657	703	3589	2127
O120C-C	40	82	27	2358	1905	734	2900	1363
O120C-D	21	64	20	1825	1189	576	2165	849
O120C-E*	5	67	15	1812	686	696	2145	354
O120C-F	-7	37	0	812	30	500	1056	-214
O120C-G	-17	-1	-2	-55	-515	19	-54	-516
O120C-H	-14	-22	-3	-527	-586	-253	-302	-812
O120C-J	-20	-38	-8	-981	-893	-405	-529	-1344
O120C-K	-13	-36	-18	-1166	-749	-234	-644	-1271
O120C-L	-9	-25	-19	-961	-559	-82	-543	-978
I120N-A	-144	-18	65	1182	-3979	-1102	1408	-4204
I120N-B	-42	20	82	2281	-570	-823	2501	-791
I120N-C	18	35	67	2237	1198	-431	2392	1043
I120N-D	45	30	45	1612	1824	-196	1941	1494
I120N-E	44	19	22	860	1584	-32	1585	859
I120N-F	21	3	-1	29	636	57	641	24
I120N-G*	0	-3	0	-63	-19	-38	3	-85
I120N-H	11	2	2	81	367	-6	367	81
I120N-J	11	-3	0	-86	316	-32	319	-88
O120N-A	128	98	132	4903	5320	-450	5607	4616
O120N-B	24	79	79	3451	1762	6	3451	1762
O120N-C	-21	42	38	1778	-108	63	1780	-110
O120N-D	-26	20	3	530	-625	228	573	-668
O120N-E	-21	1	-16	-300	-732	234	-198	-834
O120N-F	2	-5	-11	-358	-36	76	-19	-375
O120N-G	10	-6	-10	-355	179	44	182	-359
O120N-H	13	-2	2	-4	398	-57	406	-12
O120N-J	9	-1	-6	-156	210	63	221	-166

AXIAL FORCE LOADING, FYN, ON NOZZLE (300 LB)

	MICRO-STRAIN			STRESSES			PRIN STRESSES	
ROSETTE	GAGE1	GAGE2	GAGE3	TRANS	LONG	SHEAR	SIGMX	SIGMN
I150C-A	-66	22	-2	511	-1828	317	553	-1870
I150C-B	-37	23	-15	218	-1032	513	401	-1216
I150C-C*	-23	17	0	402	-578	228	452	-629
I150C-D*	29	10	-32	-523	727	564	943	-740
I150C-E*	0	-54	-37	-1984	-595	-228	-559	-2021
I150C-F	-3	-4	-40	-978	-393	481	-123	-1249
I150C-G	4	-16	-42	-1289	-273	348	-165	-1397
I150C-H	1	-19	-31	-1108	-304	165	-272	-1140
I150C-J	1	-37	-27	-1401	-378	-127	-362	-1416
I150C-K	3	-38	-25	-1382	-315	-177	-286	-1411
I150C-L	6	-20	5	-341	69	-342	263	-534
O150C-A	42	66	64	2805	2110	32	2806	2109
O150C-B	26	54	31	1851	1339	304	1993	1198
O150C-C	16	48	20	1476	913	374	1663	727
O150C-D*	4	0	15	330	213	-203	482	61
O150C-E	6	39	11	1090	498	374	1271	318
O150C-F	10	34	5	835	564	386	1108	290
O150C-G	13	21	-3	372	497	323	763	106
O150C-H	7	19	-2	358	321	272	612	67
O150C-J	4	2	-4	-46	100	89	142	-88
O150C-K	I	-1	-5	-126	-9	51	9	-145
O150C-L	3	-2	-17	-432	-30	196	50	-512
I150N-A	-62	6	45	1175	-1501	-519	1272	-1598
I150N-B	-11	15	44	1297	61	-386	1407	-50
I150N-C	23	20	35	1186	1054	-203	1333	907
I150N-D	31	17	26	896	1195	-120	1238	853
I150N-E	30	13	11	489	1045	25	1046	488
I150N-F*	18	1	0	11	545	19	546	11
I150N-G	7	2	0	44	227	32	233	39
I150N-H	13	0	1	6	401	-13	402	6
I150N-J	10	0	1	10	288	-13	289	10
O150N-A	38	55	67	2621	1941	-158	2656	1906
O150N-B	3	40	34	1616	570	82	1622	564
O150N-C	-17	20	10	697	-290	133	715	-307
O150N-D	-17	6	-4	50	-498	133	81	-529
O150N-E	-15	-2	-5	-150	-501	38	-146	-505
O150N-F	-1	-7	-8	-312	-122	13	-121	-313
O150N-G	7	-4	-5	-206	138	19	139	-207
O150N-H	6	-2	-3	-132	132	13	132	-132
O150N-J	6	-1	-1	-59	168	-6	168	-59

AXIAL FORCE LOADING, FYN, ON NOZZLE (300 LB)

	MICRO-STRAIN			STRESSES			PRIN STRESSES	
ROSETTE	GAGE1	GAGE2	GAGE3	TRANS	LONG	SHEAR	SIGMX	SIGMN
I180C-A	-47	12	10	532	-1252	25	533	-1252
I180C-B	-19	11	9	460	-432	38	461	-434
I180C-C	-6	8	3	236	-100	63	248	-112
I180C-D	4	1	2	69	135	-6	135	68
I180C-E*	2	-5	-2	-170	20	-38	28	-177
I180C-F*	10	-15	-13	-617	114	-25	115	-618
I180C-G	2	-21	-19	-870	-190	-32	-188	-871
I180C-H*	-2	-22	-21	-948	-356	-19	-355	-948
I180C-J	-5	-26	-25	-1101	-487	-13	-487	-1102
I180C-K	-10	-31	-30	-1336	-714	-19	-714	-1336
I180C-L	-13	-24	-26	-1082	-724	19	-723	-1083
O180C-A	16	47	43	1946	1068	51	1949	1065
O180C-B	6	37	29	1445	605	95	1456	594
O180C-C*	-3	21	13	745	124	108	763	106
O180C-D	-2	19	13	713	143	89	726	129
O180C-E	-2	18	13	692	136	63	699	129
O180C-F	2	4	6	217	122	-19	221	119
O180C-G	11	8	9	343	445	-13	447	341
O180C-H	8	9	12	440	374	-44	463	352
O180C-J	0	14	11	563	183	38	567	180
O180C-K	0	11	10	480	144	13	481	144
O180C-L	-11	11	11	493	-194	0	493	-194
I180N-A	-34	28	27	1228	-658	13	1228	-658
I180N-B	7	26	30	1225	567	-51	1229	563
I180N-C	20	20	20	866	859	-6	870	855
I180N-D	25	16	18	703	967	-25	969	701
I180N-E	22	7	10	341	772	-32	775	339
I180N-F	0	-2	0	-52	-16	-32	3	-71
I180N-G	10	0	-1	-32	304	25	306	-34
I180N-H	0	1	1	42	13	0	42	13
I180N-J	9	0	2	32	266	-25	269	30
O180N-A	31	48	43	1971	1518	63	1980	1509
O180N-B	-2	28	25	1161	291	32	1163	290
O180N-C	-15	9	13	497	-293	-51	500	-296
O180N-D	-16	3	1	112	-451	32	114	-453
O180N-E	-12	-3	-2	-112	-390	-13	-112	-391
O180N-F	3	-4	-3	-160	52	-19	53	-162
O180N-G	0	-6	-5	-240	-72	-19	-70	-242
O180N-H	2	-2	-2	-86	45	0	45	-86
O180N-J	1	-3	-3	-126	-9	0	-9	-126

AXIAL FORCE LOADING, FYN, ON NOZZLE (300 LB)

	MICRO-STRAIN			STRESSES			PRIN STRESSES	
ROSETTE	GAGE1	GAGE2	GAGE3	TRANS	LONG	SHEAR	SIGMX	SIGMN
I270C-A	-120	-33	-34	-1340	-4009	6	-1340	-4009
I270C-B	-90	-31	-32	-1300	-3099	13	-1300	-3099
I270C-C	-39	-16	-19	-719	-1399	32	-718	-1400
I270C-D	1	-9	-6	-315	-52	-38	-46	-320
I270C-E	31	-1	5	39	938	-82	946	32
I270C-F	73	13	27	787	2417	-184	2438	767
I270C-G	93	22	26	953	3080	-57	3081	951
I270C-H	90	13	16	538	2870	-32	2870	537
I270C-J	47	-6	-2	-229	1343	-44	1344	-231
I270C-K	21	-20	-8	-639	436	-171	462	-666
I270C-L	-9	-14	-10	-523	-414	-44	-398	-539
I270C-M	-6	10	11	476	-28	-6	476	-28
O270C-A	114	119	94	4554	4773	329	5011	4317
O270C-B*	0	0	87	1922	577	-1165	2594	-96
O270C-C	61	85	69	3307	2817	209	3384	2740
O270C-D	22	64	52	2535	1416	158	2557	1394
O270C-E	0	48	39	1912	559	108	1920	551
O270C-F	-46	3	-1	103	-1352	57	105	-1354
O270C-G	-63	-26	-31	-1194	-2254	70	-1190	-2259
O270C-H	-59	-36	-45	-1700	-2278	120	-1676	-2302
O270C-J	-35	-34	-45	-1706	-1552	146	-1465	-1794
O270C-K	-19	-23	-23	-993	-854	-6	-854	-993
O270C-L	9	-2	-10	-271	176	108	200	-285
I270N-A	-296	-5	-10	2	-8881	70	2	-8882
I270N-B	-134	47	22	1651	-3525	329	1672	-3546
I270N-C	-7	63	37	2190	457	348	2257	390
I270N-D	60	53	44	2065	2416	127	2457	2024
I270N-E	64	37	40	1612	2394	-44	2396	1609
I270N-F	36	7	-2	65	1103	114	1115	52
I270N-G	15	-1	-3	-111	423	19	424	-111
I270N-H	19	-2	0	-73	548	-19	549	-74
I270N-J	14	1	1	37	425	-6	425	37
O270N-A	288	188	169	7537	10900	253	10920	7518
O270N-B	106	144	152	6390	5110	-108	6399	5101
O270N-C	5	85	95	3932	1322	-133	3939	1315
O270N-D	-29	43	51	2089	-243	-108	2094	-248
O270N-E	-33	10	10	475	-841	13	475	-841
O270N-F	8	-11	-10	-468	88	-25	89	-469
O270N-G	18	-3	-1	-103	511	-25	512	-105
O270N-H	14	-3	0	-67	393	-44	397	-72
O270N-J	14	-2	-3	-141	371	13	372	-141

AXIAL FORCE LOADING, FYN, ON NOZZLE (300 LB)

	MICRO-STRAIN			STRESSES			PRIN STRESSES	
ROSETTE	GAGE1	GAGE2	GAGE3	TRANS	LONG	SHEAR	SIGMX	SIGMN
I300C-A	-105	32	-58	-459	-3288	1197	-21	-3726
I300C-B	-87	24	-76	-1053	-2939	1330	-366	-3626
I300C-C	-58	19	-70	-1053	-2069	1197	-261	-2861
I300C-D	-32	18	-70	-1103	-1286	1171	-20	-2370
I300C-E	-16	15	-70	-1205	-832	1133	130	-2167
I300C-F	27	4	-47	-970	522	671	779	-1227
I300C-G	33	-6	-25	-715	783	247	823	-755
I300C-H	34	-11	-9	-476	870	-25	870	-476
I300C-J	29	-19	14	-137	843	-431	1005	-299
I300C-K	13	-25	23	-56	368	-633	824	-512
I300C-L	-9	-22	7	-335	-357	-386	40	-733
0300C-A	71	104	52	3347	3143	684	3936	2554
0300C-B	71	100	30	2784	2959	924	3800	1943
0300C-C	51	86	24	2357	2232	829	3126	1463
0300C-D	37	66	10	1641	1604	741	2363	882
0300C-E	17	59	10	1506	965	646	1936	535
0300C-F	-7	26	3	644	-6	298	760	-122
0300C-G	-14	-1	-6	-141	-470	57	-131	-480
0300C-H	-18	-25	-3	-597	-707	-285	-362	-942
0300C-J	-25	-40	-14	-1163	-1090	-342	-783	-1471
0300C-K	-22	-39	-19	-1250	-1045	-279	-851	-1444
0300C-L	-18	-18	-22	-858	-785	51	-759	-884
I300N-A	-174	-27	68	1100	-4902	-1260	1354	-5156
I300N-B	-53	14	69	1896	-1014	-734	2071	-1188
I300N-C	14	27	67	2053	1029	-545	2288	794
I300N-D	43	31	52	1791	1834	-279	2092	1533
I300N-E	44	24	30	1132	1665	-82	1678	1119
I300N-F	22	5	1	112	689	44	693	108
I300N-G	17	-3	8	75	536	-146	578	33
I300N-H	10	-3	4	0	285	-95	314	-29
I300N-J	14	0	-1	-26	420	19	421	-27
0300N-A	134	104	142	5263	5599	-507	5965	4897
0300N-B	36	85	86	3700	2179	-13	3700	2179
0300N-C	-13	54	38	2019	221	215	2045	196
0300N-D	-26	29	9	853	-514	260	901	-562
0300N-E	-25	11	-6	142	-699	234	203	-760
0300N-F	0	-4	-15	-418	-111	152	-49	-481
0300N-G	13	-4	-7	-244	326	38	328	-247
0300N-H	13	-2	-2	-109	367	6	367	-109
0300N-J	15	-3	-7	-225	374	51	379	-229

AXIAL FORCE LOADING, FYN, ON NOZZLE (300 LB)

	MICRO-STRAIN			STRESSES			PRIN STRESSES	
ROSETTE	GAGE1	GAGE2	GAGE3	TRANS	LONG	SHEAR	SIGMX	SIGMN
I330C-A	-59	35	-25	285	-1697	791	562	-1974
I330C-B	-41	27	-34	-101	-1271	810	314	-1685
I330C-C	-26	20	-36	-316	-879	753	207	-1402
I330C-D	-15	13	-40	-569	-613	709	119	-1300
I330C-E	-8	10	-46	-785	-478	734	119	-1382
I330C-F	6	-7	-52	-1301	-219	595	44	-1565
I330C-G	0	-16	-48	-1400	-406	418	-254	-1552
I330C-H	0	-23	-40	-1399	-434	228	-383	-1450
I330C-J	2	-23	-25	-1067	-263	25	-262	-1068
I330C-K	4	-21	-13	-757	-99	-101	-83	-772
I330C-L	1	-14	1	-294	-60	-203	57	-410
0330C-A	34	48	44	1978	1620	57	1987	1611
0330C-B	27	43	43	1851	1354	0	1851	1354
0330C-C	27	38	36	1579	1272	25	1581	1270
0330C-D	17	39	26	1412	937	171	1467	882
0330C-E	13	38	21	1301	790	228	1388	703
0330C-F	12	30	13	926	649	228	1054	521
0330C-G	17	26	8	723	730	234	961	492
0330C-H	11	20	11	688	534	120	754	468
0330C-J	7	12	9	452	335	38	464	324
0330C-K	-8	-4	-2	-127	-266	-32	-121	-273
0330C-L	-10	-17	-13	-658	-483	-51	-469	-672
I330N-A	-59	4	42	1078	-1444	-513	1178	-1545
I330N-B	-12	24	44	1507	81	-260	1553	36
I330N-C	18	26	38	1380	956	-165	1436	899
I330N-D	24	18	29	997	1012	-139	1144	865
I330N-E	30	16	16	666	1112	6	1112	666
I330N-F	14	8	5	266	508	32	512	262
I330N-G	11	0	5	92	356	-63	370	78
I330N-H	11	2	2	72	349	0	349	72
I330N-J	10	0	5	94	313	-76	337	70
0330N-A*	0	48	68	2548	765	-266	2587	726
0330N-B	3	36	34	1532	545	32	1533	544
0330N-C	-13	20	18	861	-141	32	862	-142
0330N-D	-14	10	5	350	-323	76	358	-331
0330N-E	-18	6	-1	124	-504	89	137	-517
0330N-F	5	2	-5	-79	133	95	170	-115
0330N-G	8	1	0	12	246	13	247	11
0330N-H	0	0	-8	-188	-56	101	-1	-243
0330N-J	5	-3	-5	-172	91	25	93	-175

A.7 Out-of-Plane Force, F_{ZN}, on Nozzle

OUT-OF-PLANE FORCE LOADING, FZN, ON NOZZLE (100 LB)

	MICRO-STRAIN			STRESSES			PRIN STRESSES	
ROSETTE	GAGE1	GAGE2	GAGE3	TRANS	LONG	SHEAR	SIGMX	SIGMN
I-O-C-A	13	4	-1	48	414	63	424	37
I-O-C-B	2	-9	19	227	139	-367	553	-187
I-O-C-C	-1	-19	29	231	27	-646	783	-525
I-O-C-D	-4	-28	38	235	-58	-874	974	-798
I-O-C-E	-4	-33	45	265	-34	-1045	1171	-940
I-O-C-F	0	-46	51	125	38	-1292	1374	-1211
I-O-C-G	7	-48	57	170	265	-1399	1617	-1183
I-O-C-H	0	-46	56	209	63	-1355	1493	-1221
I-O-C-J	0	-40	52	251	61	-1228	1388	-1076
I-O-C-K	5	-35	47	245	216	-1089	1320	-858
I-O-C-L	11	-27	32	103	359	-779	1020	-558
O-O-C-A	-3	36	-54	-404	-221	1197	888	-1512
O-O-C-B	1	31	-40	-200	-17	956	852	-1069
O-O-C-C	6	32	-34	-48	157	886	947	-838
O-O-C-D	7	32	-30	24	207	829	950	-719
O-O-C-E	5	28	-29	-47	129	760	806	-724
O-O-C-F	4	25	-22	69	135	627	730	-526
O-O-C-G	1	18	-14	93	56	424	499	-350
O-O-C-H	-1	11	-6	127	-5	228	298	-176
O-O-C-J	-3	1	3	98	-71	-32	103	-76
O-O-C-K	-3	-2	0	-49	-100	-32	-34	-115
O-O-C-L*	29	-6	6	-32	874	-165	903	-61
I-O-N-A	19	21	-2	397	689	304	880	206
I-O-N-B	12	27	-9	383	486	469	906	-37
I-O-N-C	10	26	-11	313	0	500	848	-155
I-O-N-D	5	22	-10	266	237	431	682	-180
I-O-N-E	8	26	-4	472	384	393	823	33
I-O-N-F*	11	0	38	813	586	-500	1212	186
I-O-N-G	10	15	2	365	423	177	573	214
I-O-N-H	9	14	0	293	359	196	525	127
I-O-N-J	11	15	5	416	467	133	577	306
O-O-N-A	1	24	-19	103	74	570	658	-482
O-O-N-B	2	17	-15	39	83	431	492	-370
O-O-N-C	6	17	-4	276	254	272	537	-8
O-O-N-D	10	14	-1	271	381	196	530	122
O-O-N-E	8	13	3	347	332	139	479	200
O-O-N-F	4	5	5	215	179	6	216	178
O-O-N-G	6	10	8	369	296	25	377	288
O-O-N-H	8	7	10	378	342	-44	408	312
O-O-N-J	8	7	11	399	348	-57	436	311

OUT-OF-PLANE FORCE LOADING, FZN, ON NOZZLE (100 LB)

	MICRO-STRAIN			STRESSES			PRIN STRESSES	
ROSETTE	GAGE1	GAGE2	GAGE3	TRANS	LONG	SHEAR	SIGMX	SIGMN
I-90C-A	-474	-112	-130	-4784	-15660	241	-4779	-15670
I-90C-B	-387	-118	-120	-4797	-13040	25	-4797	-13040
I-90C-C	-236	-93	-95	-3866	-8231	32	-3866	-8231
I-90C-D	-100	-39	-44	-1718	-3509	70	-1715	-3512
I-90C-E	-5	-2	-7	-204	-204	63	-140	-267
I-90C-F	113	66	47	2351	4084	247	4119	2317
I-90C-G	202	95	76	3517	7114	253	7132	3499
I-90C-H	202	78	64	2900	6943	184	6951	2892
I-90C-J	141	30	33	1245	4593	-38	4594	1244
I-90C-K	85	5	5	126	2575	6	2575	126
I-90C-L	28	-1	-8	-218	761	89	769	226
O-90C-A	612	531	457	21040	24670	981	24920	20790
O-90C-B	474	373	361	15610	18910	158	18920	15610
O-90C-C	334	314	321	13600	14110	-95	14130	13580
O-90C-D	186	250	278	11420	9014	-374	11480	8957
O-90C-E	88	198	227	9251	5413	-386	9289	5374
O-90C-F	-75	62	91	3445	-1219	-380	3476	-1250
O-90C-G	-135	-18	-10	-447	-4183	-108	-444	-4186
O-90C-H	-144	-66	-55	-2505	-5071	-146	-2497	-5079
O-90C-J	-107	-76	-67	-3026	-4130	-108	-3015	-4140
O-90C-K	-66	-53	-47	-2131	-2621	-82	-2118	-2634
O-90C-L	-13	-33	0	-706	-611	-437	-219	-1098
I-90N-A	-893	116	-51	2413	-26080	2235	2587	-26250
I-90N-B	-269	278	196	10720	-4853	1102	10800	-4931
I-90N-C	84	277	258	11670	6024	241	11680	6013
I-90N-D	251	215	225	9405	10360	-133	10380	9387
I-90N-E	246	134	143	5808	9127	-114	9131	5804
I-90N-F	162	-14	17	-105	4830	-412	4864	-139
I-90N-G	75	-19	-9	-709	2026	-139	2033	-716
I-90N-H	75	-12	-8	-511	2099	-57	2100	-512
I-90N-J	67	-13	-5	-482	1880	-108	1885	-486
O-90N-A	526	415	374	16770	20800	538	20870	16700
O-90N-B	390	612	590	25970	19480	291	25990	19470
O-90N-C	66	331	381	15580	6642	-665	15630	6593
O-90N-D	-86	144	185	7332	-367	-538	7369	-404
O-90N-E	-85	35	57	2130	-1899	-298	2151	-1921
O-90N-F	70	-11	-12	-589	1933	6	1933	-589
O-90N-G	100	21	18	747	3218	51	3219	746
O-90N-H	84	23	25	962	2812	-19	2812	962
O-90N-J	67	22	20	846	2250	25	2250	846

OUT-OF-PLANE FORCE LOADING, FZN, ON NOZZLE (100 LB)

	MICRO-STRAIN			STRESSES			PRIN STRESSES	
ROSETTE	GAGE1	GAGE2	GAGE3	TRANS	LONG	SHEAR	SIGMX	SIGMN
I120C-A	-370	163	-237	-1202	-11450	5331	1068	-13720
I120C-B	-248	144	-257	-2202	-8116	5350	954	-11270
I120C-C	-200	137	-278	-2883	-6852	5527	1005	-10740
I120C-D	-141	133	-284	-3145	-5178	5559	1490	-9812
I120C-E	-82	128	-277	-3190	-3409	5407	2109	-8707
I120C-F*	52	87	-269	-4057	351	4755	3388	-7094
I120C-G	67	55	-173	-2674	1194	3045	2867	-4347
I120C-H	82	42	-95	-1250	2091	1817	2889	-2047
I120C-J	96	17	6	407	2987	146	2996	399
I120C-K	99	10	62	1489	3426	-690	3647	1268
I120C-L	55	2	79	1726	2157	-1019	2983	900
O120C-A	407	437	222	14040	16410	2855	18320	12130
O120C-B	274	385	105	10470	11350	3729	14660	7154
O120C-C	241	351	80	9197	10000	3609	13230	5968
O120C-D	190	317	66	8209	8165	3356	11540	4831
O120C-E	143	333	58	8439	6808	3653	11370	3881
O120C-F	102	266	39	6603	5046	3020	8943	2706
O120C-G	40	121	57	3862	2356	848	4244	1975
O120C-H	18	43	60	2257	1205	-228	2305	1157
O120C-J	-17	-47	41	-117	-548	-1171	858	-1524
O120C-K	-37	-86	10	-1631	-1587	-1266	-342	-2875
O120C-L	-38	-78	-25	-2225	-1808	-715	-1271	-2761
I120N-A	-574	-29	185	4056	-15990	-2849	4453	-16390
I120N-B	-187	83	278	8143	-3160	-2608	8716	-3733
I120N-C	61	127	264	8518	4394	-1823	9208	3704
I120N-D	158	116	188	6521	6703	-956	7572	5652
I120N-E	158	85	119	4307	6025	-462	6142	4191
I120N-F	88	30	31	1250	3027	-6	3027	1250
I120N-G*	0	12	25	804	241	-171	852	193
I120N-H	49	11	26	760	1711	-190	1747	724
I120N-J	48	9	22	616	1625	-177	1655	585
O120N-A	512	368	524	19050	21080	-2077	22380	17760
O120N-B	106	299	340	13930	7372	-551	13980	7326
O120N-C	-26	88	89	3924	393	-19	3924	393
O120N-D	-48	41	21	1431	-996	266	1460	-1025
O120N-E	-33	18	-13	141	-956	418	282	-1097
O120N-F	10	2	-19	-387	183	291	306	-509
O120N-G	17	7	-10	-81	489	215	561	-154
O120N-H	22	9	-2	112	689	146	724	77
O120N-J	21	9	-2	134	667	146	705	97

OUT-OF-PLANE FORCE LOADING, FZN, ON NOZZLE (100 LB)

	MICRO-STRAIN			STRESSES			PRIN STRESSES	
ROSETTE	GAGE1	GAGE2	GAGE3	TRANS	LONG	SHEAR	SIGMX	SIGMN
I150C-A	-138	114	-53	1478	-3691	2222	2302	-4515
I150C-B	-99	116	-110	244	-2892	3020	2079	-4727
I150C-C*	-88	100	0	2301	-1961	1336	2685	-2345
I150C-D	-39	82	-169	-1868	-1744	3337	1531	-5143
I150C-E*	0	59	-178	-2621	-786	3159	1586	-4994
I150C-F	-52	39	-205	-3587	-2644	3261	179	-6410
I150C-G	-25	-15	-219	-5111	-2289	2710	-645	-6755
I150C-H	-16	-21	-198	-4797	-1924	2349	-607	-6114
I150C-J*	46	-85	-182	-5920	-407	1304	-114	-6213
I150C-K*	86	-151	-171	-7175	414	266	423	-7184
I150C-L	32	-22	-44	-1487	523	285	563	-1527
O150C-A	128	115	137	5394	5467	-291	5724	5137
O150C-B*	113	137	70	4430	4708	886	5466	3671
O150C-C*	111	139	66	4379	4650	981	5505	3524
O150C-D*	101	0	65	1320	3418	-867	3730	1008
O150C-E	90	171	64	5060	4227	1431	6134	3153
O150C-F	86	185	62	5336	4195	1633	6496	3035
O150C-G	71	165	56	4768	3569	1456	5743	2593
O150C-H	59	159	56	4656	3165	1368	5468	2353
O150C-J	38	129	55	4010	2344	988	4469	1885
O150C-K	30	87	44	2839	1750	576	3087	1502
O150C-L	19	32	26	1242	957	82	1264	935
I150N-A	-121	47	71	2733	-2801	-323	2752	-2820
I150N-B	-22	35	85	2656	127	-659	2818	-34
I150N-C	28	29	74	2246	1515	-595	2579	1182
I150N-D	40	20	57	1658	1695	-488	2165	1189
I150N-E	36	14	40	1161	1432	-348	1670	923
I150N-F	15	8	0	161	504	108	535	130
I150N-G	11	10	24	740	550	-190	857	433
I150N-H	14	11	26	809	671	-196	948	532
I150N-J	16	13	29	912	758	-222	1070	601
O150N-A	50	92	148	5229	3080	-747	5463	2846
O150N-B	-20	61	86	3250	362	-336	3288	323
O150N-C	-43	30	38	1541	-835	-95	1545	-839
O150N-D	-42	13	9	537	-1093	57	539	-1095
O150N-E	-32	5	-7	-17	-974	158	9	-1000
O150N-F	-4	-1	-19	-435	-244	228	-92	-586
O150N-G	4	2	-11	-192	56	177	149	-284
O150N-H	5	4	-13	-204	81	222	202	-325
O150N-J	7	-1	-16	-394	96	196	165	-463

OUT-OF-PLANE FORCE LOADING, FZN, ON NOZZLE (100 LB)

	MICRO-STRAIN			STRESSES			PRIN STRESSES	
ROSETTE	GAGE1	GAGE2	GAGE3	TRANS	LONG	SHEAR	SIGMX	SIGMN
I180C-A	8	12	5	368	338	89	443	263
I180C-B	8	22	-9	284	313	405	704	-107
I180C-C	7	29	-19	222	280	646	898	-395
I180C-D	8	38	-24	304	334	836	1155	-517
I180C-E	7	44	-29	326	312	962	1281	-643
I180C-F	7	48	-35	275	282	1108	1386	-830
I180C-G	9	52	-35	356	378	1159	1525	-792
I180C-H	3	48	-34	310	193	1102	1354	-852
I180C-J	6	52	-29	484	331	1083	1493	-678
I180C-K	8	49	-26	514	382	1000	1451	-555
I180C-L	11	36	-16	437	473	690	1145	-236
O180C-A	-6	-32	21	-233	-255	-703	459	-947
O180C-B	-5	-29	19	-203	-218	-633	423	-844
O180C-C	-6	-32	17	-327	-284	-646	341	-952
O180C-D	-7	-30	15	-327	-298	-595	283	-908
O180C-E	-5	-26	14	-256	-219	-538	301	-776
O180C-F	-2	-19	10	-175	-124	-386	238	-536
O180C-G	-4	-11	2	-194	-186	-171	-19	-361
O180C-H	-4	-5	-4	-184	-169	-13	-162	-191
O180C-J*	-27	-21	-35	-1203	-1159	177	-1003	-1360
O180C-K	0	9	-14	-115	-34	298	226	-375
O180C-L	-1	8	-17	-197	-102	336	190	-488
I180N-A	11	4	17	448	462	-177	632	277
I180N-B	10	-5	22	365	409	-355	742	32
I180N-C	9	-9	22	273	338	-412	718	-107
I180N-D	9	-9	23	303	362	-418	752	-86
I180N-E	8	-7	20	274	310	-361	653	-69
I180N-F*	0	25	19	961	288	76	969	280
I180N-G	8	0	15	325	340	-203	535	130
I180N-H*	0	-57	14	-950	-285	-943	383	-1618
I180N-J	10	3	17	428	428	-177	605	250
O180N-A	-4	-16	7	-194	-172	-298	115	-481
O180N-B	0	-12	6	-125	-38	-241	163	-326
O180N-C	1	-8	4	-85	3	-152	117	-199
O180N-D	1	-3	3	-11	25	-82	91	-78
O180N-E	6	2	10	265	251	-114	372	144
O180N-F	5	6	6	255	233	-6	257	232
O180N-G*	0	75	4	1734	520	937	2243	11
O180N-H	2	7	4	228	125	38	240	113
O180N-J	1	8	-1	145	86	114	233	-2

OUT-OF-PLANE FORCE LOADING, FZN, ON NOZZLE (100 LB)

	MICRO-STRAIN			STRESSES			PRIN STRESSES	
ROSETTE	GAGE1	GAGE2	GAGE3	TRANS	LONG	SHEAR	SIGMX	SIGMN
I270C-A	489	148	162	6272	16570	-190	16570	6268
I270C-B	413	143	147	5917	14160	-51	14160	5917
I270C-C	245	91	91	3731	8461	6	8461	3731
I270C-D	114	48	32	1629	3924	203	3942	1611
I270C-E	16	12	-4	149	530	215	627	52
I270C-F	-116	-34	-56	-1836	-4029	291	-1798	-4067
I270C-G	-195	-61	-81	-2919	-6721	266	-2901	-6739
I270C-H	-198	-54	-68	-2466	-6685	196	-2457	-6694
I270C-J	-118	-10	-10	-309	-3642	13	-309	-3642
I270C-K	-73	15	11	654	-1985	44	655	-1986
I270C-L	-1	25	23	1056	288	19	1056	288
I270C-M	6	9	7	349	276	25	357	268
O270C-A	-492	-452	-370	-17530	-20030	-1102	-17110	-20440
O270C-B*	0	0	-351	-7718	-2315	4679	386	-10420
O270C-C	-348	-350	-296	-13800	-14580	-722	-13370	-15010
O270C-D	-151	-212	-181	-8482	-7078	-405	-6969	-8590
O270C-E	-84	-164	-143	-6665	-4523	-272	-4489	-6699
O270C-G	43	-64	-60	-2784	462	-51	463	-2785
O270C-G	104	12	17	533	3282	-63	3283	532
O270C-H	119	48	53	2073	4186	-70	4188	2071
O270C-J	84	52	57	2321	3205	-70	3211	2315
O270C-K	51	38	35	1563	1994	44	1999	1558
O270C-L	4	15	19	737	349	-44	742	344
I270N-A	1280	92	111	3064	39310	-253	39310	3062
I270N-B	630	-117	-16	-3627	17820	-1349	17900	-3712
I270N-C	96	-201	-93	-6570	909	-1437	1175	-6837
I270N-D	-189	-175	-140	-6707	-7672	-469	-6517	-7862
I270N-E	-209	-124	-127	-5295	-7861	32	-5295	-7862
I270N-F	-126	3	22	682	-3587	-253	697	-3602
I270N-G	-51	22	36	1340	-1123	-184	1354	-1137
I270N-H	-50	18	26	1016	-1192	-101	1020	-1197
I270N-J	-39	21	19	931	-890	19	931	-890
O270N-A	-894	-548	-496	-21960	-33400	-703	-21920	-33450
O270N-B	-362	-433	-467	-19380	-16660	443	-16590	-19450
O270N-C	-46	-275	-296	-12480	-5127	279	-5117	-12490
O270N-D	67	-142	-166	-6852	-45	323	-30	-6867
O270N-E	84	-49	-50	-2265	1844	13	1844	-2265
O270N-F	-8	6	0	134	-202	76	151	-219
O270N-G	-24	-4	-6	-193	-785	19	-192	-786
O270N-H	-20	-4	-6	-186	-669	25	-185	-670
O270N-J	-17	-5	-6	-211	-577	13	-211	-577

OUT-OF-PLANE FORCE LOADING, FZN, ON NOZZLE (100 LB)

	MICRO-STRAIN			STRESSES			PRIN STRESSES	
ROSETTE	GAGE1	GAGE2	GAGE3	TRANS	LONG	SHEAR	SIGMX	SIGMN
I300C-A	361	-158	279	2266	11510	-5818	14320	-542
I300C-B*	328	-125	0	-3118	8915	-1671	9143	-3346
I300C-C	273	-105	344	4943	9680	-5989	13750	871
I300C-D	198	-104	335	4869	7391	-5844	12110	152
I300C-E	128	-94	346	5405	5471	-5856	11290	-419
I300C-F	-15	-65	255	4183	813	-4261	7080	-2084
I300C-G	-57	-47	157	2486	-965	-2710	3973	-2452
I300C-H	-68	-35	86	1193	-1695	-1602	1905	-2408
I300C-J	-89	-7	-19	-476	-2823	158	-466	-2834
I300C-K	-75	8	-71	-1307	-2644	1057	-724	-3227
I300C-L	-33	19	-64	-956	-1271	1108	6	-2232
O300C-A	-347	-445	-171	-13140	-14360	-3653	-10050	-17460
O300C-B	-359	-444	-124	-12100	-14410	-4267	-8830	-17670
O300C-C	-327	-407	-110	-10990	-13110	-3957	-7954	-16150
O300C-D	-254	-359	-90	-9591	-10490	-3577	-6435	-13650
O300C-E	-181	-325	-81	-8709	-8059	-3248	-5120	-11650
O300C-F	-85	-218	-65	-6121	-4374	-2045	-3024	-7471
O300C-G	-34	-110	-62	-3743	-2149	-633	-1928	-3564
O300C-H	-11	-30	-60	-1972	-920	405	-782	-2110
O300C-J	22	52	-49	39	667	1355	1744	-1038
O300C-K	22	90	-3	1887	1236	1235	2838	285
O300C-L	36	67	25	1976	1676	564	2409	1243
I300N-A	736	122	-176	-1999	21470	3976	22120	-2654
I300N-B	259	-14	-227	-5580	6110	2843	6764	-6235
I300N-C	2	-68	-229	-6540	-1905	2140	-1068	-7377
I300N-D*	-124	-83	-169	-5400	-5326	1140	-4223	-6503
I300N-E	-134	-61	-103	-3445	-5054	557	-3271	-5228
I300N-F	-63	0	10	299	-1806	-139	308	-1815
I300N-G	-32	18	6	547	-791	158	565	-810
I300N-H	-30	19	2	514	-758	228	553	-798
I300N-J	-29	19	6	575	-697	165	596	-718
O300N-A	-520	-370	-529	-19190	-21370	2115	-17900	-22660
O300N-B	-155	-299	-341	-13910	-8834	557	-8774	-13970
O300N-C	22	-194	-169	-8003	-1745	-342	-1727	-8022
O300N-D	76	-114	-62	-3937	1086	-690	1179	-4030
O300N-E	68	-55	6	-1150	1693	-804	1905	-1362
O300N-F	-11	1	46	1046	-14	-602	1318	-286
O300N-G	-50	-9	17	243	-1438	-342	310	-1505
O300N-H*	0	-8	12	104	31	-266	336	-201
O300N-J	-38	-6	10	125	-1089	-215	162	-1126

OUT-OF-PLANE FORCE LOADING, F7N, ON NOZZLE (100 LB)

	MICRO-STRAIN			STRESSES			PRIN STRESSES	
ROSETTE	GAGE1	GAGE2	GAGE3	TRANS	LONG	SHEAR	SIGMX	SIGMN
I330C-A	141	-147	111	-949	3949	-3444	5726	-2726
I330C-B	124	-118	162	845	3974	-3735	6460	-1640
I330C-C	99	-100	184	1750	3490	-3786	6505	-1264
I330C-D	86	-76	213	2924	3443	-3856	7048	-681
I330C-E	56	-66	223	3385	2684	-3849	6900	-831
I330C-F	15	1	236	5195	2015	-3134	7119	90
I330C-G	12	39	238	6086	2196	-2646	7425	857
I330C-H	17	49	215	5789	2236	-2203	6842	1182
I330C-J	0	65	174	5254	1562	-1463	5763	1053
I330C-K	-11	53	120	3814	802	-886	4056	561
I330C-L	-22	38	54	2051	-55	-203	2070	-74
O330C-A	-127	-129	-112	-5166	-5356	-228	-5014	-5508
O330C-B	-116	-133	-111	-5241	-5051	-304	-4827	-5464
O330C-C*	-126	-140	-104	-5230	-5347	-469	-4816	-5760
O330C-D	-98	-148	-93	-5197	-4510	-734	-4043	-5665
O330C-E	-91	-158	-77	-5080	-4261	-1076	-3519	-5822
O330C-F	-90	-169	-79	-5353	-4314	-1203	-3523	-6144
O330C-G*	-75	-165	-178	-7459	-4476	165	-4467	-7468
O330C-H	-61	-161	-68	-4978	-3318	-1235	-2660	-5635
O330C-J	-14	-135	-66	-4413	-1751	-924	-1462	-4702
O330C-K	-35	-107	-60	-3638	-2146	-633	-1914	-3870
O330C-L	-20	-39	-41	-1743	-1136	32	-1134	-1744
I330N-A	197	-34	-70	-2514	5148	481	5178	-2544
I330N-B	65	-45	-94	-3121	1017	659	1119	-3223
I330N-C	-10	-34	-81	-2517	-1040	621	-814	-2743
I330N-D	-30	-23	-60	-1784	-1448	494	-1094	-2137
I330N-E	-33	-13	-39	-1113	-1317	355	-846	-1584
I330N-F	-11	2	-5	-61	-360	95	-33	-388
I330N-G	0	3	-8	-104	-31	139	76	-212
I330N-H	0	3	-9	-115	-34	158	89	-238
I330N-J	-3	1	-11	-216	-150	158	-22	-345
O330N-A	0	-65	-146	-4648	-1394	1083	-1067	-4975
O330N-B	30	-51	-79	-2885	47	374	94	-2931
O330N-C	58	-18	-33	-1192	1382	203	1398	-1208
O330N-D	58	-3	0	-126	1701	-51	1703	-128
O330N-E	39	5	18	459	1307	-165	1337	428
O330N-F	15	12	29	892	710	-234	1053	550
O330N-G	1	9	26	772	260	-228	859	173
O330N-H	-5	10	20	664	42	-146	696	10
O330N-J	-8	5	22	604	-47	-222	672	-115

A.8 Torsional Moment Loading, M_{XC}, on Cylinder

TORSIONAL MOMENT LOADING, MXC, ON CYLINDER (20000 IN-LB)

	MICRO-STRAIN			STRESSES			PRIN STRESSES	
ROSETTE	GAGE1	GAGE2	GAGE3	TRANS	LONG	SHEAR	SIGMX	SIGMN
I-0-C-A	-4	-15	-1	-361	-223	-184	-96	-488
I-0-C-B	-10	-29	14	-313	-393	-564	212	-918
I-0-C-C	-11	-32	20	-249	-417	-690	363	-1028
I-0-C-D	-9	-36	25	-220	-337	-810	534	-1091
I-0-C-E	-11	-36	26	-207	-390	-817	523	-1121
I-0-C-F	0	-36	19	-376	-113	-734	502	-991
I-0-C-G	-6	-36	19	-359	-279	-728	410	-1048
I-0-C-H	0	-33	20	-282	-85	-715	539	-906
I-0-C-J	-10	-31	22	-178	-338	-709	456	-972
I-0-C-K	-9	-32	19	-273	-338	-690	385	-996
I-0-C-L	-5	-32	15	-381	-257	-627	311	-949
O-0-C-A	3	39	-38	17	105	1026	1088	-966
O-0-C-B	6	38	-32	119	207	937	1101	-775
O-0-C-C	5	41	-31	204	204	962	1166	-759
O-0-C-D	3	42	-34	174	152	1007	1170	-844
O-0-C-E	6	44	-35	203	232	1051	1268	-834
O-0-C-F	4	44	-38	132	154	1083	1225	-940
O-0-C-G	2	39	-37	39	83	1013	1074	-952
O-0-C-H	3	38	-33	91	113	943	1045	-842
O-0-C-J	0	31	-28	84	11	785	834	-738
O-0-C-K*	2	29	0	635	248	386	873	9
O-0-C-L*	-72	26	-23	142	-2124	646	313	-2295
I-0-N-A	5	10	4	298	232	70	342	188
I-0-N-B	5	12	-3	182	212	203	400	-6
I-0-N-C	2	10	-5	112	105	209	318	-100
I-0-N-D	2	10	-2	155	103	158	289	-31
I-0-N-E*	7	0	2	45	213	-32	219	39
I-0-N-F	5	0	-31	-685	-49	412	154	-887
I-0-N-G*	0	-1	-1	-42	-13	-377	-13	-42
I-0-N-H*	-1	-4	0	-83	-53	-51	-15	-121
I-0-N-J	2	0	2	61	75	-25	94	42
O-0-N-A	0	22	-25	-63	-19	621	580	-662
O-0-N-B	-4	12	-18	-111	-147	399	270	-528
O-0-N-C	-2	7	-10	-71	-78	222	147	-296
O-0-N-D	-2	0	-5	-102	-102	76	-26	-178
O-0-N-E	-1	1	0	12	-39	19	18	-45
O-0-N-F	0	-4	4	1	-14	-101	95	-108
O-0-N-G	2	0	3	61	75	-38	107	29
O-0-N-H	6	-1	4	56	188	-63	214	31
O-0-N-J	-3	-6	2	-80	-110	-101	7	-197

TORSIONAL MOMENT LOADING, MXC, ON CYLINDER (20000 IN-LB)

	MICRO-STRAIN			STRESSES			PRIN STRESSES	
ROSETTE	GAGE1	GAGE2	GAGE3	TRANS	LONG	SHEAR	SIGMX	SIGMN
I-90C-A	-6	69	-72	-46	-185	1880	1766	-1997
I-90C-B	-10	83	-83	11	-296	2203	2066	-2351
I-90C-C	-9	101	-104	-74	-293	2735	2554	-2921
I-90C-D	-11	99	-102	-61	-346	2678	2478	-2886
I-90C-E*	-10	90	-98	-157	-332	2507	2264	-2753
I-90C-F	-6	61	-73	-255	-248	1792	1541	-2043
I-90C-G	-7	29	-40	-223	-266	924	680	-1169
I-90C-H	-3	6	-17	-237	-171	310	108	-516
I-90C-J	-5	0	-13	-287	-229	165	-91	-425
I-90C-K	-5	8	-20	-256	-219	374	136	-612
I-90C-L	-4	15	-26	-236	-199	551	334	-768
O-90C-A	2	-40	38	-44	44	-1038	1039	-1039
O-90C-B	3	-38	36	-45	72	-988	1003	-976
O-90C-C	5	-54	49	-110	124	-1380	1392	-1378
O-90C-D	5	-59	57	-37	146	-1551	1608	-1500
O-90C-E	3	-62	63	18	91	-1671	1726	-1618
O-90C-F	9	-76	74	-62	252	-1994	2096	-1906
O-90C-G	-6	-68	77	195	-127	-1925	1965	-1897
O-90C-H	-4	-57	61	88	-88	-1583	1585	-1585
O-90C-J	0	-35	34	-21	-6	-924	911	-938
O-90C-K	1	-23	21	-43	30	-595	590	-603
O-90C-L*	-1	-28	0	-604	-224	-367	-1	-828
I-90N-A	7	16	-19	-70	193	469	548	-426
I-90N-B	2	-6	10	81	96	-203	291	-115
I-90N-C	0	-17	20	84	25	-494	549	-440
I-90N-D	1	-16	21	103	60	-494	576	-413
I-90N-E	4	-11	16	100	144	-367	490	-246
I-90N-F	1	-1	4	72	50	-70	132	-9
I-90N-G	2	2	-1	29	66	44	95	0
I-90N-H	0	1	1	41	27	0	41	27
I-90N-J	0	-1	2	31	24	-44	72	-17
O-90N-A	-1	-52	46	-145	-72	-1304	1196	-1413
O-90N-B*	1	-45	30	-325	-69	-994	805	-1199
O-90N-C	-1	-24	20	-83	-53	-583	515	-651
O-90N-D	-1	-7	5	-41	-41	-165	124	-205
O-90N-E	-3	1	-6	-90	-127	95	-12	-205
O-90N-F	-2	12	-15	-61	-75	367	299	-435
O-90N-G	-4	8	-14	-131	-168	285	136	-435
O-90N-H	-3	6	-13	-154	-132	247	105	-390
O-90N-J	-6	4	-13	-192	-229	234	25	-445

TORSIONAL MOMENT LOADING, MXC, ON CYLINDER (20000 IN-LB)

	MICRO-STRAIN			STRESSES			PRIN STRESSES	
ROSETTE	GAGE1	GAGE2	GAGE3	TRANS	LONG	SHEAR	SIGMX	SIGMN
I120C-A	67	-103	-118	-4930	517	196	524	-4937
I120C-B	24	-95	-108	-4496	-636	177	-628	-4504
I120C-C	-13	-78	-103	-3975	-1592	329	-1547	-4020
I120C-D	-35	-68	-101	-3669	-2156	437	-2039	-3786
I120C-E	-40	-59	-93	-3298	-2201	456	-2036	-3462
I120C-F*	-13	-34	-71	-2304	-1076	494	-902	-2478
I120C-G	-19	-21	-60	-1775	-1117	519	-831	-2061
I120C-H	3	-8	-52	-1320	-296	595	-23	-1593
I120C-J	24	-3	-37	-914	439	450	574	-1050
I120C-K	27	-2	-27	-656	602	329	683	-737
I120C-L	23	-13	-20	-757	472	89	478	-763
O120C-A	-42	-166	-118	-6200	-3114	-633	-2989	-6324
O120C-B	1	-121	-80	-4408	-1294	-545	-1202	-4501
O120C-C	26	-87	-46	-2953	-102	-545	-1	-3053
O120C-D	43	-57	-22	-1802	743	-469	826	-1885
O120C-E	53	-40	-1	-967	1292	-526	1409	-1083
O120C-F	58	-8	28	365	1849	-475	1987	226
O120C-G	45	12	34	974	1646	-291	1755	865
O120C-H	34	11	31	903	1283	-266	1420	766
O120C-J	24	-11	21	204	774	-431	1005	-28
O120C-K	24	-25	10	-340	625	-469	815	-530
O120C-L	19	-31	2	-658	373	-450	541	-827
I120N-A	86	-23	-137	-3614	1482	1513	1897	-4029
I120N-B	-27	-61	-120	-3939	-1980	785	-1704	-4215
I120N-C	-77	-73	-86	-3404	-3331	177	-3186	-3548
I120N-D	-86	-61	-53	-2413	-3290	-101	-2401	-3301
I120N-E	-72	-43	-31	-1540	-2615	-158	-1517	-2637
I120N-F	-36	-19	-11	-640	-1261	-108	-622	-1279
I120N-G	0	-9	-10	-418	-125	13	-125	-418
I120N-H	-24	-7	0	-109	-760	-95	-96	-773
I120N-J	-21	-4	-3	-123	-664	-13	-123	-665
O120N-A	-95	-165	-132	-6433	-4781	-443	-4670	-6545
O120N-B	2	-105	-57	-3574	-1015	-646	-861	-3728
O120N-C	31	-42	2	-922	650	-589	846	-1118
O120N-D	24	-5	29	486	859	-450	1159	185
O120N-E	8	15	38	1140	570	-304	1272	439
O120N-F	-27	22	23	1032	-503	-13	1032	-503
O120N-G	-32	5	4	224	-902	13	224	-903
O120N-H*	-31	4	166	3773	191	-2165	4792	-828
O120N-J	-26	3	2	154	-738	13	154	-738

TORSIONAL MOMENT LOADING, MXC, ON CYLINDER (20000 IN-LB)

	MICRO-STRAIN			STRESSES			PRIN STRESSES	
ROSETTE	GAGE1	GAGE2	GAGE3	TRANS	LONG	SHEAR	SIGMX	SIGMN
I150C-A	51	-98	-50	-3314	531	-646	637	-3420
I150C-B	18	-100	-27	-2808	-301	-969	30	-3139
I150C-C*	-1	-96	0	-2098	-672	-1273	74	-2843
I150C-D	-27	-90	2	-1913	-1372	-1228	-385	-2901
I150C-E*	0	-97	5	-2016	-605	-1361	223	-2843
I150C-F	-19	-65	11	-1159	-932	-1019	-20	-2071
I150C-G	-13	-38	11	-592	-562	-659	82	-1236
I150C-H	-7	-33	3	-640	-392	-481	-19	-1013
I150C-J	3	-38	-12	-1100	-244	-348	-121	-1224
I150C-K*	17	-52	-30	-1826	-34	-285	10	-1870
I150C-L	10	-31	-16	-1044	-28	-196	8	-1081
O150C-A	-24	-77	-117	-4235	-1983	545	-1859	-4360
O150C-B	-4	-58	-77	-2972	-1006	260	-972	-3006
O150C-C	6	-38	-67	-2304	-520	393	-438	-2386
O150C-D*	12	0	-62	-1381	-58	829	341	-1781
O150C-E	15	-18	-59	-1719	-74	551	94	-1886
O150C-F	4	2	-48	-1028	-194	671	179	-1401
O150C-G	0	7	-42	-773	-232	646	198	-1202
O150C-H	-1	8	-38	-657	-226	614	210	-1092
O150C-J	5	5	-29	-517	-13	450	251	-780
O150C-K	11	8	-24	-368	232	418	446	-582
O150C-L	20	9	-18	-221	547	361	690	-364
I150N-A	39	-28	-73	-2257	506	608	634	-2385
I150N-B	-21	-30	-59	-1951	-1213	386	-1047	-2116
I150N-C	-41	-25	-40	-1385	-1656	196	-1282	-1759
I150N-D	-40	-15	-22	-781	-1432	95	-768	-1445
I150N-E	-30	-11	-11	-458	-1036	6	-458	-1036
I150N-F	-15	-8	0	-161	-490	-108	-129	-522
I150N-G	-13	-7	-6	-257	-462	-13	-257	-463
I150N-H	-12	-5	-6	-227	-425	19	-225	-426
I150N-J	-12	-5	-6	-217	-421	13	-216	-422
O150N-A	-13	-80	-92	-3766	-1529	165	-1517	-3778
O150N-B	17	-45	-42	-1930	-66	-32	-65	-1931
O150N-C	21	-20	-9	-671	426	-152	447	-691
O150N-D	13	-8	7	-35	374	-190	449	-110
O150N-E	-2	0	13	295	17	-177	381	-69
O150N-F	-19	3	15	418	-445	-152	444	-471
O150N-G	-22	-3	6	87	-630	-127	108	-652
O150N-H	-20	-4	7	85	-588	-152	118	-620
O150N-J	-21	-2	4	55	-625	-82	65	-635

TORSIONAL MOMENT LOADING, MXC, ON CYLINDER (20000 IN-LB)

	MICRO-STRAIN			STRESSES			PRIN STRESSES	
ROSETTE	GAGE1	GAGE2	GAGE3	TRANS	LONG	SHEAR	SIGMX	SIGMN
I180C-A	-6	-16	4	-244	-244	-266	22	-510
I180C-B	-6	-27	17	-213	-249	-589	358	-820
I180C-C	-7	-35	22	-285	-299	-760	468	-1052
I180C-D	-9	-38	28	-230	-340	-880	597	-1167
I180C-E*	-8	-39	4	-754	-468	-576	-17	-1205
I180C-F	-6	-35	22	-265	-251	-760	502	-1018
I180C-G	-9	-37	21	-325	-354	-772	433	-1112
I180C-H	-5	-34	19	-329	-241	-709	425	-996
I180C-J	-7	-34	21	-275	-282	-728	450	-1006
I180C-K	-4	-34	20	-299	-204	-715	466	-968
I180C-L	-8	-31	17	-315	-323	-640	320	-959
O180C-A	2	31	-33	-44	58	848	857	-843
O180C-B	0	35	-34	20	20	912	932	-891
O180C-C	2	38	-36	40	69	988	1042	-934
O180C-D	3	40	-40	7	88	1070	1118	-1023
O180C-E	0	40	-41	-21	-6	1089	1075	-1103
O180C-F	1	41	-40	19	49	1089	1123	-1055
O180C-G	4	38	-40	-67	108	1038	1062	-1022
O180C-H	2	34	-37	-75	34	943	925	-965
O180C-J*	-20	7	-53	-991	-910	791	-158	-1743
O180C-K	0	32	-24	188	56	747	872	-628
O180C-L	2	29	-21	175	124	678	827	-529
I180N-A	4	5	2	142	171	38	197	115
I180N-B	3	10	-4	122	136	190	319	-61
I180N-C	3	10	-4	122	122	190	312	-68
I180N-D	2	10	-2	165	121	165	309	-24
I180N-E	5	7	-1	120	179	101	255	44
I180N-F*	0	-12	0	-251	-75	-165	24	-350
I180N-G	1	2	4	135	69	-32	148	56
I180N-H*	0	69	5	1619	486	855	2078	27
I180N-J	3	2	2	101	130	751	130	101
O180N-A	-8	21	-24	-65	-248	602	452	-765
O180N-B	-6	11	-18	-139	-227	380	199	-566
O180N-C	-6	3	-14	-244	-244	228	-16	-472
O180N-D	-6	-2	-9	-244	-244	89	-156	-333
O180N-E	-5	-3	-4	-141	-185	13	-138	-188
O180N-F	-3	-6	-1	-153	-146	-70	-80	-219
O180N-G*	0	60	-3	1264	379	842	1773	-130
O180N-H	-4	-8	0	-183	-183	-101	-82	-285
O180N-J	-4	-6	0	-132	-154	-82	-60	-226

TORSIONAL MOMENT LOADING, MXC, ON CYLINDER (20000 IN-LB)

	MICRO-STRAIN			STRESSES			PRIN STRESSES	
ROSETTE	GAGE1	GAGE2	GAGE3	TRANS	LONG	SHEAR	SIGMX	SIGMN
I270C-A	-13	77	-93	-341	-487	2254	1841	-2669
I270C-B	-14	103	-109	-120	-464	2830	2543	-3127
I270C-C	-11	108	-114	-123	-379	2957	2708	-3211
I270C-D	-12	104	-105	-7	-373	2798	2614	-2994
I270C-E	-10	93	-98	-104	-331	2539	2324	-2759
I270C-F	3	68	-72	-87	60	1861	1849	-1876
I270C-G	2	36	-29	134	97	867	983	-752
I270C-H	2	13	-11	40	69	329	384	-275
I270C-J	2	10	-10	-2	56	253	282	-228
I270C-K	2	18	-15	60	89	443	518	-369
I270C-L	-2	25	-19	128	-33	595	648	-553
I270C-M	-1	25	-18	158	5	564	650	-487
O270C-A	3	-25	29	80	110	-722	817	-627
O270C-B*	0	0	48	1044	313	-633	1410	-52
O270C-C	0	-56	58	52	16	-1526	1560	-1492
O270C-D	-3	-65	64	-18	-91	-1709	1656	-1764
O270C-E	-4	-69	68	-6	-116	-1830	1769	-1892
O270C-F	-5	-77	76	-26	-150	-2045	1958	-2134
O270C-G	-3	-74	73	-17	-105	-1963	1902	-2024
O270C-H	0	-61	57	-94	-28	-1564	1503	-1625
O270C-J	-3	-39	30	-184	-155	-924	755	-1094
O270C-K	-1	-26	21	-113	-77	-627	532	-722
O270C-L	-1	-21	25	85	-17	-608	644	-576
I270N-A	-10	37	-35	53	-298	962	856	-1100
I270N-B	-4	4	3	171	-63	13	172	-63
I270N-C	6	-11	23	265	251	-456	714	-198
I270N-D	9	-16	29	272	353	-602	915	-291
I270N-E	11	-11	19	166	378	-412	697	-153
I270N-F	5	-1	1	-5	141	-25	145	-9
I270N-G	4	3	-2	17	119	63	149	-14
I270N-H	3	1	0	28	94	6	95	28
I270N-J	4	0	2	38	125	-38	140	23
O270N-A	10	-42	49	135	354	-1216	1465	-976
O270N-B	4	-34	47	267	208	-1076	1314	-839
O270N-C	0	-24	29	115	20	-715	785	-649
O270N-D	0	-7	13	135	55	-260	358	-168
O270N-E	-2	3	-3	-8	-60	82	52	-120
O270N-F	0	13	-18	-115	-34	412	339	-488
O270N-G	-4	7	-13	-131	-168	272	124	-422
O270N-H	-5	5	-13	-172	-194	247	64	-431
O270N-J	-5	3	-12	-193	-201	209	12	-406

TORSIONAL MOMENT LOADING, MXC, ON CYLINDER (20000 IN-LB)

	MICRO-STRAIN			STRESSES			PRIN STRESSES	
ROSETTE	GAGE1	GAGE2	GAGE3	TRANS	LONG	SHEAR	SIGMX	SIGMN
I300C-A	63	-109	-104	-4748	472	-76	473	-4749
I300C-B*	24	-88	0	-1969	122	-1178	652	-2498
I300C-C	-16	-76	-96	-3753	-1610	260	-1579	-3784
I300C-D	-37	-68	-94	-3531	-2171	342	-2090	-3612
I300C-E	-51	-60	-95	-3338	-2527	462	-2318	-3548
I300C-F	-38	-30	-76	-2298	-1830	608	-1412	-2715
I300C-G	-10	-10	-66	-1661	-783	734	-367	-2077
I300C-H	5	0	-58	-1279	-241	772	170	-1691
I300C-J	24	4	-39	-809	470	576	691	-1031
I300C-K	30	-5	-26	-722	682	279	735	-776
I300C-L	24	-11	-18	-664	528	82	534	-669
O300C-A	-38	-138	-103	-5253	-2716	-475	-2631	-5339
O300C-B	-12	-115	-69	-4039	-1582	-621	-1434	-4187
O300C-C	12	-84	-39	-2729	-448	-595	-302	-2875
O300C-D	31	-60	-21	-1831	392	-519	507	-1946
O300C-E	45	-37	0	-864	1081	-494	1199	-982
O300C-F	55	-2	24	420	1766	-355	1853	333
O300C-G	43	16	35	1060	1601	-253	1701	960
O300C-H	34	8	30	798	1266	-304	1415	648
O300C-J	29	-16	19	31	879	-469	1087	-177
O300C-K	24	-29	10	-433	583	-526	806	-656
O300C-L	22	-32	1	-713	442	-443	592	-864
I300N-A	79	-10	-138	-3346	1377	1697	1923	-3892
I300N-B	-19	-53	-105	-3456	-1621	703	-1383	-3695
I300N-C	-63	-61	-78	-3002	-2782	228	-2639	-3145
I300N-D	-76	-59	-50	-2309	-2959	-120	-2287	-2981
I300N-E	-55	-42	-27	-1454	-2090	-209	-1391	-2152
I300N-F	-24	-17	-4	-423	-840	-171	-362	-901
I300N-G	-19	-6	-7	-261	-649	6	-261	-649
I300N-H	-20	-5	-7	-228	-682	25	-227	-683
I300N-J	-16	-3	-4	-149	-530	13	-149	-530
O300N-A	-77	-145	-119	-5723	-4012	-355	-3941	-5793
O300N-B	-2	-96	-52	-3256	-1048	-583	-904	-3400
O300N-C	18	-50	-8	-1284	157	-564	351	-1478
O300N-D	12	-20	13	-160	323	-443	586	-423
O300N-E	2	0	22	468	197	-298	660	6
O300N-F	-26	16	18	760	-556	-25	760	-557
O300N-G	-35	4	1	163	-992	38	165	-993
O300N-H*	0	3	0	73	22	32	88	7
O300N-J	-25	0	-3	-25	-763	44	-22	-766

TORSIONAL MOMENT LOADING, MXC, ON CYLINDER (20000 IN-LB)

	MICRO-STRAIN			STRESSES			PRIN STRESSES	
ROSETTE	GAGE1	GAGE2	GAGE3	TRANS	LONG	SHEAR	SIGMX	SIGMN
I330C-A	45	-112	-35	-3277	371	-1019	637	-3542
I330C-B	18	-103	-12	-2547	-223	-1216	297	-3067
I330C-C	-5	-97	0	-2146	-801	-1292	-17	-2929
I330C-D	-20	-90	6	-1827	-1147	-1273	-170	-2804
I330C-E	-27	-80	9	-1537	-1260	-1178	-213	-2584
I330C-F	-28	-48	-6	-1171	-1178	-564	-611	-1738
I330C-G	-15	-36	12	-516	-611	-640	78	-1205
I330C-H	-6	-33	4	-620	-371	-494	14	-1005
I330C-J	0	-31	-5	-794	-238	-342	-75	-957
I330C-K	0	-34	-10	-961	-274	-329	-142	-1094
I330C-L	7	-34	-12	-1031	-96	-291	-12	-1115
O330C-A	-23	-59	-95	-3359	-1692	481	-1563	-3488
O330C-B	-9	-41	-89	-2841	-1123	640	-911	-3053
O330C-C	-2	-26	-78	-2275	-739	696	-471	-2544
O330C-D	7	-16	-68	-1856	-357	690	-88	-2125
O330C-E	9	-9	-57	-1461	-182	652	92	-1735
O330C-F	4	5	-48	-934	-152	703	261	-1347
O330C-G	-3	11	-40	-644	-293	684	238	-1174
O330C-H	-4	10	-38	-622	-315	646	195	-1132
O330C-J	6	11	-28	-382	56	519	401	-727
O330C-K	12	5	-26	-473	229	418	424	-668
O330C-L	18	7	-23	-364	418	399	586	-532
I330N-A	40	-32	-82	-2550	432	659	571	-2689
I330N-B	-16	-38	-66	-2270	-1151	374	-1038	-2383
I330N-C	-39	-33	-48	-1732	-1703	190	-1527	-1908
I330N-D	-41	-26	-31	-1208	-1589	76	-1194	-1603
I330N-E	-33	-18	-18	-758	-1211	0	-758	-1211
I330N-F	-19	-8	-1	-178	-609	-95	-158	-629
I330N-G	-12	-9	-8	-352	-476	-19	-349	-479
I330N-H	-12	-8	-7	-300	-461	-13	-299	-462
I330N-J	-11	-7	-7	-290	-429	6	-290	-430
O330N-A	0	-43	-85	-2799	-840	557	-692	-2946
O330N-B	24	-40	-37	-1718	197	-51	199	-1719
O330N-C	25	-19	-11	-636	550	-108	559	-695
O330N-D	19	-5	8	32	566	-171	616	-18
O330N-E*	-2	-4	14	211	6	-241	370	-153
O330N-F	-12	1	15	369	-260	-190	422	-313
O330N-G	-18	0	10	239	-456	-146	268	-485
O330N-H	-21	-7	2	-71	-663	-120	-47	-686
O330N-J	-19	-3	5	63	-551	-101	79	-568

A.9 Out-of-Plane Moment Loading, M_{YC}, on Cylinder

OUT-OF-PLANE MOMENT LOADING, MYC, ON CYLINDER (20000 IN-LB)

	MICRO-STRAIN			STRESSES			PRIN STRESSES	
ROSETTE	GAGE1	GAGE2	GAGE3	TRANS	LONG	SHEAR	SIGMX	SIGMN
I-O-C-A	-10	8	5	294	-226	32	295	-228
I-O-C-B	-5	3	5	193	-85	-25	196	-87
I-O-C-C	0	1	5	136	27	-44	152	11
I-O-C-D	1	0	3	72	50	-32	95	28
I-O-C-E	0	-1	2	31	23	-44	72	-17
I-O-C-F	0	-4	0	-94	-28	-44	-6	-116
I-O-C-G	-7	-3	-2	-97	-243	-13	-96	-244
I-O-C-H	-10	0	0	0	-285	-6	0	-285
I-O-C-J	-8	1	0	29	-219	13	30	-220
I-O-C-K	-12	2	0	55	-354	25	57	-356
I-O-C-L	-13	1	2	98	-370	-13	99	-370
O-O-C-A	-1	18	1	419	83	228	534	-32
O-O-C-B*	-5	-1	-3	-78	-180	25	-72	-186
O-O-C-C	-5	11	-6	121	-121	222	252	-252
O-O-C-D*	-8	3	-40	-806	-470	570	-44	-1232
O-O-C-E	-7	5	-10	-107	-246	209	44	-397
O-O-C-F	-10	0	-11	-230	-354	158	-122	-462
O-O-C-G	-6	-2	-10	-265	-265	114	-151	-379
O-O-C-H	-11	-2	-7	-186	-398	70	-165	-419
O-O-C-J	-11	-4	-7	-238	-414	38	-230	-422
O-O-C-K	-14	-1	0	-16	-432	-19	-15	-433
O-O-C-L	0	-8	-5	-292	-102	-38	-95	-299
I-O-N-A	-1	9	6	325	69	32	329	65
I-O-N-B	2	7	6	290	144	13	291	143
I-O-N-C	6	6	6	244	244	0	244	244
I-O-N-D	8	4	6	211	291	-19	296	207
I-O-N-E	5	4	6	204	204	-25	229	178
I-O-N-F*	5	0	0	-6	155	0	155	-6
I-O-N-G	8	3	3	138	270	0	270	138
I-O-N-H	3	2	2	91	113	-6	115	89
I-O-N-J	4	2	4	142	171	-25	185	127
O-O-N-A	4	17	11	612	298	70	627	283
O-O-N-B	2	10	4	321	168	82	357	132
O-O-N-C	0	4	5	188	56	-13	189	55
O-O-N-D*	6	4	2	130	210	32	221	119
O-O-N-E	2	-1	3	40	69	-51	107	2
O-O-N-F*	7	2	4	128	252	-19	255	125
O-O-N-G	6	1	3	98	201	-25	207	92
O-O-N-H	5	0	1	15	161	-13	162	14
O-O-N-J	5	-1	1	-16	138	-32	144	-22

OUT-OF-PLANE MOMENT LOADING, MYC, ON CYLINDER (20000 IN-LB)

	MICRO-STRAIN			STRESSES			PRIN STRESSES	
ROSETTE	GAGE1	GAGE2	GAGE3	TRANS	LONG	SHEAR	SIGMX	SIGMN
I-90C-A	73	-77	-72	-3360	1187	-63	1188	-3361
I-90C-B	62	-78	-65	-3202	907	-177	915	-3209
I-90C-C	47	-71	-58	-2903	541	-171	549	-2911
I-90C-D	30	-71	-58	-2874	36	-177	47	-2884
I-90C-E	24	-67	-56	-2732	-92	-146	-84	-2740
I-90C-F	17	-65	-58	-2723	-318	-82	-315	-2726
I-90C-G	5	-60	-54	-2502	-594	-82	-590	-2505
I-90C-H	7	-54	-55	-2389	-503	13	-503	-2389
I-90C-J	6	-58	-53	-2440	-547	-70	-544	-2443
I-90C-K	11	-55	-55	-2425	-385	-6	-385	-2425
I-90C-L	12	-48	-53	-2238	-301	57	-299	-2240
O-90C-A	-48	-107	-100	-4501	-2776	-101	-2770	-4507
O-90C-B	-43	-93	-87	-3911	-2456	-82	-2452	-3916
O-90C-C	-29	-86	-83	-3696	-1993	-44	-1992	-3697
O-90C-D	-15	-72	-75	-3210	-1419	44	-1418	-3212
O-90C-E	-5	-64	-69	-2930	-1021	70	-1019	-2932
O-90C-F	12	-48	-45	-2061	-248	-38	-247	-2061
O-90C-G	26	-38	-44	-1825	223	76	225	-1827
O-90C-H	26	-45	-44	-1982	190	-19	190	-1982
O-90C-J	27	-47	-40	-1951	227	-89	231	-1955
O-90C-K	24	-50	-49	-2209	64	-6	64	-2209
O-90C-L	22	-59	-48	-2384	-60	-152	-50	-2394
I-90N-A	43	-77	-55	-2940	401	-298	427	-2966
I-90N-B	-24	-66	-61	-2773	-1545	-63	-1541	-2776
I-90N-C	-51	-48	-50	-2106	-2157	19	-2100	-2163
I-90N-D	-49	-32	-35	-1418	-1908	44	-1414	-1912
I-90N-E	-36	-17	-21	-796	-1322	51	-791	-1327
I-90N-F	-14	-3	-6	-173	-465	38	-168	-470
I-90N-G	-8	-3	-4	-148	-287	19	-145	-289
I-90N-H	-8	-1	-1	-43	-255	-6	-43	-256
I-90N-J	-7	2	0	60	-182	19	61	-183
O-90N-A	-52	-114	-115	-4977	-3061	13	-3061	-4977
O-90N-B	11	-56	-67	-2727	-490	152	-480	-2738
O-90N-C	32	-13	-24	-850	714	139	727	-862
O-90N-D	23	6	1	142	741	63	748	135
O-90N-E	10	14	11	543	462	32	554	451
O-90N-F	-14	8	10	402	-307	-32	404	-309
O-90N-G	-11	2	5	159	-295	-38	162	-298
O-90N-H*	-17	1	2	102	-468	-13	102	-469
O-90N-J	-7	-2	3	39	-188	-70	58	-208

OUT-OF-PLANE MOMENT LOADING, MYC, ON CYLINDER (20000 IN-LB)

	MICRO-STRAIN			STRESSES			PRIN STRESSES	
ROSETTE	GAGE1	GAGE2	GAGE3	TRANS	LONG	SHEAR	SIGMX	SIGMN
I120C-A	37	-49	7	-981	818	-747	1088	-1251
I120C-B	34	-55	10	-1008	710	-867	1071	-1370
I120C-C*	36	-62	21	-937	788	-1114	1335	-1484
I120C-D	29	-69	25	-1013	551	-1254	1247	-1708
I120C-E	22	-72	25	-1058	353	-1285	1113	-1819
I120C-F	3	-68	26	-944	-183	-1254	747	-1873
I120C-G	0	-64	17	-1034	-296	-1083	479	-1809
I120C-H	-8	-70	12	-1265	-622	-1089	192	-2079
I120C-J	-13	-78	0	-1688	-891	-1045	-172	-2408
I120C-K	-17	-77	-7	-1841	-1051	-937	-429	-2463
I120C-L	-21	-86	-13	-2139	-1269	-969	-642	-2766
O120C-A	-24	-11	-61	-1561	-1195	671	-683	-2074
O120C-B*	-21	-20	-58	-1689	-1148	507	-845	-1993
O120C-C	-29	-18	-67	-1828	-1404	646	-936	-2295
O120C-D	-27	-20	-70	-1945	-1382	665	-941	-2385
O120C-E*	-25	-26	-48	-1613	-1225	298	-1064	-1774
O120C-F*	-19	-33	-82	-2507	-1322	646	-1038	-2791
O120C-G	-14	-16	-82	-2147	-1057	880	-567	-2637
O120C-H	-11	-23	-80	-2265	-1007	760	-650	-2622
O120C-J*	21	-6	-73	-1757	100	899	464	-2121
O120C-K	0	4	-84	-1755	-512	1165	187	-2454
O120C-L	0	1	-82	-1776	-519	1102	121	-2416
I120N-A	9	-19	-21	-887	5	25	5	-888
I120N-B	-5	-8	-17	-538	-304	114	-258	-584
I120N-C	-6	1	-9	-150	-216	133	-46	-320
I120N-D	-3	5	-3	35	-89	108	97	-151
I120N-E	0	6	1	146	58	63	179	25
I120N-F	4	1	4	111	147	-44	177	81
I120N-G*	0	0	0	0	0	0	0	0
I120N-H	3	0	0	-14	81	-6	82	-14
I120N-J	1	-2	1	-22	36	-38	55	-41
O120N-A	19	-9	-38	-1044	257	380	360	-1147
O120N-B	23	-2	-19	-506	533	228	581	-553
O120N-C*	19	0	-9	-208	494	114	512	-226
O120N-D	13	0	0	-25	378	6	378	-25
O120N-E	8	-2	2	2	229	-57	242	-11
O120N-F	1	-8	0	-158	-19	-108	40	-216
O120N-G*	3	-6	4	-45	72	-139	165	-138
O120N-H	-1	-6	5	-19	-49	-139	106	-174
O120N-J	-4	-5	1	-90	-141	-82	-29	-202

OUT-OF-PLANE MOMENT LOADING, MYC, ON CYLINDER (20000 IN-LB)

	MICRO-STRAIN			STRESSES			PRIN STRESSES	
ROSETTE	GAGE1	GAGE2	GAGE3	TRANS	LONG	SHEAR	SIGMX	SIGMN
I150C-A	-8	22	14	803	-2	114	819	-17
I150C-B	-2	13	10	504	80	51	510	74
I150C-C*	6	11	0	234	241	146	383	92
I150C-D*	15	2	5	140	498	-32	501	137
I150C-E*	0	-15	7	-178	-53	-285	176	-407
I150C-F	3	-11	13	28	94	-323	386	-264
I150C-G*	-6	-15	0	-318	-266	-196	-94	-490
I150C-H	-15	-21	20	-15	-461	-551	357	-832
I150C-J	-15	-20	26	142	-414	-621	544	-816
I150C-K*	-20	2	33	784	-364	-412	917	-496
I150C-L	-34	-40	29	-214	-1076	-912	364	-1654
O150C-A	-3	29	4	745	138	336	894	-11
O150C-B	-9	25	-1	522	-114	348	675	-268
O150C-C	-10	10	-10	32	-290	266	182	-440
O150C-D	-10	10	-14	-93	-342	317	123	-557
O150C-E	-14	5	-15	-204	-489	272	-39	-654
O150C-F	-18	-5	-25	-638	-733	272	-409	-962
O150C-G	-21	-4	-32	-770	-873	380	-438	-1205
O150C-H	-22	-3	-36	-821	-917	437	-430	-1308
O150C-J	-36	-1	-38	-828	-1318	500	-516	-1630
O150C-K	-39	-1	-50	-1085	-1509	646	-617	-1976
O150C-L	-48	8	-52	-929	-1733	798	-437	-2224
I150N-A	-6	15	24	874	77	-120	891	59
I150N-B	10	18	20	824	561	-38	829	556
I150N-C	16	16	16	672	686	0	686	672
I150N-D	15	11	10	453	592	19	595	451
I150N-E	12	9	6	311	450	32	457	304
I150N-F*	6	6	14	432	315	-114	501	245
I150N-G	4	3	3	131	168	-6	169	130
I150N-H	5	2	3	120	179	-13	181	118
I150N-J	5	2	2	78	180	0	180	78
O150N-A	8	28	15	942	525	171	1003	464
O150N-B	-1	14	3	378	70	152	440	8
O150N-C	-8	4	-5	-12	-246	114	34	-292
O150N-D	-2	0	-7	-134	-97	95	-19	-212
O150N-E	6	-3	-7	-216	121	51	128	-223
O150N-F	10	-4	-7	-251	224	32	226	-253
O150N-G	10	0	-3	-84	274	32	277	-87
O150N-H*	6	-3	-3	-132	146	0	146	-132
O150N-J	9	0	0	-9	254	13	254	-10

OUT-OF-PLANE MOMENT LOADING, MYC, ON CYLINDER (20000 IN-LB)

	MICRO-STRAIN			STRESSES			PRIN STRESSES	
ROSETTE	GAGE1	GAGE2	GAGE3	TRANS	LONG	SHEAR	SIGMX	SIGMN
I180C-A	-5	8	2	225	-89	70	240	-104
I180C-B	-1	10	-3	148	2	165	255	-105
I180C-C	1	8	-8	-2	42	203	224	-183
I180C-D	1	8	-7	30	38	196	230	-162
I180C-E	1	7	-10	-75	20	222	200	-254
I180C-F	-2	3	-9	-112	-105	158	50	-267
I180C-G	-2	6	-8	-40	-69	177	124	-232
I180C-H	-2	2	-8	-134	-97	133	19	-250
I180C-J	-6	5	-2	69	-165	101	107	-202
I180C-K	-4	7	-4	77	-91	146	161	-175
I180C-L	-3	3	-1	56	-83	57	76	-103
O180C-A	1	-7	15	187	85	-291	432	-160
O180C-B	-1	-7	13	148	2	-266	351	-201
O180C-C*	-5	-25	14	-235	-227	-526	295	-756
O180C-D*	-6	-28	11	-359	-279	-513	195	-834
O180C-E	-5	-14	12	-37	-154	-355	264	-454
O180C-F	1	-12	10	-43	16	-304	292	-319
O180C-G	0	-7	5	-42	-13	-152	126	-180
O180C-H	-1	-6	5	-9	-31	-146	126	-166
O180C-J	-8	-9	-2	-231	-312	-95	-168	-375
O180C-K*	-9	-34	-1	-753	-497	-437	-169	-1080
O180C-L	-8	-3	1	-43	-255	-57	-29	-270
I180N-A	-3	4	6	223	-33	-32	227	-37
I180N-B	3	4	8	257	177	-44	277	157
I180N-C	5	2	6	172	208	-44	238	142
I180N-D	5	3	5	172	194	-19	205	161
I180N-E	2	3	1	92	85	19	108	69
I180N-F	0	6	2	178	53	57	200	31
I180N-G	3	4	1	122	122	38	160	84
I180N-H	0	0	2	52	16	-32	71	-3
I180N-J	3	3	3	122	136	0	136	122
O180N-A	2	0	16	342	174	-209	483	33
O180N-B	-1	0	9	189	28	-127	259	-41
O180N-C	-2	0	6	138	-16	-70	165	-43
O180N-D	0	0	1	31	9	-19	42	-2
O180N-E	0	0	-1	-31	-9	19	2	-42
O180N-F	1	0	-5	-116	-6	57	18	-140
O180N-G	0	6	-3	52	16	120	156	-88
O180N-H	2	1	-2	-13	53	44	76	-35
O180N-J	2	-1	-5	-138	16	44	28	-150

OUT-OF-PLANE MOMENT LOADING, MYC, ON CYLINDER (20000 IN-LB)

	MICRO-STRAIN			STRESSES			PRIN STRESSES	
ROSETTE	GAGE1	GAGE2	GAGE3	TRANS	LONG	SHEAR	SIGMX	SIGMN
I270C-A	-14	35	46	1802	113	-146	1814	100
I270C-B	-13	32	44	1685	121	-165	1702	104
I270C-C	-15	32	41	1625	45	-127	1635	35
I270C-D	-17	29	39	1533	-39	-133	1544	-50
I270C-E	-20	31	39	1568	-129	-114	1575	-136
I270C-F	-21	38	36	1652	-132	38	1653	-132
I270C-G	-25	37	38	1667	-241	-19	1667	-241
I270C-H*	-28	0	41	939	-545	-551	1121	-727
I270C-J	-27	48	54	2275	-130	-82	2278	-133
I270C-K*	0	52	56	2360	708	-51	2362	707
I270C-L	-20	52	67	2644	180	-209	2661	163
I270C-M	2	1	4	113	91	-32	135	68
O270C-A	9	21	22	931	536	-13	931	535
O270C-B*	0	0	18	397	119	-241	536	-20
O270C-C	-10	25	22	1034	25	38	1035	24
O270C-D	-9	29	24	1179	97	63	1183	93
O270C-E	-7	30	22	1167	136	108	1178	125
O270C-F	-6	38	29	1469	255	127	1482	242
O270C-G	-8	45	35	1763	287	127	1774	276
O270C-H	-10	50	44	2069	307	82	2073	303
O270C-J	-12	56	51	2374	342	63	2376	340
O270C-K	0	62	59	2663	799	44	2664	798
O270C-L	-22	62	58	2667	130	44	2668	129
I270N-A	27	32	36	1454	1234	-51	1465	1223
I270N-B	29	23	21	950	1140	25	1144	947
I270N-C	25	16	9	506	893	95	915	484
I270N-D*	17	12	8	410	622	57	636	396
I270N-E	4	5	5	215	193	6	216	191
I270N-F	1	3	3	135	69	-6	135	68
I270N-G	0	2	3	125	52	-13	127	50
I270N-H	1	3	2	114	63	6	115	62
I270N-J	-1	1	0	32	-19	6	33	-20
O270N-A	-32	18	12	704	-758	76	708	-762
O270N-B	-30	2	-2	43	-885	57	47	-889
O270N-C	-17	-6	-10	-326	-611	44	-319	-618
O270N-D	-10	-10	-11	-448	-448	13	-435	-461
O270N-E	-1	-9	-6	-322	-139	-32	-134	-328
O270N-F	3	-5	-1	-139	58	-44	67	-149
O270N-G	3	-1	-1	-66	80	0	80	-66
O270N-H	1	-3	-2	-117	8	-6	8	-117
O270N-J	0	0	1	21	6	-13	28	-1

OUT-OF-PLANE MOMENT LOADING, MYC, ON CYLINDER (20000 IN-LB)

	MICRO-STRAIN			STRESSES			PRIN STRESSES	
ROSETTE	GAGE1	GAGE2	GAGE3	TRANS	LONG	SHEAR	SIGMX	SIGMN
I300C-A	-3	12	18	651	96	-76	661	85
I300C-B	-1	23	14	806	199	120	829	176
I300C-C	0	28	10	836	237	241	921	152
I300C-D*	-3	31	8	860	158	304	973	45
I300C-E	-1	33	7	879	221	355	1034	66
I300C-F*	0	39	-3	794	238	557	1139	-107
I300C-G	1	48	5	1169	379	583	1478	70
I300C-H	-1	57	3	1327	370	728	1720	-23
I300C-J	-5	66	-5	1342	260	937	1883	-281
I300C-K	4	75	-14	1333	514	1190	2182	-336
I300C-L	1	87	-11	1680	533	1311	2537	-324
0300C-A	-16	-19	14	-77	-494	-437	199	-769
0300C-B	-12	-14	28	317	-276	-551	646	-605
0300C-C*	-15	-15	4	-224	-509	-260	-70	-663
0300C-D*	-6	-8	34	581	-11	-551	911	-340
0300C-E	-3	-7	34	598	94	-551	952	-260
0300C-F	-3	1	41	933	194	-526	1206	-79
0300C-G*	-1	-2	43	910	244	-602	1264	-110
0300C-H	1	1	53	1190	385	-684	1581	-6
0300C-J	8	8	66	1620	729	-772	2066	283
0300C-K	5	5	76	1770	674	-950	2319	125
0300C-L	6	12	88	2207	848	-1013	2747	307
I300N-A	18	7	7	284	613	-6	613	283
I300N-B	12	1	3	81	381	-32	384	78
I300N-C	6	0	-1	-38	160	6	160	-38
I300N-D	2	-2	-3	-107	25	13	26	-108
I300N-E	-1	-2	-4	-124	-80	25	-68	-135
I300N-F	-2	1	-3	-29	-80	57	8	-117
I300N-G	-1	0	-2	-30	-52	32	-7	-74
I300N-H	0	1	-1	10	3	32	39	-25
I300N-J	-2	0	0	13	-67	-6	14	-68
0300N-A	-19	0	7	167	-520	-89	178	-531
0300N-B*	-11	-3	3	2	-342	-82	21	-360
0300N-C	-7	0	3	70	-179	-38	76	-184
0300N-D*	0	1	0	31	9	19	42	-2
0300N-E	1	1	0	9	45	19	54	1
0300N-F	1	1	0	19	49	25	63	5
0300N-G	0	2	0	52	16	32	71	-3
0300N-H	-2	1	-1	13	-53	32	25	-66
0300N-J	-1	1	1	53	-13	6	54	-13

OUT-OF-PLANE MOMENT LOADING, MYC, ON CYLINDER (20000 IN-LB)

	MICRO-STRAIN			STRESSES			PRIN STRESSES	
ROSETTE	GAGE1	GAGE2	GAGE3	TRANS	LONG	SHEAR	SIGMX	SIGMN
I330C-A	-3	-14	1	-278	-183	-209	-17	-445
I330C-B	-3	-10	6	-70	-107	-209	122	-298
I330C-C	2	-4	8	71	78	-158	233	-84
I330C-D	2	-2	8	123	108	-139	255	-24
I330C-E	3	0	9	195	158	-120	298	55
I330C-F	9	9	8	345	374	13	379	340
I330C-G	13	11	5	351	490	82	529	313
I330C-H	17	16	2	389	616	184	718	287
I330C-J	23	21	-2	403	819	310	985	237
I330C-K	29	24	-7	333	984	412	1183	134
I330C-L	41	34	-15	372	1352	659	1683	41
0330C-A	-10	-10	-8	-376	-412	-32	-357	-430
0330C-B	-1	-9	-3	-271	-110	-76	-79	-301
0330C-C*	-3	-4	-3	-153	-146	-19	-130	-169
0330C-D	-4	-6	-3	-194	-186	-44	-146	-235
0330C-E	-2	-8	-3	-238	-143	-70	-106	-274
0330C-F*	-1	-11	22	252	47	-443	604	-306
0330C-G	5	-13	3	-225	75	-222	193	-342
0330C-H	10	-14	7	-178	246	-279	384	-316
0330C-J	19	-16	18	32	566	-450	822	-224
0330C-K	19	-22	21	-31	561	-576	913	-383
0330C-L	37	-26	26	-41	1100	-684	1420	-361
I330N-A	-1	-9	-2	-250	-103	-89	-62	-291
I330N-B	0	-5	-2	-146	-44	-38	-31	-159
I330N-C*	-1	-3	-2	-124	-80	-13	-77	-127
I330N-D	0	-2	-1	-63	-5	-13	-2	-66
I330N-E	0	-1	-1	-53	-2	6	-1	-54
I330N-F	3	0	-1	-24	78	13	80	-26
I330N-G	2	0	1	39	83	-13	86	36
I330N-H*	0	-1	-1	-63	-5	0	-5	-63
I330N-J	-1	0	0	12	-39	6	13	-40
0330N-A*	0	-2	1	-10	-3	-44	38	-51
0330N-B	1	4	3	156	75	6	156	75
0330N-C	4	0	6	110	161	-82	222	50
0330N-D*	3	4	5	206	147	-13	208	145
0330N-E	12	6	6	238	428	0	428	238
0330N-F	2	3	4	154	118	-19	162	109
0330N-G	3	2	3	101	116	-13	123	94
0330N-H	3	-2	4	49	114	-82	170	-7
0330N-J	1	1	2	61	61	-13	74	48

A.10 In-Plane Moment Loading, M_{ZC}, on Cylinder

IN-PLANE MOMENT LOADING, MZC, ON CYLINDER (20000 IN-LB)

	MICRO-STRAIN			STRESSES			PRIN STRESSES	
ROSETTE	GAGE1	GAGE2	GAGE3	TRANS	LONG	SHEAR	SIGMX	SIGMN
I-O-C-A	0	38	33	1556	467	57	1559	464
I-O-C-B	11	29	29	1251	718	6	1251	717
I-O-C-C	15	22	22	944	739	0	944	739
I-O-C-D	17	15	18	702	710	-32	738	674
I-O-C-E	14	10	12	465	567	-25	573	459
I-O-C-F	0	0	2	42	13	-25	56	-2
I-O-C-G	0	-4	-1	-114	-49	-32	-36	-127
I-O-C-H	0	-5	-4	-188	-56	-13	-55	-189
I-O-C-J	-7	-5	-3	-170	-251	-19	-166	-255
I-O-C-K	-10	-6	-3	-178	-338	-38	-169	-347
I-O-C-L	-15	-4	-2	-130	-495	-25	-128	-497
O-O-C-A	-6	22	23	998	129	-6	999	128
O-O-C-B	-6	14	14	633	5	0	633	5
O-O-C-C	-7	10	14	530	-41	-51	534	-45
O-O-C-D	-3	7	8	317	9	-13	317	9
O-O-C-E	1	7	7	302	119	-6	302	119
O-O-C-F	3	7	5	258	163	19	262	159
O-O-C-G	1	8	8	343	146	-6	343	146
O-O-C-H	0	10	10	439	118	13	440	117
O-O-C-J	-10	13	12	564	-116	19	565	-117
O-O-C-K	-15	14	0	330	-343	190	379	-393
O-O-C-L	-47	11	13	584	-1236	-19	585	-1236
I-O-N-A	20	29	27	1200	959	19	1201	957
I-O-N-B	24	24	25	1050	1028	-6	1051	1026
I-O-N-C	22	21	21	895	938	0	938	895
I-O-N-D	21	18	18	750	852	0	852	750
I-O-N-E*	19	0	16	334	685	-215	787	231
I-O-N-F*	11	0	-38	-859	85	513	310	-1084
I-O-N-G	7	13	13	578	373	0	578	373
I-O-N-H	10	13	12	554	451	13	555	450
I-O-N-J	9	10	10	418	396	6	420	395
O-O-N-A	-8	19	19	844	11	13	845	11
O-O-N-B	-11	8	8	368	-232	0	368	-232
O-O-N-C	-7	3	4	164	-150	-19	165	-152
O-O-N-D	0	1	1	53	2	6	54	1
O-O-N-E	5	0	1	5	158	-19	161	2
O-O-N-F	10	0	1	20	320	-6	320	20
O-O-N-G	10	0	0	-21	279	-6	279	-21
O-O-N-H	10	0	0	-31	276	0	276	-31
O-O-N-J	11	0	-1	-43	315	6	315	-43

IN-PLANE MOMENT LOADING, MZC, ON CYLINDER (20000 IN-LB)

	MICRO-STRAIN			STRESSES			PRIN STRESSES	
ROSETTE	GAGE1	GAGE2	GAGE3	TRANS	LONG	SHEAR	SIGMX	SIGMN
I-90C-A	95	-97	-104	-4511	1484	89	1485	-4513
I-90C-B	80	-86	-95	-4056	1178	114	1181	-4059
I-90C-C	52	-71	-80	-3379	555	127	559	-3383
I-90C-D	33	-65	-75	-3097	69	133	75	-3102
I-90C-E	20	-59	-67	-2790	-238	108	-234	-2794
I-90C-F	15	-49	-58	-2377	-271	114	-265	-2383
I-90C-G	-3	-38	-38	-1678	-603	6	-603	-1678
I-90C-H	0	-26	-25	-1118	-335	-6	-335	-1118
I-90C-J	6	-12	-8	-455	34	-57	41	-462
I-90C-K	10	-2	0	-42	273	-32	276	-45
I-90C-L	7	10	11	452	349	-25	458	343
O-90C-A	-47	-131	-125	-5578	-3085	-70	-3083	-5580
O-90C-B	-39	-104	-104	-4521	-2539	6	-2539	-4521
O-90C-C	-24	-88	-89	-3879	-1891	13	-1891	-3879
O-90C-D	-6	-71	-73	-3169	-1122	25	-1121	-3169
O-90C-E	6	-55	-58	-2492	-562	38	-562	-2493
O-90C-F	20	-29	-30	-1307	221	19	221	-1307
O-90C-G	25	-17	-11	-643	548	-82	554	-649
O-90C-H	21	-9	-6	-347	537	-32	539	-348
O-90C-J	15	-7	-6	-288	356	-13	356	-288
O-90C-K	7	-4	-5	-217	149	13	149	-217
O-90C-L	0	-2	0	-52	-30	-32	-7	-74
I-90N-A	36	-101	-84	-4102	-147	-222	-135	-4115
I-90N-B	-37	-84	-78	-3521	-2168	-70	-2165	-3524
I-90N-C	-68	-59	-58	-2505	-2790	-19	-2504	-2791
I-90N-D	-60	-38	-38	-1605	-2278	0	-1605	-2278
I-90N-E	-36	-20	-19	-817	-1328	-13	-816	-1329
I-90N-F	-14	-2	-4	-110	-447	25	-108	-448
I-90N-G	-7	-3	-4	-149	-259	6	-149	-259
I-90N-H	-8	-3	-3	-127	-280	-6	-127	-281
I-90N-J	-7	-2	-1	-55	-216	-13	-54	-217
O-90N-A	-25	-127	-126	-5539	-2417	-19	-2417	-5539
O-90N-B	38	-57	-64	-2715	326	89	328	-2718
O-90N-C	57	-4	-10	-386	1581	82	1584	-389
O-90N-D	47	22	17	805	1653	63	1657	800
O-90N-E	22	29	27	1198	1015	32	1203	1010
O-90N-F	-10	20	19	867	-39	25	868	-40
O-90N-G	-11	10	10	451	-207	-13	451	-207
O-90N-H	-9	9	9	396	-152	6	396	-152
O-90N-J	-7	8	9	362	-91	-13	363	-91

IN-PLANE MOMENT LOADING, MZC, ON CYLINDER (20000 IN-LB)

	MICRO-STRAIN			STRESSES			PRIN STRESSES	
ROSETTE	GAGE1	GAGE2	GAGE3	TRANS	LONG	SHEAR	SIGMX	SIGMN
I120C-A	61	-73	-16	-2020	1233	-753	1399	-2186
I120C-B	50	-75	-8	-1872	935	-899	1198	-2135
I120C-C	45	-79	8	-1616	855	-1165	1318	-2078
I120C-D	33	-78	17	-1383	569	-1260	1186	-2001
I120C-E	28	-75	22	-1200	467	-1292	1171	-1904
I120C-F	9	-60	24	-804	30	-1114	803	-1577
I120C-G	0	-46	19	-606	-182	-861	493	-1281
I120C-H	-5	-39	11	-601	-323	-671	224	-1147
I120C-J	-6	-32	1	-673	-373	-437	-61	-985
I120C-K	-4	-18	-2	-424	-255	-209	-114	-565
I120C-L	3	-2	-1	-87	60	-13	61	-88
O120C-A	-24	-33	-88	-2637	-1504	728	-1148	-2993
O120C-B	-19	-31	-82	-2464	-1324	671	-1013	-2775
O120C-C	-20	-25	-82	-2338	-1300	760	-899	-2739
O120C-D	-19	-18	-83	-2194	-1214	861	-713	-2695
O120C-E	-14	-23	-81	-2272	-1109	766	-729	-2652
O120C-F	-9	-16	-76	-1996	-855	798	-445	-2406
O120C-G*	-7	-4	-68	-1569	-685	855	-165	-2089
O120C-H	-8	5	-55	-1098	-572	798	5	-1675
O120C-J	-2	11	-37	-572	-229	640	262	-1063
O120C-K	0	14	-26	-262	-64	526	372	-698
O120C-L	1	10	-6	83	53	203	271	-135
I120N-A	22	-23	-45	-1518	201	298	251	-1568
I120N-B	-13	-19	-40	-1270	-780	285	-649	-1401
I120N-C	-24	-12	-25	-789	-949	177	-674	-1064
I120N-D	-21	-7	-12	-395	-746	63	-384	-757
I120N-E	-10	-1	-3	-83	-338	32	-79	-342
I120N-F	0	0	2	41	27	-38	73	-5
I120N-G*	0	-4	-1	-115	-34	-32	-23	-126
I120N-H	-1	-3	-7	-207	-105	51	-84	-228
I120N-J	-1	-2	-2	-103	-60	0	-60	-103
O120N-A	20	-34	-59	-2079	-25	336	28	-2133
O120N-B	38	-15	-25	-930	876	133	886	-940
O120N-C	36	3	3	86	1109	0	1109	86
O120N-D	28	8	16	491	989	-114	1013	467
O120N-E	16	8	19	578	644	-146	760	462
O120N-F	5	6	15	465	282	-120	524	222
O120N-G	5	3	12	329	241	-114	407	163
O120N-H	4	5	15	435	244	-127	498	181
O120N-J	3	6	10	352	191	-51	367	177

IN-PLANE MOMENT LOADING, MZC, ON CYLINDER (20000 IN-LB)

	MICRO-STRAIN			STRESSES			PRIN STRESSES	
ROSETTE	GAGE1	GAGE2	GAGE3	TRANS	LONG	SHEAR	SIGMX	SIGMN
I150C-A	9	24	21	972	562	38	975	559
I150C-B	16	16	19	756	697	-38	774	678
I150C-C*	21	8	0	144	685	101	703	125
I150C-D*	-30	-1	17	378	-799	-234	423	-844
I150C-E*	0	-8	15	167	50	-304	418	-201
I150C-F	8	-16	18	33	238	-443	591	-319
I150C-G	-2	-12	27	316	24	-519	709	-370
I150C-H	-5	-13	30	382	-42	-583	790	-450
I150C-J	-1	-5	35	659	169	-538	1005	-177
I150C-K*	0	19	40	1285	385	-285	1367	303
I150C-L	-7	-9	26	384	-99	-456	658	-373
C150C-A	2	36	-10	551	223	614	1023	-249
O150C-B	-4	25	-16	203	-53	538	628	-479
O150C-C	-6	21	-24	-46	-185	602	490	-721
C150C-D*	-6	0	-29	-620	-371	380	-96	-895
C150C-E	-2	14	-33	-405	-193	627	337	-934
C150C-F	-10	4	-43	-845	-567	621	-70	-1342
C150C-G	-11	1	-41	-854	-598	564	-149	-1304
C150C-H	-16	2	-39	-797	-710	545	-207	-1300
C150C-J	-24	-3	-38	-862	-971	462	-451	-1382
O150C-K	-23	0	-35	-737	-920	462	-357	-1299
C150C-L	-22	4	-27	-467	-796	412	-188	-1075
I150N-A	7	24	25	1068	534	-6	1068	534
I150N-B	18	27	21	1025	835	76	1052	808
I150N-C	19	24	17	887	851	95	966	772
I150N-D*	20	20	285	6683	2618	-3533	8726	574
I150N-E	18	17	13	649	736	51	759	625
I150N-F*	13	13	0	278	483	177	585	176
I150N-G	12	11	12	509	523	-13	531	501
I150N-H	13	10	11	456	522	-19	527	451
I150N-J	11	8	10	374	454	-19	459	370
O150N-A	10	23	-1	470	426	317	765	131
O150N-B	3	14	-4	205	161	241	425	-58
O150N-C*	8	6	-4	33	238	139	309	-37
O150N-D*	5	3	-2	26	165	70	193	-3
C150N-E	8	1	-2	-40	216	44	224	-47
C150N-F	11	-2	0	-54	326	-25	328	-56
C150N-G	11	0	1	29	351	-13	351	29
C150N-H	10	3	2	94	313	13	314	93
C150N-J	8	2	4	117	277	-25	281	113

IN-PLANE MOMENT LOADING, MZC, ON CYLINDER (20000 IN-LB)

	MICRO-STRAIN			STRESSES			PRIN STRESSES	
ROSETTE	GAGE1	GAGE2	GAGE3	TRANS	LONG	SHEAR	SIGMX	SIGMN
I180C-A	4	35	35	1531	588	-6	1531	587
I180C-B	14	28	29	1228	782	-6	1228	782
I180C-C	19	22	22	950	855	-6	951	855
I180C-D*	20	17	0	344	702	222	808	238
I180C-E	18	10	11	461	680	-11	681	460
I180C-F	10	1	1	42	298	-6	298	42
I180C-G	0	-4	-5	-199	-45	6	-45	-199
I180C-H	-4	-3	-3	-121	-165	0	-121	-165
I180C-J	-6	-3	-1	-77	-208	-25	-72	-213
I180C-K	-4	-9	-7	-330	-213	-25	-208	-335
I180C-L	-13	-1	0	-17	-404	-6	-17	-404
O180C-A	-4	23	21	966	161	25	966	161
O180C-B	-7	15	15	665	0	6	665	0
O180C-C	-6	10	10	456	-49	-6	456	-49
O180C-D	-4	6	7	297	-39	-13	298	-40
O180C-E	-1	6	6	263	36	-6	263	36
O180C-F	4	7	7	288	215	0	288	215
O180C-G	3	10	8	393	218	25	397	214
O180C-H	0	10	10	429	114	-6	429	114
O180C-J	-7	14	14	624	-27	6	624	-27
O180C-K*	0	13	13	574	172	6	575	172
O180C-L	-19	13	11	553	-390	32	554	-391
I180N-A	16	28	29	1236	841	-13	1236	841
I180N-B	22	23	23	979	949	0	979	949
I180N-C	22	18	18	759	884	6	884	759
I180N-D	17	14	13	577	686	6	687	576
I180N-E	14	13	12	538	589	19	595	532
I180N-F*	0	123	11	2956	887	1488	3733	109
I180N-G	9	10	10	419	382	-6	420	381
I180N-H*	0	63	13	1671	501	659	1967	206
I180N-J	9	9	10	398	376	-6	400	374
O180N-A	-7	21	23	979	94	-32	980	93
O180N-B	-11	7	9	357	-235	-32	359	-237
O180N-C	-10	-1	1	21	-279	-32	24	-282
O180N-D	-4	-3	-3	-142	-171	0	-142	-171
O180N-E	1	-4	-5	-189	-28	13	-27	-190
O180N-F	9	-2	-2	-103	226	6	226	-104
O180N-G*	0	124	3	2789	837	1614	3699	-74
O180N-H	9	0	-1	-41	259	6	259	-41
O180N-J	10	-2	-2	-94	257	0	257	-94

IN-PLANE MOMENT LOADING, MZC, ON CYLINDER (20000 IN-LB)

	MICRO-STRAIN			STRESSES			PRIN STRESSES	
ROSETTE	GAGE1	GAGE2	GAGE3	TRANS	LONG	SHEAR	SIGMX	SIGMN
I270C-A	86	-92	-103	-4377	1267	139	1271	-4380
I270C-B	64	-77	-87	-3673	808	133	812	-3677
I270C-C	38	-73	-78	-3363	132	76	133	-3365
I270C-D	21	-66	-72	-3052	-288	89	-285	-3055
I270C-E	11	-63	-66	-2853	-528	38	-527	-2853
I270C-F	-3	-61	-56	-2555	-866	-70	-864	-2558
I270C-G	-5	-42	-44	-1885	-708	19	-708	-1885
I270C-H	0	-30	-31	-1358	-407	13	-407	-1358
I270C-J	6	-13	-16	-643	-22	32	-20	-645
I270C-K	9	-5	-7	-271	176	19	176	-271
I270C-L	3	9	8	351	205	13	353	204
I270C-M	-10	30	34	1421	127	-57	1423	124
O270C-A	-31	-122	-114	-5156	-2488	-108	-2483	-5161
O270C-B*	0	0	-102	-2235	-671	1355	112	-3017
O270C-C	-16	-86	-81	-3638	-1576	-63	-1574	-3640
O270C-D	0	-68	-63	-2872	-862	-70	-859	-2875
O270C-E	9	-53	-48	-2234	-400	-57	-398	-2236
O270C-F	24	-29	-27	-1258	335	-25	336	-1259
O270C-G	27	-13	-12	-593	620	-13	621	-593
O270C-H	26	-8	-10	-436	639	32	640	-436
O270C-J	15	-8	-8	-372	345	0	345	-372
O270C-K	8	-5	-9	-322	132	51	137	-327
O270C-L	-1	5	5	231	27	0	231	27
I270N-A	78	-86	-90	-3971	1161	51	1161	-3972
I270N-B	-8	-86	-70	-3417	-1253	-203	-1234	-3436
I270N-C	-59	-67	-40	-2274	-2464	-355	-2002	-2736
I270N-D	-69	-45	-38	-1752	-2593	-82	-1744	-2601
I270N-E	-36	-23	-25	-1005	-1371	25	-1003	-1373
I270N-F	-13	-4	-2	-132	-439	-25	-130	-441
I270N-G	-6	-3	-3	-130	-210	-6	-129	-210
I270N-H	-6	-3	-1	-88	-197	-19	-85	-201
I270N-J	-2	0	0	3	-71	-13	5	-73
O270N-A	-51	-134	-128	-5709	-3252	-76	-3250	-5711
O270N-B	33	-68	-72	-3118	63	44	63	-3118
O270N-C	51	-19	-21	-923	1249	32	1249	-923
O270N-D	48	12	8	385	1570	51	1572	383
O270N-E	25	24	21	976	1034	38	1053	957
O270N-F	-11	20	18	848	-88	25	849	-88
O270N-G	-12	11	11	515	-216	0	515	-216
O270N-H	-9	10	10	448	-122	13	448	-123
O270N-J	-6	7	8	330	-72	-6	330	-72

IN-PLANE MOMENT LOADING, MZC, ON CYLINDER (20000 IN-LB)

	MICRO-STRAIN			STRESSES			PRIN STRESSES	
ROSETTE	GAGE1	GAGE2	GAGE3	TRANS	LONG	SHEAR	SIGMX	SIGMN
I300C-A	51	-69	-16	-1926	962	-715	1129	-2093
I300C-B	45	-75	0	-1699	830	-1000	1178	-2047
I300C-C	41	-77	23	-1215	862	-1330	1510	-1863
I300C-D	33	-75	30	-1029	689	-1299	1472	-1812
I300C-E	28	-68	33	-803	586	-1355	1414	-1631
I300C-F	8	-56	35	-468	88	-1203	1045	-1425
I300C-G	-1	-45	18	-594	-207	-842	464	-1265
I300C-H	-2	-40	9	-677	-260	-652	216	-1153
I300C-J	-4	-28	0	-591	-291	-374	-39	-844
I300C-K	-2	-19	0	-426	-185	-260	-19	-592
I300C-L	4	-1	2	16	133	-38	144	5
O300C-A	-12	-28	-78	-2315	-1065	677	-769	-2612
O300C-B	-16	-29	-82	-2406	-1192	709	-866	-2732
O300C-C	-24	-23	-87	-2396	-1446	848	-949	-2894
O300C-D	-22	-21	-92	-2461	-1408	950	-849	-3021
O300C-E	-20	-18	-89	-2328	-1297	956	-726	-2899
O300C-F	-15	-13	-81	-2062	-1075	905	-537	-2599
O300C-G	-10	0	-66	-1430	-743	874	-147	-2025
O300C-H	-10	6	-57	-1107	-617	842	15	-1739
O300C-J	-5	12	-41	-632	-332	703	237	-1201
O300C-K	-1	13	-26	-271	-110	519	335	-715
O300C-L	1	7	-6	20	34	177	205	-150
I300N-A	25	-24	-48	-1615	271	329	327	-1671
I300N-B	-12	-17	-38	-1187	-727	272	-601	-1314
I300N-C	-23	-10	-24	-726	-917	177	-620	-1023
I300N-D	-22	-5	-12	-362	-765	95	-341	-786
I300N-E	-10	0	-3	-51	-329	38	-46	-334
I300N-F	2	-1	6	112	105	-95	204	14
I300N-G	2	1	5	123	94	-51	161	56
I300N-H	1	0	0	9	31	-6	33	8
I300N-J	1	-2	0	-53	13	-19	18	-58
O300N-A	22	-29	-59	-1967	80	393	153	-2040
O300N-B	36	-12	-25	-844	830	171	848	-861
O300N-C	34	-2	-2	-142	984	0	984	-142
O300N-D	23	4	9	257	761	-57	768	251
O300N-E	13	4	12	330	498	-108	551	278
O300N-F	2	2	13	332	157	-139	409	80
O300N-G	1	1	9	208	91	-101	266	32
O300N-H	0	3	9	261	78	-82	293	47
O300N-J	0	3	9	251	75	-76	279	47

IN-PLANE MOMENT LOADING, MZC, ON CYLINDER (20000 IN-LB)

	MICRO-STRAIN			STRESSES			PRIN STRESSES	
ROSETTE	GAGE1	GAGE2	GAGE3	TRANS	LONG	SHEAR	SIGMX	SIGMN
I330C-A	9	15	9	512	425	89	567	370
I330C-B	14	5	11	329	526	-82	556	299
I330C-C	16	-4	11	149	530	-203	617	62
I330C-D	16	-8	16	170	536	-317	719	-13
I330C-E	10	-12	15	52	315	-367	573	-207
I330C-F	-5	-18	22	99	-113	-526	529	-543
I330C-G	-10	-15	29	304	-223	-583	680	-599
I330C-H	-13	-16	29	307	-307	-608	681	-681
I330C-J	-17	-12	33	478	-370	-608	795	-687
I330C-K	-19	-9	31	523	-428	-532	761	-666
I330C-L	-20	-6	29	534	-439	-462	718	-623
O330C-A	-3	32	-12	431	44	589	858	-382
O330C-B	-5	27	-23	89	-130	659	647	-688
O330C-C	-11	20	-31	-218	-393	684	384	-995
O330C-D*	-9	18	-35	-367	-367	696	330	-1063
O330C-E	-6	14	-36	-474	-313	659	270	-1057
O330C-F	-8	10	-43	-723	-445	696	126	-1294
O330C-G*	-12	36	-39	-60	-374	1007	802	-1236
O330C-H	-17	7	-41	-733	-733	633	-100	-1366
O330C-J	-25	3	-38	-735	-976	551	-292	-1419
O330C-K	-26	-2	-40	-901	-1040	513	-453	-1488
O330C-L	-27	1	-32	-649	-1007	437	-356	-1300
I330N-A	5	22	22	955	443	0	955	443
I330N-B	12	26	19	969	647	101	998	618
I330N-C	16	25	16	881	735	114	943	672
I330N-D	17	21	15	785	749	82	851	683
I330N-E	14	16	12	611	611	51	662	560
I330N-F*	12	7	6	268	451	6	451	268
I330N-G	8	8	10	398	362	-32	417	344
I330N-H	12	10	12	467	511	-25	522	455
I330N-J	11	8	10	374	440	-19	445	369
O330N-A	0	63	-1	1358	407	848	1855	-90
O330N-B	8	14	-4	221	295	241	501	15
O330N-C	3	9	-5	80	110	177	273	-83
O330N-D	1	1	-4	-64	23	76	67	-108
O330N-E*	7	-2	-5	-175	161	38	166	-179
O330N-F	7	-2	-6	-174	147	51	155	-182
O330N-G	8	-1	-1	-51	227	0	227	-51
O330N-H	10	1	3	73	307	-25	310	70
O330N-J	9	1	3	85	282	-32	287	80

A.11 Axial Force, F_{XC}, on Cylinder

AXIAL FORCE LOADING, FXC, ON CYLINDER (5000 LB)

	MICRO-STRAIN			STRESSES			PRIN STRESSES	
ROSETTE	GAGE1	GAGE2	GAGE3	TRANS	LONG	SHEAR	SIGMX	SIGMN
I-O-C-A	0	-25	-25	-1097	-329	-6	-329	-1097
I-O-C-B	-5	-18	-22	-883	-407	57	-401	-889
I-O-C-C	-7	-10	-19	-608	-396	120	-342	-663
I-O-C-D	-7	-4	-13	-368	-324	114	-230	-462
I-O-C-E	-8	0	-10	-201	-288	139	-98	-390
I-O-C-F	0	10	0	198	60	133	279	-21
I-O-C-G	4	15	8	486	274	95	523	238
I-O-C-H*	0	17	8	533	160	120	568	124
I-O-C-J	11	17	9	562	511	108	647	426
I-O-C-K	15	17	10	589	633	89	702	520
I-O-C-L	19	16	9	533	716	95	756	493
O-O-C-A	12	-13	-13	-578	197	0	197	-578
O-O-C-B	10	-8	-10	-397	166	32	168	-399
O-O-C-C	7	-2	-3	-122	163	6	163	-122
O-O-C-D	5	-2	-4	-141	100	32	104	-145
O-O-C-E	6	0	-2	-48	157	25	160	-51
O-O-C-F	0	-1	-3	-94	-28	32	-15	-107
O-O-C-G	-1	-7	-8	-312	-136	13	-135	-313
O-O-C-H	3	-9	-10	-411	-24	19	-23	-412
O-O-C-J	9	-11	-11	-511	103	0	103	-511
O-O-C-K	14	-13	0	-297	324	-171	368	-341
O-O-C-L*	68	-11	-11	-576	1866	0	1866	-576
I-O-N-A	3	0	-2	-66	66	25	71	-71
I-O-N-B	1	4	4	166	92	0	166	92
I-O-N-C	6	9	9	380	299	-6	380	299
I-O-N-D	10	11	15	564	454	-44	580	439
I-O-N-E	15	16	15	663	641	6	664	639
I-O-N-F*	19	0	-3	-84	545	38	548	-86
I-O-N-G	16	11	11	474	613	6	613	473
I-O-N-H	14	10	9	392	531	6	531	392
I-O-N-J	16	10	11	453	606	-6	607	453
O-O-N-A	22	-1	-2	-97	627	19	627	-98
O-O-N-B	20	5	5	186	669	0	669	186
O-O-N-C	16	10	11	452	620	-6	621	452
O-O-N-D	14	13	13	570	584	0	584	570
O-O-N-E	10	15	13	595	464	25	600	459
O-O-N-F	5	12	10	475	299	38	483	291
O-O-N-G	3	10	9	404	207	19	406	205
O-O-N-H	4	10	11	476	257	-13	477	256
O-O-N-J	-3	8	8	337	16	0	337	16

AXIAL FORCE LOADING, FXC, ON CYLINDER (5000 LB)

	MICRO-STRAIN			STRESSES			PRIN STRESSES	
ROSETTE	GAGE1	GAGE2	GAGE3	TRANS	LONG	SHEAR	SIGMX	SIGMN
I-90C-A*	-1037	111	123	6289	-29230	-158	6290	-29230
I-90C-B	-60	101	113	4755	-370	-158	4760	-375
I-90C-C	-38	86	96	4041	86	-120	4045	83
I-90C-D	-23	79	92	3774	448	-171	3783	439
I-90C-E	-14	73	85	3483	631	-152	3491	623
I-90C-F	-13	61	70	2897	470	-127	2904	463
I-90C-G	-1	51	50	2226	639	19	2226	639
I-90C-H	-7	43	40	1825	348	38	1826	347
I-90C-J	-15	39	29	1521	0	139	1533	-13
I-90C-K	-21	38	29	1475	-185	120	1483	-194
I-90C-L	-24	36	32	1520	-257	57	1521	-259
O-90C-A	29	124	119	5325	2481	70	5327	2480
O-90C-B	28	100	103	4429	2156	-32	4430	2155
O-90C-C	16	85	91	3837	1621	-82	3840	1618
O-90C-D	2	72	77	3288	1043	-70	3290	1041
O-90C-E	-6	61	65	2774	647	-57	2776	646
O-90C-F	-18	38	40	1722	-11	-32	1722	-12
O-90C-G	-22	30	24	1204	-295	82	1209	-299
O-90C-H	-18	28	25	1190	-185	38	1191	-186
O-90C-J	-13	30	32	1393	33	-25	1393	32
O-90C-K	-9	36	38	1639	221	-38	1640	220
O-90C-L*	-7	35	0	781	20	469	1004	-203
I-90N-A	13	118	109	4988	1896	120	4993	1891
I-90N-B	68	95	94	4081	3277	13	4082	3277
I-90N-C	86	69	70	2966	3470	-6	3470	2965
I-90N-D	71	50	50	2125	2776	-6	2776	2125
I-90N-E	49	34	33	1429	1897	13	1897	1429
I-90N-F	26	20	23	922	1061	-32	1067	915
I-90N-G	20	19	19	814	843	-13	848	809
I-90N-H	21	19	18	791	879	13	881	789
I-90N-J	19	16	16	669	757	0	757	669
O-90N-A	10	116	118	5149	1830	-25	5149	1830
O-90N-B	-41	51	58	2437	-495	-95	2440	-498
O-90N-C*	-48	7	10	408	-1332	-38	409	-1332
O-90N-D	-29	-13	-12	-532	-1043	-13	-531	-1044
O-90N-E	-8	-19	-18	-795	-481	-6	-481	-795
O-90N-F	20	-8	-7	-356	492	-13	492	-356
O-90N-G	15	-4	-4	-183	387	0	387	-183
O-90N-H	15	-2	-1	-89	415	-6	415	-89
O-90N-J	9	0	-3	-83	246	44	252	-89

AXIAL FORCE LOADING, FXC, ON CYLINDER (5000 LB)

	MICRO-STRAIN			STRESSES			PRIN STRESSES	
ROSETTE	GAGE1	GAGE2	GAGE3	TRANS	LONG	SHEAR	SIGMX	SIGMN
I120C-A*	-28	32	11	992	-544	279	1041	-593
I120C-B*	-24	33	8	924	-436	342	1005	-517
I120C-C*	-19	37	0	815	-340	494	998	-522
I120C-D	-23	79	-2	1727	-166	1083	2219	-658
I120C-E	-19	78	-8	1567	-100	1140	2145	-679
I120C-F	-10	62	-16	1034	11	1038	1680	-635
I120C-G	5	55	-10	997	442	861	1624	-185
I120C-H	9	53	-7	1014	561	798	1617	-42
I120C-J	6	53	-2	1111	519	728	1601	29
I120C-K	9	49	0	1066	577	665	1530	113
I120C-L	8	60	-5	1203	589	861	1810	-18
O120C-A	15	26	88	2490	1203	-823	2891	802
O120C-B	13	25	88	2482	1130	-842	2886	726
O120C-C	17	22	91	2456	1250	-918	2952	755
O120C-D	15	17	91	2365	1166	-988	2920	610
O120C-E	15	17	88	2302	1147	-950	2836	613
O120C-F	10	14	85	2172	937	-943	2682	427
O120C-G	10	2	74	1660	797	-962	2283	174
O120C-H	10	-3	66	1368	710	-912	2008	69
O120C-J	8	-7	58	1120	564	-861	1747	-63
O120C-K	9	-5	54	1066	577	-779	1638	5
O120C-L	7	2	58	1329	613	-747	1799	142
I120N-A*	12	41	61	2232	1040	-260	2286	986
I120N-B	36	31	49	1736	1604	-241	1919	1421
I120N-C	46	31	40	1516	1838	-127	1881	1472
I120N-D	38	25	29	1138	1496	-44	1501	1132
I120N-E	30	22	22	928	1177	0	1177	928
I120N-F	20	22	18	844	866	57	913	797
I120N-G*	0	-12	18	125	38	-405	489	-326
I120N-H	19	20	19	836	821	13	843	814
I120N-J	18	20	18	805	783	32	828	761
O120N-A	-24	33	54	1938	-146	-272	1973	-181
O120N-B	-32	17	23	913	-696	-76	916	-699
O120N-C	-17	10	10	447	-379	-6	447	-379
O120N-D	-8	6	0	134	-202	76	151	-219
O120N-E	2	7	-1	134	97	108	225	6
O120N-F	10	10	2	250	389	108	447	191
O120N-G*	6	6	-4	45	199	133	276	-31
O120N-H	8	5	5	211	291	6	292	211
O120N-J	9	7	1	168	307	70	336	139

AXIAL FORCE LOADING, FXC, ON CYLINDER (5000 LB)

	MICRO-STRAIN			STRESSES			PRIN STRESSES	
ROSETTE	GAGE1	GAGE2	GAGE3	TRANS	LONG	SHEAR	SIGMX	SIGMN
I150C-A	-12	-20	-14	-739	-578	-89	-539	-778
I150C-B	-13	-17	-12	-623	-586	-70	-532	-676
I150C-C*	-13	-11	0	-226	-467	-146	-157	-535
I150C-D*	-36	-8	-9	-316	-1164	13	-316	-1164
I150C-E	0	-4	-9	-292	-88	63	-70	-310
I150C-F	-5	3	-7	-78	-180	127	8	-266
I150C-G	1	3	-10	-148	-2	177	117	-266
I150C-H	3	4	-11	-160	38	209	170	-292
I150C-J	-5	1	-15	-308	-235	215	-53	-490
I150C-K*	-15	-11	-21	-694	-650	139	-531	-813
I150C-L	6	7	-18	-257	108	329	302	-451
O150C-A	9	-21	19	-62	238	-526	635	-458
O150C-B	8	-14	27	273	324	-538	838	-240
O150C-C	10	-7	36	626	501	-576	1143	-16
O150C-D*	11	0	40	865	588	-532	1276	177
O150C-E	11	-6	42	781	577	-633	1320	38
O150C-F	8	-8	41	712	456	-652	1248	-81
O150C-G	12	-7	39	697	566	-608	1243	20
O150C-H	16	-7	38	672	672	-608	1280	64
O150C-J	24	-9	38	632	902	-627	1408	126
O150C-K	32	-4	38	707	1167	-551	1534	340
O150C-L	39	-3	37	709	1382	-532	1675	416
I150N-A	11	-9	4	-117	307	-165	364	-173
I150N-B	5	-6	3	-68	136	-114	187	-119
I150N-C	3	-1	4	60	103	-76	161	2
I150N-D	6	5	8	276	254	-32	298	231
I150N-E	8	7	9	326	326	-25	351	301
I150N-F*	12	9	0	175	409	114	455	129
I150N-G	10	10	10	438	445	-6	449	434
I150N-H	11	12	10	478	486	19	501	463
I150N-J	11	12	11	489	475	13	497	467
O150N-A	-2	-19	7	-259	-135	-336	144	-538
O150N-B	2	-3	5	40	69	-114	169	-61
O150N-C	5	1	8	193	201	-95	292	102
O150N-D	1	4	9	280	127	-70	307	100
O150N-E	-2	8	8	337	30	0	337	30
O150N-F	-5	5	8	288	-70	-32	291	-73
O150N-G	-4	4	5	192	-56	-13	193	-57
O150N-H	-2	5	5	221	9	-6	222	9
O150N-J	-1	3	2	127	-5	13	128	-6

AXIAL FORCE LOADING, FXC, ON CYLINDER (5000 LB)

	MICRO-STRAIN			STRESSES			PRIN STRESSES	
ROSETTE	GAGE1	GAGE2	GAGE3	TRANS	LONG	SHEAR	SIGMX	SIGMN
I180C-A	0	-22	-24	-1024	-307	25	-306	-1024
I180C-B	-8	-14	-19	-723	-462	70	-445	-750
I180C-C	-11	-10	-14	-510	-495	63	-439	-566
I180C-D	-10	-5	-12	-376	-412	95	-297	-491
I180C-E	-10	-1	-10	-219	-351	114	-154	-417
I180C-F	-3	8	-20	-278	-183	374	146	-607
I180C-G*	-5	-56	9	-1039	-454	-861	163	-1656
I180C-H	5	12	10	496	306	25	499	302
I180C-J	8	22	15	806	470	89	828	448
I180C-K	11	22	21	938	624	19	939	622
I180C-L	15	19	14	704	667	70	758	614
O180C-A	8	-15	-10	-562	74	-57	79	-568
O180C-B	7	-10	-5	-321	118	-63	126	-330
O180C-C	5	-7	-1	-183	102	-82	124	-205
O180C-D	3	-5	-1	-139	44	-57	60	-155
O180C-E	0	-7	-1	-167	-50	-76	-13	-205
O180C-F	-4	-6	-1	-152	-174	-57	-105	-221
O180C-G	-6	-10	-8	-380	-299	-19	-295	-384
O180C-H	-1	-12	-10	-500	-193	-25	-191	-502
O180C-J	12	-7	-4	-253	280	-44	284	-257
O180C-K*	0	-6	-6	-251	-75	0	-75	-251
O180C-L	21	-7	-9	-357	520	25	521	-358
I180N-A	1	0	-3	-64	9	38	26	-80
I180N-B	0	1	1	63	19	0	63	19
I180N-C	1	4	5	197	102	-6	197	101
I180N-D	5	7	8	308	249	-13	310	247
I180N-E	9	8	9	346	360	-13	368	338
I180N-F*	0	11	9	449	135	32	452	132
I180N-G	12	8	6	290	443	19	446	288
I180N-H*	0	-37	6	-679	-204	-576	182	-1064
I180N-J	10	8	7	313	393	19	398	309
O180N-A	19	-7	-5	-282	486	-32	487	-283
O180N-B	18	2	2	64	547	0	547	64
O180N-C	12	5	4	195	429	13	430	195
O180N-D	6	6	7	275	268	-6	279	264
O180N-E	4	8	9	361	237	-6	361	236
O180N-F	0	8	8	334	114	0	334	114
O180N-G*	0	-19	5	-303	-91	-323	143	-537
O180N-H	-1	7	6	283	56	6	283	56
O180N-J	-3	7	5	265	-20	19	266	-22

AXIAL FORCE LOADING, FXC, ON CYLINDER (5000 LB)

	MICRO-STRAIN			STRESSES			PRIN STRESSES	
ROSETTE	GAGE1	GAGE2	GAGE3	TRANS	LONG	SHEAR	SIGMX	SIGMN
I270C-A	-65	116	143	5753	-213	-355	5774	-234
I270C-B	-43	97	125	4924	194	-374	4954	165
I270C-C	-22	90	114	4515	699	-329	4543	671
I270C-D	-10	81	105	4106	918	-317	4137	887
I270C-E	-4	79	96	3868	1046	-228	3887	1028
I270C-F	15	87	91	3911	1615	-51	3912	1614
I270C-G	12	71	80	3308	1363	-114	3314	1356
I270C-H	4	65	66	2867	989	-19	2868	988
I270C-J	-10	50	58	2392	418	-101	2397	413
I270C-K	-17	49	52	2243	160	-32	2244	159
I270C-L	-19	47	56	2276	127	-114	2282	121
I270C-M	6	48	48	2082	810	0	2082	810
O270C-A	16	122	119	5278	2054	32	5278	2053
O270C-B*	0	0	105	2308	692	-1399	3116	-115
O270C-C	4	93	85	3912	1288	108	3917	1283
O270C-D	-5	77	70	3222	810	89	3226	807
O270C-E	-11	70	59	2843	511	146	2852	502
O270C-F	-21	48	38	1913	-53	120	1921	-61
O270C-G	-23	42	34	1686	-179	108	1692	-185
O270C-H	-15	41	32	1614	42	120	1623	33
O270C-J	-10	45	36	1786	251	114	1794	242
O270C-K	-3	51	36	1915	475	196	1941	448
O270C-L	-3	52	49	2228	583	44	2229	582
I270N-A	-5	118	130	5457	1495	-152	5463	1489
I270N-B	59	106	99	4457	3119	95	4464	3112
I270N-C*	89	84	60	3066	3600	310	3742	2924
I270N-D	86	61	55	2444	3299	82	3307	2436
I270N-E	51	41	39	1698	2049	25	2051	1696
I270N-F	26	22	22	953	1070	0	1070	953
I270N-G	22	22	21	926	934	6	937	923
I270N-H	22	20	21	884	935	-6	936	883
I270N-J	18	19	19	805	783	-6	807	782
O270N-A	-1	124	115	5244	1545	114	5247	1541
O270N-B	-57	56	53	2464	-957	38	2465	-958
O270N-C	-56	6	7	354	-1562	-13	354	-1562
O270N-D	-46	-17	-19	-733	-1589	32	-732	-1590
O270N-E	-20	-26	-24	-1064	-918	-25	-914	-1068
O270N-F	15	-17	-15	-716	227	-19	228	-716
O270N-G	11	-9	-5	-315	248	-44	251	-319
O270N-H	10	-6	-6	-273	232	-6	232	-273
O270N-J	8	-3	-4	-166	193	6	193	-166

AXIAL FORCE LOADING, FXC, ON CYLINDER (5000 LB)

	MICRO-STRAIN			STRESSES			PRIN STRESSES	
ROSETTE	GAGE1	GAGE2	GAGE3	TRANS	LONG	SHEAR	SIGMX	SIGMN
I300C-A	-38	81	48	2872	-265	437	2931	-325
I300C-B*	-30	90	-47	994	-600	1823	2187	-1793
I300C-C	-30	93	10	2279	-229	1108	2698	-648
I300C-D	-14	94	0	2094	201	1247	2713	-419
I300C-E	-9	89	-2	1931	323	1216	2584	-331
I300C-F*	9	76	-2	1599	736	1038	2292	43
I300C-G	11	70	-1	1502	793	943	2155	140
I300C-H	9	67	7	1609	739	804	2089	260
I300C-J	7	63	7	1518	655	747	1949	224
I300C-K	5	64	-4	1321	553	905	1920	-47
I300C-L	-6	56	-12	967	119	912	1549	-462
O300C-A	3	21	91	2461	838	-924	2880	420
O300C-B	5	16	99	2512	896	-1108	3075	333
O300C-C	10	11	100	2433	1015	-1190	3110	339
O300C-D*	9	10	110	2622	1043	-1342	3390	276
O300C-E	10	2	103	2287	985	-1342	3128	144
O300C-F	11	-2	95	2024	949	-1285	2880	94
O300C-G	8	-4	86	1787	779	-1203	2587	-21
O300C-H	10	-13	81	1483	744	-1260	2426	-200
O300C-J	11	-5	73	1471	783	-1038	2221	33
O300C-K	11	4	68	1564	812	-855	2122	254
O300C-L	15	16	67	1812	985	-678	2192	605
I300N-A	17	47	75	2644	1307	-374	2742	1209
I300N-B	46	38	60	2112	2002	-285	2347	1767
I300N-C	50	30	42	1543	1974	-158	2026	1491
I300N-D	42	25	29	1123	1606	-51	1611	1118
I300N-E	30	19	17	750	1137	19	1138	749
I300N-F	14	19	10	611	611	127	738	484
I300N-G	17	20	15	765	729	70	819	675
I300N-H	19	19	17	783	805	32	828	761
I300N-J	18	19	16	764	771	44	812	723
O300N-A	-32	32	59	2051	-354	-361	2104	-407
O300N-B	-41	15	24	901	-956	-127	910	-964
O300N-C	-30	3	2	148	-868	19	149	-868
O300N-D	-19	-2	-8	-198	-630	82	-183	-645
O300N-E	-10	-1	-10	-219	-365	114	-157	-427
O300N-F	1	1	-10	-179	-11	146	73	-263
O300N-G	3	4	-5	-14	81	120	163	-95
O300N-H	0	3	-3	-10	-3	82	76	-89
O300N-J	5	2	-2	-6	155	63	177	-28

AXIAL FORCE LOADING, FXC, ON CYLINDER (5000 LB)

	MICRO-STRAIN			STRESSES			PRIN STRESSES	
ROSETTE	GAGE1	GAGE2	GAGE3	TRANS	LONG	SHEAR	SIGMX	SIGMN
I330C-A	-6	-14	2	-265	-265	-215	-49	-480
I330C-B	-9	-1	3	62	-238	-57	72	-249
I330C-C	-7	9	3	268	-119	82	285	-136
I330C-D	-1	18	4	482	102	177	552	32
I330C-E	4	23	1	528	287	285	717	98
I330C-F	19	29	-11	377	669	532	1074	-29
I330C-G	26	30	-8	473	912	507	1244	141
I330C-H	28	30	-11	387	957	557	1298	46
I330C-J	33	31	-16	287	1084	627	1428	-57
I330C-K	38	27	-19	136	1167	602	1444	-140
I330C-L	45	30	-20	170	1391	665	1683	-122
O330C-A	6	-26	21	-111	138	-633	659	-632
O330C-B	10	-17	32	324	382	-646	1000	-293
O330C-C	14	-14	42	601	608	-741	1345	-137
O330C-D	11	-14	44	646	522	-766	1352	-185
O330C-E	11	-13	43	646	522	-741	1327	-160
O330C-F	10	-16	46	658	483	-823	1398	-258
O330C-G*	15	-25	45	412	580	-931	1430	-439
O330C-H	20	-12	44	667	813	-747	1491	-11
O330C-J	30	-12	48	760	1140	-810	1783	118
O330C-K	30	-19	44	531	1072	-836	1679	-77
O330C-L	39	-16	44	562	1352	-798	1847	67
I330N-A	17	-1	9	148	558	-139	601	105
I330N-B	14	1	10	214	492	-114	533	173
I330N-C	12	3	12	311	450	-120	519	241
I330N-D*	12	6	11	373	483	-70	516	339
I330N-E	11	6	11	374	454	-70	495	334
I330N-F	13	10	10	445	533	0	533	445
I330N-G	14	12	10	476	556	32	567	465
I330N-H	11	11	10	458	465	19	481	442
I330N-J	11	12	10	468	483	25	502	449
O330N-A	0	-67	18	-1076	-323	-1121	483	-1881
O330N-B	7	-1	13	264	293	-190	469	88
O330N-C	6	4	12	349	276	-101	420	205
O330N-D	3	6	11	372	212	-76	403	181
O330N-E*	-9	5	9	302	-180	-51	308	-185
O330N-F	-3	5	7	275	-17	-25	277	-19
O330N-G	-4	4	7	234	-44	-38	239	-49
O330N-H	-4	7	2	203	-67	70	220	-84
O330N-J	0	3	2	115	20	6	116	20

A.12 In-Plane Force, F_{YC}, on Cylinder

IN-PLANE FORCE LOADING, FYC, ON CYLINDER (2000 LB)

	MICRO-STRAIN			STRESSES			PRIN STRESSES	
ROSETTE	GAGE1	GAGE2	GAGE3	TRANS	LONG	SHEAR	SIGMX	SIGMN
I-0-C-A	-13	109	90	4380	929	253	4398	911
I-0-C-B	20	84	73	3424	1640	139	3435	1629
I-0-C-C	34	54	52	2302	1703	25	2303	1702
I-0-C-D	38	34	33	1421	1552	13	1554	1420
I-0-C-E	36	16	18	691	1291	-25	1292	690
I-0-C-F*	0	-22	-19	-909	-273	-32	-271	-910
I-0-C-G	-13	-40	-39	-1730	-918	-6	-918	-1730
I-0-C-H*	0	-45	-44	-1953	-586	-19	-586	-1953
I-0-C-J	-33	-47	-45	-1979	-1592	-32	-1589	-1982
I-0-C-K	-39	-45	-40	-1837	-1734	-63	-1704	-1867
I-0-C-L	-41	-34	-34	-1459	-1664	0	-1459	-1664
0-0-C-A	-30	62	65	2812	-69	-38	2812	-69
0-0-C-B	-33	38	42	1791	-447	-51	1792	-448
0-0-C-C	-26	22	24	1041	-457	-19	1042	-458
0-0-C-D	-19	12	16	637	-365	-57	640	-368
0-0-C-E	-15	8	11	424	-329	-44	427	-332
0-0-C-F	10	7	11	376	412	-57	454	334
0-0-C-G	12	19	20	853	627	-19	855	625
0-0-C-H	1	27	28	1200	389	-19	1200	388
0-0-C-J	-21	32	33	1464	-188	-13	1464	-188
0-0-C-K*	-34	36	0	820	-766	475	952	-897
0-0-C-L	-96	22	30	1265	-2514	-108	1268	-2517
I-0-N-A	58	91	93	3978	2947	-19	3978	2946
I-0-N-B	74	73	73	3114	3158	-776	3158	3114
I-0-N-C	67	54	52	2255	2701	32	2703	2253
I-0-N-D	56	43	42	1798	2207	13	2208	1798
I-0-N-E	42	38	37	1593	1747	6	1747	1593
I-0-N-F	23	0	70	1521	1140	-937	2287	374
I-0-N-G	22	39	35	1605	1151	63	1613	1143
I-0-N-H	22	44	41	1834	1220	38	1837	1218
I-0-N-J	23	36	35	1531	1158	6	1531	1158
0-0-N-A	-50	57	54	2499	-761	38	2500	-762
0-0-N-B	-53	20	15	842	-1344	70	844	-1346
0-0-N-C	-40	-6	-9	-270	-1278	38	-268	-1280
0-0-N-D	-25	-20	-20	-861	-1000	6	-860	-1000
0-0-N-E	-9	-23	-19	-920	-547	-44	-542	-925
0-0-N-F	15	-16	-12	-632	252	-44	254	-635
0-0-N-G	20	-13	-14	-617	414	6	414	-617
0-0-N-H	20	-17	-18	-795	360	13	361	-795
0-0-N-J	23	-16	-17	-736	478	13	478	-736

IN-PLANE FORCE LOADING, FYC, ON CYLINDER (2000 LB)

	MICRO-STRAIN			STRESSES			PRIN STRESSES	
ROSETTE	GAGE1	GAGE2	GAGE3	TRANS	LONG	SHEAR	SIGMX	SIGMN
I-90C-A	399	-409	-501	-20450	5840	1228	5898	-20510
I-90C-B	324	-358	-468	-18510	4170	1456	4263	-18600
I-90C-C	207	-286	-421	-15750	1477	1798	1663	-15930
I-90C-D	118	-259	-397	-14540	-813	1836	-572	-14780
I-90C-E	64	-240	-368	-13450	-2124	1703	-1874	-13700
I-90C-F*	34	-198	-317	-11360	-2381	1583	-2110	-11630
I-90C-G	-41	-151	-221	-8132	-3680	931	-3493	-8319
I-90C-H	-25	-99	-157	-5591	-2433	772	-2254	-5770
I-90C-J	10	-36	-91	-2790	-523	734	-306	-3007
I-90C-K	24	12	-57	-997	414	918	866	-1450
I-90C-L	16	69	-11	1256	862	1064	2141	-23
O-90C-A	-216	-615	-543	-25210	-14050	-956	-13970	-25300
O-90C-B	-188	-514	-454	-21070	-11970	-791	-11900	-21140
O-90C-C	-120	-437	-385	-17930	-8984	-690	-8931	-17980
O-90C-D	-37	-364	-307	-14730	-5516	-760	-5454	-14790
O-90C-E	13	-300	-242	-11940	-3183	-772	-3116	-12010
O-90C-F	88	-181	-104	-6363	729	-1013	870	-6505
O-90C-G	97	-125	-17	-3240	1936	-1444	2312	-3615
O-90C-H	84	-95	0	-2181	1869	-1254	2226	-2538
O-90C-J	47	-78	3	-1712	898	-1083	1288	-2103
O-90C-K	19	-73	6	-1493	122	-1045	635	-2006
O-90C-L*	-20	-34	0	-730	-818	-456	-316	-1232
I-90N-A	159	-442	-383	-18320	-733	-791	-698	-18350
I-90N-B	-179	-379	-352	-15880	-10120	-361	-10100	-15900
I-90N-C	-314	-276	-258	-11390	-12840	-228	-11360	-12880
I-90N-D	-274	-172	-170	-7218	-10390	-38	-7218	-10390
I-90N-E	-173	-98	-92	-3987	-6400	-89	-3984	-6403
I-90N-F	-70	-17	-27	-884	-2375	127	-873	-2386
I-90N-G	-38	-21	-29	-1044	-1468	101	-1021	-1491
I-90N-H	-41	-18	-20	-780	-1474	32	-778	-1476
I-90N-J	-36	-10	-11	-409	-1206	19	-409	-1207
O-90N-A	-151	-609	-556	-25450	-12160	-703	-12120	-25490
O-90N-B	148	-292	-291	-12970	558	-13	558	-12970
O-90N-C	230	-49	-57	-2592	6122	114	6124	-2594
O-90N-D*	175	74	64	2826	6108	133	6114	2820
O-90N-E	75	110	99	4513	3606	152	4538	3581
O-90N-F	-64	79	60	3130	-971	247	3145	-986
O-90N-G	-63	37	30	1531	-1422	89	1534	-1425
O-90N-H	-51	33	21	1257	-1162	158	1268	-1173
O-90N-J	-41	23	16	912	-953	95	917	-957

IN-PLANE FORCE LOADING, FYC. ON CYLINDER (2000 LB)

	MICRO-STRAIN			STRESSES			PRIN STRESSES	
ROSETTE	GAGE1	GAGE2	GAGE3	TRANS	LONG	SHEAR	SIGMX	SIGMN
I120C-A	252	-412	-154	-12730	3738	-3432	4424	-13410
I120C-B	193	-423	-113	-12000	2201	-4134	3317	-13120
I120C-C	158	-435	-34	-10490	1599	-5344	3622	-12520
I120C-D	115	-422	9	-9213	700	-5736	3325	-11840
I120C-E	85	-409	29	-8449	17	-5837	2995	-11430
I120C-F	22	-327	44	-6239	-1202	-4945	1829	-9269
I120C-G	-15	-258	10	-5436	-2073	-3558	181	-7690
I120C-H	-33	-224	-20	-5322	-2580	-2716	-909	-6993
I120C-J	-19	-189	-61	-5483	-2215	-1703	-1489	-6209
I120C-K	-8	-128	-79	-4545	-1592	-659	-1452	-4685
I120C-L	32	-66	-75	-3127	31	114	35	-3131
O120C-A	-121	-211	-445	-14290	-7908	3109	-6644	-15550
O120C-B*	-90	-194	-411	-13200	-6653	2893	-5557	-14290
O120C-C	-101	-165	-417	-12680	-6827	3362	-5297	-14210
O120C-D	-86	-130	-414	-11860	-6154	3780	-4272	-13750
O120C-E	-67	-139	-396	-11690	-5502	3432	-3975	-13210
O120C-F	-36	-106	-368	-10390	-4202	3489	-2633	-11960
O120C-G	-24	-43	-321	-7974	-3105	3710	-1102	-9977
O120C-H	-10	-7	-266	-5983	-2109	3457	-83	-8009
O120C-J	21	14	-184	-3751	-498	2640	976	-5226
O120C-K	36	19	-128	-2431	340	1956	1352	-3443
O120C-L	45	-17	-42	-1345	951	342	1001	-1394
I120N-A	98	-137	-267	-8985	241	1735	557	-9300
I120N-B	-88	-112	-221	-7225	-4805	1463	-4117	-7913
I120N-C	-139	-86	-143	-4861	-5621	760	-4391	-6090
I120N-D	-124	-53	-74	-2652	-4531	285	-2609	-4573
I120N-E	-78	-25	-29	-1084	-2663	51	-1082	-2665
I120N-F	-14	-17	4	-256	-490	-279	-71	-676
I120N-G*	0	20	-2	386	116	298	578	-76
I120N-H	-13	-15	2	-257	-462	-228	-110	-610
I120N-J	-11	-9	-7	-322	-439	-25	-316	-444
O120N-A	63	-220	-317	-11890	-1686	1292	-1525	-12050
O120N-B	165	-106	-139	-5581	3273	437	3294	-5602
O120N-C	151	-19	-5	-699	4324	-196	4331	-706
O120N-D	109	19	66	1750	3790	-627	3967	1573
O120N-E	47	25	78	2205	2059	-709	2844	1419
O120N-F	-10	15	62	1702	226	-633	1937	-9
O120N-G	-8	3	40	970	49	-494	1184	-166
O120N-H	-9	6	46	1148	74	-538	1371	-150
O120N-J	-9	7	31	835	-20	-323	943	-129

IN-PLANE FORCE LOADING, FYC, ON CYLINDER (2000 LB)

	MICRO-STRAIN			STRESSES			PRIN STRESSES	
ROSETTE	GAGE1	GAGE2	GAGE3	TRANS	LONG	SHEAR	SIGMX	SIGMN
I150C-A	10	61	62	2684	1104	-13	2684	1104
I150C-B	42	14	50	1363	1678	-475	2021	1020
I150C-C*	58	-31	0	-743	1531	-412	1603	-815
I150C-D*	122	-61	51	-343	3547	-1494	4055	-850
I150C-E*	0	-140	49	-1984	-595	-2520	1324	-3904
I150C-F	9	-126	56	-1555	-210	-2431	1640	-3405
I150C-G	-53	-124	88	-715	-1797	-2824	1619	-4131
I150C-H	-74	-133	104	-566	-2394	-3166	1815	-4775
I150C-J*	-50	-116	115	44	-1484	-3083	2457	-3896
I150C-K*	-37	-19	123	2328	-414	-1893	3294	-1380
I150C-L	-73	-138	85	-1079	-2519	-2969	1256	-4854
O150C-A	-21	152	-90	1381	-227	3216	3892	-2738
O150C-B	-47	96	-128	-659	-1595	2988	1898	-4152
O150C-C	-59	70	-168	-2076	-2391	3172	942	-5409
O150C-D*	-57	0	-203	-4396	-3044	2703	-933	-6507
O150C-E	-51	35	-234	-4310	-2818	3584	96	-7224
O150C-F	-58	17	-247	-4991	-3251	3508	-507	-7734
O150C-G	-58	5	-237	-5022	-3260	3223	-800	-7482
O150C-H	-75	7	-231	-4837	-3703	3172	-1048	-7492
O150C-J	-104	4	-228	-4804	-4578	3096	-1593	-7789
O150C-K	-117	2	-217	-4592	-4885	2912	-1822	-7654
O150C-L	-105	21	-189	-3571	-4222	2792	-1086	-6708
I150N-A	1	81	83	3591	1120	-25	3591	1120
I150N-B	46	93	64	3396	2402	393	3532	2265
I150N-C	66	85	50	2894	2836	456	3322	2408
I150N-D	67	65	60	2684	2801	63	2829	2656
I150N-E	58	51	34	1805	2295	222	2380	1720
I150N-F*	35	26	0	536	1202	348	1351	387
I150N-G	30	18	26	938	1180	-108	1221	897
I150N-H	29	16	23	835	1134	-95	1162	807
I150N-J	25	10	19	599	935	-114	970	564
O150N-A	45	101	-27	1591	1817	1703	3411	-3
O150N-B	17	57	-29	587	689	1152	1792	-515
O150N-C	7	17	-30	-300	110	633	570	-760
O150N-D	11	-2	-25	-597	163	304	270	-704
O150N-E	20	-14	-22	-805	357	108	367	-815
O150N-F	36	-22	-14	-843	816	-108	823	-850
O150N-G	37	-9	-3	-302	1021	-70	1025	-306
O150N-H	32	-4	0	-130	931	-57	934	-133
O150N-J	27	-7	8	-9	810	-190	852	-51

IN-PLANE FORCE LOADING, FYC, ON CYLINDER (2000 LB)

	MICRO-STRAIN			STRESSES			PRIN STRESSES	
ROSETTE	GAGE1	GAGE2	GAGE3	TRANS	LONG	SHEAR	SIGMX	SIGMN
I180C-A	-27	147	148	6505	1139	-13	6505	1139
I180C-B	29	105	111	4710	2268	-76	4713	2266
I180C-C	57	71	75	3154	2657	-51	3159	2652
I180C-D	58	44	48	1952	2325	-44	2330	1947
I180C-E	48	20	22	867	1686	-25	1686	866
I180C-F	2	-27	-28	-1193	-287	13	-287	-1193
I180C-G	-45	-48	-50	-2102	-1985	25	-1980	-2107
I180C-H	-72	-48	-51	-2114	-2787	38	-2112	-2789
I180C-J	-92	-59	-59	-2500	-3501	-6	-2500	-3501
I180C-K*	-93	-76	-73	-3177	-3747	-38	-3175	-3750
I180C-L	-153	-40	-46	-1711	-5118	76	-1710	-5120
O180C-A	-40	112	110	4932	268	25	4932	268
O180C-B	-54	70	70	3140	-669	6	3140	-669
O180C-C	-51	41	39	1810	-982	25	1811	-983
O180C-D	-43	21	21	987	-987	0	987	-987
O180C-E	-36	10	11	489	-937	-19	489	-937
O180C-F	-14	6	10	350	-323	-51	354	-327
O180C-G	-18	25	25	1105	-196	0	1105	-196
O180C-H	-41	35	37	1633	-750	-25	1633	-751
O180C-J	-85	41	37	1806	-2010	51	1807	-2011
O180C-K*	0	41	36	1702	511	70	1706	507
O180C-L	-166	26	32	1467	-4535	-82	1468	-4536
I180N-A	55	125	135	5674	3342	-133	5681	3334
I180N-B	98	106	108	4603	4318	-32	4606	4314
I180N-C	99	79	78	3338	3967	13	3967	3338
I180N-D	81	62	56	2501	3174	76	3182	2493
I180N-E	59	52	46	2097	2411	82	2431	2076
I180N-F*	0	49	33	1817	545	215	1853	510
I180N-G	29	38	39	1649	1379	-19	1650	1377
I180N-H*	0	120	43	3572	1072	1026	3939	705
I180N-J	37	35	34	1464	1537	13	1539	1462
O180N-A	-48	107	111	4846	28	-44	4846	28
O180N-B	-75	29	41	1638	-1747	-158	1646	-1754
O180N-C	-59	-10	-6	-280	-1852	-57	-278	-1854
O180N-D	-32	-30	-27	-1207	-1332	-44	-1193	-1346
O180N-E	-10	-33	-37	-1535	-746	51	-743	-1538
O180N-F	28	-28	-27	-1232	472	-6	472	-1232
O180N-G*	0	48	-18	668	201	886	1351	-482
O180N-H	32	-19	-20	-912	682	13	682	-912
O180N-J	36	-17	-18	-802	829	6	829	-802

IN-PLANE FORCE LOADING, FYC, ON CYLINDER (2000 LB)

	MICRO-STRAIN			STRESSES			PRIN STRESSES	
ROSETTE	GAGE1	GAGE2	GAGE3	TRANS	LONG	SHEAR	SIGMX	SIGMN
I270C-A	358	-465	-433	-20140	4692	-424	4699	-20150
I270C-B	266	-410	-352	-17030	2873	-779	2904	-17060
I270C-C	154	-393	-306	-15550	-33	-1159	53	-15640
I270C-D	78	-368	-285	-14450	-1982	-1108	-1884	-14540
I270C-E	30	-356	-262	-13620	-3188	-1247	-3041	-13770
I270C-F	-23	-308	-201	-11170	-4036	-1431	-3759	-11450
I270C-G	-30	-226	-164	-8531	-3472	-823	-3341	-8661
I270C-H	-15	-174	-112	-6281	-2340	-829	-2173	-6448
I270C-J	13	-101	-40	-3116	-536	-804	-306	-3346
I270C-K	15	-73	8	-1458	19	-1076	586	-2025
I270C-L	5	-13	74	1227	525	-1216	2141	-390
I270C-M	-45	128	142	5982	440	-177	5987	435
O270C-A	-171	-536	-546	-23610	-12200	133	-12200	-23620
O270C-B*	0	0	-492	-10820	-3246	6559	541	-14610
O270C-C	-103	-363	-404	-16740	-8117	557	-8081	-16780
O270C-D	-24	-277	-329	-13280	-4711	696	-4654	-13340
O270C-E	17	-213	-273	-10700	-2712	791	-2634	-10780
O270C-F	87	-93	-182	-6143	766	1184	963	-6340
O270C-G	104	-25	-118	-3257	2131	1247	2405	-3532
O270C-H	96	-1	-95	-2215	2215	1254	2545	-2545
O270C-J	59	6	-83	-1746	1244	1184	1656	-2158
O270C-K	32	15	-71	-1278	586	1146	1131	-1823
O270C-L	-10	68	-22	1034	11	1203	1830	-785
I270N-A	372	-398	-381	-17540	5901	-228	5904	-17540
I270N-B	-28	-385	-321	-15490	-5474	-861	-5400	-15560
I270N-C	-274	-302	-209	-10940	-11510	-1241	-9948	-12490
I270N-D	-323	-205	-204	-8637	-12290	-19	-8637	-12290
I270N-E	-194	-119	-130	-5249	-7405	146	-5239	-7415
I270N-F	-73	-29	-19	-974	-2488	-120	-965	-2497
I270N-G	-39	-26	-19	-949	-1468	-82	-936	-1481
I270N-H	-43	-21	-17	-789	-1520	-51	-785	-1523
I270N-J	-27	-10	-10	-399	-918	6	-399	-918
O270N-A	-265	-601	-616	-26460	-15890	209	-15890	-26460
O270N-B	116	-308	-361	-14830	-971	696	-936	-14870
O270N-C	210	-86	-124	-4847	4847	507	4873	-4873
O270N-D	204	40	22	1144	6459	234	6469	1134
O270N-E*	98	90	85	3736	4057	76	4075	3719
O270N-F	-53	71	76	3286	-611	-70	3287	-612
O270N-G	-66	29	38	1535	-1521	-127	1540	-1526
O270N-H	-52	26	34	1363	-1159	-108	1368	-1164
O270N-J	-43	16	24	924	-1006	-114	931	-1012

IN-PLANE FORCE LOADING, FYC, ON CYLINDER (2000 LB)

	MICRO-STRAIN			STRESSES			PRIN STRESSES	
ROSETTE	GAGE1	GAGE2	GAGE3	TRANS	LONG	SHEAR	SIGMX	SIGMN
I300C-A	150	-287	-55	-7685	2199	-3090	3086	-8571
I300C-B	142	-324	43	-6329	2364	-4894	4563	-8528
I300C-C	136	-333	103	-5204	2516	-5799	5623	-8311
I300C-D	112	-329	136	-4373	2038	-6198	5811	-8146
I300C-E	82	-306	156	-3390	1435	-6154	5632	-7588
I300C-F	-12	-246	143	-2242	-1043	-5192	3583	-6869
I300C-G	-54	-211	95	-2510	-2378	-4077	1634	-6522
I300C-H	-61	-193	54	-2993	-2723	-3286	431	-6147
I300C-J	-86	-138	14	-2620	-3381	-2026	-939	-5062
I300C-K	-93	-86	1	-1747	-3304	-1159	-1129	-3921
I300C-L	-64	-11	11	60	-1907	-298	104	-1951
0300C-A	-62	-93	-298	-8538	-4415	2735	-3051	-9901
0300C-B	-96	-96	-334	-9346	-5684	3159	-3863	-11170
0300C-C	-139	-89	-360	-9717	-7078	3615	-4549	-12250
0300C-D	-134	-81	-367	-9712	-6934	3811	-4266	-12380
0300C-E	-128	-69	-373	-9582	-6724	4058	-3850	-12460
0300C-F	-122	-48	-345	-8503	-6215	3957	-3240	-11480
0300C-G	-95	-11	-290	-6518	-4792	3723	-1833	-9476
0300C-H	-85	31	-245	-4606	-3934	3685	-570	-7970
0300C-J	-63	74	-167	-1968	-2472	3210	1000	-5440
0300C-K	-47	91	-102	-178	-1465	2571	1828	-3471
0300C-L	-37	78	-19	1335	-697	1292	1962	-1324
I300N-A	86	-101	-170	-6048	766	924	889	-6171
I300N-B	-48	-64	-138	-4386	-2756	981	-2295	-4847
I300N-C	-88	-34	-96	-2755	-3464	829	-2207	-4011
I300N-D	-80	-14	-48	-1280	-2779	462	-1149	-2910
I300N-E	-41	0	-14	-268	-1307	177	-239	-1336
I300N-F	1	-7	17	218	108	-310	478	-152
I300N-G	3	-8	8	7	102	-209	269	-160
I300N-H	-1	-8	-1	-197	-88	-95	-33	-252
I300N-J	-2	-9	-7	-343	-160	-32	-155	-348
0300N-A	85	-98	-237	-7445	304	1849	722	-7864
0300N-B	136	-42	-115	-3606	2995	969	3135	-3745
0300N-C	121	-13	-32	-1115	3301	253	3315	-1129
0300N-D	82	1	13	234	2522	-158	2533	223
0300N-E	46	0	33	671	1570	-437	1747	493
0300N-F	7	-7	35	609	382	-564	1070	-79
0300N-G	5	-4	26	465	282	-399	783	-36
0300N-H	0	2	29	689	207	-355	877	19
0300N-J	0	7	29	784	221	-298	912	93

IN-PLANE FORCE LOADING, FYC, ON CYLINDER (2000 LB)

	MICRO-STRAIN			STRESSES			PRIN STRESSES	
ROSETTE	GAGE1	GAGE2	GAGE3	TRANS	LONG	SHEAR	SIGMX	SIGMN
I330C-A	-3	67	8	1653	410	785	2033	31
I330C-B	26	25	10	744	1007	190	1107	645
I330C-C	36	-7	17	170	1120	-317	1216	74
I330C-D	32	-30	23	-182	915	-709	1263	-530
I330C-E	15	-49	29	-476	299	-1038	1020	-1197
I330C-F	-38	-70	52	-355	-1247	-1633	892	-2494
I330C-G	-69	-66	78	337	-1980	-1919	1420	-3063
I330C-H	-83	-63	91	697	-2272	-2051	1744	-3319
I330C-J	-96	-40	107	1588	-2389	-1963	2393	-3195
I330C-K	-106	-19	98	1840	-2641	-1564	2332	-3133
I330C-L	-109	-1	72	1676	-2762	-981	1883	-2969
0330C-A	-21	115	-40	1663	-129	2070	3023	-1489
0330C-B	-38	84	-78	167	-1076	2165	1798	-2708
0330C-C	-57	62	-107	-929	-2004	2248	845	-3777
0330C-D	-52	47	-123	-1603	-2049	2260	445	-4097
0330C-E	-49	34	-128	-2025	-2076	2159	109	-4209
0330C-F	-51	10	-150	-3014	-2444	2140	-570	-4888
0330C-G	-64	0	-140	-2990	-2821	1868	-1036	-4775
0330C-H	-79	-7	-133	-3005	-3268	1684	-1447	-4826
0330C-J	-108	-15	-126	-2983	-4131	1488	-1963	-5152
0330C-K	-116	-23	-120	-3016	-4383	1298	-2233	-5167
0330C-L	-117	-8	-81	-1824	-4068	969	-1464	-4429
I330N-A*	-11	70	75	3187	628	-63	3189	627
I330N-B	29	81	62	3102	1786	253	3149	1739
I330N-C	49	78	50	2766	2312	367	2970	2107
I330N-D	51	64	41	2252	2215	310	2544	1923
I330N-E	45	49	35	1799	1880	196	2040	1639
I330N-F	32	20	18	810	1213	32	1215	808
I330N-G	25	18	26	923	1018	-108	1088	853
I330N-H	28	16	22	805	1068	-76	1089	785
I330N-J	24	10	16	538	874	-89	896	516
0330N-A	0	133	-2	2883	865	1811	3946	-199
0330N-B	5	50	-19	674	345	931	1454	-436
0330N-C	-3	20	-27	-133	-125	627	498	-756
0330N-D	2	1	-29	-618	-129	399	95	-841
0330N-E	10	-10	-30	-878	50	272	124	-952
0330N-F	23	-12	-26	-861	440	190	467	-888
0330N-G	28	-7	-12	-449	707	76	712	-454
0330N-H	27	-5	-5	-260	735	0	735	-260
0330N-J	24	-2	-1	-110	694	-13	694	-110

A.13 Out-of-Plane Force, F_{ZC}, on Cylinder

OUT-OF-PLANE FORCE LOADING, FZC, ON CYLINDER (1200 LB)

	MICRO-STRAIN			STRESSES			PRIN STRESSES	
ROSETTE	GAGE1	GAGE2	GAGE3	TRANS	LONG	SHEAR	SIGMX	SIGMN
I-O-C-A	2	-12	6	-138	16	-234	185	-308
I-O-C-B	-4	-25	21	-79	-138	-621	513	-730
I-O-C-C	-7	-29	26	-76	-223	-734	589	-887
I-O-C-D	-7	-33	30	-55	-230	-848	710	-996
I-O-C-E*	-19	-33	32	11	-581	-867	631	-1202
I-O-C-F	0	-34	29	-104	-31	-848	781	-917
I-O-C-G	0	-33	28	-115	-34	-817	743	-892
I-O-C-H	0	-31	28	-73	-22	-791	744	-839
I-O-C-J	-7	-31	29	-34	-210	-798	680	-925
I-O-C-K	-4	-31	28	-69	-135	-791	690	-894
I-O-C-L	1	-31	24	-158	-19	-741	656	-832
O-O-C-A	0	27	-39	-283	-71	880	710	-1063
O-O-C-B	0	27	-31	-105	-17	772	713	-835
O-O-C-C	2	29	-30	-13	67	791	820	-765
O-O-C-D	1	31	-32	-22	22	848	849	-849
O-O-C-E	-2	32	-35	-61	-75	899	831	-967
O-O-C-F	0	34	-38	-83	-39	962	902	-1024
O-O-C-G	-2	32	-41	-196	-116	981	826	-1138
O-O-C-H	-6	31	-37	-109	-204	905	751	-1063
O-O-C-J	-5	27	-33	-131	-182	804	648	-961
O-O-C-K*	0	29	0	638	177	386	857	-42
O-O-C-L	-11	28	-28	12	-324	747	610	-922
I-O-N-A	-1	0	-1	-30	-38	6	-27	-41
I-O-N-B	-1	6	-8	-51	-58	184	129	-238
I-O-N-C	-2	7	-10	-50	-86	222	155	-290
I-O-N-D	-4	5	-9	-90	-141	184	70	-301
I-O-N-E	-4	0	-7	-152	-174	95	-67	-259
I-O-N-F*	0	0	-65	-1430	-443	867	61	-1935
I-O-N-G	-1	1	1	54	-27	6	54	-27
I-O-N-H	2	1	3	92	85	-19	108	69
I-O-N-J	-1	-1	1	12	-39	-32	27	-54
O-O-N-A	-10	9	-32	-501	-450	551	76	-1027
O-O-N-B	-8	2	-26	-503	-393	374	-71	-826
O-O-N-C	-10	-3	-20	-490	-447	228	-239	-697
O-O-N-D	-11	-7	-14	-458	-465	95	-367	-557
O-O-N-E	-11	-9	-10	-416	-453	19	-408	-461
O-O-N-F	-10	-12	-8	-428	-414	-63	-357	-485
O-O-N-G	-9	-12	-8	-429	-400	-63	-349	-479
O-O-N-H	-11	-13	-10	-500	-478	-44	-443	-534
O-O-N-J	-10	-12	-5	-366	-395	-89	-290	-470

OUT-OF-PLANE FORCE LOADING. FZC. ON CYLINDER (1200 LB)

	MICRO-STRAIN			STRESSES			PRIN STRESSES	
ROSETTE	GAGE1	GAGE2	GAGE3	TRANS	LONG	SHEAR	SIGMX	SIGMN
I-90C-A	-61	157	5	3629	-750	2032	4427	-1548
I-90C-B	-59	170	-10	3574	-710	2406	4654	-1789
I-90C-C	-45	182	-41	3151	-395	2969	4836	-2080
I-90C-D	-37	179	-38	3143	-169	2881	4809	-1836
I-90C-E	-29	167	-34	2966	34	2678	4553	-1553
I-90C-F	-26	128	-6	2723	47	1785	3616	-846
I-90C-G	-19	90	28	2601	210	829	2860	-50
I-90C-H	-19	60	55	2559	183	70	2561	181
I-90C-J	-19	59	66	2758	243	-89	2761	240
I-90C-K	-19	67	65	2925	293	38	2925	292
I-90C-L	-24	64	69	2940	169	-70	2942	167
O-90C-A	25	47	119	3618	1827	-969	4041	1403
O-90C-B	23	40	110	3264	1678	-931	3694	1248
O-90C-C	19	15	119	2935	1437	-1387	3762	610
O-90C-D	9	1	122	2696	1065	-1602	3678	83
O-90C-E	0	-6	123	2579	788	-1716	3619	-252
O-90C-F	-7	-32	127	2097	415	-2127	3543	-1032
O-90C-G	-30	-16	121	2352	-207	-1823	3300	-1155
O-90C-H	-33	-5	104	2209	-335	-1469	2880	-1006
O-90C-J	-33	29	78	2407	-276	-652	2557	-426
O-90C-K	-36	51	67	2630	-295	-215	2646	-310
O-90C-L*	-36	63	0	1429	-655	842	1726	-953
I-90N-A	-12	92	36	2322	490	753	3045	268
I-90N-B	28	49	60	2361	1535	-146	2386	1510
I-90N-C	45	21	58	1695	1863	-500	2286	1271
I-90N-D	39	5	47	1085	1509	-557	1893	701
I-90N-E	23	-2	30	602	865	-431	1183	283
I-90N-F	10	-2	7	93	327	-114	374	47
I-90N-G	3	-4	2	-45	72	-76	110	-82
I-90N-H	4	1	2	58	146	-13	148	56
I-90N-J	1	-2	0	-54	27	-32	38	-65
O-90N-A	23	39	142	3954	1885	-1361	4629	1209
O-90N-B	-16	0	86	1928	108	-1146	2482	-445
O-90N-C	-24	-12	40	632	-537	-696	957	-862
O-90N-D	-17	-11	4	-138	-555	-209	-51	-641
O-90N-E	-4	-5	-14	-403	-249	120	-183	-469
O-90N-F	16	11	-19	-174	432	399	630	-372
O-90N-G	14	13	-10	58	431	298	596	-107
O-90N-H	12	11	-8	50	371	253	510	-90
O-90N-J	10	11	-4	145	357	209	486	17

OUT-OF-PLANE FORCE LOADING. FZC, ON CYLINDER (1200 LB)

	MICRO-STRAIN			STRESSES			PRIN STRESSES	
ROSETTE	GAGE1	GAGE2	GAGE3	TRANS	LONG	SHEAR	SIGMX	SIGMN
I120C-A	51	-52	-115	-3743	403	842	567	-3907
I120C-B	2	-37	-109	-3219	-895	962	-548	-3566
I120C-C	-41	-12	-116	-2775	-2059	1380	-991	-3843
I120C-D	-62	4	-118	-2438	-2599	1621	-896	-4141
I120C-E	-65	15	-110	-2017	-2558	1659	-607	-3968
I120C-F*	-22	41	-87	-989	-967	1716	738	-2693
I120C-G	-26	57	-70	-254	-846	1690	1166	-2266
I120C-H	8	81	-52	629	417	1766	2292	-1247
I120C-J	30	102	-29	1575	1371	1747	3224	-277
I120C-K	38	110	-8	2203	1816	1564	3585	434
I120C-L	37	129	16	3145	2055	1501	4196	1004
O120C-A	-35	-179	-75	-5549	-2706	-1387	-2141	-6114
O120C-B	15	-122	-27	-3275	-526	-1266	-32	-3770
O120C-C	44	-88	16	-1625	824	-1387	1449	-2250
O120C-D	62	-56	49	-225	1786	-1399	2504	-942
O120C-E	69	-25	77	1052	2383	-1355	3227	208
O120C-F	72	12	111	2626	2940	-1323	4116	1451
O120C-G	54	31	124	3366	2635	-1241	4294	1707
O120C-H	41	29	123	3307	2232	-1247	4128	1412
O120C-J	21	3	119	2650	1437	-1545	3703	384
O120C-K	17	-17	116	2154	1145	-1773	3493	-194
O120C-L	-2	-22	118	2101	573	-1868	3355	-681
I120N-A	87	-13	-137	-3407	1601	1652	2097	-3903
I120N-B	-24	-64	-121	-4036	-1938	766	-1688	-4286
I120N-C	-79	-81	-88	-3641	-3473	95	-3430	-3684
I120N-D	-90	-72	-57	-2742	-3531	-203	-2693	-3580
I120N-E	-83	-52	-36	-1952	-3036	-215	-1814	-3074
I120N-F	-45	-22	-15	-765	-1584	-89	-756	-1593
I120N-G*	0	-89	-19	-2371	-711	-943	-285	-2797
I120N-H	-29	-6	-1	-125	-907	-70	-119	-913
I120N-J	-26	-3	-2	-87	-796	-6	-87	-796
O120N-A	-128	-164	-105	-5792	-5572	-785	-4889	-6475
O120N-B	-15	-109	-39	-3231	-1426	-931	-1032	-3625
O120N-C	22	-43	10	-745	447	-703	772	-1071
O120N-D	22	-2	33	665	855	-469	1238	282
O120N-E	12	22	41	1365	780	-253	1459	686
O120N-F	-24	34	26	1332	-313	108	1339	-320
O120N-G	-29	16	12	648	-661	44	649	-663
O120N-H	-30	12	10	524	-741	32	525	-742
O120N-J	-24	9	4	309	-635	70	314	-640

OUT-OF-PLANE FORCE LOADING, FZC, ON CYLINDER (1200 LB)

	MICRO-STRAIN			STRESSES			PRIN STRESSES	
ROSETTE	GAGE1	GAGE2	GAGE3	TRANS	LONG	SHEAR	SIGMX	SIGMN
I150C-A	77	-124	-60	-4126	1072	-855	1208	-4263
I150C-B	31	-120	-29	-3313	-67	-1216	337	-3718
I150C-C	3	-108	0	-2385	-616	-1444	193	-3193
I150C-D	-18	-93	7	-1861	-1086	-1330	-88	-2858
I150C-E*	0	-81	13	-1493	-448	-1260	393	-2335
I150C-F	-9	-44	17	-586	-432	-804	299	-1317
I150C-G	10	-11	10	-21	279	-285	451	-193
I150C-H	23	3	-2	-4	683	76	691	-12
I150C-J	28	4	-27	-543	678	412	804	-668
I150C-K*	39	-34	-57	-2027	561	304	596	-2062
I150C-L	63	48	-47	-49	1881	1254	2498	-666
O150C-A	-37	-126	-151	-6049	-2912	336	-2877	-6084
O150C-B	-7	-97	-94	-4201	-1474	-44	-1473	-4202
O150C-C	6	-67	-76	-3140	-757	114	-751	-3145
O150C-D*	17	0	-61	-1356	107	810	467	-1716
O150C-E	20	-32	-50	-1829	64	234	93	-1858
O150C-F	25	3	-20	-403	620	317	710	-493
O150C-G	21	8	-9	-44	628	215	691	-107
O150C-H	28	6	4	178	895	25	895	177
O150C-J	47	1	23	471	1552	-291	1626	397
O150C-K	64	2	42	891	2178	-532	2369	700
O150C-L	86	-4	63	1200	2955	-886	3324	830
I150N-A	45	-62	-110	-3830	191	646	292	-3931
I150N-B	-38	-56	-91	-3186	-2082	475	-1906	-3362
I150N-C	-68	-49	-66	-2452	-2789	228	-2337	-2904
I150N-D	-67	-37	-44	-1701	-2535	101	-1689	-2547
I150N-E	-56	-28	-27	-1140	-2010	-6	-1140	-2010
I150N-F	-29	-18	0	-365	-979	-241	-282	-1062
I150N-G	-24	-16	-16	-663	-912	0	-663	-912
I150N-H	-25	-15	-14	-610	-924	-19	-609	-925
I150N-J	-24	-10	-10	-433	-843	0	-433	-843
O150N-A	-14	-102	-106	-4549	-1778	57	-1777	-4550
O150N-B	29	-57	-41	-2173	218	-209	236	-2191
O150N-C	38	-21	3	-439	1023	-317	1089	-505
O150N-D	25	2	24	558	909	-291	1073	393
O150N-E	10	11	33	950	570	-291	1108	413
O150N-F	-17	19	35	1188	-143	-215	1222	-177
O150N-G	-21	10	21	702	-431	-146	721	-449
O150N-H	-21	9	19	629	-439	-139	647	-457
O150N-J	-20	9	15	545	-450	-89	553	-458

OUT-OF-PLANE FORCE LOADING, FZC, ON CYLINDER (1200 LB)

	MICRO-STRAIN			STRESSES			PRIN STRESSES	
ROSETTE	GAGE1	GAGE2	GAGE3	TRANS	LONG	SHEAR	SIGMX	SIGMN
I180C-A	3	-17	13	-87	60	-405	398	-425
I180C-B	0	-32	31	-31	-9	-842	822	-863
I180C-C	-2	-40	44	76	-49	-1121	1136	-1109
I180C-D	-2	-46	46	3	-71	-1216	1182	-1250
I180C-E	-1	-46	46	11	-25	-1222	1215	-1229
I180C-F	0	-41	42	21	6	-1102	1115	-1088
I180C-G*	-10	-48	38	-209	-348	-1146	870	-1426
I180C-H	4	-32	38	111	147	-931	1060	-802
I180C-J	3	-34	35	7	88	-918	966	-871
I180C-K	2	-41	31	-212	8	-962	867	-1070
I180C-L	-2	-30	32	34	-61	-829	817	-844
O180C-A	-1	46	-57	-260	-107	1374	1193	-1559
O180C-B	-1	48	-60	-250	-103	1444	1269	-1622
O180C-C	0	56	-63	-157	-47	1576	1476	-1679
O180C-D	3	59	-66	-139	44	1665	1620	-1715
O180C-E	0	62	-65	-62	-33	1684	1637	-1732
O180C-F	-2	59	-61	-39	-83	1608	1547	-1669
O180C-G	6	48	-60	-267	91	1450	1373	-1549
O180C-H	0	44	-52	-177	-67	1273	1152	-1396
O180C-J	0	33	-45	-261	-78	1045	879	-1218
O180C-K	0	26	-42	-355	-107	912	689	-1151
O180C-L	-5	24	-36	-266	-237	798	547	-1049
I180N-A	-2	-7	-8	-332	-157	13	-156	-333
I180N-B	-6	2	-15	-276	-254	222	-43	-487
I180N-C	-5	4	-13	-193	-201	234	37	-431
I180N-D	-5	4	-10	-120	-193	177	25	-337
I180N-E	-7	1	-5	-76	-223	89	-34	-264
I180N-F*	0	-22	1	-460	-138	-317	56	-654
I180N-G	0	-2	1	-20	-20	-38	18	-58
I180N-H*	0	-77	-1	-1734	-520	-1013	54	-2308
I180N-J	-2	-1	-1	-50	-72	-6	-48	-74
O180N-A	-6	32	-38	-140	-213	937	761	-1114
O180N-B	-5	20	-25	-99	-186	595	454	-739
O180N-C	-5	7	-15	-162	-191	291	115	-468
O180N-D	-4	-1	-8	-194	-172	95	-88	-279
O180N-E	-5	-8	-5	-277	-226	-44	-200	-302
O180N-F	-5	-11	0	-235	-227	-146	-85	-377
O180N-G*	0	-63	0	-1399	-420	-836	59	-1878
O180N-H	-4	-10	0	-204	-190	-139	-57	-336
O180N-J	-5	-11	3	-162	-191	-190	14	-367

OUT-OF-PLANE FORCE LOADING, FZC, ON CYLINDER (1200 LB)

	MICRO-STRAIN			STRESSES			PRIN STRESSES	
ROSETTE	GAGE1	GAGE2	GAGE3	TRANS	LONG	SHEAR	SIGMX	SIGMN
I270C-A	36	30	-173	-3183	129	2716	1654	-4709
I270C-B	28	66	-185	-2642	49	3343	2307	-4900
I270C-C	25	71	-186	-2565	-28	3425	2356	-4949
I270C-D	18	68	-174	-2348	-177	3223	2138	-4663
I270C-E	19	54	-163	-2424	-143	2887	1821	-4387
I270C-F	31	20	-126	-2374	229	1950	1272	-3417
I270C-G	31	-15	-82	-2165	291	886	578	-2451
I270C-H	34	-46	-61	-2377	299	203	315	-2392
I270C-J	33	-57	-61	-2637	207	44	208	-2638
I270C-K	32	-62	-66	-2834	119	51	120	-2835
I270C-L	37	-67	-68	-3017	193	19	193	-3017
I270C-M	3	-24	33	205	161	-760	943	-577
0270C-A	-9	-98	-43	-3092	-1184	-741	-931	-3346
0270C-B*	0	0	-17	-376	-113	228	19	-508
0270C-C	-10	-124	3	-2642	-1078	-1697	8	-3728
0270C-D	7	-116	19	-2148	-445	-1804	699	-3292
0270C-E	6	-120	28	-2022	-436	-1969	894	-3352
0270C-F	14	-130	37	-2052	-188	-2222	1290	-3530
0270C-G	23	-127	26	-2239	13	-2039	1216	-3442
0270C-H	27	-115	1	-2536	38	-1557	771	-3269
0270C-J	34	-89	-40	-2888	146	-652	280	-3023
0270C-K	35	-81	-63	-3193	97	-241	115	-3210
0270C-L	31	-67	-82	-3324	-56	196	-45	-3336
I270N-A	-1	-17	-106	-2693	-851	1190	-267	-3277
I270N-B	-32	-50	-49	-2158	-1617	-13	-1616	-2158
I270N-C	-40	-56	-12	-1450	-1632	-576	-958	-2124
I270N-D	-33	-47	1	-967	-1274	-646	-456	-1784
I270N-E	-20	-35	3	-667	-799	-507	-222	-1244
I270N-F	-4	-10	-7	-351	-219	-38	-209	-361
I270N-G	-5	-4	-9	-277	-226	57	-189	-314
I270N-H	-4	-3	-4	-163	-163	13	-150	-176
I270N-J	-5	-3	-1	-89	-169	-19	-85	-174
0270N-A	18	-104	-2	-2359	-180	-1368	479	-3018
0270N-B	44	-60	29	-727	1093	-1197	1687	-1320
0270N-C	39	-21	35	250	1244	-747	1644	-151
0270N-D	31	6	29	738	1162	-304	1321	580
0270N-E	17	23	15	817	744	114	900	661
0270N-F	-1	30	-1	638	163	424	887	-86
0270N-G	0	21	-4	366	96	336	593	-131
0270N-H	0	17	-3	303	91	272	489	-95
0270N-J	0	13	-4	208	77	228	380	-95

OUT-OF-PLANE FORCE LOADING, FZC, ON CYLINDER (1200 LB)

	MICRO-STRAIN			STRESSES			PRIN STRESSES	
ROSETTE	GAGE1	GAGE2	GAGE3	TRANS	LONG	SHEAR	SIGMX	SIGMN
I300C-A	97	-147	-122	-6029	1114	-336	1130	-6044
I300C-B	52	-134	-122	-5697	-155	-165	-150	-5702
I300C-C	7	-124	-94	-4802	-1227	-399	-1183	-4846
I300C-D	-19	-121	-88	-4574	-1943	-431	-1874	-4643
I300C-E	-36	-112	-88	-4358	-2377	-323	-2325	-4409
I300C-F	-38	-86	-67	-3321	-2137	-266	-2080	-3378
I300C-G	-15	-71	-61	-2887	-1322	-139	-1310	-2899
I300C-H	4	-65	-55	-2636	-677	-139	-667	-2646
I300C-J	19	-67	-33	-2235	-100	-456	-7	-2328
I300C-K	12	-79	-9	-1945	-227	-931	180	-2353
I300C-L	-2	-83	8	-1648	-566	-1216	224	-2437
O300C-A	-54	-165	-165	-7209	-3788	0	-3788	-7209
O300C-B	-29	-142	-136	-6077	-2707	-70	-2706	-6079
O300C-C	-10	-105	-109	-4700	-1695	57	-1694	-4701
O300C-D	17	-72	-89	-3570	-558	228	-541	-3587
O300C-E	35	-51	-71	-2722	224	272	249	-2747
O300C-F	38	-9	-45	-1211	777	481	887	-1322
O300C-G	32	10	-37	-620	783	621	1018	-855
O300C-H	21	6	-45	-879	363	684	666	-1182
O300C-J	13	-16	-60	-1696	-124	589	72	-1892
O300C-K	5	-24	-77	-2220	-509	696	-262	-2468
O300C-L	-7	-18	-86	-2259	-877	905	-429	-2707
I300N-A	88	-26	-178	-4567	1281	2026	1915	-5200
I300N-B	-35	-68	-140	-4525	-2413	956	-2044	-4894
I300N-C	-86	-78	-103	-3874	-3757	329	-3481	-4150
I300N-D	-98	-70	-65	-2848	-3791	-70	-2843	-3796
I300N-E	-75	-50	-35	-1787	-2774	-209	-1745	-2817
I300N-F	-31	-20	-5	-519	-1097	-196	-459	-1157
I300N-G	-25	-11	-11	-453	-877	0	-453	-877
I300N-H	-26	-9	-9	-368	-895	0	-368	-895
I300N-J	-22	-5	-6	-205	-732	13	-205	-732
O300N-A	-62	-162	-154	-6888	-3920	-101	-3916	-6891
O300N-B	21	-104	-63	-3689	-479	-538	-392	-3777
O300N-C	43	-50	-1	-1165	948	-652	1133	-1350
O300N-D	33	-11	25	256	1075	-481	1297	34
O300N-E	19	7	36	919	846	-393	1277	488
O300N-F	-18	21	29	1116	-207	-108	1125	-216
O300N-G	-28	11	15	605	-645	-44	606	-647
O300N-H*	0	12	10	480	144	25	482	142
O300N-J	-20	9	8	377	-486	13	377	-486

OUT-OF-PLANE FORCE LOADING. FZC, ON CYLINDER (1200 LB)

	MICRO-STRAIN			STRESSES			PRIN STRESSES	
ROSETTE	GAGE1	GAGE2	GAGE3	TRANS	LONG	SHEAR	SIGMX	SIGMN
I330C-A	60	-103	-29	-2970	920	-988	1156	-3206
I330C-B	30	-104	-7	-2477	155	-1292	683	-3005
I330C-C	3	-104	6	-2155	-547	-1456	313	-3014
I330C-D	-13	-98	13	-1855	-956	-1488	149	-2960
I330C-E	-24	-90	18	-1571	-1198	-1437	64	-2834
I330C-F	-34	-64	25	-819	-1272	-1190	166	-2257
I330C-G	-27	-52	27	-513	-967	-1051	335	-1815
I330C-H	-20	-53	19	-730	-818	-950	177	-1725
I330C-J	-19	-51	11	-856	-841	-836	-13	-1684
I330C-K	-24	-51	8	-924	-990	-791	-165	-1749
I330C-L	-25	-54	7	-996	-1054	-810	-214	-1836
0330C-A	-40	-61	-111	-3737	-2319	671	-2051	-4004
0330C-B	-18	-44	-105	-3260	-1520	823	-1192	-3587
0330C-C	-12	-29	-98	-2775	-1189	919	-769	-3196
0330C-D	-4	-17	-88	-2303	-819	956	-351	-2772
0330C-E	-2	-9	-77	-1867	-631	905	-153	-2345
0330C-F	-7	6	-70	-1403	-620	1007	69	-2091
0330C-G	-17	18	-62	-953	-785	1070	204	-1942
0330C-H	-18	17	-60	-941	-824	1026	145	-1910
0330C-J	-13	19	-58	-848	-782	1032	218	-1847
0330C-K	-21	9	-64	-1178	-931	969	-106	-2053
0330C-L	-25	13	-60	-996	-1040	975	-43	-1994
I330N-A*	44	-29	-83	-2513	558	722	719	-2674
I330N-B	-18	-38	-72	-2403	-1263	456	-1103	-2563
I330N-C	-46	-33	-51	-1809	-1911	241	-1614	-2106
I330N-D	-47	-25	-33	-1223	-1764	101	-1205	-1782
I330N-E	-41	-18	-20	-791	-1463	25	-790	-1464
I330N-F	-21	-10	-3	-269	-722	-89	-252	-739
I330N-G	-15	-9	-6	-308	-534	-32	-303	-539
I330N-H	-16	-10	-8	-369	-595	-19	-367	-597
I330N-J	-17	-6	-9	-315	-608	38	-311	-613
0330N-A	0	-101	-104	-4512	-1354	51	-1353	-4513
0330N-B	14	-51	-50	-2240	-259	-19	-258	-2240
0330N-C	22	-31	-20	-1152	310	-139	323	-1165
0330N-D	14	-15	-5	-454	291	-139	317	-480
0330N-E*	5	-7	8	5	158	-196	292	-129
0330N-F	-14	-2	11	225	-360	-177	274	-410
0330N-G	-20	-6	3	-51	-628	-120	-27	-652
0330N-H	-19	-1	5	115	-536	-82	125	-546
0330N-J	-19	-2	6	94	-542	-108	112	-560

ORNL-4553
UC-80 – Reactor Technology

Internal Distribution

1. S. E. Beall
2. H. W. Behrman
3. M. Bender
4. J. P. Blakely
5. R. Blanco
6-8. S. E. Bolt
9. R. H. Bryan
10. J. W. Bryson
11. J. R. Buchanan
12. J. P. Callahan
13. D. W. Cardwell
14. H. P. Carter
15. S. J. Chang
16. R. D. Cheverton
17. C. E. Childress
18. C. J. Claffey
19. C. W. Collins
20-34. J. M. Corum
35. W. B. Cottrell
36. J. S. Crowell
37. F. L. Culler
38. W. G. Dodge
39. D. E. Ferguson
40. M. H. Fontana
41. A. P. Fraas
42. W. R. Gall
43. D. L. Gray
44-46. W. L. Greenstreet
47. A. G. Grindell
48-50. R. C. Gwaltney
51. W. O. Harms
52. P. N. Haubenreich
53. R. F. Hibbs (Y-12)
54. H. W. Hoffman
55. P. R. Kasten
56. K. C. Liu
57. M. I. Lundin
58. R. N. Lyon
59. R. E. MacPherson
60. W. R. Martin
61. W. J. McAfee
62. H. E. McCoy
63. H. C. McCurdy
64. J. G. Merkle
65. A. J. Miller
66. S. E. Moore
67. H. A. Nelms
68. Paul Nelson
69. R. B. Parker
70. A. M. Perry
71. T. W. Pickel
72. C. E. Pugh
73. M. Richardson
74. P. L. Rittenhouse
75. G. C. Robinson
76. O. A. Rogers (Y-12)
77. M. W. Rosenthal
78. G. Samuels
79. W. K. Sartory
80. R. A. Schmidt
81. M. R. Sheldon
82. J. E. Smith
83. I. Spiewak
84. D. A. Sundberg
85. R. W. Swindeman
86. D. B. Trauger
87. R. S. Valachovic
88. R. D. Waddell, Jr.
89. A. M. Weinberg
90. J. R. Weir
91. G. D. Whitman
92. F. J. Witt
93. G. T. Yahr
94. H. C. Young
95. ORNL Patent Office
96-98. Central Research Library
99. Y-12 Document Reference Section
100-125. Laboratory Records
126. Laboratory Records (RC)

External Distribution

127. R. W. Aderholdt, Auburn University, Auburn, Ala.
128. D. W. Allwein, Annapolis Division, Naval Ship Research and Development Center, Annapolis, Md.

129. L. E. Alsager, USAEC, Washington, D.C.
130. R. L. Anderson, Pennsylvania Power and Light Co., Allentown, Pa.
131. W. F. Anderson, Liquid Metal Engineering Center, Canoga Park, Calif.
132. J. S. V. Andrews, British Embassy, Washington, D.C.
133. H. L. Arnold, RDT, USAEC, Washington, D.C.
134. C. V. Backlund, USAEC, Berkeley, Calif.
135. J. F. Bailey, University of Tennessee, Knoxville, Tenn.
136. N. Balai, Argonne National Laboratory, Argonne, Ill.
137. R. E. Ball, Byron Jackson Pump, Inc., Los Angeles, Calif.
138. R. H. Ball, Gulf General Atomic, Inc., San Diego, Calif.
139. R. A. Barnes, General Electric Co., KAPL, Schenectady, N.Y.
140. D. L. Becker, Westinghouse Hanford Co., Richland, Wash.
141. R. E. Benson, Tube Turns Corp., Chemetron Division, Louisville, Ky.
142. D. J. Bergman, Winnetka, Ill.
143. I. Berman, Foster Wheeler Corp., Livingston, N.J.
144. M. D. Bernstein, Foster Wheeler Corp., Livingston, N.J.
145. T. N. Bernstein, Air Force Flight Dynamics Laboratory, AFFDL (FDTR), Wright-Patterson AFB, Ohio
146. C. C. Bigelow, USAEC, Washington, D.C.
147-148. C. W. Bills, Idaho Operations Office, AEC, Idaho Falls, Idaho
149. E. C. Bishop, Westinghouse Electric Corp., ARD, Madison, Pa.
150. L. D. Blackburn, Westinghouse Hanford Co., Richland, Wash.
151. N. Blair, Holmes and Narver, Inc., Anaheim, Calif.
152. F. J. Bogden, Westinghouse Electric Corp., Cheswick, Pa.
153. M. Bolotsky, Division of Reactor Standards, USAEC, Washington, D.C.
154. M. Booth, USAEC, Washington, D.C.
155. T. Branca, Teledyne Materials Research Co., Waltham, Mass.
156. E. B. Branch, Sargent and Lundy, Chicago, Ill.
157. H. F. Brannon, Yankee Atomic Electric Co., Boston, Mass.
158. A. P. Bray, General Electric Co., San Jose, Calif.
159. G. O. Bright, Idaho Nuclear Corp., Idaho Falls, Idaho
160. C. R. Brinkman, Aerojet Nuclear Co., Idaho Falls, Idaho
161. W. E. Bristow, Monsanto Co., St. Louis, Mo.
162. George Brockett, Idaho Nuclear Corp., Idaho Falls, Idaho
163. J. E. Brock, U.S. Naval Postgraduate School, Monterey, Calif.
164-165. R. S. Brodsky, Division of Naval Reactors, USAEC, Washington, D.C.
166. Harry Brown, Idaho Nuclear Corp., Idaho Falls, Idaho
167. G. Burley, Division of Reactor Licensing, USAEC, Washington, D.C.
168. J. P. Burn, Westinghouse Hanford Co., Richland, Wash.
169. S. H. Bush, Battelle-Northwest Laboratory, Richland, Wash.
170. D. R. Campbell, Liquid Metal Engineering Center, Canoga Park, Calif.
171-172. W. Carbiener, Battelle Memorial Institute, Columbus, Ohio
173. M. W. Carbon, University of Wisconsin, Madison, Wis.
174. A. E. Carden, University of Connecticut, Storrs, Conn.
175. L. H. Carr, San Luis Obispo, Calif.
176-177. E. G. Case, Director, Division of Reactor Standards, USAEC, Washington, D.C.
178. J. A. Casner, Youngstown Sheet and Tube Co., Youngstown, Ohio
179. A. K. Chakraborty, General Electric Co., San Jose, Calif.
180. J. R. Chamberlain, Borg-Warner Corp., York, Pa.

181. S. K. Chan, Westinghouse Research Laboratory, Pittsburgh, Pa.
182. T. Y. Chang, The University of Akron, Akron, Ohio
183. C. H. Chen, Auburn University, Auburn, Ala.
184. F. L. Cho, Sargent and Lundy, Chicago, Ill.
185. D. C. Church, General Dynamics Corp., Electric Boat Division, Groton, Conn.
186. J. R. Clapp, Burns and Roe, Inc., Hempstead, N.Y.
187. T. T. Claudson, Westinghouse Hanford Co., Richland, Wash.
188. F. J. Climent, Aerojet General Corp., Sacramento, Calif.
189. R. L. Cloud, Westinghouse Electric Corp., Pittsburgh, Pa.
190. R. W. Clough, University of California, Berkeley, Calif.
191. W. S. Clouser, Los Alamos Scientific Laboratory, Los Alamos, N.M.
192. R. H. Clute, Interprovincial Pipe Line Co., Edmonton, Alberta, Canada
193. J. C. Cochran, Liquid Metal Engineering Center, Canoga Park, Calif.
194. Combustion Engineering, Inc., Chattanooga, Tenn., Attention: Librarian MR & D
195. J. B. Conway, Mar-Test, Inc., Cincinnati, Ohio
196. John Conway, Naval Ships Engineering Center, Code 6154I, Hyattsville, Md.
197. W. E. Cooper, Teledyne Materials Research Co., Waltham, Mass.
198. L. M. Corcoran, MPR Associates, Inc., Washington, D.C.
199. J. E. Corr, General Electric Co., San Jose, Calif.
200. H. T. Corten, University of Illinois, Urbana, Ill.
201. J. Grady Cox, Auburn University, Auburn, Ala.
202. J. W. Crawford, RDT, USAEC, Washington, D.C.
203. A. W. Crittenden, Niagara Mohawk Power Corp., Buffalo, N.Y.
204. G. W. Cunningham, RDT, USAEC, Washington, D.C.
205. S. A. Davis, Argonne National Laboratory, Argonne, Ill.
206. A. J. Del Buono, Taylor Forge and Pipe Works, Chicago, Ill.
207. R. F. Detman, C. F. Braun and Co., Alhambra, Calif.
208. G. S. Dhaliwal, Valcor Engineering Corp., Kenilworth, N.J.
209. R. W. Dickinson, Liquid Metal Engineering Center, Canoga Park, Calif.
210. Paul Dimitroff, Atomic Energy of Canada, Ltd., Sheridan Park, Ontario, Canada
211. R. J. Dohrmann, Babcock and Wilcox Co., Alliance, Ohio
212. H. W. Dolfi, Combustion Engineering, Inc., Chattanooga, Tenn.
213. W. L. Dornaus, Bechtel Corp., San Francisco, Calif.
214. W. D. Doty, U.S. Steel Corp., Monroeville, Pa.
215. J. J. Droher, Liquid Metal Engineering Center, Canoga Park, Calif.
216. A. R. Duffy, Battelle Memorial Institute, Columbus, Ohio
217. J. M. Duke, Westinghouse Electric Corp., Tampa, Fla.
218. F. W. Dunham, David Taylor Model Basin, Code 703.1, Washington, D.C.
219. A. J. Durelli, The Catholic University of America, Washington, D.C.
220. A. F. Eckert, Babcock and Wilcox Co., Lynchburg, Va.
221. A. J. Edmondson, University of Tennessee, Knoxville, Tenn.
222. G. R. Edwards, Pittsburgh Des Moines Steel Co., Pittsburgh, Pa.
223. R. W. Elkins, Byron Jackson Pump, Inc., Los Angeles, Calif.
224. F. E. Ellyin, University of Sherbrooke, Sherbrooke, Canada
225. E. P. Esztergar, La Jolla, Calif.
226. Harold Etherington, Jupiter, Fla.
227. N. J. Ettenson, Westinghouse Electric Corp., ARD, Madison, Pa.
228. J. R. Farr, Babcock and Wilcox Co., Barberton, Ohio

229. J. H. Faupel, E. I. Du Pont De Nemours and Co., Wilmington, Del.
230. L. F. Fidrych, General Electric Co., Sunnyvale, Calif.
231. John Field, General Electric Co., Sunnyvale, Calif.
232. W. N. Findley, Brown University, Providence, R.I.
233. D. M. Fischer, Amoco Chemicals Corp., Chicago, Ill.
234. G. Fischer, Argonne National Laboratory, Argonne, Ill.
235. J. D. Fishburn, Combustion Engineering, Inc., Windsor, Conn.
236. S. Fistedis, Argonne National Laboratory, Argonne, Ill.
237. J. W. Flora, Division of Compliance, USAEC, Washington, D.C.
238-239. P. Fox, Westinghouse Electric Corp., ARD, Madison, Pa.
240-242. R. F. Fraley, Advisory Committee on Reactor Safeguards, USAEC, Washington, D.C.
243. A. L. Gaines, Combustion Engineering, Inc., Windsor, Conn.
244. W. M. Gajewski, Westinghouse Hanford Co., Richland, Wash.
245. R. H. Gallagher, Cornell University, Ithaca, N.Y.
246. A. C. Gangadharan, Foster Wheeler Corp., Livingston, N.J.
247. D. M. Gardiner, USAEC, Argonne, Ill.
248. J. W. Gascoyne, C. F. Braun and Co., Alhambra, Calif.
249. P. Gast, Argonne National Laboratory, Argonne, Ill.
250. H. H. George, Tube Turns, Inc., Chemetron Div., Louisville, Ky.
251. J. C. Gerdeen, Michigan Technological University, Houghton, Mich.
252. E. F. Gerwin, M. W. Kellogg Co., Williamsport, Pa.
253. R. G. Gilliland, University of Wisconsin, Milwaukee, Wis.
254. J. D. Gilman, General Electric Co., San Jose, Calif.
255. A. B. Glickstein, General Dynamics Corp., Groton, Conn.
256-257. A. J. Goodjohn, Gulf General Atomic, San Diego, Calif.
258. J. J. Gough, Annapolis Division, Naval Ship Research and Development Center, Annapolis, Md.
259. C. T. Grace, University of New Mexico, Albuquerque, N.M.
260. H. Graves, Westinghouse Electric Corp., APD, Pittsburgh, Pa.
261. G. R. Graves, California State Polytechnic College, Pomona, Calif.
262. R. C. Green, Southwest Fabricating and Welding Co., Houston, Tex.
263. G. A. Greenbaum, Mechanics Research, Inc., Los Angeles, Calif.
264. D. K. Greenwald, Ladish Co., Cudahy, Wis.
265. J. H. Griffin, Los Alamos Scientific Laboratory, Los Alamos, N.M.
266. S. C. Grigory, Southwest Research Institute, San Antonio, Tex.
267. Nicholas Grossman, USAEC, Washington, D.C.
268. John Grund, Portland General Electric Co., Portland, Ore.
269. Manuel Gutiervez, American Society of Mechanical Engineers, New York, N.Y.
270. R. Haelsig, Mechanics Research, Inc., Tacoma, Wash.
271. O. Hagen, Westinghouse Electric Corp., EMD, Cheswick, Pa.
272. J. Hagstrom, Chicago Bridge and Iron Co., Oak Brook, Ill.
273. Curt Haire, Idaho Nuclear Corp., Idaho Falls, Idaho
274. G. R. Halford, NASA Lewis Research Center, Cleveland, Ohio
275. E. E. Hamer, Argonne National Laboratory, Chicago, Ill.
276. D. G. Harman, Westinghouse Electric Corp., Tampa, Fla.
277. D. R. Harting, Boeing Co. Aerospace Group, Seattle, Wash.
278. R. W. Haupt, Engineering Data Systems, San Francisco, Calif.
279. E. E. Hay, Imperial Chemical Industries, Manchester 9, England
280. K. Hayashi, Esso Research and Engineering Co., Florham Park, N.J.
281. J. K. Hayes, Combustion Engineering, Inc., Chattanooga, Tenn.

282. F. M. Heck, Westinghouse Electric Corp., APD, Pittsburgh, Pa.
283. D. B. Heilig, Bechtel Corp., San Francisco, Calif.
284. J. M. Hendrie, Brookhaven National Laboratory, Upton, L.I., N.Y.
285. K. Hikido, General Electric Co., Sunnyvale, Calif.
286. F. P. Hill, Combustion Engineering, Inc., Chattanooga, Tenn.
287. H. M. Hill, Excelsior, Minn.
288. R. W. Holland, University of Tennessee, Knoxville, Tenn.
289. R. J. Hollmeier, Pioneer Service and Engineering Co., Chicago, Ill.
290. A. B. Holt, RDT, USAEC, Washington, D.C.
291. F. I. Horan, NASA Langley Field, Hampton, Va.
292. J. P. Houstrup, Combustion Engineering, Inc., Chattanooga, Tenn.
293. L. L. Hsu, General Electric Co., San Jose, Calif.
294. K. A. Huber, Byron Jackson Pump, Inc., Los Angeles, Calif.
295. L. E. Hulbert, Battelle Memorial Institute, Columbus, Ohio
296. H. Huner, Auburn University, Auburn, Ala.
297. J. R. Hunter, RDT, USAEC, Washington, D.C.
298. T. Iltis, Westinghouse Electric Corp., ARD, Madison, Pa.
299. H. S. Isbin, University of Minnesota, Minneapolis, Minn.
300. M. E. Jackson, Argonne National Laboratory, Argonne, Ill.
301. R. W. Jackson, National Valve and Manufacturing Co., Pittsburgh, Pa.
302. M. T. Jakub, Westinghouse Hanford Co., Richland, Wash.
303. Marion Janicke, ARCO, Harvey, Ill.
304. C. E. Jaske, Battelle Memorial Institute, Columbus, Ohio
305. R. I. Jetter, Atomics International, Canoga Park, Calif.
306. R. L. Johnson, Westinghouse Electric Corp., Research and Development Center, Pittsburgh, Pa.
307. A. W. Jones, Rolls Royce and Associates, Ltd., Derby, England
308. Norman Jones, Massachusetts Institute of Technology, Cambridge, Mass.
309. Ralph Jones, USAEC, Washington, D.C.
310. S. M. Jorgensen, Foster Wheeler Corp., Livingston, N.J.
311. L. M. Kaldor, U.S. Navy, Annapolis, Md.
312. W. J. Kaufman, University of California, Richmond, Calif.
313. R. E. Keever, Nuclear Services Corp., Campbell, Calif.
314. E. J. Keith, Engineering Data Systems, San Francisco, Calif.
315. Reese Kern, Idaho Nuclear Corp., Idaho Falls, Idaho
316. H. B. Ketchum, Westinghouse Electric Corp., ARD, Madison, Pa.
317. R. J. Kiessel, U.S. Coast Guard, Washington, D.C.
318. W. C. Kinsel, Westinghouse Hanford Co., Richland, Wash.
319. E. E. Kintner, RDT, USAEC, Washington, D.C.
320. Ronald Kitching, University of Manchester, Manchester, England
321. W. G. Knecht, Darling Valve and Manufacturing Co., Williamsport, Pa.
322. Robert Koester, The Wm. Powell Co., Cincinnati, Ohio
323. L. Kornblith, Division of Compliance, USAEC, Washington, D.C.
324. R. E. Kosiba, RDT, USAEC, Washington, D.C.
325. H. Kraus, Rensselaer Polytechnic Institute of Connecticut, Hartford, Conn.
326. Z. A. Kravets, Consolidated Edison Co. of New York, New York, N.Y.
327. E. Krempl, Rensselaer Polytechnic Institute, Troy, N.Y.
328. N. Krishnamurthy, Auburn University, Auburn, Ala.
329. J. G. Kuang, Esso Production Research Co., Houston, Tex.
330. Y. S. Lai, Chicago Bridge and Iron Co., Oak Brook, Ill.
331. B. Lamar, Argonne National Laboratory, Argonne, Ill.

332. D. F. Landers, Teledyne Materials Research Co., Waltham, Mass.
333. G. Landler, Atomics International, Canoga Park, Calif.
334. E. P. Lang, Lunkenheimer Co., Cincinnati, Ohio
335. D. F. Lange, USAEC, Washington, D.C.
336. B. F. Langer, Westinghouse Electric Corp., Pittsburgh, Pa.
337. C. F. Larson, Welding Research Council, New York, N.Y.
338. R. E. Lawther, Westinghouse Electric Corp., APD, Pittsburgh, Pa.
339. C. W. Lawton, Combustion Engineering, Inc., Windsor, Conn.
340. W. H. Layman, RDT, USAEC, Washington, D.C.
341. M. M. Lemcoe, Battelle Memorial Institute, Columbus, Ohio
342. M. R. Lesh, Esso Research and Engineering Co., Florham, N.J.
343. M. J. Letich, American Bureau of Shipping, New York, N.Y.
344. M. M. Leven, Westinghouse Electric Corp., Research and Development Center, Pittsburgh, Pa.
345. D. J. Lewis, Berkeley Nuclear Laboratories, Berkeley, Gloucestershire, England
346. Librarian, Bechtel Corp., Gaithersburg, Md.
347. Librarian, Westinghouse Electric Corp., Pittsburgh, Pa.
348. G. E. Lien, American Electric Power Service Corp., New York, N.Y.
349. N. C. Lind, University of Waterloo, Waterloo, Ontario, Canada
350. E. M. Livingston, Nuclear Power Division, Babcock and Wilcox Co., Barberton, Ohio
351. R. G. Lloyd, Babcock and Wilcox Co., Barberton, Ohio
352. A. Lohmeier, Westinghouse Electric Corp., Philadelphia, Pa.
353. R. H. Luhta, Darling Valve and Manufacturing Co., Williamsport, Pa.
354. C. J. Lung, Taylor Forge Division, Cicero, Ill.
355. J. Lytton, Virginia Polytechnic Institute, Blacksburg, Va.
356. Josef Maatuk, Crane Co., Chicago, Ill.
357. J. B. Mahoney, Applied Technology Associates, Ramsey, N.J.
358. J. R. Maison, U.S. Naval Civil Engineering Laboratory, Port Hueneme, Calif.
359. L. J. Malandra, Westinghouse Electric Corp., Pittsburgh, Pa.
360. M. V. Malkmus, Tube Turns, Division of Chemetron, Louisville, Ky.
361. R. H. Mallett, Westinghouse Electric Corp., ARD, Madison, Pa.
362. J. R. Maloney, Westinghouse Electric Corp., EMD, Cheswick, Pa.
363. H. G. Mangelsdorf, Short Hills, N.J.
364. M. J. Manjoine, Westinghouse Electric Corp., Pittsburgh, Pa.
365. J. Marchaterre, Argonne National Laboratory, Argonne, Ill.
366. P. V. Marcal, Brown University, Providence, R.I.
367. L. P. Marchesani, Sun Oil Co., Philadelphia, Pa.
368. A. Mathews, University of Tennessee, Knoxville, Tenn.
369. J. D. Mattimore, Louisville, Ky.
370. J. M. Matusz, Rockwell Manufacturing Co., Pittsburgh, Pa.
371. R. L. Maxwell, University of Tennessee, Knoxville, Tenn.
372. J. D. McAdoo, Westinghouse Electric Corp., APD, Pittsburgh, Pa.
373. George McClure, Battelle Memorial Institute, Columbus, Ohio
374. J. E. McConnelee, General Electric Co., Schenectady, N.Y.
375. C. M. McCullar, Bechtel Corp., San Francisco, Calif.
376. J. T. McKeon, M. W. Kellogg Co., Houston, Tex.
377. N. R. McKinney, Southern Services, Inc., Birmingham, Ala.
378. J. L. McLean, Teledyne Materials Research Co., Waltham, Mass.
379. W. N. McLean, Crane Co., Chicago, Ill.

380. G. R. McNutt, Tennessee Valley Authority, Knoxville, Tenn.
381. W. W. McPherson, McPherson Associates, Inc., Waltham, Mass.
382. E. A. McPhillamy, Sandusky Foundry and Machine Co., Sandusky, Ohio
383. R. Mello, Westinghouse Electric Corp., ARD, Madison, Pa.
384-388. J. L. Mershon, USAEC, RDT, Washington, D.C.
389. W. R. Mikesell, CBI Nuclear Co., Memphis, Tenn.
390. C. E. Miller, Argonne National Laboratory, Argonne, Ill.
391. B. J. Milleville, Rockwell Manufacturing Co., Pittsburgh, Pa.
392. R. A. Moen, Westinghouse Hanford Co., Richland, Wash.
393. A. T. Molin, United Engineers and Constructors, Philadelphia, Pa.
394. H. O. Monson, Argonne National Laboratory, Argonne, Ill.
395. C. A. Moore, Idaho Nuclear Corp., Idaho Falls, Idaho
396. R. L. Morgan, Atomics International, Canoga Park, Calif.
397. W. I. Morita, Bechtel Corp., San Francisco, Calif.
398. D. L. Morrison, Battelle Memorial Institute, Columbus, Ohio
399-401. P. A. Morris, Director, Division of Reactor Licensing, USAEC, Washington, D.C.
402. J. K. Morse, Combustion Engineering, Inc., Chattanooga, Tenn.
403. I. Mortman, General Electric Co., South Portland, Me.
404. F. N. Mosehini, Nuclear Systems Europe, Brussels, Belgium
405. C. Muehlhause, National Bureau of Standards, Washington, D.C.
406. E. D. Mysinger, Tennessee Valley Authority, Knoxville, Tenn.
407. A. D. Nalbandian, Grinnell Corp., Providence, R.I.
408. R. M. Nelson, Bingham-Williamette Co., Portland, Ore.
409. D. J. Nolan, United Nuclear Corp., Elmsford, N.Y.
410. E. C. Norman, USAEC, Washington, D.C.
411. NRTS Technical Library, Idaho Falls, Idaho
412. W. J. O'Donnell, O'Donnell and Associates, Bethel Park, Pa.
413. A. A. O'Kelly, Littleton, Colo.
414. David Okrent, University of Arizona, Tucson, Ariz.
415. E. T. Onat, Yale University, New Haven, Conn.
416. J. A. Paget, Gulf General Atomic, San Diego, Calif.
417-418. R. E. Pahler, RDT, USAEC, Washington, D.C.
419. D. H. Pai, Foster Wheeler Corp., Livingston, N.J.
420. M. Pakstys, General Dynamics, Electric Boat Division, Groton, Conn.
421. W. B. Palijenko, Ontario Hydro, Toronto, Ontario, Canada
422. N. J. Palladino, The Pennsylvania State University, University Park, Pa.
423. A. J. Palmer, Esso Research and Engineering Co., Florham Park, N.J.
424. E. C. Pandorf, Cincinnati Gas and Electric Co., Cincinnati, Ohio
425. J. S. Panesar, Atomic Energy of Canada, Ltd., Sheridan Park, Ontario, Canada
426. G. W. Pangborn, Combustion Engineering, Inc., Windsor, Conn.
427-428. S. Paprocki, Battelle Memorial Institute, Columbus, Ohio
429. C. S. Parker, General Electric Co., San Jose, Calif.
430. G. L. Parkinson, Bechtel Corp., San Francisco, Calif.
431. J. R. Payne, Esso Research Engineering Co., Florham Park, N.J.
432. M. H. Pedell, Stone and Webster Engineering Corp., Boston, Mass.
433. W. Pennell, Westinghouse Electric Corp., ARD, Madison, Pa.

434. R. K. Penny, University of Liverpool, Liverpool, England
435. N. T. Peters, Giffels and Rosetti, Inc., Detroit, Mich.
436. D. B. Peterson, KPA Computer Techniques, Inc., Large, Pa.
437. R. Peterson, Westinghouse Hanford Co., Richland, Wash.
438-439. N. Petrick, Westinghouse Electric Corp., ARD, Madison, Pa.
440. A. G. Pickett, Southwest Research Institute, San Antonio, Tex.
441-442. D. L. Platus, Mechanics Research, Inc., Los Angeles, Calif.
443. R. W. Pochmann, U.S. Industries, Inc., Wyatt Division, Houston, Tex.
444. C. H. Powell, University of California, Berkeley, Calif.
445-449. A. J. Pressesky, RDT, USAEC, Washington, D.C.
450. James Proctor, Naval Ordnance Laboratory, White Oak, Silver Spring, Md.
451. J. C. Quinn, Lunkenheimer Co., Cincinnati, Ohio
452. F. C. Rally, General Electric Co., Sunnyvale, Calif.
453. Y. R. Rashid, General Electric Co., San Jose, Calif.
454. G. S. Rasmussen, G. S. Rasmussen and Associates, Glendale, Calif.
455. R. T. Reid, Aerojet Nuclear Systems Co., Sacramento, Calif.
456. B. T. Resnick, USAEC, Washington, D.C.
457. J. W. Riches, Douglas United Nuclear, Richland, Wash.
458. D. R. Riley, USAEC, Washington, D.C.
459. B. Roberts, Combustion Engineering, Inc., Chattanooga, Tenn.
460. T. Rockwell III, MPR Associates, Inc., Washington, D.C.
461. E. C. Rodabaugh, Battelle Memorial Institute, Columbus, Ohio
462. D. Rose, Argonne National Laboratory, Argonne, Ill.
463. M. A. Rosen, RDT, USAEC, Washington, D.C.
464. G. S. Rosenberg, Argonne National Laboratory, Argonne, Ill.
465. F. A. Ross, USAEC, Washington, D.C.
466. H. D. Ross, Babcock and Wilcox Co., Lynchburg, Va.
467. B. J. Round, Combustion Engineering, Inc., Windsor, Conn.
468. E. J. Rozic, Babcock and Wilcox Co., Beaver Fall, Pa.
469. Robert Rung, Applied Technology Associates, Inc., Ramsey, N.J.
470. P. H. Sager, Gulf General Atomic, San Diego, Calif.
471. R. F. Sammataro, General Dynamics Corp., Groton, Conn.
472. R. I. Sann, Gulf United Nuclear Fuel Corp., Elmsford, N.Y.
473. A. W. Savolainen, American National Standard Institute, New York, N.Y.
474. A. O. Schaefer, Metals Properties Council, New York, N.Y.
475. Robert Schmidt, Ladish Co., Cudahy, Wis.
476. W. R. Schmidt, MPR Associates, Inc., Washington, D.C.
477. R. W. Schneider, Bonney Forge and Foundry, Inc., Allentown, Pa.
478. J. J. Schreiber, USAEC, Washington, D.C.
479. J. Schroeder, University of Waterloo, Waterloo, Ontario, Canada
480. C. C. Schultz, Babcock and Wilcox Co., Alliance, Ohio
481. F. Sebring, C. F. Braun and Co., Alhambra, Calif.
482. R. A. Selbey, Westinghouse Hanford Co., Richland, Wash.
483. H. R. Selby, Bechtel Corp., Gaithersburg, Md.
484. Jagmohan Seoni, Bechtel Corp., Gaithersburg, Md.
485. L. K. Severud, Westinghouse Hanford Co., Richland, Wash.
486. R. Sevy, Argonne National Laboratory, Argonne, Ill.
487. M. Shaw, RDT, USAEC, Washington, D.C.
488. W. A. Shaw, Auburn University, Auburn, Ala.

489. E. F. Sheaffer, Liquid Metal Engineering Center, Canoga Park, Calif.
490. D. W. Sher, Combustion Engineering, Inc., Chattanooga, Tenn.
491. P. Shewmon, Argonne National Laboratory, Argonne, Ill.
492. R. L. Shively, General Electric Co., San Jose, Calif.
493. L. R. Shobe, University of Tennessee, Knoxville, Tenn.
494. Sidney Siegel, Atomics International, Canoga Park, Calif.
495. M. Siegler, General Electric Co., San Jose, Calif.
496. C. P. Siess, University of Illinois, Urbana, Ill.
497. J. M. Simmons, USAEC, Washington, D.C.
498-501. W. Simmons, Argonne National Laboratory, Argonne, Ill.
502. E. E. Sinclair, USAEC, Washington, D.C.
503. G. Skochko, General Electric Co., MAO, Schenectady, N.Y.
504. V. Skoglund, University of New Mexico, Albuquerque, N.M.
505. R. J. Slember, Westinghouse Electric Corp., ARD, Madison, Pa.
506. E. R. Sliwinski, EBASCO Services, New York, N.Y.
507. W. L. Smalley, Oak Ridge Operations Office, Oak Ridge, Tenn.
508. G. V. Smith, 104 Berkshire Road, Ithaca, N.Y.
509. H. B. Smith, Combustion Engineering, Inc., Windsor, Conn.
510. W. R. Smith, Bechtel Corp., San Francisco, Calif.
511. A. L. Snow, Westinghouse Electric Corp., ARD, Madison, Pa.
512. R. E. Soderberg, Walworth Co., Greensburg, Pa.
513. J. E. Soehrens, C. F. Braun and Co., Alhambra, Calif.
514-515. D. Spencer, Westinghouse Electric Corp., ARD, Madison, Pa.
516. J. L. V. Sperry, Detroit Edison Co., Detroit, Mich.
517. Lombard Squires, Naples, Fla.
518. E. D. Ssinegurski, Combustion Engineering, Inc., Windsor, Conn.
519. R. E. Stanbridge, Liquid Metal Engineering Center, Canoga Park, Calif.
520. E. H. Steigerwald, Bechtel Corp., Gaithersburg, Md.
521. K. O. Stein, Babcock and Wilcox Co., Alliance, Ohio
522. W. R. Stratton, Los Alamos Scientific Laboratory, Los Alamos, N.M.
523. R. G. Sturm, Brown Engineering-Teledyne Co., Huntsville, Ala.
524. W. A. Sutherland, General Electric Co., San Jose, Calif.
525. W. H. Sutherland, Westinghouse Hanford Co., Richland, Wash.
526. E. O. Swain, General Electric Co., San Jose, Calif.
527. J. A. Swanson, Elizabeth, Pa.
528-529. R. Swanson, Idaho Operations Office, USAEC, Idaho Falls, Idaho
530. W. F. Swinson, Auburn University, Auburn, Ala.
531. A. N. Tardiff, USAEC, Washington, D.C.
532-533. J. Taylor, Westinghouse Electric Corp., ARD, Madison, Pa.
534. R. E. Taylor, Reinhold Publishing Co., Chicago, Ill.
535. B. E. Tenzer, EBASCO Services, Inc., New York, N.Y.
536. H. J. Thailer, Westinghouse Electric Corp., Pittsburgh, Pa.
537. K. Thomas, Westinghouse Electric Corp., ARD, Madison, Pa.
538. J. C. Tobin, Westinghouse Hanford Co., Richland, Wash.
539. C. H. A. Townley, Berkeley Nuclear Laboratories, Central Electricity Generating Board, Berkeley, Gloucestershire, England
540. R. E. Tschirch, Hartwell Co., Inc., East Providence, R.I.
541. I. S. Tuba, Basic Technology, Inc., Pittsburgh, Pa.
542. W. H. Tuppeny, Combustion Engineering, Inc., Windsor, Conn.
543. A. J. Turner, Combustion Engineering, Inc., Chattanooga, Tenn.

544. A. B. Ungar, Public Service Electric and Gas Co., Newark, N.J.
545. R. A. Valentin, Argonne National Laboratory, Argonne, Ill.
546. M. F. Valerino, General Electric Co., San Jose, Calif.
547. W. A. Van der Sluys, Babcock and Wilcox Co., Alliance, Ohio
548. F. E. Vinson, Bechtel Corp., San Francisco, Calif.
549. R. Vogel, Argonne National Laboratory, Argonne, Ill.
550. G. E. Wade, General Electric Co., San Jose, Calif.
551. E. A. Wais, Holmes and Narver, Inc., Anaheim, Calif.
552. Robert Wascher, Babcock and Wilcox Co., Lynchburg, Va.
553. E. O. Waters, 28F Heritage Village, Southbury, Conn.
554. R. F. Webster, U.S. Steel Corp., Pittsburgh, Pa.
555. R. W. Weeks, Argonne National Laboratory, Argonne, Ill.
556. B. C. Wei, RDT, USAEC, Washington, D.C.
557. W. H. Wepfer, Westinghouse Electric Corp., Cheswick, Pa.
558. D. H. White, Westinghouse Electric Corp., Tampa, Fla.
559. M. J. Whitman, RDT, USAEC, Washington, D.C.
560. K. R. Wichman, USAEC, Washington, D.C.
561. R. A. Wiesemann, Westinghouse Electric Corp., APD, Pittsburgh, Pa.
562. F. S. G. Williams, Frank S. G. Williams and Associates, Inc., Chicago, Ill.
563. B. V. Winkel, Idaho Nuclear Corp., Idaho Falls, Idaho
564. B. Wolfe, Westinghouse Hanford Co., Richland, Wash.
565. Christopher Wright, Underseas Engineering, Inc., Riviera Beach, Fla.
566. L. E. Wright, C. F. Braun and Co., Alhambra, Calif.
567. W. B. Wright, Westinghouse Electric Corp., APD, Pittsburgh, Pa.
568. J. N. Wu, Babcock and Wilcox Co., Alliance, Ohio
569. B. M. Wundt, Schenectady, N.Y.
570. J. C. M. Yu, Auburn University, Auburn, Ala.
571. Lin Yung-Lo, Bliss R and D Co., Swarthmore, Pa.
572. S. Y. Zamrik, Pennsylvania State University, University Park, Pa.
573. E. Zebroski, General Electric Co., Sunnyvale, Calif.
574. Zenons Zudans, Franklin Institute Research Laboratories, Philadelphia, Pa.
575. M. P. Zyne, Southern Services, Inc., Birmingham, Ala.
576-592. Manager, Technical Information Center (TIC)
593. Patent Office, AEC, ORO
594. Research and Technical Support Division, AEC, ORO
595-809. Given distribution as shown in TID-4500 under Reactor Technology category (including 25 copies to NTIS)